The regulation of plastidial proteins by calmodulins

Elisa Dell'Aglio

UNIVERSITÉ DE GRENOBLE

THÈSE

Pour obtenir le grade de

DOCTEUR DE L'UNIVERSITÉ DE GRENOBLE

Spécialité : **Biologie Végétale**

Arrêté ministériel : 7 août 2006

Présentée par

Elisa DELL'AGLIO

Thèse dirigée par **Norbert ROLLAND**
codirigée par **Gilles CURIEN**

préparée au sein du **Laboratoire de Physiologie Cellulaire et Végétale**

dans **l'École Doctorale Chimie et Sciences du Vivant**

La Régulation des Protéines Plastidiales par la Calmoduline

Thèse soutenue publiquement le **29 novembre 2013**,
devant le jury composé de :

Mme Christelle BRETON
Professeur à l'Université Joseph Fourier, Grenoble (Président)
M. Christian MAZARS
Directeur de Recherche à LRSV, Toulouse (Rapporteur)
Mme Dominique RUMEAU
Chargée de Recherche CNRS à SBVME, CEA-Cadarache (Rapporteur)
M. Andrea GENRE
Chargé de Recherche à DSVBS, Torino, Italie (Examinateur)
M. Norbert ROLLAND
Directeur de Recherche à iRTSV, Grenoble (Directeur de thèse)
M. Gilles CURIEN
Chargé de Recherche CNRS à iRTSV, Grenoble (Codirecteur de thèse)

Université Joseph Fourier / Université Pierre Mendès France /
Université Stendhal / Université de Savoie / Grenoble INP

Dans l’œuvre de la science seulement on peut aimer ce qu’on détruit, on peut continuer le passé en le niant, on peut vénérer son maître en le contredisant.

Gaston Bachelard, *La formation de l’esprit scientifique*, 1938

Le cose che un racconto non dice sono necessariamente più numerose di quelle che dice e solo una speciale aureola intorno a ciò che è scritto può dare l'illusione che stai leggendo qualcosa che non è scritto.

Italo Calvino, 1923-1985

Acknowledgements

This study was funded by an IRTELIS international PhD fellowship and conducted in the Laboratory of Cell and Plant Physiology (LPCV) of the CEA-Grenoble. I express my gratitude to Marylin Vantard who welcomed me in her laboratory in 2010, and to Norbert Rolland and Laurent Blanchoin who subsequently undertook the direction of the laboratory.

I am grateful to Christelle Breton, Andrea Genre, Christian Mazars and Dominique Rumau for having accepted to judge my PhD work.

Norbert Rolland supervised this work and directed the team. I acknowledge the time spent in discussing my results and the help in writing this manuscript and the associated publication.

Gilles Curien closely supervised this work day-by-day. I express him my deepest gratitude for all the technical and theoretical knowledge he shared with me, his enthusiasm and his patience.

Many thanks to Giovanni Finazzi for the direction and supervision of the photosynthetic measurements, his moral support, and all the discussions in Italian.

I am grateful also to Cécile Breyton and Stefan Hörtensteiner for the critical supervision of my work during the PhD thesis committees.

Je suis reconnaissante à tous les membres de l'équipe1 du laboratoire PCV car ils ont tous contribué à l'accomplissement de ce travail. Je remercie en particulier Cécile Giustini et Faustine Delpierre pour le clonage et la purification de certaines protéines et pour l'aide dans l'optimisation des overlays.

Merci également à tous les autres membres du laboratoire présents et passés pour l'harmonie que l'on respire toujours dans les couloirs, et aussi à tousles amis que j'ai connus pendant mon séjour en France et qui m'ont permis de profiter le plus possible de cette expérience de vie. Merci surtout à Héléna, Matthieu, Nina, Sarah, Marta, Valentina, Dimitris, James, Manu, Marie, Camille, Sophie, Hicham, Fanny, Martino, Guillaume, Serena, Valeria et à L'Aplomb d'la Plume.

Grazie di cuore a tutte le persone a me care da cui mi sono allontanata per svolgere questo lavoro: ai "torinesi", ai "rivolesi", a quelli che sono ancoralà e a quelli che come me hanno deciso di partire. Un forte abbraccio a Monica e Valeria, i miei punti di riferimento. Tutto il mio affetto alla mia famiglia, in particolare alla mia cara Mamma e a Luigi.

Summary

Preface

Acquired by endosymbiosis from an ancient cyanobacterium, the chloroplast is the most peculiar organelle of autotrophic eukaryotes, which include algae and land plants. It represents the site of the photosynthetic process, *i.e.* the chain of reactions allowing the conversion of solar energy and CO_2 into organic molecules and reductive power for plant development and reproduction. The chloroplast hosts also many metabolic pathways for the synthesis of various metabolites such as amino acids, lipids and hormones. Many of these molecules cannot be produced by heterotrophic organisms, which need to assimilate them by nutrition. Several plastidial metabolites have a variety of industrial applications and plant tissues are used to produce fibers, fuels and other products.

Regulation of chloroplast physiology takes place at various levels. Firstly, it must be taken into account that the most part of plastidial proteins were horizontally transferred to the nuclear genome. To be efficiently targeted to the chloroplast they need a plastidial signal peptide, normally located at the *N*-terminal of the protein. Mechanisms regulating protein synthesis and transport are therefore essential. Moreover, the metabolic activity of chloroplast needs to be finely modulated according to the environmental conditions (*e.g.* season, light intensity, temperature, availability of nutrients) and the plant need (organ, developmental state). This regulation implicates the presence in the chloroplast of sensors of the redox state and of changes in external conditions (*e.g.* the transition from light to dark), coupled with effective and rapid strategies of adaptation.

Understanding the general physiology of the chloroplast and how the different processes are modulated is essential for many practical purposes, such as:

- The amelioration of the photosynthetic yield of crops and plant productivity;
- The improvement of the metabolic pathways that lead to the production of molecules of interest;
- The improvement of the adaptation capacity of plants in a context of deep climate change and shortage of fertilizers.

One of the most ubiquitous eukaryotic secondary messengers is calcium. Calcium variations are observed in response to cell processes such as fertilization and muscle contraction in mammals or

stomatal aperture and symbiotic interactions in plants. In particular, in the chloroplast, calcium signals were associated to the transition from light to dark and to the control of protein import.

Calcium signaling is decoded by a variety of proteins, especially the calcium sensor Calmodulin. In animals, calmodulin is a cytosolic protein present as only one (sometimes two) isoforms per species. In plants, Calmodulins and Calmodulin-like proteins form an extended protein family and some isoforms are found in cell compartments such as the nucleus and the mitochondria. This peculiarity suggests that plants evolved specific ways of dealing with calcium signaling. Moreover, few plastidial proteins were previously shown to interact with Calmodulin, suggesting the existence of calcium-Calmodulin regulatory processes in this organelle. Understanding these responsive mechanisms could reveal important and useful aspects of plant adaptation.

This thesis work aimed to explore the plastidial Calmodulin-binding proteome. In the **Introduction**, we discuss the calcium regulation of the plant cell with particular emphasis on the chloroplast. We describe the most important families of plant calcium-binding proteins with a particular focus on Calmodulins, their specificity, their calcium affinity and their regulatory functions. The Results section comprises a better quantitative characterization by fluorescence anisotropy measurements of the interaction between Calmodulin 1 and the NAD kinase 2 of Arabidopsis (**Chapter 1**). We then present a proteomics survey on plastidial Calmodulin interactors (**Chapter 2**), and a finer analysis of two of them: ceQORH and Tic32 (**Chapters 3** and **4**). The search for Calmodulin or Calmodulin-like proteins in the chloroplast is described in **Chapter 5**. Finally, a more detailed analysis of NADK2 and the *in vivo* dependency of NADK on CaM is the subject of **Chapter 6**.

Introduction

1- Plant calcium signaling

1.1- Distribution and roles of calcium in living organisms

Calcium (Ca^{2+}) is a macro-element essential for all living organisms, an important constituent of the plant cell wall, and a stabilizer of plant protein complexes (*e.g.* photosystem II, Barry et al, 2005). Ca^{2+} can, however, form insoluble precipitates with phosphate, thereby interfering with energy metabolism and other cell pathways. Cytosolic [Ca^{2+}] is therefore maintained at sub-micromolar levels by active extrusion of Ca^{2+} in excess outside the cell or accumulation in cell compartments, especially the endoplasmic reticulum and the vacuole. Ca^{2+} plays also a pivotal role as a signaling molecule which triggers cell responses to a wide variety of environmental and developmental stimuli.

Ca^{2+} signaling has been for long considered a "eukaryotic invention" but recent data suggest that it could have a regulatory role also in bacteria, through the action of some Ca^{2+}-binding proteins sometimes similar to those found in eukaryotes. The same differences in cytosolic and external [Ca^{2+}] found in eukaryotes are common also to bacteria, but current knowledge not yet allows making a satisfactory comparison of the two systems (Dominguez, 2004).

1.2- Ca^{2+} measurements inside plant cells

Ca^{2+} homeostasis was extensively studied in animal cells and knowledge about plant systems is lagging behind. One reason is that the peculiar shape of the plant cell (*i.e.* the presence of the cell wall and the huge vacuole that limits the cytoplasmic volume) challenged microelectrode measurements that were rarely performed (Felle, 1988). Nevertheless, many discoveries were made during the last decades, thanks to plant genome sequencing projects and the development of new tools for quantitative measurements of intracellular Ca^{2+} levels *in vivo*. These techniques include fluorescent dyes that bind Ca^{2+}, such as Quin-2, Fura-2 and Indo-1 (see Takahashi et al, 1999 for a review), and various biosensors, especially aequorin (Knight, 1991) and cameleon (Miyawaki 1997).

Aequorin is constituted of apo-aequorin (189 amino acids) and the chromophore coelenterazine. Aequorin contains three Ca^{2+}-binding sites. Ca^{2+} chelation triggers a protein conformational change that causes the oxidation of the coelenterazine, which is observed by the luminescence emitted at 469

nm (**Fig. I.1A**). The protein was engineered by mutagenesis (Stepanyuk et al., 2005, Tricoire et al., 2006) in order to create several variants with optimized properties, such as higher stability and Ca^{2+} sensitivity. Aequorin can be targeted to different cell types or cell compartments, in order to measure [Ca^{2+}] variations in specific developmental stages or organelles (Johnson et al, 1995; Sai & Johnson, 2002).

The low fluence rate of aequorin does not allow measurements in single cells. This resolution can be achieved with cameleon, a Ca^{2+} sensor composed of two fluorescent proteins (for example CFP and YFP), that surround a calmodulin and the calmodulin binding peptide of the skeletal muscle myosin light chain kinase (named M13). After Ca^{2+} binding, this construct undergoes a conformational change that triggers a shift in the protein fluorescence emission (**Fig. I.1B**). Cameleon allowed following [Ca^{2+}] variations in single cells and the analysis of many Ca^{2+}-regulated processes such as those associated to the stomatal closure or the symbiosis interactions with rhizobia or mycorrhizal fungi (see Batistič and Kudla 2012 for a review).

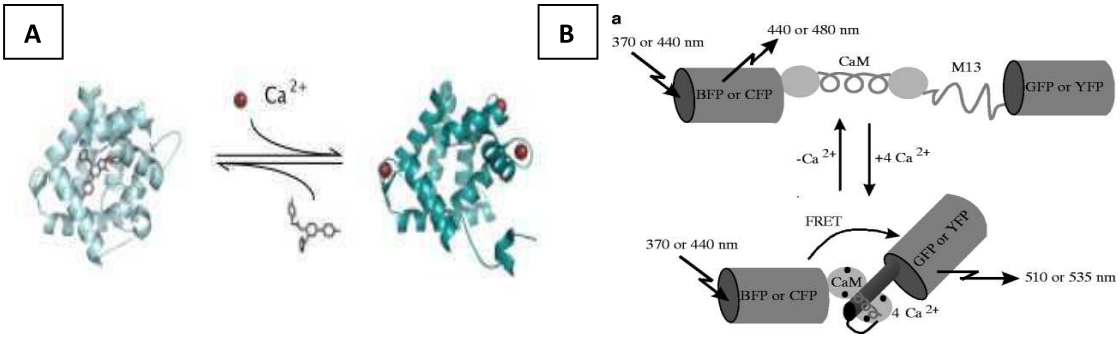

Fig. I.1 Schematical representation of aequorin and cameleon binding to calcium. **A**. Aequorin binds three Ca^{2+} ions, triggering the oxidation and release of the chromophore coelenterazine and the development of a detectable luminescence (McCombs et al, 2008). **B**. The CaM-like region of cameleon chelates four Ca^{2+} ions. The calmodulin binding peptide (M13) situated next to it rotates and binds tightly to the calmodulin region. This causes the approaching of the *N*-terminal protein region that contains a BFP or CFP domain with the *C*-terminal GFP or YFP domain. A FRET (Förster resonance energy transfer) change detected by confocal microscopy occurs (Miyawaki 1997).

1.3- Ca^{2+} homeostasis and Ca^{2+} fluxes in the plant cell

The central dogma of Ca^{2+} signaling states that, in response of an environmental stimulus or stress conditions, the [Ca^{2+}] of the cytoplasm or of an organelle increases, shifting from nanomolar to micromolar levels. This Ca^{2+} is then bound by proteins called "Ca^{2+} sensors", whose role is to transfer the signal up to effectors that determine a cell response (*i.e.* enzymes, channels and transcription factors).

This dogma is valid for all eukaryotes and general assumptions on Ca^{2+} fluxes and the properties of Ca^{2+}-binding proteins can be extended from animals to plants. However, important differences need to be underlined, especially in what concerns the Ca^{2+} storage and release in the various organelles and the variety of Ca^{2+} sensors.

The difference in $[Ca^{2+}]$ between the cytosol and Ca^{2+}-storing organelles or the apoplast allows rapid and deep changes in cytosolic $[Ca^{2+}]$ (10 to 100 folds) following the opening of Ca^{2+} channels situated on the Ca^{2+}-storing organelles or the plasma membrane. Changes in the kinetics of opening of these channels were shown in response to many stimuli: abiotic, biotic and developmental (reviewed in Reddy, 2001).

In order to generate various cell responses, the Ca^{2+} signals must be extremely controlled, *i.e.* Ca^{2+} channels, transporters and Ca^{2+} buffering proteins must be finely modulated. Ca^{2+} channels and transporters have undergone a high degree of duplication and differentiation. Particular tissues or cell types are therefore able to generate and respond to various Ca^{2+} signals by modulation of gene expression of Ca^{2+} channels and transporters and/or their post-translational modifications.

a) Transport of Ca^{2+} outside the cytoplasm

Many proteins are involved in order to keep the cytosolic $[Ca^{2+}]$ under control. These include P-type ATPases of the P2 class, in particular the AUTO-INHIBITED Ca^{2+} ATPases (ACAs). They are probably key controllers of cytosolic Ca^{2+} homeostasis and are localized in the vacuole as well as at the plasma membrane (Sanders et al, 2002). Their expression was shown to be increased in stress conditions such as cold, ABA treatment or pathogen infiltration. Moreover, mutants of some of these Ca^{2+} pumps show impairment in processes that are known to require cytosolic $[Ca^{2+}]$ variations, such as pollen germination (*aba9*) and flower development (*aca10*). These proteins are regulated by calmodulin, acidic phospholipids and phosphorylation (Boursiac and Harper, 2007). Another type of ATPases, (ER-type Ca^{2+} ATPases or ECAs), are located on the endoplasmic reticulum and the vacuole (Geisler et al, 2000).

In addition to pumps, cytosolic Ca^{2+} is also extruded by Ca^{2+}-proton exchangers. In Arabidopsis there are at least six cation exchangers (CAX) proteins which are localized at the plasma membrane or

at the tonoplast. They are often auto-inhibited by an *N*-terminal regulatory domain. Among CAX proteins, CAX1 was shown to be a key controller of Ca^{2+} homeostasis, with implications in lateral root formation and inflorescence (Hirschi et al, 1996; Cheng et al, 2005).

b) Entry of Ca^{2+} in the cytosol

The entry of Ca^{2+} in the cytosol occurs through Ca^{2+} channels. These channels are relatively inactive during normal conditions but their opening can be stimulated by a wide variety of factors. Some of these channels are voltage-dependent and their opening is driven by changes in the potential of the plasma membrane (depolarization- or hyperpolarization-activated channels), or mechanical stimuli. Many secondary messengers can be involved in triggering the release of Ca^{2+} by specific channels, for example inositol 3-phosphate (InsP3), cyclic ADP ribose (cADPR) and Nicotinic Acid Adenine Dinucleotide Phosphate (NAADP), a derivative of NADP. Vast classes of channels are that of cyclic nucleotide-gated channels (CNGCs), and that of the glutamate-receptor-like channels. They can form heteromultimeric complexes, with different sensitivities and properties that might explain the differences in the modulation of cell responses (see for reviews Dennison & Spalding, 2000 and Demidchik et al, 2002).

c) Ca^{2+} fluxes across the cell and cell responses

Cytosolic transient influxes of Ca^{2+} can be highly localized in the cellular space and have been divided into monophasic and biphasic, although caution should be applied in analyzing these data when taken from a cell population rather than from single cells (see Dodd et al, 2010 for a review). Different dynamics in the opening and activity of channels and transporters result in Ca^{2+} spikes of different lifetimes (**Table I.1**). The duration of the stimulus can be extremely short (microseconds or milliseconds) or longer (seconds or even minutes). This depends on the properties of Ca^{2+} channels and transporters involved. Generally, the opening of Ca^{2+} channels (controlled by several factors such as InsP3) lasts for a short time and is followed by a period of inactivation when the channel is no more able to transfer Ca^{2+} in the cytosol. At the same time, Ca^{2+}-dependent Ca^{2+} ATPases become activated and contribute to re-establish the normal cytoplasmic [Ca^{2+}]. Periodic and localized [Ca^{2+}] increases in the cytosol can also originate “waves” that spread in the surrounding regions and sometimes throughout the cell. This is especially possible thanks to Ca^{2+}-dependent Ca^{2+} channels: when cytosolic [Ca^{2+}] transiently in-

creases in a certain region, the Ca^{2+}-dependent Ca^{2+} channels located nearby will be activated and temporary opened, thus contributing to the transmission of the Ca^{2+} wave, sometimes throughout the cytoplasm (Trewavas, 1999).

Signal	Lag Period	Rise Time	Total Transient
		s	
Oxidative shock	30	10	90
Wind	0	0.3	15
Cold shock	0	4–5	30
Hyperosmotic shock	5	10	30
Anoxia	60	120	300
Elicitors	5–10	20	45–60
Blue light	3–6	20–30	90
Heat shock	several min	10 min	30 min

Table I.1 Characteristics of Ca^{2+} signatures in tobacco seedlings after the imposition of different perturbations. The seedlings were transformed with aequorin (Malhó et al, 1998).

Specific patterns of spatial and temporal variations in [Ca^{2+}] are often called "Ca^{2+} signatures". They can lead to a wide number of cell responses that determine plant development and environmental adaptation such as stomatal aperture, growth of pollen tubes, and abiotic stress responses (see Kudla et al, 2010 for a complete and exhaustive review).

Mechanical stresses for example originate specific Ca^{2+} signatures in roots. Touching originates a monophasic wave that spreads throughout the cell, while bending provokes a biphasic response in the cells under tension, but not in those under contraction (Monshausen et al, 2009).

Ca^{2+} signatures are also needed to establish root symbiosis with both mycorrhizal fungi and rhizobia. Indeed, this process is the most well-known and studied. In order to successfully develop these two associations, Ca^{2+} oscillations at the proximity of the nucleus and a specific cell signaling pathway (the so-called Sym pathway) are activated in both cases. However, the shape and duration of the Ca^{2+} oscillations are qualitatively different (**Fig. I.2**, Kosuta et al, 2008).

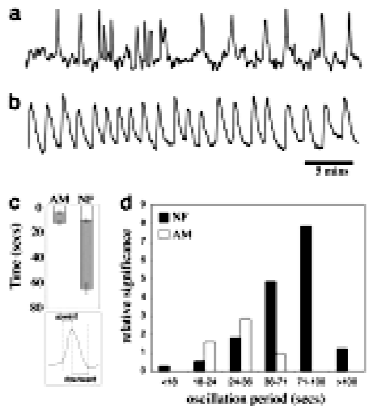

Fig. I.2 Differences between the Ca^{2+} signatures produced by Nod factor of Rhizobia and mycorrhizal fungi. A. A root hair cell showing mycorrhizal-induced Ca^{2+} oscillations. **B.** A root hair cell showing Nod factor-induced Ca^{2+} spiking. **C.** Analysis of individual transients in arbuscular mycorrhizal-induced and Nod factor-induced [Ca^{2+}] changes. The upward phase of the spike (white) is compared with the downward phase (gray). D: A histogram showing significant peaks from Fourier analysis of 10 Nod factor-treated cells and 10 mycorrhizal-treated cells. Components within each trace that showed significance were separated and plotted by the oscillation period (Kosuta et al, 2008).

The extreme variety of Ca^{2+} signatures and associated cell responses led to speculate that they could be compared to neural networks. Indeed, as well as neural networks, *i)* they are spatially structured; *ii)* they can integrate various stimuli at the same time; *iii)* they can originate rhythmic oscillations, *iv)* they can "learn" (*i.e.* transcription of Ca^{2+} channels, transporters and Ca^{2+} binding proteins, as well as specific responsive genes can be triggered by Ca^{2+} signals); and *v)* memory of previous signals can be accessed and used to modify current signal information (Trewavas, 1999). This audaceous hypothesis shows the importance of the understanding how Ca^{2+} signatures are originated from the different cell compartments, and how the Ca^{2+} message is transmitted up to the final cell effectors.

1.4- Compartments involved in Ca^{2+} signaling in plants

Ca^{2+} distribution in plant and animal cells is similar, but the presence of the apoplast and the plastids adds more complexity to the plant system. Here we report a list of all Ca^{2+} storing organelles of the plant cell and their characteristics (**Fig. I.3**).

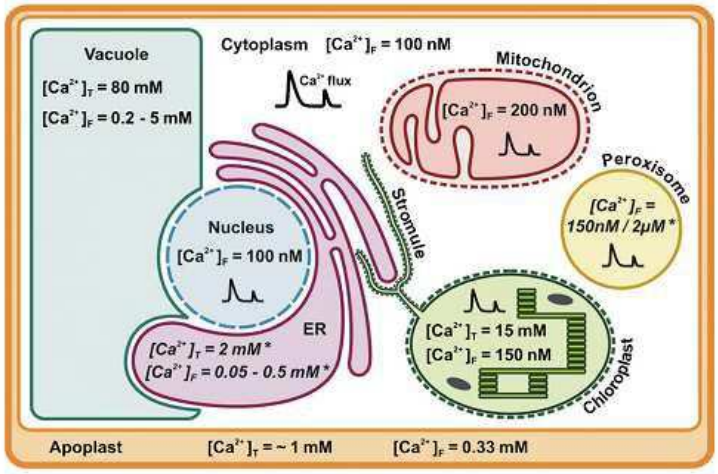

Fig. I.3 Summary of organelle Ca^{2+} concentrations in the plant cell (Stael et al, 2012b). For each organelle, total (T) and free (F) resting Ca^{2+} concentrations are reported. Asterisks indicate that measurements were taken from animal cells.

a) Endoplasmic reticulum (ER)

In animals, the role of the ER in Ca^{2+} signaling was studied in detail because of its importance in the regulation of muscle contraction. Few data are available for plants, especially because the Ca^{2+} channels involved do not belong to the same protein families as in animals (*i.e.* InsP3 and ryanodine receptor channel), thus making difficult to evaluate analogies between the two kingdoms. Even the internal concentration of $[Ca^{2+}]$ in the ER of plant cells has not yet been measured (for animals, it has been estimated approximately 2 mM for total $[Ca^{2+}]$ and 50-500 µM for free $[Ca^{2+}]$, Coe and Michalak, 2009).

Fluxes of Ca^{2+} from the ER in plant cells were measured upon stimulation by InsP3 (Muir and Sanders, 1997), cADPR (Navazio et al, 2000) and NAADP, a derivative of NADP (Navazio et al, 2001). Some of the channels involved appear to be voltage-gathered (Klusener et al, 1997).

The ER-localized Ca^{2+}-binding protein calreticulin was estimated to be the major Ca^{2+} storage protein in plants and was also associated to protein folding control. Ca^{2+}-transport experiments in isolated tobacco or Arabidopsis microsomes overexpressing maize calreticulin showed an increase in Ca^{2+} uptake and, *vice versa*, down-regulation causes enhanced sensitivity of the plant to Ca^{2+} depletion (Persson et al, 2001).

b) Apoplast

In the apoplast Ca^{2+} has a structural role. Indeed, the rigidity of cross-linking of the pectate molecules depends on the Ca^{2+} concentration. A high concentration of Ca^{2+} was also linked to impairment of guard cell mobility. Entry of Ca^{2+} in the cytoplasm is regulated by a wide variety of channels, such as voltage-gated channels or ligand-gated ion channels (CNGCs and GLRs, Stael et al 2012b).

c) Mitochondria

Mitochondrial Ca^{2+} transporters were only characterized in animals, but several homologues of animal proteins were found in plants, suggesting that the control mechanisms of Ca^{2+} uptake could be similar.

Free mitochondrial Ca^{2+} concentration was estimated approximately 200 nM (Logan and Knight, 2003) and isolated plant mitochondria are able to take up external Ca^{2+} up to micromolar concentrations, if the respiratory substrates are present (Chen & Lehninger, 1973). It has been proposed that the Ca^{2+} intake could be modulated by the light intensity through the action of mitochondrial phytochrome (Roux, 1981).

In animals, release of mitochondrial proteins such as the cytochrome *c* is associated to apoptosis. Mitochondrial disruption is due to the swelling of the mitochondrial matrix that ends up in the rupture of the inner membrane. A similar event (*i.e.* a fast shrinkage followed by swelling of the mitochondrial matrix) is triggered in isolated plant mitochondria by high external concentrations of Pi and Ca^{2+}. Substitution of Ca^{2+} with magnesium still provokes the shrinking but abolishes the swelling (Virolainen et al, 2002). This Ca^{2+}-dependent mitochondrial rupture and apoptosis was observed in wheat isolated mitochondria or Arabidopsis cell cultures in response to anoxia as well as to oxidative stress, by measurements of membrane potentials and electron microscopy (Virolainen 2002, Tiwari et al, 2002).

In addition, plant specific Ca^{2+} control of the import of nuclear encoded proteins in the mitochondria has recently been reported (Kuhn et al 2009), similarly to what observed for plastids (see paragraph 1.4).

d) Vacuole

The vast majority of intracellular Ca^{2+} is stored in the vacuole of plant cells and hypersensitivity is observed when the vacuolar Ca^{2+} uptake is hampered. For example, overexpression of the Ca^{2+}/ H^{+} antiporter of the tonoplast, CAX1, results in symptoms of Ca^{2+} deficiencies, including hypersensitivity to ion imbalances, and to cold shock. Increasing the Ca^{2+} in the media abrogated these sensitivities. Tobacco plants expressing CAX1 also showed increased Ca^{2+} accumulation in the vacuole (Hirschi, 1999, Conn et al, 2011).

The Ca^{2+} stored in the vacuole is buffered by many ligands, especially little molecules such as malate and citrate, or proteins. Free vacuolar Ca^{2+} is in the range of 0.2-5 mM (Reid &Smith, 1991).

The tonoplast possesses a long series of Ca^{2+} channels regulated by cADPR or InsP3 (Allen et al, 1995) and voltage (Islam et al, 2010), but no solid data are available concerning the role of these channels in determining cell responses to Ca^{2+}.

e) Nucleus

Nuclear [Ca^{2+}] is similar to the cytosolic one in resting conditions (100 nM). The presence of large pores on the nuclear envelope suggested that [Ca^{2+}] variations in the nucleus simply mimicked the cytosolic events and dynamics. However, it was observed that the Ca^{2+} gradients in the nucleus are delayed with respect to the cytoplasm. This delay can be of few or several minutes, up to one hour (Van der Luit, 1999). Moreover, when Ca^{2+} fluxes are studied in isolated nuclei, Ca^{2+} chelation of the external medium or increase of external [Ca^{2+}] does not influence the nuclear compartment or the specificity of the nuclear Ca^{2+} variations (Xiong, 2004).

These observations strongly suggest the existence of a specific Ca^{2+} homeostasis apparatus in the nucleus (**Fig. I.4**). The current hypothesis is that Ca^{2+} is accumulated in the perinuclear space (*i.e.* the space between the outer and inner nuclear membrane) and enters the nucleoplasm in response to stimuli that activate Ca^{2+} channels located at the inner nuclear membrane. A simple mathematical model (Brière 2006) was drawn in order to simulate the nuclear [Ca^{2+}] variations in response to mechanical stimuli, based on the experimental data obtained by Xiong et al. 2004 in nuclei isolated from tobacco cells. At acidic pH and low temperature, a series of mechanical stimuli induced a periodic stable varia-

tion of the nuclear Ca^{2+} concentration. In contrast, at neutral-alkaline pH, the system was apparently desensitized to mechanical stimulation and the concentration of nucleoplasmic free Ca^{2+} depended on the temperature of the incubation medium, which determined the steady-state concentration level of Ca^{2+} at equilibrium.

The model strongly supports the hypothesis of an active regulation of Ca^{2+} fluxes rather than simple adjustments of the nucleoplasm Ca^{2+} intake by diffusion.

Unfortunately, the identity of possible nuclear envelope Ca^{2+} channels and transporters of plants is still unknown, with the exception of a putative Ca^{2+} ATPase on the cytosolic side of the outer nuclear envelope membrane (Downie et al, 1998), and the two-pore channel (TPC, controlled by NAADP in mammals, Peiter et al, 2005).

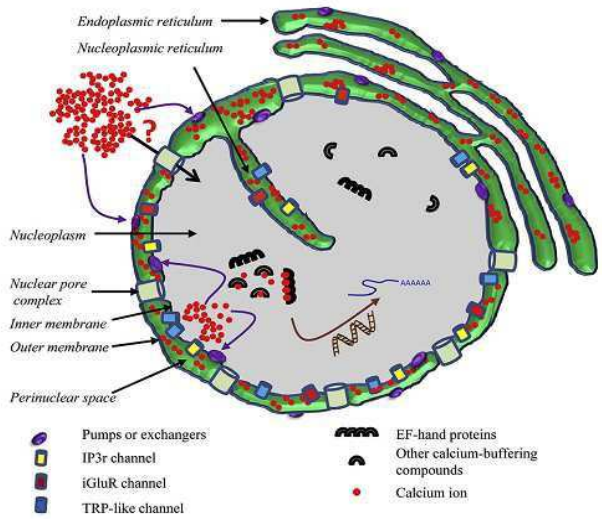

Fig. I.4 Ca^{2+} storage and release in plant cell nuclei (Mazars et al., 2011). Ca^{2+} accumulates in the perinuclear space, and, upon stress, enters the nucleoplasm through Ca^{2+} channels where it can interact with Ca^{2+} binding proteins that ultimately regulate gene expression. Diffusion phenomena (illustrated by a question mark) might also be possible.

Nuclear Ca^{2+} fluxes were associated to many biotic and abiotic stimuli ultimately leading to the control of gene expression. A wide variety of transcription factor families (CAMTA, MYB, WRKY, bZIP, MADS-box, GT(L), NAC, SCL, NAM) were shown to be modulated by Ca^{2+}, either directly or indirectly, by the mediation of Ca^{2+}-binding proteins such as calmodulin or Ca^{2+}-dependent protein kinases and phosphatases (see Galon, 2010 for a review). The existence of a cross-talk between nuclear Ca^{2+}-

signaling and ROS signaling was also recently pointed out (reviewed by Mazars et al, 2011) and associated to gene expression regulation.

f) Peroxysomes

The internal [Ca^{2+}] in peroxisomes was measured twice, with contradictory results: 150 nM (Drago et al, 2008) or 2 µM (Lasorsa et al 2008). Peroxisomal [Ca^{2+}] and [H_2O_2] variations were observed by the use of a cameleon Ca^{2+} probe and a peroxisomal-localized HyPer, a H_2O_2 sensor protein. These observations allowed linking variations of peroxisomal [Ca^{2+}] to an enhancement in the detoxification of ROS (Costa 2010). To date, no peroxisomal Ca^{2+} transporters were characterized.

g) Plastids

As mitochondria, plastids originated from a bacterial ancestor and therefore one could expect them to escape from the Ca^{2+} control, at least as evolved in eukaryotes. However, Ca^{2+} fluxes have been observed even in this cell compartment. A deeper analysis of what happens in the chloroplasts will be provided in section 1.4.

In conclusion, the Ca^{2+} distribution in plant cells seems to be finely controlled and dynamic, enabling different responses at the organelle and cellular levels.

2- Plant Ca^{2+} sensors

Besides the specificity of the Ca^{2+} signatures, the extreme diversity of responses to Ca^{2+} signals is due to the Ca^{2+} sensors. Ca^{2+} sensors are proteins containing one or more Ca^{2+}-binding sites. Ca^{2+} binding triggers deep changes in the properties of these proteins, influencing their activity or and/or affinity for other partners. This allows the decoding of the Ca^{2+} signal and the transfer of the message up to the final actors.

Most of these proteins contain Ca^{2+}-binding sites called EF-hands. We will firstly show the properties of this domain and then illustrate the main families of plant Ca^{2+}-binding proteins.

2.1- Plant Ca^{2+} binding domains

a) The EF-hand domain

The EF-hand (**Fig. I.5A**) is the most widespread Ca^{2+}-binding motif among eukaryotes. The motif is 29-residues long and presents a helix-loop-helix structure, where the first helix is called "E" and the second is called "F". The name "EF-hand" is due to the fact that it was observed for the first time in the structure of parvalbumin, where it constitutes the 5^{th} (E) and 6^{th} (F) helices, and the in-between loop (Kretsinger et al, 1973).

Ca^{2+} binding occurs in the loop between the two helices, which consists of 12 residues containing the conserved pattern: X*Y*Z*-Y*(or #)-X*-Z, also called 1, 3, 5, 9 and 12. Residues indicated by an asterisk are those involved in the binding of Ca^{2+}. Some amino acids are usually conserved at key positions. Aspartate and asparagine are common at positions X and Y. Z position is usually occupied by aspartate, asparagine or serine. –Y and –X are variable but aspartate and asparagine are quite common. Glutamate is often found at –Z (Nakayama 2000). By these residues, a single Ca^{2+} ion is bound to pentagonal bipyramidal geometry (see **Fig. I.5B**). The interaction with Ca^{2+} occurs in all cases through the side chain oxygens, except residue 7, which acts through its main chain oxygen. Chelation by residue 9 can occur indirectly through a hydrogen-bonded water molecule. Moreover, position 6 is frequently filled by glycine, probably in order to provide a sharp turn in the loop, and position 8 by isoleucine (Mc Cormack 2005). Notably, cysteine in position 7 is common only in plant Calmodulins (Zielinski, 1998). Hydrophobic amino acids are regularly distributed in the two helices: in the E helix, this gives the pattern h**hh**h, where 'h' represents hydrophobic amino acids and * represents any amino acid (Kawasaki et al, 1998).

EF-hand motifs are extremely common and EF-hand containing proteins were divided in 66 subfamilies. The proposed classification contained proteins from animals, plants, fungi and protists (Kawasaki et al, 1998).

More recently, a Ca^{2+}-binding motif similar to the EF-hand domain was found in bacterial proteins and named Excalibur. The existence of this motif suggests that the eukaryotic EF-hand domain could

have an ancient evolutionary origin. Excalibur-containing proteins often contain also other domains (such as endonuclease domains) whose activity is controlled by the Ca^{2+}-binding (Rigden, 2003).

Variants of the classic EF-hand pattern are found in eukaryotes or prokaryotes. In these cases, the loop sequence is normally conserved, but the two surrounding helices are substituted by other structures. A superposition of the classic EF-hand motif of calmodulin and all the new combinations reported is given in **Fig. I.5C** (Rigden et al 2011).

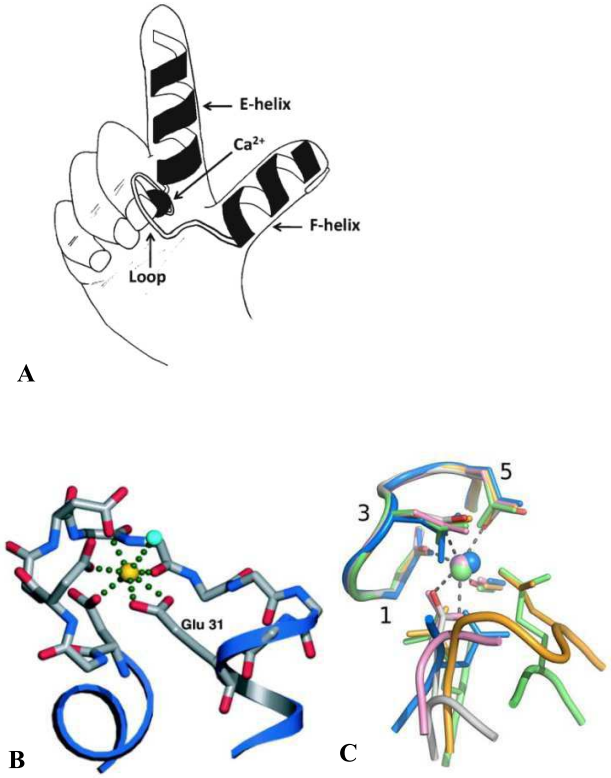

Fig I.5 The EF-hand motif. A. Schematic representation of the EF-hand Ca^{2+}-binding motif (Lewit-Bentley et al, 2000). **B.** The classic structure of the EF-hand motif bound to Ca^{2+} (McCormack et al, 2005). **C**. New suggested conformations of Ca^{2+}-loaded EF-hand motif (Rigden et al, 2011).

b) Other plant Ca^{2+}-binding domains

Besides the most common EF-hand domain, two other Ca^{2+}-binding folds are present in plant membrane-associated proteins.

The first is the "annexin" fold of 70 amino acids (Clark and Roux, 1995, Nelson and Creutz, 1995). Annexins contain four to eight repeats of the 70 amino acid module. Generally they require the presence of phospholipids to exhibit Ca^{2+}-binding at physiological [Ca^{2+}]. Their main role is linked to maintaining the stability and the organization of membrane structures, but some of them are also catalytically active (such as ATPases) or were shown to interact with enzymes. Like EF-hand containing proteins, annexins constitute a large family. Annexins could be involved in the control of many developmental processes and cell responses (Jami et al, 2012).

The second domain is named C2 (similar to the conserved region 2 in protein kinase C). It comprises 130-145 amino acids that form a β sheet scaffold with eight antiparallel strands connected by loops. The first three loops are placed on the top of the β sheet and coordinate the Ca^{2+}-binding of 3-4 Ca^{2+} ions. In this case, no deep conformational change is produced by Ca^{2+}, but the ion increases the affinity of the protein for lipids (Rizo and Sudhof, 1998). The vairety of C2 containing proteins (142 in Arabidopsis) challenges the understanding of their functions, but they are generally linked to the regulation of vesicular trafficking and membrane stability.

In addition, few proteins without a typical Ca^{2+}-binding site were experimentally shown to bind to Ca^{2+}. These include caleosins (Naested et al., 2000), 14-3-3 proteins (1 mol Ca^{2+} per mol of protein with constant of association of $5.5*10^4$/M, *i.e.* K_D = 18 μM, Lu et al, 1994), SUB1 (Guo et al, 2001), PCP, calreticulin and the CAS protein. The last three proteins were shown to be high-capacity and low-affinity Ca^{2+} binding proteins (for PCP: 29 mol of Ca^{2+} per mol of PCP and a constant of association of $32*10^2$/M, or K_D=312 μM, Furuyama and Dzelzkalns, 1999; for calreticulin: K_d = 2 mM; B_{max} 25 mol of Ca^{2+}/mol of protein, Nauseef et al, 1995; Corbett et al, 2000; for CAS: 10 to 12 mol Ca^{2+} per mol of CAS and K_d<1.2 mM, Han et al, 2003).

2.2- Major families of plant Ca^{2+} binding proteins

In the classification of EF-hand containing proteins proposed by Kawasaki in 1998, nine out of 66 identified subfamilies contain plant proteins. Despite this, a high number of such proteins are present in plants, thanks to gene duplication. In 2002 by Day et al performed a genome search in order to obtain a comprehensive picture of EF-hand proteins in Arabidopsis, retriving more than 250 proteins. The number of EF-hand domains present in each sequence ranged from 1 to 6. The majority of these proteins

contain EF-hand domains organized in pairs (**Fig I.6**). This is thought to facilitate the Ca^{2+} binding (Kawasaki et al, 1998).

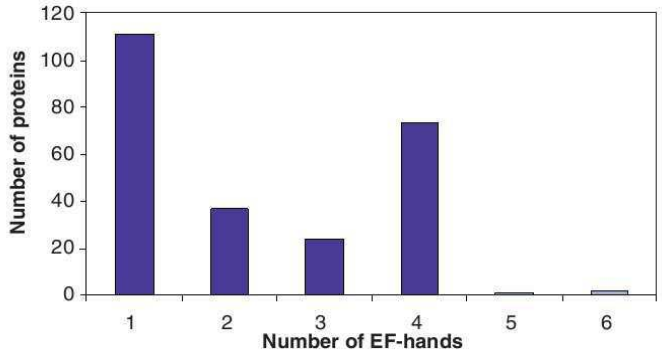

Fig. I.6 Number of EF-hands in EF-hand containing proteins of the Arabidopsis genome (Day et al, 2002).

The bioinformatics analysis (Day et al, 2002) allowed a phylogenetic classification in six subfamilies of plant EF-hand containing proteins. Several ones have no additional motifs in their sequence and are called "sensor relayers". Because of their simple structure, they probably function only as Ca^{2+} chelators and might be involved in Ca^{2+} signaling by modulating the activity of their partners - ion channels, enzymes or structural molecules. These proteins include calmodulin and calmodulin-like proteins, S100 proteins, centrin and others. In other cases, next to the EF-hand sites, other additional domains are found, such as protein kinase or GTPase domains or ion channels. These are called "responders", since their activity is differentially modulated by Ca^{2+}-binding to the EF-hand sites of the same protein.

Group 1

None of the proteins belonging to Group 1 was characterized in detail so far. Some of them contain additional motifs (*e.g.* DNA or ATP/GTP binding domains) that allow speculations about their function.

Group 2

Group 2 is quite heterogeneous. These proteins contain additional domains other than one or more Ca^{2+}-binding sites and some of them were studied in detail. This is the case of a Ca^{2+}-regulated potassium transporter (KCO1, Czempinski, 1997) and of a particular isoform of phospholipase C (AtPLC1, Otterhag 2001), whose activity was shown to be completely Ca^{2+} dependent.

Group 3

This group shows again heterogeneity in protein functions. Many of them are up-regulated in response to stress such as salt, cold or wounding. This is the case of calcineurin B like (CBL) proteins. In animals, calcineurin B is a Ca^{2+}-binding protein that forms a complex with calcineurin A, a calmodulin-dependent serine/threonine protein phosphatase. The primary sequence of both subunits and heterodimeric quaternary structure is highly conserved from yeast to mammals and the protein participates in Ca^{2+} signaling by regulating several cellular events such as apoptosis and cardiac morphogenesis (Rusnak & Mertz, 2000). Despite the high degree of conservation with the animal protein, plant CBLs do not regulate calcineurin A or other phosphatases, but interact with a family of protein kinases named CIPKs (CBL-interacting Protein Kinases, Pandey et al, 2008). The subcellular localization of CBLs is quite heterogeneous, since they were found at the tonoplast, at the plasma membrane, in the nucleus and in the cytoplasm (Weinl and Kudla, 2009). The different localizations and possible combinations between CBLs and CIPKs could account for a wide variety of signal responses mediated by these proteins. So far, CBLs were shown to be implicated in salt and cold stress responses, but the signaling pathways implicated still wait for characterization (Cheong et al, 2003).

Some other proteins of this group contain only one Ca^{2+}-binding site, *e.g.* homologues to the protein phosphatase 2A regulatory B subunit, and the KIC protein.

Group 4

The group 4 comprises calmodulin and Calmodulin-like proteins. Due to the major role of calmodulin and their importance for this work, the discussion about these proteins will be postponed to the next paragraph.

Group 5

Almost all the proteins of this group belong to the category of the Ca^{2+} dependent protein kinases (CDPKs), more recently called CPKs. They are serine/threonine protein kinases with a Calmodulin-Like Domain (CLD), usually with two EF-hands. Thirty-seven proteins of this subfamily contain the characteristic structure of CDPKs, and three can be classified as CDPK-related proteins (CRKs).

CDPKs are only found in plants and protozoans. According to bioinformatics predictions, some of these proteins could be targeted to organelles such as mitochondria or chloroplasts, even if their exact localization still needs to be proven experimentally.

The schematic structure of CDPK1 is illustrated in **Fig I.7** and is representative of all other isoforms of this subfamily. It contains a variable *N*-terminal region, the serine/threonine protein kinase domain in the center of the sequence followed by an autoinhibitory domain, and the regulatory calmodulin-like domain, with four Ca^{2+} binding sites, at the *C*-terminus. The size of CDPKs ranges from 453 to 646 amino acids.

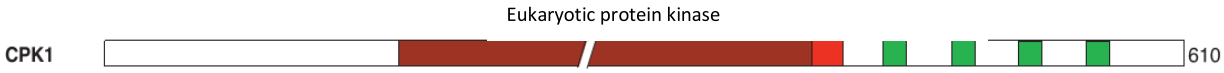

Fig. I.7 Structure of CPK1, representative of all other proteins of this group. It contains a variable *N*-terminus (white), a protein kinase domain (dark red), an autoinhibitory domain (light red) and a calmodulin-like site with four EF-hand motifs (in green). From Day et al, 2002.

In the absence of Ca^{2+}, the basal enzyme activity is very low, since the kinase domain is inhibited by the protein autoinhibitory domain. Binding of Ca^{2+} to the *C*-terminal region disrupts the inhibition thereby activating the protein. A recently proposed model (Harper et al, 2004, **Fig. I.8**) states that under *in vivo* basal Ca^{2+} ion concentrations, the *C*-terminal lobe of the Ca^{2+}-binding domain, which comprises the last two Ca^{2+}-binding sites, is loaded with Ca^{2+} and pre-bound to the inhibitory domain. This implies that activation occurs through Ca^{2+}-binding to the *N*-terminal lobe of the Ca^{2+}-binding domain. Consistent with this prediction, the *N*-terminal lobe displays a K_d for Ca^{2+} ions approximately 1 μM.

The *N*-terminal variable region could have additional regulatory roles or be involved in determining the substrate specificity.

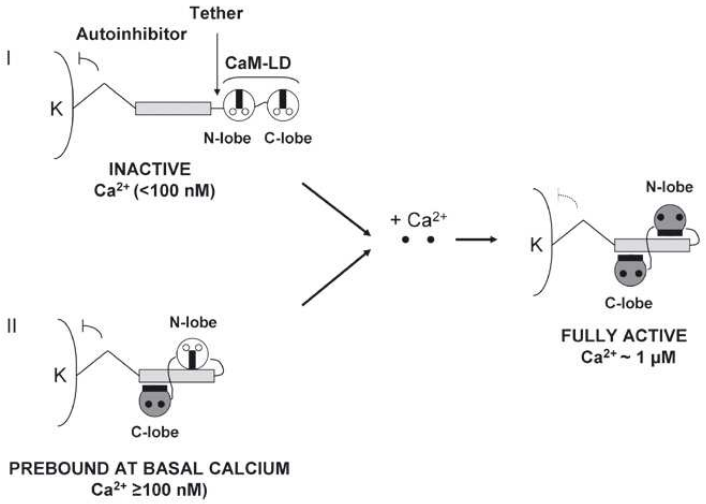

Fig. I.8 Mechanism of Ca^{2+} response of CDPKs. K, kinase domain; CaM-LD, calmodulin-like domain; white dots within *N*- and *C*-lobes, empty Ca^{2+} binding sites; black dots within N- and C-lobes, Ca^{2+} binding sites with bound Ca^{2+}. Modified from Harper et al, 2004.

CDPKs act on a wide variety of substrates containing particular phosphorylation motifs (**Table I.2**). Putative substrates tested by *in vitro* phosphorylation assays include proteins involved in nitrogen and carbon metabolism, defense related processes, protein degradation, cytoskeletal organization and ABA signaling (Klimecka and G. Muszyńska 2007).

Motif	Sequence	Reference
Simple 1	$Basic_{-3}$-X_{-2}-X_{-1}-**S/T_0**	Roberts & Harmon, 1992
Simple 2	S_0-X_{+1}-$Basic_{+2}$	Neumann *et al.*, 1996
Motif 1		
minimal	ϕ_{-5}-X_{-4}-$Basic_{-3}$-X_{-2}-X_{-1}-**S_0**-X_{+1}-X_{+2}-X_{+3} –ϕ_{+4}	Neumann *et al.*, 1996
optimal	$Basic_{-6}$ ϕ_{-5}-X_{-4}-$Basic_{-3}$-X_{-2}-X_{-1}-**S_0**-X_{+1}-X_{+2}-X_{+3}-ϕ_{+4}-$Basic_{+5}$	Huang & Huber 2001
Motif 2	$Basic_{-9}$-$Basic_{-8}$-X_{-7}-$Basic_{-6}$- ϕ_{-5}-X_{-4}-X_{-3}-X_{-2}-X_{-1}- **S/T_0**-X_{+1}-$Basic_{+2}$	Huang *et al.*, 2001; Huang & Huber, 2001
Motif 3	ϕ_{-1}- **S/T_0**-ϕ_{+1}-X_{+2}-$Basic_{+3}$-$Basic_{+4}$	Sebastià *et al.*, 2004
Motif 4	A/L_{-5}-X_{-4}-R_{-3}-X_{-2}-X_{-1}-S_0-X_{+1}-R_{+2}-Z_{+3}-R_{+4}	Loog *et al.*, 2000

Table I.2 Motifs phosphorylated by CDPKs and their sequence. Bold residues denote the phosphorylation site. Basic: -R or –K. –X: any residue except R. –Φ: hydrophobic residue. From Harper and Harmon, 2005.

Group 6

In this last group are included all the proteins that do not fall in any of the other categories. They are often members of protein families involved in plant defense and redox control. Homologues of

these proteins are present in animals, but Ca^{2+}-binding is a characteristic of only some plant isoforms. For example, among the Rboh proteins, that are intrinsic plasma membrane protein oxydases, only the Arabidopsis RbohF isoform contains EF-hand motifs (Keller et al, 1998). Other proteins of this group are ABI1 (a protein phosphatase induced by abscissic acid and linked to meristem development and stomatal aperture, see Leung et al, 1994 and Meyer et al, 1994), the glutamate dehydrogenase isoform GHD2 (Turano et al, 1997) and the two-pore channel TPC1 (Furuichi et al, 2001).

3- Structure and function of calmodulins

Calmodulin (CALcium MODULated proteIN, CaM) was discovered by Cheung (1970) and Kakiuchi and Yamazaki (1970) in the bovine brain and rat brain, respectively.

Due to its central role in cell physiology, the simplicity of its structure and its stability, CaM is the most studied Ca^{2+} sensor.

CaM is a little protein (approximately 150 amino acids, depending on the species) composed of four EF-hand Ca^{2+}-binding sites and lacks any catalytic activity. Upon binding to Ca^{2+}, it undergoes a deep structural change in conformation that modifies its properties and affinity for other proteins. Binding to CaM was shown to be a major regulator of protein activity, especially for kinases. Therefore, even if CaM has no direct effect, it is able to transduce the Ca^{2+} signal by modifying the properties of its partners (Wylie and Vanaman, 1988).

By the use of a fluorescent biosensor for intracellular detection of both free Ca^{2+}-CaM and apo-CaM, an intracellular CaM concentration of 8.8 ±2.2 µM was determined. Measurements were performed under resting conditions in a human kidney cell line stably expressing the biosensor (Black et al, 2004). Quantification of CaM in carrot cell suspensions gave similar results (4 µM, Fisher et al, 1996). Ling and Assmann measured [CaM] in *Vicia faba* tissues by gel densitometry and enzyme activation assays. On the basis of their data, a similar value of 2 µM total [CaM] was calculated (Zielinski 1998). In plants, the CaM control is more complex since several CaM isoforms are present as well as a high number of CaM-like proteins (see paragraph 3.9 and **Chapter 5**).

3.1- CaM sequence and conservation

In the sequence of CaM, the four Ca^{2+} binding EF-hand sites are localized in two pairs, one at the *N*-terminus and the other at the *C*-terminus.

This protein is ubiquitously found in eukaryotes. Animal genomes normally contain only one CaM isoform, or sometimes two genes coding for identical or almost identical protein sequences and/or CaM pseudogenes (Cohen 1988). A KO mutation on the CaM yeast gene is lethal (Davis, 1986) and this represents another clue of the central function of this protein in ruling Ca^{2+} homeostasis and responses.

Plant genomes contain a number of CaM genes remarkably higher with respect to animals. In Arabidopsis, for example, CaM is encoded by seven genes. Despite minor differences in the gene sequence, some of them code for the same amino acid sequence and the others are pretty conserved also if compared with mammal CaMs (**Fig. I.9**).

```
AtCaM3          MADQLTDDQISEFKEAFSLFDKDGDGCITTKELGTVMRSLGQNPTEAELQDMINEVDADG  60
AtCaM5          MADQLTDDQISEFKEAFSLFDKDGDGCITTKELGTVMRSLGQNPTEAELQDMINEVDADG  60
AtCaM2          MADQLTDDQISEFKEAFSLFDKDGDGCITTKELGTVMRSLGQNPTEAELQDMINEVDADG  60
AtCaM6          MADQLTDDQISEFKEAFSLFDKDGDGCITTKELGTVMRSLGQNPTEAELQDMINEVDADG  60
AtCaM7          MADQLTDDQISEFKEAFSLFDKDGDGCITTKELGTVMRSLGQNPTEAELQDMINEVDADG  60
AtCaM1          MADQLTDEQISEFKEAFSLFDKDGDGCITTKELGTVMRSLGQNPTEAELQDMINEVDADG  60
AtCaM4          MADQLTDEQISEFKEAFSLFDKDGDGCITTKELGTVMRSLGQNPTEAELQDMINEVDADG  60
Hs              MADQLTEEQIAEFKEAFSLFDKDGDGTITTKELGTVMRSLGQNPTEAELQDMINEVDADG  60
                ******::******************.********************************

AtCaM3          NGTIDFPEFLNLMARKMKDTDSEEELKEAFRVFDKDQNGFISAAELRHVMTNLGEKLTDE  120
AtCaM5          NGTIDFPEFLNLMARKMKDTDSEEELKEAFRVFDKDQNGFISAAELRHVMTNLGEKLTDE  120
AtCaM2          NGTIDFPEFLNLMARKMKDTDSEEELKEAFRVFDKDQNGFISAAELRHVMTNLGEKLTDE  120
AtCaM6          NGTIDFPEFLNLMARKMKDTDSEEELKEAFRVFDKDQNGFISAAELRHVMTNLGEKLSDE  120
AtCaM7          NGTIDFPEFLNLMARKMKDTDSEEELKEAFRVFDKDQNGFISAAELRHVMTNLGEKLTDE  120
AtCaM1          NGTIDFPEFLNLMAKKMKDTDSEEELKEAFRVFDKDQNGFISAAELRHVMTNLGEKLTDE  120
AtCaM4          NGTIDFPEFLNLMAKKMKDTDSEEELKEAFRVFDKDQNGFISAAELRHVMTNLGEKLTDE  120
Hs              NGTIDFPEFLTMMARKMKDTDSEEEIREAFRVFDKDGNGYISAAELRHVMTNLGEKLTDE  3
                **********.:**:**********:*********.**:*****************:**
```

```
AtCaM3          EVDEMIKEADVDGDGQINYEEFVKVMMAK 149
AtCaM5          EVDEMIKEADVDGDGQINYEEFVKVMMAKRRGKRVMAAKRSSNSAEYKEKNGRRKSHCRIL 181
AtCaM2          EVDEMIKEADVDGDGQINYEEFVKVMMAK 149
AtCaM6          EVDEMIREADVDGDGQINYEEFVKVMMAK 149
AtCaM7          EVDEMIREADVDGDGQINYEEFVKVMMAK 149
AtCaM1          EVEEMIREADVDGDGQINYEEFVKIMMAK 149
AtCaM4          EVEEMIREADVDGDGQINYEEFVKIMMAK 149
Hs              EVDEMIREADIDGDGQVNYEEFVQMMTAK
                **:***:***:*****:*******:*:**
```

Fig. I.9 Primary sequence of Arabidopsis calmodulins compared with the human one. The long extension of Arabidopsis CaM5 contains a myristilation site. Accession numbers: AtCaM1: AT5G37780, AtCaM2 AT2G41110, AtCaM3: AT3G56800, AtCaM4: AT1G66410, AtCaM5: AT2G27030, AtCaM6: At5g21274, AtCaM7: AT3G43810, Homo sapiens CaM: P62158. EF-hands motifs are represented on the basis of the prediction of the 3CLN structure, with helices in pink and Ca^{2+}-binding loops in gray. The central region that constitutes the long centlal helix upon binding to Ca^{2+} is shown as italic characters.

3.2- Three-dimensional structure

The three-dimensional structure of CaM was determined both in the presence and in the absence of Ca^{2+}. The Ca^{2+}-bound form of CaM was firstly crystallized and analyzed (Babu, 1986). The protein shows a dumbbell conformation with the two lobes connected by an eight-turn α helix and no contacts between the two lobes. The length of the molecule is approximately 65 Å, with each lobe having approximate dimensions of 25x20x20 $Å^3$. Lobes are composed of a couple of EF-hand motifs and share 46% of identity in their amino acid sequence. The helices of two EF-hands motifs create a Phe and Met-rich hydrophobic cleft that is exposed to solvent and involved in target binding (Wilson 2000). (**Fig. I.10**)

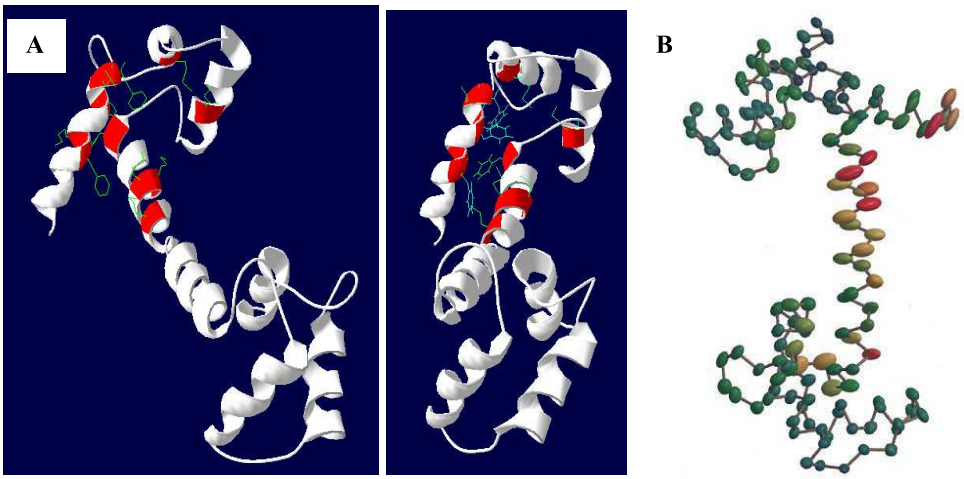

Fig. I.10 Ca^{2+}-bound CaM structure profiles. A. Ribbon structure of Calcium-binding CaM, with the methionine and phenylalanine residues of the N terminal region forming the hydrophobic pocket highlighted (1.0 Å crystal structure, Wilson et al, 2000). **B.** A Cα trace of CaM, with thermal ellipsoids for the Cα atoms represented at the 90% probability level. The ellipsoids are colored according to their isotropic displacement parameter (U_{eq}), a parameter that measures the flexibility of a protein region. Amino acids colors range from blue (lowest U_{eq} , *i.e.* low flexibility) to red (highest U_{eq} *i.e.* high flexibility). The largest values of U_{eq} are found in the central helix and the hydrophobic binding pockets, as well as the two termini.

NMR and solution X-ray scattering results indicate that the central helix in the Ca^{2+}-loaded protein is flexible (Van der Spoel et al, 1996) and allows considerable movement of the two lobes with respect to one another in solution (Wilson 2000). This flexible central helix and the two hydrophobic regions surrounding it are the key elements that allow CaM to interact with basic amphiphilic helices (*i.e.* constituted of one polar and one non-polar side) of a wide variety of target proteins.

By NMR spectroscopy, it was shown that in apoCaM (Ca^{2+}-free), the α-helices in the EF-hand motifs are positioned almost parallel to each other and the interhelical angles of the four EF-hand motifs increase by 36°–44°. In this condition, the hydrophobic cavities are no more accessible and the overall protein appears to be in a closer conformation (Zhang 1995).

The clear difference in the CaM conformation in the presence and in the absence of Ca^{2+} explains why the protein binding to its targets can be extremely conditioned by the [Ca^{2+}] (**Fig. I.11**).

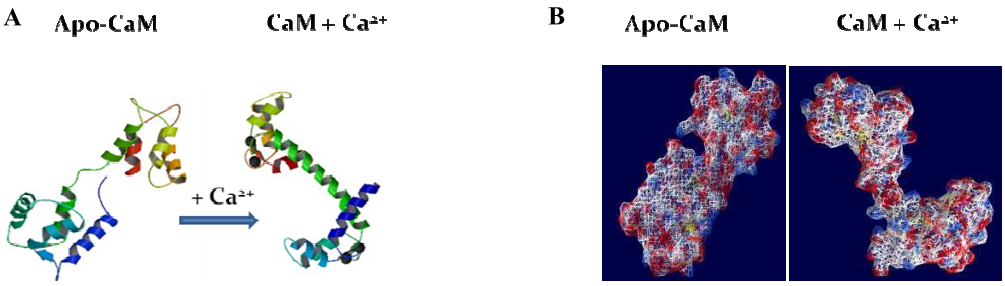

Fig. I.11 Variation of CaM structure in the presence and absence of Ca^{2+}. A. Ribbon and **B.** Surface representation of apo-CaM and the Ca^{2+}-loaded CaM structure. Structures were downloaded from www.rcsb.org/. Accessions: apo-CaM: 1CFD; Ca^{2+}-CaM: 1CLN.

Recently, this simple and elegant paradigm has been challenged by the discovery of possible alternative CaM conformations (**Fig. I.12**).

A new kind of Ca^{2+}-CaM X–ray conformation was reported (Fallon et al 2003). In this case, the N-domain appears contracted and a sharp reverse turn is present in the linker helix. This compact Ca^{2+}-CaM is more globular because its hydrophobic surfaces are at least partially shielded from the bulk solvent.

Even more recently, Kumar et al (2013) reported a new crystal structure for the Ca^{2+}-loaded CaM (**Fig. I.12**). In this model, residues Ala74-Asp79 of the central helix (amino acids 65–92) are unwound, and the C-lobe is reoriented in a perpendicular direction to the central helix. The side chain of Arg75 is exposed on the surface of the molecule, which makes four hydrogen bonding contacts only with symmetry-related molecules (Arg38 and Arg127). Interestingly, for the first time one zinc ion was observed in the protein structure.

These new CaM folds might be involved in the establishment of special CaM-partner interactions. However, further investigations still need to be performed in order to assess the importance of these alternative conformations in CaM affinity to its target.

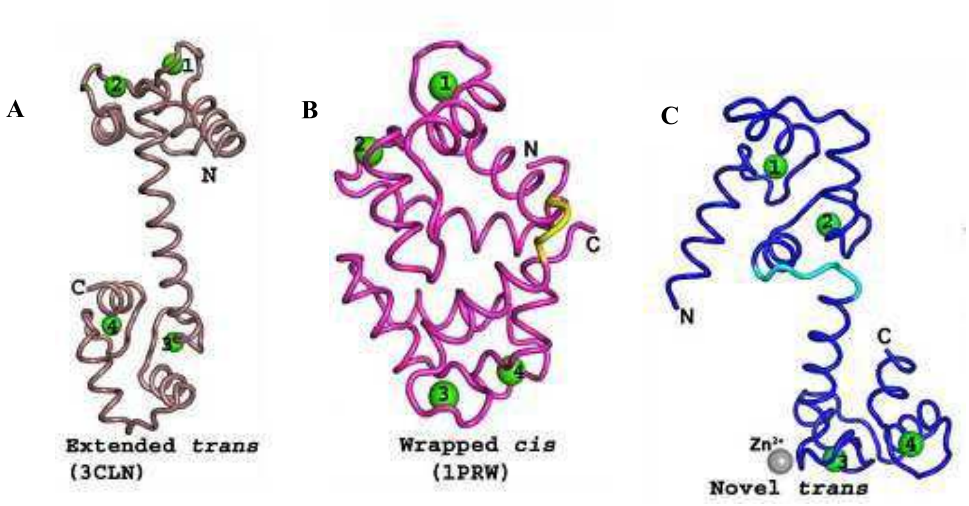

Fig. I.12 The classic Ca^{2+}-loaded CaM structure (A), compared with new observed folds. B: Fallon et al, 2003; **C:** Kumar et al 2013. From Kumar et al, 2013.

3.3- Ca^{2+}-binding

The presence of four EF-hand motifs allows CaM to interact with up to 4 moles of Ca^{2+} per mole of protein. These four sites were shown to differ for Ca^{2+} affinity.

First measurements of Ca^{2+} binding by equilibrium dialysis with $^{45}Ca^{2+}$ led to the conclusion that all four CaM sites had almost the same affinity for Ca^{2+} (K_a approximately $2.5*10^5$/M, *i.e.* K_d= 4 µM Potter et al, 1983). Effects of ionic strength and magnesium concentration on Ca^{2+} affinity were reported (Ogawa et al, 1984). Soon after, it appeared that a remarkable difference in Ca^{2+} affinity occurs between the *N*-terminal and the *C*-terminal lobe. At sites III and IV (*C*-terminal lobe) a binding constant K_a of $5*10^6$/M was measured (K_D= 0.2 µM), while at sites I and II (*N*-terminal lobe) K_a of $5*10^5$/M was reported (K_D= 5 µM), with a certain degree of positive cooperativity between the two sites in each class (**Fig. I.13**). Analogous differences and cooperativity in the dissociation constants were subsequently measured. The $^{45}Ca^{2+}$ NMR and stopped-flow kinetics gave k_{off} values of 1150 and 650 s^{-1}, respectively, for the low-affinity sites and <40 and 9 s^{-1}, respectively, for the high-affinity sites (Drakenberg et al, 1983; Martin et al, 1985).

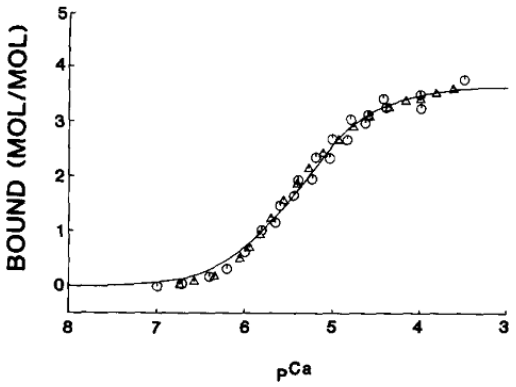

Fig. I.13 Ca^{2+}-binding to calmodulin. The plot shows the moles of Ca^{2+} bound as a function of the free metal concentration. Data were obtained from equilibrium-dialysis experiments (white circles) and with a Ca^{2+} electrode (white triangles). The line is the best fit obtained by a Hill equation (from Potter et al, 1983).

More recently, studies of Ca^{2+} binding were carried out with tryptic fragments of CaM molecules from various sources, including vertebrate and yeast (Weinstein 1994). These fragments were obtained by trypsin digestion that cleaves the central tether helix at Lys77 and separates the pair of EF-hands in the *N*-terminal domain from those in the *C*-terminus. These experiments further confirmed previous studies. By NMR of ^{45}Ca, at room temperatures and at 0.1-0.2 M KCl off-rates of 470 s^{-1} were measured for the 1-77 fragment, and of 300-500 s^{-1} with ^{1}H NMR. On the contrary, the *C*-terminal fragment 78-148 was shown to contain high affinity binding sites with stopped-flow dissociation rates of 37 or 10-11 s^{-1}. Similar values were obtained by NMR (3-10 s^{-1}).

Since CaM function is mainly of modifying the properties of its protein targets, the influence of CaM-target interactions on CaM bindig to Ca^{2+} was also investigated with several CaM-binding peptides. A modulation of CaM affinity for Ca^{2+} by CaM-binding peptides was indeed frequently reported (Yazawa, 1987, **Figure I.14,** Johnson et al, 1996).

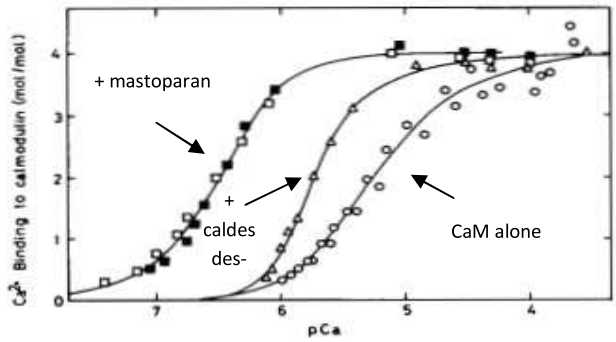

Fig. I.14 Effect of CaM-binding peptides on the CaM affinity for Ca^{2+}. Ca^{2+} binding to scallop testis CaM was measured by the flow-dialysis method. Concentration of CaM was 16.2 µM. White circles: CaM alone. White squares, CaM +60.2 µM mastoparan peptide (a toxin from wasp venom with a CaM affinity of less than 1 nM). Black squares, CaM +301 µM mastoparan. White triangles, CaM +28.5 µM of the CaM-binding peptide of caldesmon (a protein that tonically inhibits the ATPase activity of myosin in smooth muscle with an affinity for CaM of approximately 1 µM). Solid lines are the calculated best fit curves with four macroscopic binding constants. With a 19-fold molar excess of mastoparan (301 µM) the cooperative effect increases (Yazawa, 1987).

Similar measurements were also conducted in order to determine the affinity of CaM for magnesium, a highly abundant cellular ion (total concentration of approximately 10 mM, free concentration in the millimolar range). These measurements revealed that the affinity for the *N*-terminal lobe is higher than that of the *C*-terminal region (K_a=3.5×10^3/M, *i.e.* K_D= 3.5 mM for the *N*-terminal domain and *K*a=2–3×10^2/M, *i.e.* K_D= 20-30 mM for the *C*-terminal domain, according to Tsai et al, 1987). Due to the high abundance of Mg^{2+} in resting cells, it has been proposed that in these conditions CaM might be always bound to Mg^{2+}. This binding is thought having a stabilizing effect on CaM but a mild effect on the protein conformation if compared to Ca^{2+} (Malmendal et al, 1998). The dynamics of Mg^{2+} replacement by Ca^{2+} are complex to analyze and up to now still controversial (Grabarek et al, 2011).

3.4- CaM-binding sites

CaM partners have an affinity for CaM ranging from 1 nM or even less to the µM range, which is considered the upper limit for a genuine CaM partner (Crivici and Ikura, 1995, Tidow et al, 2012). CaM-binding sites of different affinities can be present on the same CaM target (Reddy et al, 2003) and these differences might be important in the modulation of the protein properties (Tidow et al, 2012).

CaM partners are usually identified on the basis of the activatory/inhibitory effect produced by CaM (*e.g.* adenylate cyclase, McNeil et al, 1985; Glutamate decarboxylase, Snedden et al, 1996; NAD

kinase, Delumeau et al, 1998 and 2000). The peptides containing CaM-binding sites are used to determine the CaM affinity of a CaM partner by NMR and spectroscopic techniques (see Buschmeier et al, 1987 and Bayley et al, 1996, for examples).

As shown in the previous section, CaM interaction with target proteins usually depends on the conformational changes it undergoes upon binding to Ca^{2+}. In particular, a central flexible helix surrounded by two hydrophobic regions is thought to be the main actor that mediates the interactions.

a) Ca^{2+}-dependent CaM-binding sites

Ca^{2+}-dependent CaM-binding sites often occur within or near a pseudosubstrate domain (*e.g.*, protein kinases and protein phosphatases), phosphorylation sites for serine/threonine protein kinases (*e.g.*, CaM-dependent protein kinase II, neuromodulin, MARCKS protein), regions responsible for interaction with other proteins (*e.g.,* the actin binding site of caldesmon or MARCKS protein) (Rhoads et al, 1997) or regulatory domains (in the case of GAD2, Snedden et al, 1996).

Many of the known CaM-binding proteins possess a region that is characterized by a basic amphipathic helix of approximately 20 residues. Specific characteristics of this region include a net positive charge and moderate hydrophilicity (O'Neil, 1990).

Most common Ca^{2+}-dependent CaM-binding motifs are the 1-8-14 and 1-5-10 motifs. Numbers indicate the position of conserved hydrophobic residues (Crivici and Ikura, 1995).

The 1-8-14 motifs can be of A or B type. Both subtypes have flanking hydrophobic residues (positions 1 and 14), with internal conserved hydrophobic residues occurring at positions 5 and 8. The type B motif possesses a lower net electrostatic charge or lacks a hydrophobic residue in position 5. Most of the high-affinity CaM-binding proteins contain the 1-8-14 motif with a net charge of 3+ to 6+ (**Table I.3**).

A 1-16 CaM-binding site was also identified. It contains a tryptophan in position 1 and a hydrophobic amino acid in position 16 (Bhattacharya et al, 2004).

Type	Motif[a]	Proteins	Charge
1-8-14 Motif			
Type A	(FILVW)xxx(FAILVW)xx(FAILVW)xxxxx(FILVW)	Calcineurin, NO synthase, skeletal muscle MLCK, and most other Ca^{2+}-dependent binding proteins	3+ → 6+
Type B	(FILVW)xxxxxx(FAILVW)xxxxx(FILVW)	α-Fodrin Caldesmon, smooth muscle MLCK, and Titin	2+ → 4+
1-5-10 Motif	xxx(FILVW)xxx(FILV)xxxx(FILVW)	CaM kinases I and II, MARCKS, HSP90 heat shock protein, and synapsins	3+ → 6+

[a] The standard amino acid letter code is used. The letter x stands for any amino acid. Net electrostatic charge for the 14-residue or 13-residue (1-5-10 motif) motif was based on assigning −1 for residues E and D and + 1 for K and R.

Table I.3 Sequence of Ca^{2+}-dependent CaM-binding motifs (Rhoads et al, 1997).

In certain CaM-binding proteins, a bend in the binding region coupled with the flexibility of the central helix of CaM may result in other arrangements. Due to the pseudo-twofold symmetry of the two lobes of CaM, some peptides might also be bound in the reverse orientation (Osawa et al, 1999**, Fig. I.15** and PDB code 1CKK).

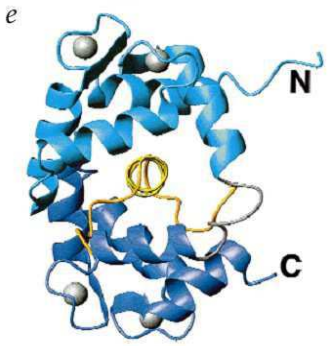

Fig. I.15 CaM-binding to the CaM-binding peptide of the rat Ca^{2+}/CaM-dependent protein kinase kinase (CaMKK). It shows a compact conformation and the flexibility of the central helix and binding in the reverse orientation. From Osawa et al, 1999.

b) Ca^{2+}-independent CaM-binding sites

Some proteins can interact with CaM in a Ca^{2+}-independent manner. Animal proteins of this type are, for example, PEP19 (with an apparent CaM affinity of 1.2 μM, Slemmon, 1996), neuromodulin and unconventional myosins. The affinity of neuromodulin for CaM decreases in the presence of Ca^{2+} (Alexander et al, 1987).

In some cases even if Ca^{2+} is not required for the interaction, it can strengthen the CaM-protein interaction. This is the case for certain myosin CaM-binding sites that require Ca^{2+} for maximal binding and may occur in addition to the Ca^{2+}-independent CaM-binding sites (Wolenski, 1995). In a similar manner, the animal NO synthase binds to CaM with high affinity both in the presence of Ca^{2+} (less than 1 nM affinity) and in its absence (45-80 nM affinity) (Anagli, 1995). Another interesting case is the one of the enzyme phosphorylase kinase (see below).

Motifs responsible for CaM-binding in the absence of Ca^{2+} are known as IQ motifs (**Table I.4**). Cheney and Mooseker (1992) were the first to recognize that the IQ motif of unconventional myosin shares sequence similarity with the CaM-binding region of neuromodulin and neurogranin. Conservation occurs at positions 1, 2, 6, 11, and 14 and to some extent at position 5 (Rhoads et al, 1997).

Class	Motif[a]	Tissue
Myosin light chain binding motifs: conventional myosins (type II); smooth, skeletal, and cellular myosins		
Site 1 (type 1A)	FQxxxRGxxxRxx(FY)	Smooth muscle, cellular, and mollusc myosins
Site 1 (type 1B)	TQxxxRGxxxRxx(FY)	Skeletal
Site 1 (type 1C)	IQxxxRGxxxRxx(FY)	Cardiac
Site 2 (type 2A)	(IVL)QxxxRxxxx(VL)(KR)xW	Skeletal, cardiac, and mollusc myosins, α-fodrin
Site 2 (type 2B)	(IL)QxxCxxxxKxRxW	Cellular, smooth muscle
CaM binding motif: unconventional myosins, neuromodulin, and neurogranin		
Site 1	(IVL)QxxxRxxxx(RK)xx(FILVWY)	Neuromodulin, neurogranin, myosins I, III, V–VII, IX

[a] The standard amino acid letter code is used. The letter x stands for any amino acid.

Table I.5 Sequence of Ca^{2+} independent CaM-binding motifs (Rhoads et al, 1997).

c) Predictions of CaM-binding sites

As it appears from the classification presented above, CaM-binding sites are characterized by weak conserved amino acids and no signatures allowing recognizing them with certitude on protein primary sequences. This means that CaM-binding proteins cannot be identified on the basis of informatics predictions.

However, once a CaM-binding protein identified, algorithms can be used in order to localize the most probable CaM-binding site within the protein sequence. One of these algorithms is open access (http://calcium.uhnres.utoronto.ca/ctdb/ctdb/sequence.html, Yap, 2000). It compares the user's query to

a bank of 300 CaM-binding protein sequences for which the CaM-binding site was identified and proven experimentally.

As mentioned before (paragraph 3.4a), a common feature of many Ca^{2+}-dependent CaM-binding sites is that they usually constitute an amphipathic helix, with a charged and a hydrophobic side. Helical wheel projections (see **Fig. I.16**) can be useful to visualize the CaM-binding site and identify residues important in determining the affinity.

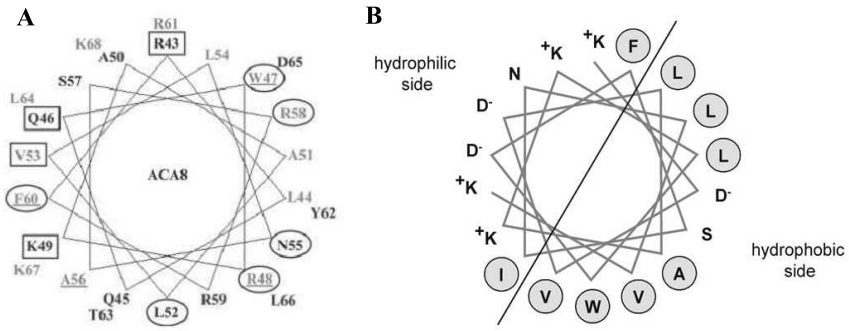

Fig. I.16 Helical wheel projection of the CaM-binding site of two CaM-binding proteins. A. CaM-binding site of the plant plasma membrane calcium pump ACA8. Residues important for CaM-binding are shown in grey and the four most important ones are underlined. Residues important for CaM recognition are boxed and residues involved in autoinhibition are circled. From Bækgaard et al, 2005. **B**. CaM-binding site of the plastidial protein Tic32 of *Pisum sativum*, showing the presence of a hydrophilic and two hydrophobic regions (according to Chigri et al, 2006, supplementary material).

3.5- CaM-partners interactions

Several structures are now available of CaM-Ca^{2+} bound to isolated CaM-binding peptides and, more rarely, to entire protein partner. Recently, a detailed survey of all the available structures of CaM-protein complexes was cured, starting from the analysis of 80 unique structures of CaM-partner deposited in the Protein Data Bank (**Fig. I.17**). This analysis revealed a remarkable variety of modes of interaction (Tidow and Nissen, 2013).

The most classical case is that of serine/threonine protein kinases and phosphatases. Generally, CaM interaction disrupts the protein inhibition produced by an inhibitory domain of the same protein. The first complex of this type (the CaM-binding peptide of the myosin light-chain kinase, MLCK with CaM) was resolved in 1992 (Ikura et al, 1992; Meador et al, 1992, PDB codes 1CDL and 2BBM), revealing a CaM conformation similar to what observed in the unbound CaM but with the central helix

more flexible, allowing the two lobes to wrap around the target. Similar conformations were observed for CaM-binding peptides of other kinases, such as CaM-dependent protein kinase II (PDB code: 2WEL), death-associated protein kinases (PDB code: 1WRZ) and phosphatases, in particular calcineurin (PDB code: 2F2O), and the nitric oxide synthase (PDB code: 1NIW). In the case of several ion channels the CaM interaction occurs in a similar manner at the *C*-terminus of the protein where an IQ motif is localized.

In other cases CaM is placed in an extended conformation. The two lobes bind to two different protein regions not in contact with each other. Interestingly, in this case CaM usually binds only two Ca^{2+} ions at the high affinity *C*-terminal lobe. This occurs in the case of the *Bacillus anthracis* edema factor (PDB code: 1LVC) and several ion channels, especially small conductance Ca^{2+}-activated potassium channels and voltage-activated sodium channels.

Myosin V heavy chain contains two IQ motifs placed in the same helix and two CaM molecules are bound to them in a Ca^{2+}-free conformation. The C-lobe has a semi-open conformation and interacts with apolar side chains in the first part of the IQ motif. The *N*-lobe retains a closed, non-gripping conformation and binds only weakly to the second part of the IQ motif (PDB code: 2IX7). Something similar occurs also in the case of the Na^{+}/H^{+} exchanger NHE1 (PDB code: 2YGG). However, in this case, the two CaM-binding sites are placed in two proximal helices and the interaction is Ca^{2+} dependent.

Only two structures of plant CaM-target complexes were obtained so far.

The first one is the Arabidopsis plasma membrane Ca^{2+} ATPases (PMCA) ACA8 bound to CaM. The structure of the complex revealed an unexpected stoichiometry of 2 CaMs per ACA8, one in parallel and the other in antiparallel orientation (PDB code: 4AQR). The importance of this double CaM regulation is illustrated in the next paragraph.

The second case is the enzyme glutamate decarboxylase (GAD, PDB code: 1NWD) that was seen to be activated up to 20-folds by CaM in Petunia. The structure of CaM bound to the GAD CaM-binding peptide was obtained in 2003 (Yap et al, 2003). This structure clearly demonstrated a 2:1 stoichiometry, with two GAD peptides bound to one CaM molecule. The two GAD CaM-binding peptides are placed in opposite orientations and are bound one to the *N*-terminal and the other to the *C*-terminal lobe

of CaM, allowing therefore the predicted formation of a complex comprising two GAD molecules linked together by one CaM. Structural analyses showed that the CaM-binding peptide is almost unstructured in the absence of CaM. For the interaction to take place, a well conserved tryptophan residue (W) plays a major role. These results were further confirmed later with a low-resolution structure of CaM bound to the entire AtGAD1 protein (Gut et al, 2009).

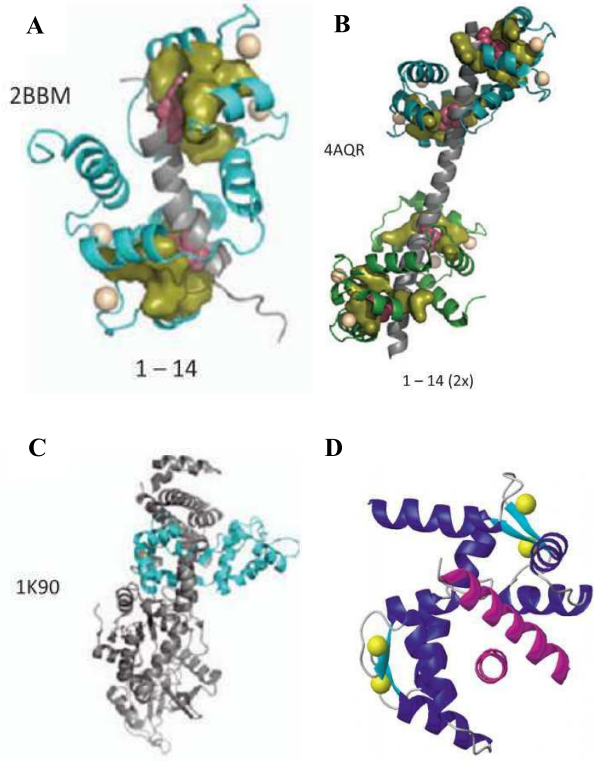

Fig I.16 Different modes of CaM-partner binding. A. CaM-MLCK. **B**. CaM-PMCA of Arabidopsis; **C.** CaM-EF protein from Bacillus anthracis (from Tidow and Nissen, 2013) and **D**. CaM in complex with two CaM-binding peptides of Petunia GAD (Yap et al, 2003).

3.6- Functional roles of CaM interactions.

CaM targets are incredibly heterogeneous and include Ca^{2+} pumps, phosphatases, the adenylate cyclase, cytoskeletal proteins, cyclic nucleotide phosphodiesterases, and many kinases. Here, we chose to illustrate four examples that should give an idea of the different functions and modes of action of CaM and of the complexity of their interactions, in both animals and plants.

a) Activation of phosphorylase kinase

In mammals, muscle contraction is triggered by Ca^{2+} fluxes from the sarcoplasmic reticulum. The energy that supports the muscular activity is given by the glycogenolysis and the limiting step of this pathway is the glycogen phosphorylase. This enzyme is activated by phosphorylation by the phosphorylase kinase - a tetramer of four subunits, one of which is a CaM. It was demonstrated that CaM is constantly present in the complex, and tightly bound to the other subunits, since high urea concentrations cannot dissociate the complex and classic CaM inhibitors are less effective on the phosphorylase kinase than on other CaM-regulated enzymes. CaM accounts for the phosphorylase kinase affinity for Ca^{2+} (four ions per complex unit) and the protein activation when Ca^{2+} levels increase (Cohen, 1988).

b) Regulation of small protein secretion

Small secreted proteins with functions in cell recognition and signaling are translated very rapidly. This means that the available time for their recognition and targeting to the ER is short and specific mechanisms were proposed to account for avoiding protein degradation and allow their secretion. It was demonstrated *in vitro* and *in vivo* (Shao and Hedge, 2011) that classic chaperone proteins stabilizing the *N*-terminal hydrophobic sequences for the protein insertion in the ER in yeast are not effective in mammals. Surprisingly, this role can successfully be covered by CaM if Ca^{2+} is present at physiological concentrations. Indeed, CaM is able to bind to N-terminus of these small proteins in the presence of Ca^{2+} in excess (10 μM), preventing their aggregation and degradation. The CaM-binding to the *N*-terminus of the small proteins to be targeted to the ER is inhibited by EGTA, while their release is inhibited at high [Ca^{2+}]. A finer analysis of the process is needed in order to unravel how it is regulated by Ca^{2+} and other factors.

c) Dual modulation of the P-type ATPases by CaM

Plasma-membrane Ca^{2+}-ATPases (PMCAs) are key regulators of intracellular Ca^{2+} in eukaryotes. They contain a unique amino- or carboxy-terminal regulatory domain responsible for autoinhibition. Pump activity is stimulated by binding of Ca^{2+}-loaded calmodulin to the regulatory domain, thereby inducing a conformational change that displaces the autoinhibitory domain from the pump core structure. CaM substantially increases both Ca^{2+} affinity and pump rate in PMCAs. Thanks to the structure resolution of an intact regulatory domain (residues 40–95) of the Arabidopsis PMCA combined with bioinformatics, biophysics and biochemistry, both *in vivo* and *in vitro*, the mechanism of CaM control of the pump was recently elucidated (Tidow et al, 2012). The authors demonstrated the presence of two CaM-binding sites per pump – one with high Ca^{2+} affinity and the other with low Ca^{2+} affinity – and then analyzed protein mutants unable to bind to CaM in one or both sites. These studies showed the importance of both the high-affinity and the low- affinity CaM-binding site in triggering steep pump activation at high Ca^{2+} concentration and in maintaining the protein completely inactive at normal or low cytoplasmic Ca^{2+} levels.

d) Activation of plant GAD by CaM

CaM-GAD interaction occurs only in plants thanks to the presence of a *C*-terminal protein extension that contains a CaM-binding site. In Petunia, CaM-GAD interaction was shown to increase the protein activity by a factor of 20. The GAD CaM-binding domain is located near an autoinhibitory region situated at the *C*-terminus of the protein. CaM-GAD interaction is thus suggested to cause the release of the autoinhibition, similar to what frequently observed in kinases. Moreover, the ability of CaM to interact simultaneously with two GAD subunits suggested the possibility of cooperative activation mechanisms (Yap et al, 2003), possibly by also inducing GAD dimerization (Yuan et al, 1998).

3.7- CaM inhibition

Several molecules are known to inhibit CaM–protein interaction.

Most of these molecules are hydrophobic and bind to CaM in its Ca^{2+}-loaded conformation, thus preventing the interaction with Ca^{2+} dependent CaM partners. This category includes phenothiazine

antipsychotic drugs, local-anesthetics, muscle relaxants, drugs for treatment of neoplasm, other chemical agents such as Triton X-100 and 2-p-toluidinylnaphthaline-6-sulfonate, but also natural metabolites such as Ophiobolin A, a fungal phytotoxin (Au and Leung, 1998).

The antipsychotic drug trifluoperazine (TFP, Levin and Weiss, 1977) is not completely CaM-specific, since it also binds to S100 proteins, troponin C and protein kinase C. The complex of CaM bound to TFP was resolved and revealed that each CaM molecule can bind at least 4 molecules of TFP (see pdb codes 1LIN, 1A29 and 1CTR for structures). When this happens, the central helix of CaM bends. This probably affects the CaM affinity for its targets (Vandonselaar et al, 1994).

The molecule N-(6-aminohexl)-5-chloro-1-naphtalensulfonamide, also known as W7, is another strong CaM antagonist. The structure of the CaM-W7 complex shows a slightly different mode of action in comparison to TFP. W7 binding occurs in correspondence of the two CaM lobes (one molecule of W7 per lobe; Osawa et al, 1998, pdb code 1MUX).

Another way to control CaM activity is to act on the Ca^{2+} concentration by using Ca^{2+} chelators. The most common ones are EGTA and EDTA. These two molecules are quite similar and both bind to Ca^{2+} with a stoichiometry of 2 molecules per Ca^{2+} ion. However, EGTA is almost completely Ca^{2+}specific (K_d = 123 nM, Qin et al, 1999), while EDTA has high affinity also for other divalent cations such as magnesium (Raaflaub, 1956, Holleman and Wiberg, 2001).

3.8- Post translational modifications of CaM

The most studied post-translational modification of plant CaMs is the methylation. CaM often occurs to be trimethylated at position K115 by a *S*-adenosyl-L-methionine:lysine N-methyltransferase (Roberts et al, 1986, Magnani et al, 2010). Lysine 115 is found within a highly conserved six-amino acid loop (LGEKLT) that forms a 90° turn between EF-hand III and EF-hand IV in the carboxyl-terminal lobe. This post-translational modification is frequently observed in plants but was not detected in CaM from other organisms such as *Chlamydomonas reinhardtii* or *Dictyostelium discoideum*.

In all the cases so far analyzed, the methylation status of CaM had no effects in the activities or properties of the CaM-binding proteins. The only exception is plant NAD kinase, for which the methylation was reported to lower the activation of the enzyme by CaM by a factor of 3 or 4 (Roberts, 1992).

The same lysine involved in methylation might also be a target for ubiquitination, but these findings need to be further confirmed (Ziegenhagen & Jennissen, 1990).

A Petunia isoform of CaM, CaM53 (homologous to AtCaM5, At2g27030) contains a 35 amino acid extension at the *C*-terminus with a prenylation site that allows targeting the protein to the plasma membrane (Rodríguez-Concepción et al. 1999). The prenylated *C*-terminus cysteine can subsequently be methylated by a prenyl-cysteine methyltransferase. In the absence of this methylation, the protein localizes mainly in the nucleus instead to be addressed to the plasma membrane.

In addition, animal CaMs are known to be subjected to phosphorylation (Corti et al, 1999, Leclerc et al, 1999) but this was never observed in plant isoforms so far.

3.9- Peculiarities of plant CaMs

Where animals evolved movement and the nervous system in order to deal with environmental changes, plants cannot escape to adverse condition. This leads to the need of deep cell plasticity so that the whole plant or just some organs can adapt its phenotype to the environmental challenges. Even if many mechanisms of cell signaling are conserved between plant and animals, plants have also evolved peculiar adaptation mechanisms. This appears to be the case for CaM/Ca^{2+} signalling: while in animals only one isoform of CaM per genome is present, in plants a wide range of Ca^{2+} binding proteins of the family of CaM can be observed.

Not only plants possess a higher number of genes coding for CaMs (7 in Arabidopsis), but plant genomes contain also several CaM-like proteins or CMLs (McCormack and Braam, 2003).

Like CaMs, CMLs are short proteins composed mostly of EF-hand motifs and without any other domain. They differ from CaM in that their protein sequence is more divergent (but at least 15% homologue to the overall CaM sequence). They can contain a variable number of EF-hands, and sometimes *N*/*C*-terminal extensions that can act as transit peptides for the internal cell localization in specific or-

ganelles. The number of CMLs in plant genomes is curiously high (32 in rice and 50 in Arabidopsis, for example).

Sequence analysis suggests that they can differ for Ca^{2+} affinity since differences in the amino acids involved in the Ca^{2+} coordination are sometimes present (McCormack and Braam, 2003).

Targets of CMLs can differ with respect to CaM. For example, it has been shown that NAD kinase is highly activated by bovine CaM as well as Arabidopsis CMLs 10 and 47, while no effect was detected for CMLs 2, 3, 18, 39, 42, and 43 (see **Chapter 5**). More recently, a proteomic analysis showed many potential interactions for a group of CMLs (Popescu et al, 2007). Sometimes the target proteins were conserved among all the isoforms investigated, but others were able to bind to only some of them.

With respect to the localization, CaM is normally found in the cytoplasm and, in the case of CaM7 (At3g43810), in the cell nucleus. CMLs were variously localized in several organelles such as the vacuole (Yamaguchi et al, 2005), the plasma membrane (Rodríguez-Concepción et al, 2000), and the mitochondria (Chigri et al, 2012).

At present no plant CaM or CML was ever associated to the chloroplast even if some of them might contain a plastidial *N*-terminal transit peptide. The Ca^{2+} control of the chloroplast is therefore intriguing and will be discussed in the next paragraph.

4- Ca^{2+} regulation inside the chloroplast

Total concentration of Ca^{2+} in the chloroplast was estimated to be approximately 15 mM (Nobel et al, 1969, Portis and Held, 1976). This high value would generate precipitates with the phosphate and alter the activity of photosynthetic enzymes that were shown to be inhibited by Ca^{2+}: the fructose 1-6 bisphosphate (Racker and Schroeder, 1958) and the sedoheptulose bisphosphate (Portis and Heldt, 1976, Charles and Halliwell, 1980). Ca^{2+} is therefore mostly buffered, and the final [Ca^{2+}] in the stroma was estimated to be 150 nM in light conditions according to Johnson et al, (1995), with a stroma targeted aequorin.

Mechanisms of Ca^{2+} buffering in the chloroplast are not completely clarified. A high amount of Ca^{2+} is thought to be stored in the thylakoid lumen (Ettinger et al, 1999), but indirect evidence suggests the presence of additional Ca^{2+} stores in the stroma (Sai and Johnson 2002). One hypothesis is that the high amount of phosphorylated proteins of the thylakoids (especially by two kinases named STN7 and 8 in Arabidopsis) might account for the buffering of Ca^{2+} in excess (Stael et al, 2012a). However, given the high concentration of membrane lipids in the chloroplast (Block et al, 1983; Douce, 1985) and the affinity of Ca^{2+} for those molecules (K_D of 1,1 mM for phosphatidylcholine, Post and Langer, 1992), a high amount of plastidial Ca^{2+} might be simply buffered by membranes[1].

An overview of the chloroplast Ca^{2+} transport and of the main actors in the Ca^{2+} homeostasis and signal transduction known so far is given in **Fig I.17**.

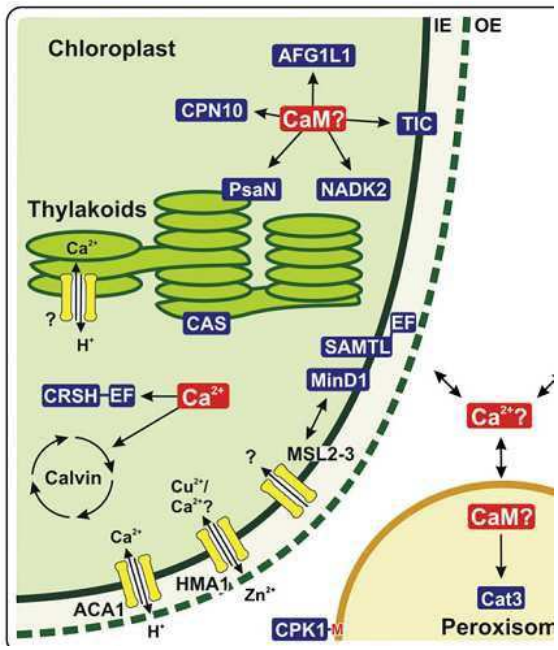

[1] In order to get an idea of the quantity of Ca^{2+} that can be stored by plastidial lipids a rough calculation can be done. Phosphatidylcholine of the chloroplast outer envelope membrane represents approximately 32% of total lipids (Block et al, 1983; Douce, 1985). Assuming that the chloroplast volume is approximately 60 fL, [phosphatidylcholine] would be 1-10 mM in solution. Considering a plastidial [Ca^{2+}] of 5 mM and the K_D of phosphotidiylcholine for Ca^{2+} previously calculated (1.1 mM according to Post and Langer, 1992), we can compute that 3.14 mM Ca^{2+} would be bound to phosphatidylcholine. In a similar manner, phosphatidyl glycerol has a high K_D for Ca^{2+} (117 mM, according to Lau et al, 1981), but represents 7% of the thylakoid lipids, that is 32 mM if it was soluble. It can be estimated that, in these simplified conditions, 1 mM of Ca^{2+} would be bound to phosphatidyl glycerol.

Fig I.17 Overview of the putative Ca^{2+} transporters and Ca^{2+} binding proteins of the chloroplast. Question marks identify lack of protein identity or protein function.

4.1- Structural and inhibitory roles of Ca^{2+} in the chloroplast

Ca^{2+} is required at the level of the thylakoid membrane for the correct functioning of the photosynthetic apparatus. Indeed, the assembly of PSII and the oxygen-evolving complex (OEC) requires Ca^{2+} and other ions as essential cofactors (Becker et al., 1985; Ghanotakis et al, 1984; Miller and Brudvig, 1989). Similarly, the reconstitution of PSII after photoinhibition needs Ca^{2+} (see for example Virgin et al, 1990). Ca^{2+} regulates also the stability of the cytochrome b-559 (McNameara and Gounaris, 1995) and the photosynthetic proton flow by binding to the 8 kDa subunit of the ATP synthase (Zakharov et al, 1993). The importance of Ca^{2+} binding for the activity of the complex and the modulation of ATP production remains to be clarified.

A high [Ca^{2+}] in the stroma tends to inhibit CO_2 fixation at various points, especially at the level of the fructose-1,6-bisphosphatase (at 0.34-0.58 mM concentrations) and sedoheptulose bisphosphatase (Kreimer 1987, Charles and Halliwell, 1980). The physiological meaning of these regulatory mechanisms is however doubtful, since free Ca^{2+} concentrations never reach mM levels. *Vice versa*, plastidial NAD kinase activity was suggested to be Ca^{2+}/CaM stimulated, even if the plastidial localization of the CaM controlled NAD kinase was frequently questioned (see **Chapter 6** for a detailed review of this topic).

4.2- Transport of Ca^{2+} into the chloroplast

As stated previously, the plastidial Ca^{2+} appears mostly concentrated into the thylakoid lumen. The chloroplast must therefore contain systems to allow the transit of Ca^{2+} through the envelope up to the thylakoid lumen.

The outer membrane of the chloroplast is permeable to Ca^{2+}, but the crossing of the inner membrane requires specific transporters. An active transport of Ca^{2+} was measured both in intact chloroplasts (Kreimer et al 1985) and across vesicles of inner envelope membrane (Roh 1998). However, only two potential transporters for Ca^{2+} transport of in the stroma were identified to date. The first one is AtACA1, an autoinhibited Ca^{2+} ATPase (Huang et al 1993) that was however localized mostly in the tonoplast and the ER. The second one is AtHMA1, a heavy metal P-type ATPase. The protein is inhibited by the thapsigargin (Moreno et al 2008), the same inhibitor of the Ca^{2+} ATPase of the mammalian

sarcoplasmatic reticulum. However, this protein was mostly linked to the physiological transport of Cu inside the chloroplast (Seigneurin-Berny 2006) or a detoxification function for the active extrusion of Zn (Kim, 2009).

Two homologues of bacterial mechanosensitive Ca^{2+} channels were also identified at the inner envelope membrane: MSL2 and MSL3. Their presence was shown to be essential for correct chloroplast division, but no direct measurements of Ca^{2+} fluxes were performed (Wilson et al, 2011).

At the level of the thylakoid membrane, only one candidate for the transport of Ca^{2+} was proposed – an integral membrane translocase named ALBINO3. Expression of this gene in human cells results in inward Ca^{2+} current, and the down-regulation of the protein results in severe growth phenotypes and disruption of Ca^{2+}-induced stomatal aperture in Arabidopsis guard cells (Li et al, 2004). The uptake of Ca^{2+} could also be due to the proton gradient generated by photosynthesis by a Ca^{2+}/H exchanger that was hypothesized on the basis of Ca^{2+}-import experiments to the lumen of isolated thylakoids (Ettinger et al, 1999). These findings were supported by the fact that the Ca^{2+} intake of the thylakoids was impaired by nigericin, a proton translocation uncoupler, while ATP had no effect. However, no candidate gene for this Ca^{2+}/H+ antiporter has ever been proposed.

4.3- Light/dark transition and Ca^{2+} fluxes

Ettinger et al (1999) also observed that in isolated chloroplasts or thylakoid membranes the Ca^{2+} transport in the thylakoids was stimulated by light and thylakoidal [Ca^{2+}] reached a plateau after 15 minutes of illumination. Their observations are in agreement with a light-dependent Ca^{2+} flux from the cytosol to the chloroplast that was observed several times (Muto et al, 1982; Kreimer et al, 1985, Miller and Sanders, 1987). This transport was shown to be dependent on photosynthesis, since it was inhibited not only by nigericin but also by the photosynthetic inhibitor DCMU. Light does not produce a significant change in the Ca^{2+} concentration of the stroma, strongly suggesting that at least a high portion of the Ca^{2+} is stored in the thylakoid lumen or in other unknown stores.

When photosynthesis is active, Ca^{2+} seems to progressively accumulate from the cytoplasm to the thylakoidal lumen.

A peak in the stromal Ca^{2+} concentration was recently observed *in vivo* some minutes after transition from light to dark (Sai and Johnson, 2002). Both the peak height and the integrated luminescence were directly proportional to the duration of the previous light exposure (**Fig I.18**).

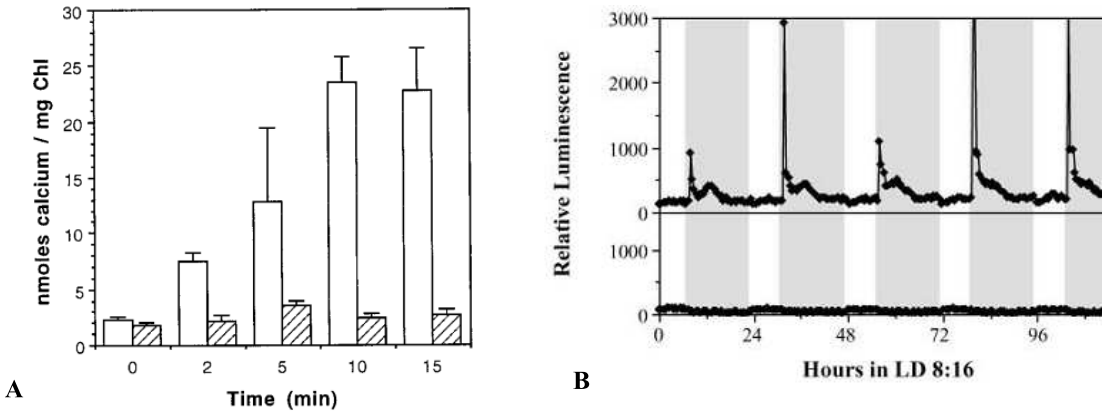

Fig I.18 [Ca^{2+}] variations in chloroplasts. A. Accumulation of Ca^{2+} in the isolated thylakoid lumen as a function of time (from Ettinger et al, 1999). White bars: light exposure; shaded bars: dark. **B**. Luminescence of stromal localized aequorin as a function of time for plants kept in short day conditions (From Sai and Johnson, 2002). An everyday occurring fluorescence peak a few minutes after lights off is visible (upper panel). No peak is detected in non-transgenic plants *i.e.* in the absence of aequorin (bottom panel).

In contrast to the postulated role of photosynthesis in Ca^{2+} flux inside the chloroplast, DCMU applied during the dark phase did not abolish the stromal Ca^{2+} peak observed in the dark. However, it did cause a significant increase in stromal Ca^{2+} levels during the light period that might have been caused by leaking of Ca^{2+} from the thylakoid lumen to the stroma or by a reduced rate of Ca^{2+} transport from the stroma to the thylakoid. This suggests the presence of another subplastidial compartment not regulated by photosynthesis where Ca^{2+} is stored, probably localized at the stromal level.

A prolonged Ca^{2+} transient within the stroma in short days could lead to a prolonged end-of-day signal and could be a means by which plants perceive the difference between long and short days.

In the dark, the chloroplast switches from a mainly anabolic metabolism (photosynthesis, starch synthesis) to a catabolic metabolism (starch degradation, glycolysis). One of the most intriguing aspects of the dark-stimulated Ca^{2+} spike is the 5- to 10-min delay between lights off and the increase of Ca^{2+} in the stroma. If the light is turned on before the Ca^{2+} spike begins, this spike is inhibited, while if the light is turned on after the Ca^{2+} spike has begun, the spike is just attenuated. Assuming that the stromal

Ca^{2+} spike functions as a signal for the chloroplast in order to adapt its metabolism to dark, a rectifying mechanism to attenuate or abolish the Ca^{2+} spike when it was triggered by a short dark period becomes extremely useful.

This suggests that Ca^{2+} could be one of the main actors that trigger the plastidial responses to light, thus permitting a rapid metabolic adaptation to the new conditions. However, the authors always measured Ca^{2+} fluxes after switching the light on and off instantaneously. It might be therefore interesting to repeat these observations on plants exposed to natural light or mimicking the more realistic situation in which light changes gradually and slowly.

A schematic representation of the light induced Ca^{2+} fluxes in the chloroplast is reported in figure **Fig I.19**.

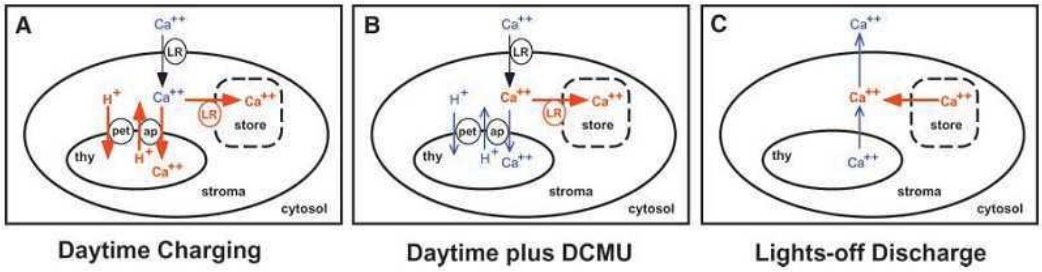

Fig I.19 Model for Ca^{2+} Fluxes into and out of the chloroplast modulated by light and dark (Sai and Johnson, 2002). Relatively high concentrations of Ca^{2+} and strong Ca^{2+} fluxes are shown with thick red lines, and relatively low concentrations of Ca^{2+} and weak Ca^{2+} fluxes are shown with thin blue lines. A hypothetical calcium store is also localized in the stroma. This calcium store is shown with dashed lines because it is not known (1) whether it is in the stromal lumen or the thylakoid, and (2) whether it is membrane bound (*e.g.*, if it is identical with the thylakoid). Calcium stores in the cytosol and extracellular space are not shown, but they certainly are involved in the regulation of cytosolic calcium. ap, Ca^{2+}/H^{+} antiporter; LR, light-regulated Ca^{2+} uptake into chloroplasts; pet, photosynthetic electron transport; thy, thylakoid lumen.

4.4- Role of Ca^{2+}/CaM in chloroplast protein import

Ca^{2+} was proposed as a regulator of the targeting to the chloroplast of nuclear-encoded proteins. Chigri et al, (2005) showed that the chloroplast import of some proteins, all containing a cleavable *N*-terminal transit peptide, was inhibited by Ophiobolin A, a membrane-permeable inhibitor of CaM (Au and Leung, 1998). Proteins located in the inner envelope or the stroma were affected in the same manner as proteins that required further translocation across the thylakoid membrane, suggesting that it is the translocation process into the chloroplast itself that is susceptible to Ophiobolin A inhibition. The

insertion of Toc34 or Tic32 into the plastidial envelope does not involve the classic chloroplast import machinery and was not affected by Ophiobolin A.

The observed effect of Ophiobolin A on chloroplast protein import questioned the role of CaM in the process. One year later, Chigri et al, (2006) showed that CaM was able to interact with Tic32, a NADPH-dependent dehydrogenase of the inner translocon complex. Tic32-CaM interaction appeared to inhibit the dehydrogenase activity of Tic32 since CaM- and NADPH-binding to Tic32 are mutually exclusive. Moreover, NADPH binding to Tic32 abolishes its ability to interact with Tic110, another member of the inner membrane translocon.

These findings suggested that Tic32 might be a central regulator of plastidial protein import, capable of integrating Ca^{2+} signals and the redox status of the chloroplast. However, more recently, it has been established that Tic32 is not an essential component of the Tic complex, and the role of its interaction with CaM in the regulation of protein import in the plastids is therefore questionable (Hormann et al, 2009).

The properties of Tic100, another component of the import machinery, were recently unraveled by spectroscopy and *in vitro* import experiments (Balsera et al, 2009). The authors showed that the protein forms a six helix cation channel localized in the inner envelope membrane. They suggest possible mechanisms of redox control by interaction with thioredoxin and showed that the activity of the channel is strongly influenced by Ca^{2+}.

To sum up, Ca^{2+} is probably involved in the control of protein import by interacting with several components of the protein import complexes. A Ca^{2+}/CaM dependent regulatory mechanism of protein import into the chloroplast like what observed for the secretion of little protein in the mammal system is therefore an intriguing hypothesis.

4.5- Plastidial CaMs and CaM-binding proteins: an open field

As illustrated in the previous paragraphs, Ca^{2+} signals are transduced by Ca^{2+} sensors, especially by EF-hand containing proteins.

For what concerns the chloroplast, the presence and the identity of Ca^{2+} sensors is still completely unknown. In addition to a group of serine-threonine phosphatases (Johnson et al, 2006), few other plastidial proteins contain Ca^{2+}-binding motifs.

CRSH (Ca^{2+}-activated RelA/SpoT homologous protein) contains two EF-hand motifs and is implicated in the Ca^{2+} dependent biosynthesis of guanosine 5'-diphosphate 3'-diphosphate (ppGpp). In plants, protein transcription was shown to be up-regulated by stress conditions and hormones (Takahashi et al, 2004). CRSH modulates specifically the activity of the bacterial type plastid-encoded plastid RNA polymerase (PEP), with no effects on the nuclear-encoded plastid RNA polymerase (NEP) (Sato et al, 2009).

Another plastidial EF-hand containing protein is AtSAMTL (At2g35800), with a single EF-hand motif. YFP fusions confirmed the plastidial localization of the protein (Stael et al, 2012b). No analyses on the function of this protein and on the Ca^{2+} regulation were done, but speculatively it could be involved in the import S-adenosylmethionine (SAM) into the chloroplast.

Finally, the CAS protein was recognized as a low affinity, high capacity Ca^{2+} binding protein without any predicted Ca^{2+}-binding sites. This peculiar protein was localized at the thylakoid membrane (Vainonen et al, 2008). It can be phosphorylated, probably by the kinase STN8, and disruption of its activity was shown to have a high impact on plant growth, development and response to pathogens (Nomura et al, 2012), as well as photoacclimation in algae (Petroutsos et al, 2011).

The presence of CaM or CMLs in the chloroplast is still unclear. Jarrett et al (1982) firstly attempted to purify CaM from chloroplast fractions and concluded that a protein with characteristics comparable with those of CaM is indeed present in this cell compartment. Another indirect evidence for the presence of CaM at the inner envelope membrane is given by Chigri et al (2006). They cross-linked plastidial inner envelope with exogenous CaM and detected by western blot a shift in the size of Tic32 from 32 to 48 kDa, corresponding to the size of the Tic32-CaM complex. A faint band at the same size was observed for the protein in the absence of exogenous CaM, thus suggesting the presence of an endogenous CaM or CML. However, this might also be due to contamination of cytoplasmic CaM, since no identification of this CaM/CML isoform was provided.

Several high-throghput studies succeeded however in detecting potential CaM interactors such as the photosystem 1 subunit PsaN and the elongation factor EF-1α (Reddy et al, 2002). Other potential plastidial CaM interactors were independently discovered and include Cpn21 (Yang and Poovaiah, 2000), AFG1-like (Bussemer 2009), NAD kinase 2 (Turner et al, 2004) and the previously mentioned Tic32 (Chigri et al, 2006). All the postulated interactions need further characterization and only in the case of NADK and Tic32 a CaM-dependent modulation of the protein activity was reported.

Concluding remarks and aim of the present work

This rapid synthesis of the role of calcium in eukaryotic cells with focus on plants shows that Ca^{2+} variations are observed in response to a wide variety of stimuli and extremely regulated by channels and pumps. Several Ca^{2+} sensors are involved in decoding these signals in order to determine cell responses. CaM is the most important of these sensors and the most extensively studied. CaM-partners interactions are very eterogeneous: they can be Ca^{2+}-dependent or independent, and can have a stimulatory or inhibitory effect. Various interaction mechanisms were described and CaM-binding sequences are not easy to identify.

The chloroplast is one of the major Ca^{2+}-storing organelles of the plant cell. Plastidial Ca^{2+} fluxes were observed and could be involved in regulating plastidial adaptations to environmental conditions, especially in regard to the light/dark cycles.

Despite the high number of Ca^{2+}-binding proteins in plant genomes, the plastidial Ca^{2+} sensors and Ca^{2+} signaling pathways are still largerly unknown. In particular, the presence of Ca^{2+}-regulated events and CaM-regulated proteins in the chloroplast, combined with the absence of an identified CaM isoform in this cell compartment open many questions about the significance and the extent of the plastidial Ca^{2+}-CaM regulation.

In order to shed some light in the field, we proceeded *via* four steps. Firstly, we developed a quantitative technique based on fluorescence anisotropy to measure the affinity of proteins for CaM. To do so, we focused on the CaM interaction with the most well studied plastidial partner, *i.e.* NADK2 (**Chapter 1**). Then, we used these same biochemical tools to validate a high-throughput approach aimed to detect other previously unknown plastidial CaM interactor (**Chapter 2**). Among the 210 pro-

teins detected by this survey, the ceQORH protein (**Chapter 3**) was analyzed more in detail together with Tic32 (**Chapter 4**). We then attempted to identify plastidial CaM isoforms in the chloroplast by various proteomics approaches and by protoplast transient transformations (**Chapter 5**). We finally improved the characterization of an Arabidopsis NADK2 mutant insertion line showing a drastic growth and photosynthetic phenotype and we developed tools to confirm the localization of NADK2, to measure its CaM affinity and the effect of CaM-binding on the protein activity of the recombinant and native protein (**Chapter 6** and **Annex IV**).

Our work allowed the development of fast and direct measurements of CaM-protein interactions and opens new perspectives on the role of CaM in regulating protein activity and localization.

Materials and Methods

1- Biological material

1.1- Arabidopsis plant cultures

Arabidopsis seeds (variety Col-0) were placed at -80 °C for two hours in order to kill parasite eggs, then surface sterilized with a sodium hypochloride solution for two minutes. Seeds were rinsed with sterilized water three times, and seeded directly on soil or on MS-medium (4 g Gamborg MS-Medium, 4 g saccharose, 8 g selected agar, pH 5.7).

Pots were watered with a solution of Bt Vectobac 0.5%, covered with a plastic film in order to keep water saturation and placed in the dark at 4 °C for vernalization. After two days, pots were put in phytotron with a day/night cycle of 8/16 hours and 65% humidity at 22 °C and 40 µE light intensity. The plastic film is removed after two weeks and plants watered once or twice a week.

If seeded into MS-medium plates, plants were transferred in soil after two weeks and pots are kept under plastic film for an additional two weeks.

1.2- Arabidopsis cell cultures

Arabidopsis cell cultures were constantly maintained in the lab (variety Col-0) in Murashige and Skoog (1962) nutrient media as described by Bligny and Leguay (1987), without antibiotic and supplemented with 30 g sucrose/L. Cells are kept at 30 µE light intensity and 22 °C, under constant agitation at 125 rpm (200 mL in 1L flask). In order to propagate the culture, 50 ml of medium of 5 days old cells is let sediment by gravity for several minutes in a 50 ml falcon under sterile conditions. The supernatant (approximately 20 mL) is removed and cells inoculated in another 200 mL flask.

For NADK purification, cells were harvested at day 5. In order to remove the medium, cells were filtered on Whatman paper and washed with milliQ water. Cells were kept at –80 °C prior to protein extraction.

1.3- *E. coli* strains

The strain DH5α (Invitrogen; F-Φ80*lac*ZΔM15 Δ(*lac*ZYA-*arg*F)U169 *deo*R *rec*A1 *end*A1 *hsd*R17(r_k^- m_k^+) *pho*A *sup*E44 *thi*-1 *gyr*A96 *rel*A1 λ-) was used for amplifications of DNA plasmids and for subclonings. This strain contains several modifications that increase the stability of transformed plasmids.

The strain BL21 Rosetta 2 (DE3) (Merck; F- *omp*T *hsd*SB($r_B^-m_B^-$) *gal dcm* (DE3) pRARE2 (Cam^R)) was used for overexpression of recombinant proteins. This strain contains a chromosomal copy of the gene *LACI* and of the T7 RNA polymerase. The product of the first gene blocks the expression of the promoter *LacUV5* on the bacterial genome and controls the expression of the RNA polymerase T7. The same strain contains also the genes for tRNAs of 7 codons that are more abundant in the eukaryotes with respect to prokaryotes, and a chloramphenicol resistant gene on the same plasmid. This enhances the translation of eukaryotic proteins.

Both strains are cultivated at 37 °C (unless otherwise indicated) in LB medium (Luria-Bertani: yeast extract, tryptone, NaCl), supplemented with agar 1% for solid media, and suitable selective antibiotics.

2- DNA techniques

2.1- DNA extraction from plant leaves for genotyping

One young leaf for each plant (or, in the case of NADK2 mutants, whole plants) were used for DNA extraction. The leaf or the plant was grinded in liquid nitrogen with a little potter. Grinding was continued with addition of 400 µL DNA extraction buffer (Edward buffer: 200 mM Tris-HCl pH 7.5, 250 mM NaCl, 25 mM EDTA, 0.5% SDS, see Edwards et al, 1991). Samples were vortexed and centrifuged at room temperature for 2 minutes at 13,000 rpm. The supernatant was recovered and supplemented with 300 µL pure isopropanol, incubated 2 minutes at room temperature and centrifuged 5 minutes at 13,000 rpm at room temperature. After removing the supernatant, the pellet is let dry at room temperature, and finally resuspended in sterile water. 1 µL of the resuspended DNA was used for PCR. DNA was stored at -20 °C for up to one month.

2.2- Genotyping of the NADK2 Salk_122250 mutant line

Heterozygous seeds of NADK2 Salk_122250 line were purchased from the Salk institute. Seeds were seeded directly on soil and the F2 generation was harvested. A proportion of 1:2:1 wt:het:mut seeds was expected. These seeds were then cultivated on MS medium.

Mutant plants were selected thanks to their reduced F_v/F_m value (see **Annex IV**).

In order to confirm the presence of the mutation, a PCR was performed with specific primers. A forward (left border) and reverse (right border) primers (NADK2 LP and RP) were designed in order to match the wild-type sequence and used to detect wild-type and heterozygous plants. An additional primer was designed in the T-DNA insertion (LbB1) and used in combination with the NADK2-RP primer in order to detect heterozygous and mutant plants (**Table M1**). The amplicon obtained with LPNADK2 and RPNADK2 in wild-type and heterozygous plants was of 902 bp, while the one obtained in heterozygous and mutant plants with primers LbB1 and RPNADK2 was of 447 bp.

LPNADK2	TATTGGGAACAGTGCCAACTC
RPNADK2	GAGAAATCCAAGAGACCCCAG
LbB1	GCGTGGACCGCTTGCTGCAACT

Table M1: primers for genotyping of the mutant line Salk_122250.

2.3- Primer design for cDNA cloning

cDNA sequences of selected proteins were downloaded from the TAIR database (http://www.arabidopsis.org/). Transit peptide cleavage sites were identified using ChloroP and by sequence comparison between homologous genes of other plant species with the BLAST tool of NCBI.

Primers contained suitable restriction sites for subcloning in the plasmid vectors.

For protein expression, the cDNA sequences corresponding to the predicted mature proteins were cloned into pET28 or pET30 expression vectors (Novagen, Darmstadt, Germany). Proteins lacking a measurable catalytic activity were expressed with a Histidine tag which was not subsequently cleaved. All other proteins were expressed in their native form without the predicted chloroplast transit peptide sequence.

For NADK2, three constructs were made: one with only the *N*-terminal region containing the CaM-binding sequence was cloned (amino acids 61–411, named NADK2.1), one with the whole CDS without the predicted transit peptide (NADK2.2), and one corresponded to the predicted *C*-terminal catalytic domain (NADK2.3). cDNAs were amplified from an Arabidopsis cDNA library in pYES (Elledge et al, 1991).

cDNAs for CML 30, 35, 36 and 41 were cloned into the pUC vector for protein expression into protoplasts. cDNA sequences were cloned in this vector in order to be in frame with a GFP protein sequence that is placed at the *C*-terminus of the CML.

Primer sequences, restriction enzymes used, the presence of the Histidine tag and the final sequence of each cloned protein are reported in **Table M2**.

2.4- Polymerase chain reaction

For subcloning, the PCR reaction was performed in 50 µL final volume of a mix containing 25 µM of each deoxyribonucleotides triphosphate (dATP, dCTP, dGTP and dTTP), 0.5 µM of each primer, and 0.5 µL of the Phusion DNA polymerase (New England Biolabs) in its buffer.

For both genotyping and subcloning, the PCR protocol was constituted of a first denaturation of the DNA at 95 °C for 5 minutes, followed by 10 cycles of a touch-down protocol (30 seconds of denaturation at 95 °C, 30 seconds of hybridization at 65 to 55 °C (minus 1 °C at each cycle), and 1 minute/kb of elongation at 72 °C). 25 cycles of amplification were then realized at 55 °C hybridization temperature. The protocol ended with 7 minutes of final elongation at 72 °C. Amplifications were checked by loading 5 µL of the PCR on a 10.7-1.5% agarose gel in TAE buffer. Amplicons of the correct size were excised with a scalpel, purified with a Macherey-Nagel kit and digested with suitable restriction enzymes for 2 hours at 37 °C unless otherwise specified.

Accession number	protein name	vector	Cloning sites	Primer 5'	Primer 3'
protein expression					
At5g23060	CAS	pet28b (+)	NdeI-XhoI	ctgagtctgagacaaCATATGgtttcacttccaac	CTATATATATCC-TCGAGTTTCAGTCGGAGCTAG
At1g53280	DJ1	pet28b (+)	NheI-XhoI	ctatctctgcaactGCTAGCtcatctactaagaag	CTTACCTAAGATACTCGA-GAGTTTACACAAGTG
At1g65260	Vipp1	pet30a (+)	NcoI-SacI	Gtgttgaccatggcttgtgataatagactcaggtgc	cggaaagagctcatatctaaaagtcgttagctttcc
At1g80480	pTAC17	pet28b (+)	NdeI-XhoI	ctcagctacgcagactCaTATGtctgatgtcac-cactaag	GCCGGTGACCATTTCCTCGA-GATACATAGAGCTAG
At5g35630	GS2	pet28b (+)	NdeI-XhoI	Ggatcatcaatccaatggctcagatc	ccacatagactcgagtgttcatcagattcatg
At5g63420	RNAseJ	pet28b (+)	NheI-EcoRI	cttgagctagcatgtcatcctctaagacgccac	caaggaattcttaagacgcaggtgtgcctagc
At1g59990	RH22	pet28b (+)	NheI-BamHI	cttggctagcAtggcagaagtcgagaaaaag	caagggatccttaatatctcacagcttgagG
At1g17220	FUG1	pet28b (+)	NdeI-SalI	cttgcatATGTCTTCAACTACTAC-TAC	caaggtcgacTTAAACTCCAGCCTC TTCAAT
At5g10910	MRAW	pet28b (+)	NdeI-HindIII	ggaaatcatatgtcgagcgagactaagaag	GTCATAAAGCTTTCA-CAACTTCTGAATCACTCTTAAC
At4g01800	SecA	pet28b (+)	EcoRI-XhoI	ctggagaattcatgtgctctcggaagagaagc	CGTTTAC-TCGAGTTAGGCGCTTGCAATT-GAGG
At2g37500	ArgJ	pet28b (+)	NdeI-SalI	gcctaagagttttgtgCATATGtcacggaga-gaattaag	CAGTAAAT-GAAACTCTGTCGACCGGTCTCA GTTCTATG
At1g74470	GGR	pet30a (+)	NcoI-XhoI	cggacctctctccgagCCaTGgcagcca-gagccactc	GAAAGGAGATAGACCTCGA-GATTTGTTTCTTAAAC
At5g01920	STN8	pet28b (+)	NdeI-XhoI	GGGTTGTATGcatatggGCAGTTTTT CTCCGC	CATCATAACTCGAGAAATCA-GAGTCACTTGCTGAAAC
At3g45140	Lox2	pet28b (+)	NdeI-BamHI	cttggctagcATGGCTAATATT-GAACAAG	gaacggatccTCAAATAGAAATAC-TATAAGG
At2g21370	XK-like1	pet28b (+)	NdeI-XhoI	Ctccgatttcagacatatgagtggcaat	gaaaatgtgttctcgagctctggtcttg
At2g33040	ATPCγMit	pet28b (+)	BamHI-XhoI	GTTGGATC-CATCTCAACTCAAGTGGTGCGTA AG	GAAAAGAGAACTAACC-TCGAGGGGCTTATTTAGCAG
At1g09795	PRT2	pet28b (+)	NdeI-BamHI	ggtgccac-cgattccCATATGgtcgtcgggcgggag	CTGACTAAAC-CAAAGGGATCCTGAGAAG-CAGCATC
At4g04640	ATPCγChl	pet28b (+)	NcoI-EcoRI	CTCCTTCCATGGCTTCCTCTGTTT CACCAC	GAAGATTCAAAGAGAATT-CAAAACAAATCAAACCTG
At1g21640	NADK2.1	pet30a (+)	NdeI-KpnI	GATTTGTGcatAtgGCGCAGCTCTC TGAAGC	CAGTCTGCTCAT-CAGGTACCCCCTTAC
At1g21640	NADK2.2	pet30a (+)	KpnI-SacI	GTAAGGGgGTACCTGATGAGCA-GACTG	CTAAAATGAgCtcATCAATCAT-CAGAGAGCC
At1g21640	NADK2.3	pet30a (+)	NdeI-SacI	GAGTCTCAGACTCAtAt-gAATAATAGTGGTTCCTCC	CTAAAATGAgCtcATCAATCAT-CAGAGAGCC
At3g50770	CML41	pet30a (+)	NcoI-XhoI	caaccttaaactctccCaTGGgcaacagtgatgac	ggtaattacgtaaaagCTCGAGttaattacac-taaac
GFP fusions					
AT2G15680	CML30-GFP	pUC	SacI-NcoI	AAAg-tcGACATGTCAAACGTGAGTTTTC TTGAG	AGAGAGccATGGA-GACATTGTTGGAAGACATC
AT2G41410	CML35-GFP	pUC	SacI-NcoI	TTCgtCGAcAT-GAAGCTCGCCGCTAGCCT	CAAcCATGgAATGATGATGAT-CATTCATCGC
AT3G10190	CML36-GFP	pUC	SacI-NcoI	AAgTcgACACTAT-GAAACTCGCCAAACTAATTCC	AAAcCATGgAACGCTGGA-GATCCATCATTCGTGAG
At3g50770	CML41-GFP	pUC	SacI-NcoI	TATAAAgTCgAcGA-TATGGCAACTCAAAAAGA-GAAACC	ATTTAATccatggAAACCGTCAT-CATTTGACGAAACTC

Table M2 List of primer sequences used in this study.

2.5- Plasmid ligation and cloning

Ligations were performed overnight at 16 °C with T4 ligase, in a final volume of 10 to 20 µL with 50 ng plasmid and a ratio of insert/plasmid of 3 (mol ratio).

E. coli competent cells (DH5α strain) were transformed with 10 µL of ligation reaction per 50 µL of cells. After 30 minutes incubation on ice, cells were heat-shocked at 42 °C for 45 seconds, and then kept on ice for other two minutes. The reaction was finally diluted in 0.5 mL of LB medium and kept under agitation at 37 °C for 45 minutes. The medium was then plated on LB plates supplemented with a suitable selective antibiotic for the vector used (either 50 µg/mL kanamycin or 100 µg/mL carbenicillin). Chloramphenicol (34 µg/mL) was used for Rosetta2 cells to maintain the plasmid carrying the rare codons. Plates were incubated overnight at 37 °C.

Several colonies for each construct were selected and put in 5 ml liquid LB medium supplemented with antibiotic for one night. Recombinant plasmids were then purified from the overnight cultures with a Macherey-Nagel kit.

Sequences of cloned cDNAs were verified by direct sequencing using T7 primers.

3- Protein techniques

3.1- Protein extraction from Arabidopsis cells, leaves and roots

Arabidopsis frozen cells were grinded in liquid nitrogen with mortar and pestle. The obtained powder was resuspended in potassium phosphate buffer: 50 mM KPi pH 7.5, 150 nM KCl, 10% glycerol, 1 mM EDTA, 1 mM DTT, 1 mM benzamidine, 5 mM ε-aminocaproic acid and 1 mM leupeptine. For leaf extraction, 1-2 leaves were used and resuspended in 500 µL of buffer; for roots, 5-10 root segments were used and resuspended in 100 µL of buffer. The solution was centrifuged at 4 °C for 30 minutes at 20,000 rpm and the pellet was grinded again in the same buffer in order to improve the protein extraction yield.

3.2- Protein expression

For protein expression, *E. coli* Rosetta2 competent cells were transformed with the recombinant plasmid (10-50 ng) and grown overnight on Petri dishes containing the suitable set of antibiotic depending on the construct (either carbecillin or kanamycin) and chloramphenicol. Ten colonies were picked and grown on 5 mL of LB medium supplemented with antibiotics at 37 °C under agitation up to saturation. Saturated cultures were transferred into 100 mL of the same medium and growth was continued until $A_{600\ nm}$ reached 0.8-1. Protein expression was induced by addition of IPTG (0.4 mM) and growth was continued for 18 hours at 20 °C.

Bacteria were harvested by centrifugation 20 minutes at 4 °C (4000 *g*) and kept at -80 °C until protein extraction.

3.3- Protein separation by SDS-PAGE

SDS-PAGE allows separating proteins according to their molecular weight after denaturation by heating in the presence of SDS. Samples are diluted in a loading buffer containing 50 mM Tris-HCl (pH 6.8), 10% glycerol [v/v], 1% SDS [v/v], 0.01% bromophenol blue [w/v] and 25 mM DTT. Samples are boiled for 5 minutes at 95 °C and loaded on a gel constituted of two layers. The upper region (concentration layer) contains 5% [v/v] acrylamide, while the lower layer contains 12% [v/v] or, for little proteins, 15% [v/v] acrylamide.

Electrophoresis was run at 160 V in a Laemmli buffer for 1 hour or until the bromophenol blue dye reaches the bottom of the gel.

3.4- Protein staining: coomassie brilliant blue and silver staining

SDS-PAGE gels were colored with Coomassie brilliant blue dye. The staining solution was composed of 10% acetic acid [v/v], 25% ethanol [v/v], and Coomassie brilliant-blue (R250, Sigma), 2.5 g/L. Destaining was obtained by washing in a solution of 10% ethanol [v/v] and 10% acetic acid [v/v].

In order to stain low abundant proteins, since the detection limit of the coomassie brilliant blue is of 0.1 µg of proteins, gels were colored by silver staining. In this case the gel is washed 30 minutes in

acetic acid 10% [v/v] and ethanol 10% [v/v], then three times 10 minutes in a solution of 10% ethanol [v/v] and 5% acetic acid [v/v] in order to remove SDS and fix the proteins into the gel.

The gel is then incubated 5 minutes in an oxidant solution containing 3.4 mM $K_2Cr_2O_7$ and 3.2 mM HNO_3, and then washed 4 times in distilled water. The gel is finally colored 30 minutes in the dark in a solution containing 12 mM $AgNO_3$, and washed in distilled water. Proteins are visualized by a solution containing 0.28 M Na_2CO_3, 0.18% formaldehyde [v/v], for 10 to 15 min. The reaction is arrested by incubation in 1% acetic acid [v/v].

3.5- Protein quantification

Proteins were quantified by the method of Bradford or, for pure proteins, by measuring protein absorbance at 280 nm using a Nanodrop 2000 (Thermo Scientific) against appropriate blank solutions.

3.6- Preparation of proteins for antibody production

All procedures were performed with freshly-prepared solutions and gloves.

Two mg of the pure protein for which we wanted to obtain an antiserum was loaded on a 15 x 10 cm SDS-PAGE in a long, single well. The gel was run overnight at 6 mA, then stained in a Biosafe staining solution (Biorad) for half an hour. The band corresponding to the purified protein was cut in little fragments placed into a 3 K dialysis membrane and electro-eluted in 50 mM ammonium bicarbonate, 0.1% SDS. The elution was run for 3 hours at 50 V or longer if needed. Before recovering the protein, the current was reversed for 30 seconds, in order to detach proteins from the dialysis membrane.

The protein was recovered and placed in a falcon tube and frozen in liquid nitrogen. The frozen protein was then lyophilized overnight, re-suspended in sterile water and checked on SDS-PAGE.

The lyophilized protein was sent to the Charles Rivers Laboratory for antibody production in guinea pig. The day 81 post-inoculation anti-serum was used for western blots.

3.7- Protein transfer on nitrocellulose membrane

After having separated protein samples by SDS-PAGE, the gel was soaked in a transfer solution (Laemmli buffer and 20% ethanol (v/v)). The gel was placed in contact with a nitrocellulose membrane and placed against 3 layers of Whatman paper and one sponge on both sides. Air bubbles were removed by rolling a pipette up and down this "sandwich" that was placed in the transfer device containing the transfer buffer. The transfer of proteins onto the nitrocellulose membrane was obtained by passing electric current at 90 V for 1 hour and 30 minutes at 4 °C. The correct transfer of the proteins and the absence of bubbles were checked by staining the gel for some minutes into the Rouge Ponceau dye (0.4 g in 200 mL in water) that colors the proteins in red. The dye was subsequently removed by washing in TBST (TBS [150 mM NaCl, 50 mM Tris/HCl pH 7.5] + 0.05% Triton X-100 [v/v]).

3.8- Immunostaining

After the transfer, the membrane was rinsed in TBST and incubated 1 hour under agitation in TBST containing 5% of powder milk. The milk was then removed and the membrane rinsed with 25 mL of TBST and incubated overnight at 4 °C under agitation in TBST containing the primary antibody against the protein of interest at 1:3500 dilution.

The membrane was then rinsed with TBST and incubated 1 hour under agitation at room temperature with secondary antibody (an antibody against Guinea pig immunoglobulins) coupled with peroxydase (dilution 1/10,000).

The membrane was washed 3 times 5 minutes in TBST. The activity of the peroxidase was detected in an alkaline medium (100 mM Tris/HCl, pH 8.5) with 12.5 mM luminol (3-aminophalhydrazine) and 0.2 mM P-coumaric acid, in the presence of H_2O_2. In these conditions, the alkaline peroxydase catalyses the oxidation of luminol. When the excited luminol comes back to its original state, it produces chemiluminescence that is transduced in blue light. The P-coumaric acid is a catalyser of the reaction enhancing it by a factor of 100.

After one minute of incubation of the membrane in this solution, it is exposed on an autoradiography film sensible to the blue light for different times depending on the intensity of the signal (one to 10 minutes).

4- Protein labeling

4.1- HRP conjugation

HRP conjugation was carried out on 1 mg of purified AtCaM1 by using the EZ-Link Plus Activated Conjugation Kit Peroxidase ThermoScientific, Rockford, IL) at pH 7.2 following the manufacturer's instructions. The protein was stored at -20 °C in an equal volume of BSA at 10 mg/mL.

4.2- Alexa^{488} conjugation

We took advantage of the presence of a single Cys in AtCAM1 to label the protein with a C5-maleimide Alexa^{488} fluorescent probe. Labeling of 8 nmol of AtCaM1 (untagged protein previously purified in the laboratory) was performed by incubating the protein with a 7-fold molar excess of C5-maleimide-Alexa^{488} from a 20 mM stock in dimethylsulfoxide (Molecular probes, Invitrogen) for 45 minutes at room temperature in 10 mM Hepes, pH 7.5, 250 mM Tris(2-carboxyethyl)phosphine (prepared in 10 mM hepes pH 7.5) and 1 mM EDTA in a final volume of 200 µL. The labeled protein was separated from the free probe by gel filtration chromatography (G25 (M) resin, 1 x 30 cm^2) equilibrated with a buffer containing 10 mM Hepes-KOH, pH 7.5, 200 mM KCl and concentrated up to 40 µM in the same buffer. The eluted protein was concentrated on a 3 K Amicon filter unit (Merck).

5- Protein purification

5.1- Purification of His-tagged soluble and insoluble proteins

The pellet of bacteria were re-suspended in 2 mL of sonication buffer (20 mM Tris-HCl pH 8.0, 5 mM β-mercaptoethanol, 0.5 M NaCl, 5% (v/v) glycerol, 5 mM ε-aminocaproic acid and 1 mM benzamidine), and sonicated for 5 minutes at 4 °C on a Benson sonifier. Streptomycin sulfate (0.1% (w/v)) was added to precipitate DNA and the solution was centrifuged for 30 minutes at 30,000 *g* at 4 °C.

All purification steps were carried out at room temperature on 2 mL of NiNTA resin (Qiagen). The column was equilibrated with 8 column volumes of buffer A (25 mM Tris-HCl pH 8.0, 0.5 M NaCl, 25 mM Imidazole pH 8.0). After loading the sample, the column was washed with 8 mL of buffer A followed by 8 mL of buffer B (25 mM Tris-HCl pH 8.0, 0.5 M NaCl, 50 mM imidazole pH 8.0). Elution was performed with 6 mL of buffer C (25 mM Tris-HCl pH 8.0, 0.5 M NaCl, 250 mM imidazole pH 8,0). Fractions containing the purified protein were pooled and dialyzed overnight at 4 °C in dialysis buffer (25 mM Tris pH 8.0, 1 mM DTT, 5% (v/v) glycerol).

Prior to purification, insoluble proteins were solubilized in a urea-containing buffer as follows. Bacterial pellet was re-suspended in 4 mL solubilization buffer (25 mM Tris-HCl pH 8.0, 0.5 M NaCl, 10 mM DTT, 5 mM ε-aminocaproic acid, 1 mM benzamidine), sonicated 5 minutes and centrifuged for 20 minutes at 14,000 *g*. The pellet was washed three times in 4 mL of Triton buffer (25 mM Tris-HCl pH 8.0, 0.5 M NaCl, 1% (v/v) Triton X-100, 2 M urea) and, each time, centrifuged 10 minutes at 14,000 *g*. The final pellet was resuspended in 5 mL of urea buffer (25 mM Tris-HCl pH 8.0, 0.5 M NaCl, 1% (v/v) Triton X-100, 8 M buffered urea and 5 mM β-mercaptoethanol) and kept under agitation for 1 hour before centrifugation for 20 minutes at 14,000 *g* and recovery of the supernatant. For NiNTA purification, buffers B and C and dialysis buffer were supplemented with 5 mM β-mercaptoethanol and 6 M urea.

SDS-PAGE profiles of these partially purified proteins are reported in **Fig. M1**.

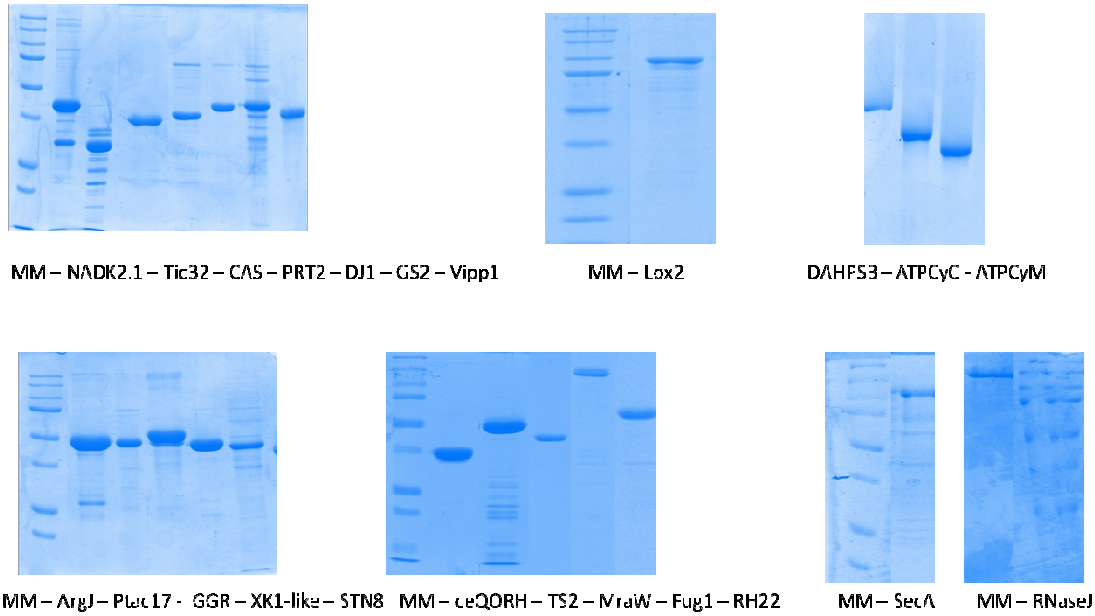

Fig M1 Profile of partially purified putative CaM-binding proteins used in this study.

5.2- CaM-affinity chromatography

CaM affinity chromatography of putative CaM-binding proteins (TS2, XK1-like, Lox2 and ceQORH, as well as NADK2.1) were carried out using 1 mL of CaM-sepharose resin (Agilent Technologies, Santa Clara, CA), poured in a PD-10 (GE-Healthcare, Milwaukee, WI) column, emptied of its G25 resin. The CaM-sepharose resin was equilibrated in a Ca^{2+} containing buffer (10 mM Hepes-KOH pH 7.5, 200 mM KCl, 1 mM DTT, 2 mM Ca^{2+}). One mg of bacterial soluble protein extract was diluted in 1.5 mL of the same buffer used for the column equilibration (final protein concentration: 0.67 mg/mL) and the pass through was reloaded three times on the column. The column was then washed with 10 mL of the same buffer. Proteins bound to the column were released with loading 5 mL of EGTA containing buffer (10 mM Hepes pH 7.5, 200 mM KCl, 1 mM DTT, and 0.5 mM EDTA).

Protein SDS gels were made by loading 2 µL of total bacterial extracts (from 2 mL sonicate corresponding to 100 ml culture) and 22 µL of the soluble extract, the pass through and the EGTA elution, all concentrated up to 0.75 mL.

5.3- Purification of recombinant AtCML41 and putative CMLs from Arabidopsis stroma and thylakoids

The purification was made following the protocol of Lee et al, 1997, with minor modifications.

30 mg of AtCML41 expressing bacterial soluble extract (3 mg/ml), Arabidopsis stroma and thylakoid highly purified subfractions were adjusted to a Ca^{2+} concentration of 5 mM, heat-shocked for 5 minutes at 95 °C, immediately cooled on ice for 2 minutes and centrifuged 20 minutes at 16 °C. In a first assay, a spinach sample was also used.

The supernatant was loaded twice on a 4 mL phenyl sepharose column poured in a recycled emptied PD10-column equilibrated with Ca^{2+} buffer (50 mM Tris-HCl pH 7.5, 1 mM $CaCl_2$). The column was washed 10 times with Ca^{2+} buffer, then with the same buffer supplemented with 200 mM NaCl. Bound proteins were eluted in EGTA bugger (50 mM Tris-HCl pH 7.5, 2 mM EGTA).

For AtCML41 the eluted fractions containing the protein were pooled and concentrated on a 3 K Amicon filter unit (Merck).

Proteins present in Stroma and thylakoid eluted fractions (10 mL) were precipitated using TCA. Firstly, they were supplemented with 1% (v/v) deoxycholate and 10% (v/v) trichloracetic acid, incubated 30 minutes on ice and centrifuged at 14,000 rpm for 30 minutes at 4 °C. The supernatant was discarded and the pellet washed with 100% acetone. Samples were centrifuged for 5 minutes at 14,000 rpm at 4 °C, the acetone was discarded and samples dried under hood. Before loading on SDS gels, aliquots of precipitates were resuspended in 1 X SDS-PAGE loading buffer and heated at 95 °C for 5 minutes.

5.4- Purification of native CaM-dependent Arabidopsis NADK

Purification of the native CaM-dependent NADK of Arabidopsis was performed following the protocol of Delumeau et al, 1998 and his PhD thesis manuscript.

Frozen Arabidopsis cells (100 g) were grinded in 150 mL of buffer (50 mM KPi pH 7.5, 150 nM KCl, 10% glycerol, 1 mM EDTA, 1 mM DTT, 1 mM benzamidine, 5 mM ε-aminocaproic acid and 1

mM leupeptine). The solution was centrifuged 20 minutes at 18,000 *g* at 4 °C. The pellet was resuspended in 50 mL of the same buffer supplemented with 1 M KCl and recentrifuged. Supernatants were precipitated with crystalline ammonium sulfate (final concentration 48% (w/v)) at 4 °C for 30 minutes under agitation, and then centrifuged at 18,000 rpm in a JA 20 Beckman rotor for 30 min at 4 °C.

Precipitates were frozen in liquid nitrogen and stored at -80 °C before use.

The ammonium sulfate precipitate was then resuspended in buffer A (50 mM Tris pH 8.0; 1 mM DTT, 1 mM EDTA, 10% glycerol (v/v) supplemented with protease inhibitors: 1 µM leupeptin (inhibitor of cysteine proteases) and 5 mM ε-aminocaproic acid and 1 mM benzamidine and 1 mM $MgCl_2$. Volume was adjusted with buffer A in order to reach a conductivity of 20 mS (*i.e.* 50 mM ammonium sulfate) using the conductivity sensor of the Biorad purification device.

The resuspension was centrifuged at 13,000 rpm in a JA 20 rotor (Beckman), for 25 min, at 4 °C, filtered on 0.2 µM filters and loaded at 1.5 mL/min on a XK-26 column (Pharmacia) containing 100 mL of EMD-DEAE 650 (M) resin (Merck), equilibrated in buffer A. After loading, the column was washed with 150 mL of the same buffer and then a linear gradient of 500 mL from 0% to 50% of KCl was applied. Pools of 50 mL of the pass-through and the wash, as well as 5 mL fractions of the linear gradient were recovered and tested for NADK activity.

NADK activity was found to be present in the pass-through of the column and in the washing fractions. These fractions were concentrated on a 10 K concentrator (Merck), frozen in liquid nitrogen and stored at -80 °C.

The DEAE pass-through was loaded either on a CaM-affinity column as described above for recombinant proteins but on 4 mL resin, after having supplemented the sample with 1 mM Ca^{2+}. The pass through and the elution (10 and 5 mL respectively) were immediately concentrated on a 10 K concentrator and the protein was immediately frozen.

6- *In vitro* CaM-binding assay (overlay assay)

Each purified candidate protein (100 pmol) in a volume of 1-2 µL were spotted onto Whatman Protran nitrocellulose blotting membranes (dots of 3-5 mm diameters on 2-3 cm^2 membrane squares) dried

and independently incubated for 1 hour in 8 mL of assay buffer (50 mM Tris–HCl, pH 7.5, 150 mM NaCl, 1% (w/v) BSA, 1% (v/v) Brij35) either in the presence of 1 mM $CaCl_2$ or of 5 mM EGTA. Incubations were performed in petri dishes of 55 mm diameter. BSA was used as a competitor and Brij35, a non ionic detergent, proved to reduce the background noise. AtCaM1–HRP (250 pmol, of AtCaM1–HRP (final concentration 30 nM) was added and incubation was extended for either 3 hours or 15 minutes at room temperature under constant agitation (55 rpm). After three washes with the assay buffer (10 minutes each), bound AtCaM1–HRP was visualized using an ECL detection system according to the manufacturer's instructions (GE Healthcare Life Sciences, Pittsburgh, PA). For each candidate CaM-binding protein, the intensity of the signal was compared to that of positive and negative controls, either in the presence of Ca^{2+} or EGTA. This was achieved by revealing at the same time (*i.e.* on the same film) the spots of the positive controls (NADK2.1 and Tic32 in the presence of Ca^{2+}) and the negative controls (Vipp1, PAT and NADK2.1 or Tic32 in the absence of Ca^{2+}).

7- Fluorescence anisotropy measurements

7.1- Experimental setup

Fluorescence anisotropy assays were carried out with a MOS-450 spectrometer in a thermostated (25 °C) 150 µL quartz cuvette. For AtCaM-Alexa^{488} measurements, a filter centered at 522.07 nm wavelength (FWHM coordinates: 517.643-526.564 nm) was used. For TAMRA peptides measurements, a 578.45 nm wavelength centered filter (FWHM coordinates: 573.897-582.999 nm) was used (Melles Griot).

Assay conditions were: 100 mM Hepes-KOH pH 7.5, 200 mM KCl, and variable amounts of AtCaM1 and its partners.

The surfactant (14 µM) Lauryldimethylamine-oxide (LDAO) was added to the assays for the measurement of the interaction of the ceQORH CaM-binding peptides with AtCaM1. In the absence of LDAO similar results were obtained but fluorescence was less stable.

Unlabeled AtCaM1 (when TamRa labeled peptides were used) or partner concentrations (when At-CaM1-Alexa^{488} was used) were increased by incremental additions of small volumes of concentrated solutions. Total added volume lead to less than 5% dilution of the assays.

Fluorescence anisotropy values detected were averaged over one minute.

In a control assay, the Alexa and the TamRA probe alone did not show any affinity for AtCaM1.

7.2- Interaction between AtCaM1-Alexa^{488} and CaM-binding proteins

Interaction of AtCaM1-Alexa^{488} (200 nM) with unlabeled candidate proteins (NADK2.1, TS2, ceQORH, Lox2 and XK1-like) was followed by the increase in fluorescence anisotropy with excitation set at 488 nm and emission set at 522 nm. The concentration of the candidate protein was increased by incremental addition of small volumes of concentrated solutions.

7.3- Interaction between AtCaM1 and the CaM-binding peptide of NADK2 and ceQORH

5-carboxytetramethylrhodamine (TamRA)-labeled peptides were bought from Peptide Specialty Laboratories (Heidelberg, Germany). Peptide sequences with label at the *N*-terminus were as follows:

NADK2 CaM-binding site	IYVHSKEGVWRTSAMVSRWK
Tic32 CaM-binding site	VKDTELAKKVWDFSTKLTDS
CeQORH CaM-binding site	AMWTYAVKKITMSKKQLVPL
CeQORH mutated CaM-binding site	AMWTYAVKKITGSAAQLVPL
Control peptide	TKALGISYGRKKRRQRRRA

Interaction of each TamRA-labeled CaM-binding peptide (50 nM, Peptide Specialty laboratories, GmbH, Heidelberg) with unlabeled AtCaM1 was followed by the increase in fluorescence anisotropy with excitation at 546 nm and emission at 579 nm.

TamRA-peptide powders were diluted in water with 30% (v/v) dimethylformamide to a final concentration of 3.6 mM and stored at -20 °C. Before use, stock solutions were diluted to a concentration of 5 µM in 100 mM Hepes, pH 7.5 and 200 mM KCl, supplemented with 5% (v/v) dimethylformamide.

Peptide concentration was measured spectrophotometrically (ε_{540nm}= 55,000 M^{-1} cm^{-1}) assuming 100% labeling.

Unlabeled AtCaM1 concentration was increased progressively by addition of small volumes of concentrated solutions.

7.4- Ca^{2+} dependency of the interaction

In order to confirm the Ca^{2+} dependency of the interaction, at the end of each curve an excess of EGTA (300 µM) was added to the reaction and fluorescence anisotropy value of AtCaM1 or the CaM-binding peptide decreased down to its minimum (*i.e.* the same value as in the absence of the partner).

In order to quantify the Ca^{2+} dependency, 50 nM of the CaM-binidng peptides of ceQORH and NADK2 were incubated with AtCaM1 at 80% saturation in the absence of Ca^{2+} and in buffer treated with chelex, in order to remove all traces of Ca^{2+}. Ca^{2+} was progressively added to the reaction mixture.

7.5- Data analysis

In all experiments the curves were analyzed using Kaleidagraph software (Synergy Software, Reading, PA).

Under our experimental conditions, the fraction of ligand (i.e. unlabeled protein) involved in complex formation with the labeled "receptor (*i.e.* AtCaM1-$Alexa^{488}$ or TamRa labeled peptide) is not negligible compared to the total ligand concentration, a fact that needs to be considered for during data analysis for deriving precise K_d values. Assuming the simple reaction:

^{Labeled}Receptor + Ligand ↔ ^{Labeled}Receptor-ligand,

the relation between anisotropy, K_d and concentrations of labeled receptor and of unlabeled "ligand" is given by **Eqn. 1** (Blanchoin et al, 1998):

$$r = r_{\text{free receptor-labeled}} + \left(r_{\text{bound receptor-labeled}} - r_{\text{free }_{\text{free receptor-labeled}}}\right) \cdot \left[\frac{\left(K_d + \left[\text{Receptor}^{\text{labeled}}\right] + [\text{Ligand}]\right) - \sqrt{\left(K_d + \left[\text{Receptor}^{\text{labeled}}\right] + [\text{Ligand}]\right)^2 - \left(4\left[\text{Receptor}^{\text{labeled}}\right] \cdot [\text{Ligand}]\right)}}{2 \cdot \left[\text{Receptor}^{\text{labeled}}\right]}\right]$$

(Eqn.1)[2]

where r is the observed anisotropy, $r_{\text{free receptor-labeled}}$ is the anisotropy of free TamRA-peptide or free AtCaM1-Alexa^{488}, $r_{\text{bound receptor-labeled}}$ is the anisotropy of TamRA-peptide bound to AtCaM1 or of At-CaM1-Alexa^{488} bound to a protein partner. [Receptor$^{\text{labeled}}$] is the total concentration of receptor, [Ligand] is the total concentration of AtCaM1when the TamRa peptides are used or protein partner when AtCaM1-Alexa^{488} is used, and K_d the dissociation equilibrium constant of the complex.

Fluorescence anisotropy of peptide1-CaM1 as a function of [Ca^{2+}] was fitted by a Hill equation:

$$r = r_{\text{free peptide}} + (r_{\text{bound peptide}} - r_{\text{free peptide}}) \cdot \frac{\left[Ca^{2+}\right]^{n_h}}{\left(K_{0.5}\right)^{n_h} + \left[Ca^{2+}\right]^{n_h}} \quad \textbf{(Eqn.2)}^3$$

where r is the observed anisotropy, r_{free} peptide is the anisotropy of free TamRA-peptide, r_{bound} peptide is the anisotropy of TamRA-peptide bound to AtCaM1, [Ca^{2+}] is the Ca^{2+} concentration total, $K_{0.5}$ is the Ca^{2+} concentration producing half of the maximal change in anisotropy value and n is the Hill number.

To fit the competition curves, we firstly needed to calculate the concentration of free AtCaM1 before the addition of the competitor. This can be done by using **Eqn.3**,

$$[L]_0 = \frac{-\left([\text{R}]_T - [\text{L}]_T + K_{d1}\right) + \sqrt{\left([\text{R}]_T - [\text{L}]_T + K_{d1}\right)^2 + 4 \cdot K_{d1} \cdot [\text{L}]_T}}{2} \quad \textbf{(Eqn. 3)}^4$$

[2] Fo interested readers, **Eqn.1** in the following form can be used for fitting or simulations: r= $r_{\text{free receptor}}$ + ($r_{\text{bound receptor}}$-$r_{\text{free receptor}}$)*(($K_D$+[receptor]+[Ligand])-sqrt((K_D+[receptor]+[Ligand])^ 2-(4*[receptor]*[ligand])))/(2*[receptor])

[3]For interested readers, **Eqn.2** in the following form can be used for fitting or simulations: r= $r_{\text{free peptide}}$ + ($r_{\text{bound peptide}}$-$r_{\text{free peptide}}$)*((Ca^{2+})^{nk}/(($K_{0,5}$)^{nk} + (Ca^{2+})^{nk}))

[4] For interested readers, **Eqn.3** in the following form can be used for fitting or simulations: L_0=(-(R_T-L_T+K_{D1}) +sqrt((R_T-L_T+K_{D1})^2+4*K_{D1}*L_T))/2

where, $[L]_0$ is the free ligand concentration (*i.e.* unlabeled protein), $[R]_T$ is total receptor concentration (*i.e.* labeled component), $[L]_T$ is total ligand concentration and K_{D1} is the K_D of the first interaction.

Fluorescence anisotropy competition experiments were then fitted with a hyperbolic equation that considers the affinity of the receptor for the first ligand and the concentration of free ligand before addition of the competitor (**Eqn. 4**, Vinson et al, 1998):

$$r = r_{\text{free labelled receptor}} + \frac{\left(r_{\text{labelled-receptor□ligand1}} - r_{\text{free labelled-receptor}}\right)}{K_{d1} \cdot \frac{\left(\left[\text{Competing Ligand2}\right] + K_{d2}\right)}{\left(K_{d2} \cdot \left[\text{Ligand1}\right]_0\right)} + 1}$$

(Eqn.4)[5]

where [Competing ligand2] is the total concentration of the competitor, K_{d1} the dissociation equilibrium constant for the binding of Ligand 1 to the receptor, $[Ligand1]_0$ is the free concentration of the first ligand (calculated using **Eqn. 3**), and K_{d2} the dissociation equilibrium constant for the binding of the competing ligand to the receptor.

8- Measurement of NADK2 activity

NAD kinase phosphorylates NAD from ATP, in the presence of excess of Mg^{2+}. Assays were carried out in 50 mM Tris-HCl pH 7.5 in a total volume of 100 µL.

Production of NADP was carried out as described by Turner et al (2004) with few modifications. The NADK-containing extract (5-20 µL) was incubated in the presence of saturating concentrations of NAD (1 mM, from a 50 mM solution in water), ATP (5 mM from a 200 mM stock solution in water), $MgCl_2$ (10 mM from a 1 M stock solution in water), and in the presence or absence of Ca^{2+}/CaM (1 mM Ca^{2+} and 300 nM bovine CaM or AtCaM1), in 50 mM Tris-HCl pH 7.5. For assays conducted in the presence of a CaM inhibitor, W7 and TFP stock solutions (20 mM) were prepared in dimethylformamide and stored at -80 °C. Inhibitors were used at a final concentration of 50 µM. Incubation was carried out at 30 °C. The reaction was stopped by heating at 95 °C. When highly concentrated protein

[5]For interested readers, **Eqn.4** in the following form can be used for fitting or simulations: $r = r_{\text{free labeled receptor}} + (r_{\text{labeled receptor + ligand1}} - r_{\text{free labeled receptor}})/(1+K_{D1}*(K_{D2}+[\text{Competing Ligand2}])/(K_{D2}*[\text{Ligand1}]))$

extracts were used the heated reaction was centrifuged at 14,000 rpm to remove proteins. The NADP produced was then quantified thanks to a coupled reaction involving the enzyme Glucose-6-P dehydrogenase (Sigma-Aldrich, 0.1 U/100 µL reaction diluted in 50 mM Tris pH 7.5). We used the protocol of Turner et al, (2004) with some modifications. The G6PDH indeed uses NADP to dehydrogenate the Glucose-6-phosphate and produce 6-phosphogluconate. The NADP reduced to NADPH is then re-oxidized thanks to a cycling assay. Firstly, the oxidizing molecule Phenazine methosulfate (PMS, 0.8 mM, from a stock solution at 5 mM in water) oxidizes NADPH. Once reduced, PMS transfers its electron to dichlorophenolindophenol (DCPIP), (0.4 mM, from a stock solution of 5 mM in water). DCPIP, a blue compound, becomes transparent upon reduction leading to a decrease in the absorbance at 600 nm. The constant re-oxidation of NADPH allows the reaction of the G6PDH to proceed linearly until all the DCPIP (limiting substrate) is consumed (**Fig M.2**).

NADP concentration is therefore proportional to the rate of the G6PDH reaction, and can be calculated thanks to a titration curve obtained in the same conditions with variable amounts of NADP (0.25-20 µM) and with the same amount of G6PDH. The second reaction (NADP quantification) was carried out in a 100 µL reaction volume in quartz cuvette. Measurements were done on a Jasco V-650 spectrophotometer (Jasco inc., Japan) at 25 °C.

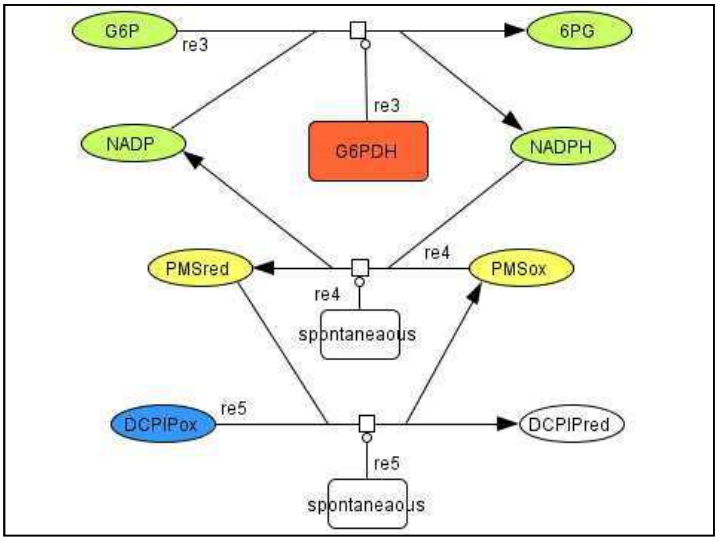

Fig M2 Reaction of the G6PDH enzyme used to quantify NADP produced by NAD kinase. G6P: glucose-6-phosphate; 6PG: 6-phosphoglucono-δ-lactone; G6PDH: glucose-6-phosphate dehydrogenase; PMSred: phenazine methosulfate reduced; PMSox: phenazine methosulfate oxidized; DCPIPox: dichlorophenolindophenol oxidized; DCPIPred: dichlorophenolindophenol reduced.

Chapter 1:

Quantitative characterization of NADK2 interaction with AtCaM1

Introduction

As illustrated in the **Introduction**, the most important challenge in the study of the role of CaM and CMLs consists in identifying their targets. In addition, several parameters (*i.e.* the Ca^{2+}-dependency of the complex formation, the affinity of the two proteins) need to be carefully considered in order to estimate the physiological importance of these interactions. Quantitative and flexible tests are difficult to develop because of the extreme variety of CaM effects and of the nature of its partners (*i.e.* enzymes, membrane transporters and structural proteins).

As a first step in our survey of plastidial CaM-binding proteins we therefore developed a qualitative and quantitative approach for the detection of plastidial Ca^{2+}/CaM-controlled proteins. To do so, we took advantage of the possibility of monitoring the formation of protein-protein complexes by fluorescence anisotropy CaM-binding tests.

In this chapter, we will illustrate the application of two fluorescence anisotropy-based tests to the study of the most well characterized plastidial CaM-binding protein, *i.e.* NADK2. We will firstly give a rapid summary of current knowledge about the CaM interaction with NADK2 and describe the use of fluorescence anisotropy for analyzing the formation of protein-protein complexes. We will then describe the results we obtained by applying the two quantitative tests we designed to the NADK2-AtCaM1 interaction. These tests will be subsequently applied to the characterization of several other interactions (**Chapters 2-4**). Our results, combined with a detailed analysis of the literature of this topic, prompted us to perform also a more careful study of the CaM-NADK interaction, which will be illustrated in **Chapter 6**.

- **Plant NAD kinases: identification of a plastidial CaM-binding isoform of *Arabidopsis thaliana***

NAD kinase (ATP:NAD 2'-phosphotransferase, *EC 2.7.1.23*) is the enzyme responsible for the phosphorylation of NAD to NADP. All organisms so far investigated possess at least one isoform of this enzyme, with the exception of some intercellular parasites that can use the NADP of the host cell (Agledal et al, 2010).

As briefly illustrated in the **Introduction**, and more in detail in **Chapter 6**, a CaM-dependent NADK activity was detected several times in plant tissues, starting from the 80s. However, during these earlier studies, the identification of the gene coding for plant NADKs was not achieved due to lack of genetic tools and the instability of the protein.

More recently, three Arabidopsis NAD kinases were identified. They were named NADK 1, 2 (Turner et al, 2004) and 3 (Turner et al, 2005). This third enzyme phosphorylates NADH rather than NAD.

Despite no signs of CaM-dependent activity, Turner et al (2004) reported that the recombinant NADK2 enzyme was able to bind to CaM in a Ca^{2+}-dependent manner. They were therefore able to purify the recombinant enzyme by CaM-affinity chromatography. Then, by the expression of several truncated versions of NADK2, the authors managed to identify a CaM-binding site in a *N*-terminal domain of the protein of unknown function that is not present in the sequence of NADK1 and 3 (**Fig. 1.1**). Interestingly, this site does not correspond to any of the putative CaM-binding sites localized in the protein sequence by the Calmodulin target database (**see Annex I**).

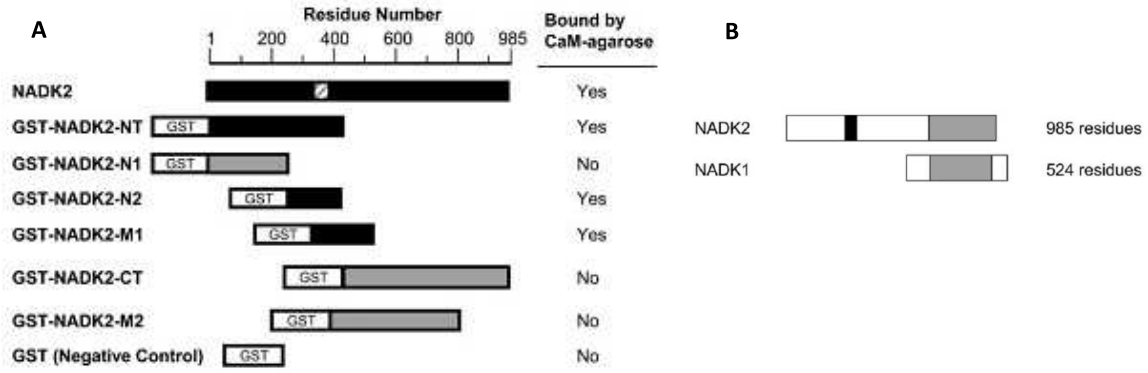

Fig 1.1 Identification of the CaM-binding site of NADK2 (from Turner et al, 2004). **A**. Several GST- NADK2 truncations were tested for their CaM affinity on a CaM column. Black sequences are those that were able to bind on the column in the presence of $CaCl_2$ in excess, while the others were not retained on the column. The striped segment in the whole NADK2 sequence represents the site where the CaM-binding site is supposed to be located, as present in all CaM-binding constructs and absent in all the others. **B**. Comparison between the sequence of NADK2 and NADK1. The CaM-binding site is represented in black and the kinase domain in gray.

The plastidial NADK2 localization was further proved by Chai et al, 2005 and by Waller et al, 2010, using expression of NADK2-GFP constructs in Arabidopsis protoplasts or cells, respectively.

Coherently with its role in photosynthesis, the same authors also showed that the NADK2 gene is preferentially expressed in photosynthetic tissues (Waller et al, 2010).

- **Fluorescence anisotropy as a parameter to study protein-protein interactions**

Fluorescent molecules are able to absorb light in a certain wavelength range and partially release the energy acquired by emitting light at a higher wavelength range (**Fig 1.2**). However, this process requires time (τ) in the range of milliseconds. If the light used to excite a fluorescent probe is polarized on a certain plane, then part of the emitted light will be polarized on the same plane, depending on the extent to which the fluorescent molecule rotates during the interval between excitation and emission. As a consequence, the more the probe is mobile, the less emitted light will be polarized on the same plane as the excitation light, since the probability of the probe to rotate between excitation and emission will increase.

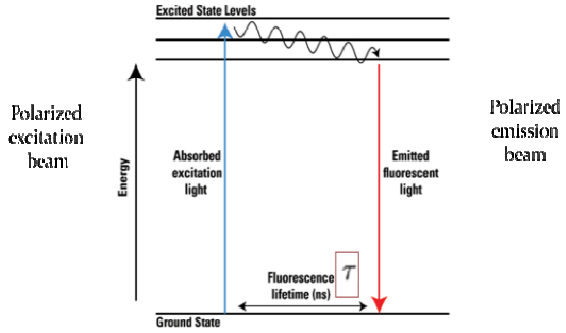

Fig. 1.2 Schematic representation of the emission of fluorescence by a molecule. Blue arrow: excitation light absorbed by the molecule that reaches an excited state level. Red arrow: emitted light released by the electrons of an excited molecule that goes back to its original state level. τ: fluorescence lifetime, *i.e.* the time needed for the fluorescence to be released after absorption. Waved arrow: electron moving through different excited state levels prior to go back to the ground state.

This inequity in the fluorescence emitted on different polarization planes is called fluorescence anisotropy (Jarrett et al, 1995). More precisely, fluorescence anisotropy (*r*) can be defined as the difference of light intensity recovered on the same plane and on one perpendicular plane, divided by the total emitted light (**Fig. 1.3**).

Fluorescence anisotropy can be measured with a spectrofluorimeter able to excite the sample with a polarized light and recover two light beams: the polarized light emitted by the sample on the same

plane, and the polarized light emitted by the sample on a 90° rotation plane (*i.e.* a perpendicular plane). The existence of two perpendicular planes to the emitted light is accounted by the "2" factor at the denominator (see the equation in **Fig.1.3**). Since light can be measured only on one of these two planes, it is assumed that the value is identical in both of them.

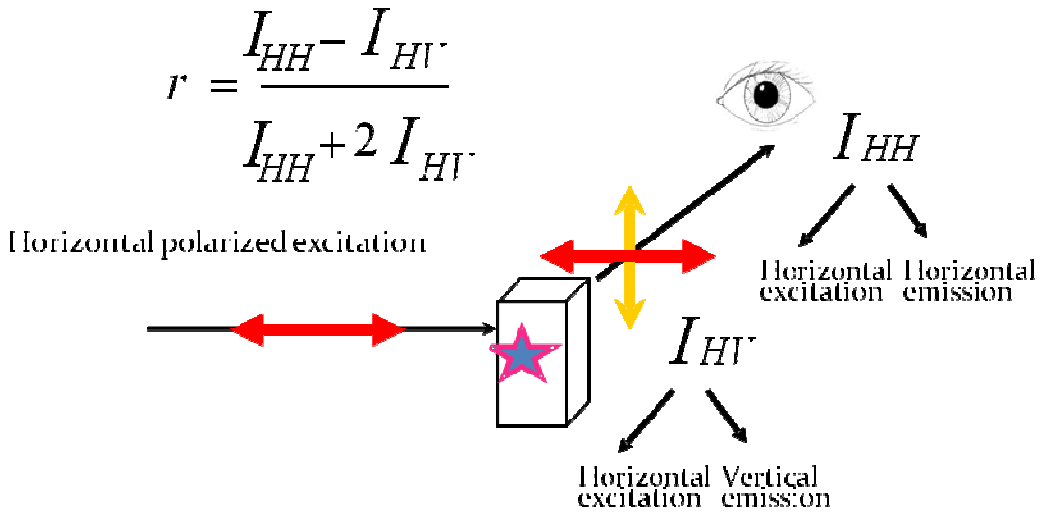

Fig. 1.3 Light path for measuring fluorescence anisotropy. The star represents the fluorescent molecule contained in a cuvette placed into the spectrofluorimeter. The horizontal arrow represents the direction of the excitation polarized light. The eye represents the direction of the emitted light. The spectrofluorimeter measures the emitted light in the same plane of the excitation light and on a perpendicular plane.

It follows that fluorescence anisotropy theoretically varies from a minimal value of 0 (when the mobility of the probe is infinite, therefore the emitted light is no more polarized and $I_{HH} = I_{HV}$, see the equation in **Fig. 1.3**) to a maximal value of 1 (when the probe is totally immobile, therefore no light will be recovered on the perpendicular plane and $I_{HV} = 0$, see the equation in **Fig. 1.3**).

In practice, every fluorescent substance has an intrinsic minimum value of fluorescence anisotropy that depends on its characteristics. For example, little fluorescent molecules will have high tendency to rotate in short periods of time, therefore their fluorescence anisotropy will be generally weaker than that of larger molecules.

However, if a little fluorescent molecule binds a bigger partner, its volume increases and, as a consequence, its rotation is slowed. This results in an increase of the fluorescence anisotropy of the mole-

cule. Intermediate anisotropy values of a given fluorescent molecule are therefore direct measures of the fraction of the molecule bound to its partner. This makes fluorescence anisotropy a valuable parameter to characterize the interactions of proteins with their protein partners (Phizicky and Fields, 1995, Wu et al, 1997) or molecules such as oligonucleotides (Lundblad et al, 1996, Ozers et al, 1997, Benlloch et al, 2011), inhibitors or other chemicals (Bolger et al, 1998). In particular, a fluorescence anisotropy-based screening of candidate CaM inhibitors was recently conducted (Audran et al, 2013).

With respect to other *in vitro* techniques, such as surface plasmon resonance, fluorescence anisotropy is characterized by the fact that both partners are in solution. Another advantage is that fluorescence anisotropy requires the fluorescent labeling of only one species instead of two, as in the case of the FRET technique, or the homogeneous time-resolved fluorescence (Parker et al, 2000). In addition, competition experiments can be designed in which none of the two partners requires a fluorescent labeling. Fluorescence-based techniques are also very sensitive to the environment and variations in fluorescence can sometimes be due to aggregation. On the contrary, when measuring fluorescence anisotropy, the fluorescence value of the labeled partner is not supposed to change during the experiment, and this is an important assessment of the fact that no aggregates or precipitates are formed during the experiment (Parker et al, 2000). Fluorescence anisotropy can also be used to measure protein/protein interactions *in vivo* (see Roberti et al, 2011, and Vishwasrao et al, 2012).

Fluorescence anisotropy appears to be particularly useful for studying CaM interactions, since CaM is a little protein: this generates larger fluorescence anisotropy variations upon complex formation that are easier to detect.

Results

Before setting our fluorescence anisotropy measurements, we needed to produce pure recombinant proteins corresponding to NADK2 and a suitable CaM isoform.

Pure recombinant AtCaM1 was already available in our laboratory (purified by Cécile Giustini, see Dell'Aglio et al 2013 for the details).

As will be discussed later in **Chapter 5**, not all CaM isoforms are able to activate plant NADK, but our activity measurements (see **Chapter 6**) showed that AtCaM1 belongs to this category, so it was suitable for our binding experiments. In addition, AtCaM1 contains a unique cysteine residue that can be useful for labeling the protein with a fluorescent probe (in our case, C_5-maleimide-Alexa^{488}).

Pure NADK2 was not available and we knew from the literature that this protein is quite unstable and difficult to purify to homogeneity. Therefore, we decided to express and purify only the NADK2 domain containing the CaM-binding site.

1- Analysis of NADK2 gene/protein structure.

The NADK2 gene is located in chromosome 1 (At1g21640) and comprises 8 exons separated by 7 introns (**Fig. 1.4**).

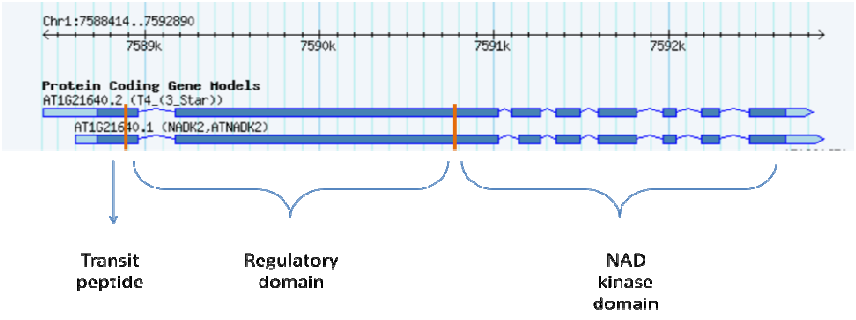

Fig. 1.4 Characteristics of the NADK2 gene. Dark blue blocks represent exons, light blue blocks represent UTRs. The double-headed arrow on the top represents the Chromosome 1 and the location of the gene therein. The regions corresponding to the putative transit peptide, the NAD kinase domain and the regulatory *N*-terminal domain are depicted with blue arrows and parenthesis.

The first of these exons is mostly constituted of the predicted plastidial transit peptide (61 amino acids). The end of the second exon and all the others contain the active domain, responsible for the phosphorylation of NAD to NADP. This region is extremely conserved among NAD kinases of all kingdoms. An alignment of this protein region with Arabidopsis NADK1, human NADK and *E. coli* NADK is reported in **Annex II**.

The end of the first exon and most of the second, which is remarkably long (approximately 1.7 Kb – 568 amino acids) constitute an *N*-terminal protein domain of unknown function. The first part of this region is conserved among plants and algae. Indeed, in all plant species for which the genome is sequenced, a NAD kinase isoform containing a similar *N*-terminal extension can be found. This is also the case for some algae, especially *Ostreococcus tauri*, the free-living algae with the most reduced genome. **Annex II** contains an alignment of available plant and algae NADK sequences containing this long *N*-terminal extension. It is in this domain of unknown function that Turner et al (2004) located the NADK2 CaM-binding sequence of NADK2.

Fig 1.5 contains a schematic representation of all peculiar features of NADK2, including the putative plastidial transit peptide (green), the identified CaM-binding site (magenta) and the active domain (red).

Fig 1.6 represents a sequence alignment of the portion of the identified CaM-binding site in *A. thaliana* NADK2 with the orthologous sequences from other plants. The identified peptide has the characteristics of a 1-8-14 CaM-binding site, (see **Introduction**), where the key residues might be a tyrosine, a valine and a methionine (in red in **Fig 1.6**). Note also the presence of a second tryptophan (position 18) in the motif that is conserved in all the analyzed sequences.

NADK2 protein sequence:

```
1-   MFLCFCPCHVPIMSRLSPATGISSRLRFSIGLSSDGRLIPFGFRFRRNDVPFKRRLRFVI
61-  RAQLSEAFSPDLGLDSQAVKSRDTSNLPWIGPVPGDIAEVEAYCRIFRSAERLHGALMET
121- LCNPVTGECRVPYDFSPEEKPLLEDKIVSVLGCILSLLNKGRKEILSGRSSSMNSFNLDD
181- VGVAEESLPPLAVFRGEMKRCCESLHIALENYLTPDDERSGIVWRKLQKLKNVCYDAGFP
241- RSDNYPCQTLFANWDPIYSSNTKEDIDSYESEIAFWRGGQVTQEGLKWLIENGFKTIVDL
301- RAEIVKDTFYQTALDDAISLGKITVVQIPIDVRMAPKAEQVELFASIVSDSSKRPIYVHS
361- KEGVWRTSAMVSRWKQYMTRPITKEIPVSEESKRREVSETKLGSNAVVSGKGVPDEQTDK
421- VSEINEVDSRSASSQSKESGRFEGDTSASEFNMVSDPLKSQVPPGNIFSRKEMSKFLKSK
481- SIAPAGYLTNPSKILGTVPTPQFSYTGVTNGNQIVDKDSIRRLAETGNSNGTLLPTSSQS
541- LDFGNGKFSNGNVHASDNTNKSISDNRGNGFSAAPIAVPPSDNLSRAVGSHSVRESQTQR
601- NNSGSSSDSSDDEAGAIEGNMCASATGVVRVQSRKKAEMFLVRTDGVSCTREKVTESSLA
661- FTHPSTQQQMLLWKTTPKTVLLLKKLGQELMEEAKEAASFLYHQENMNVLVEPEVHDVFA
721- RIPGFGFVQTFYIQDTSDLHERVDFVACLGGDGVILHASNLFKGAVPPVVSFNLGSLGFL
781- TSHPFEDFRQDLKRVIHGNNTLDGVYITLRMRLRCEIYRKGKAMPGKVFDVLNEIVVDRG
841- SNPYLSKIECYEHDRLITKVQGDGVIVATPTGSTAYSTAAGGSMVHPNVPCMLFTPICPH
901- SLSFRPVILPDSAKLELKIPDDARSNAWVSFDGKRRQQLSRGDSVRIYMSQHPLPTVNKS
961- DQTGDWFRSLIRCLNWNERLDQKAL
```

Fig. 1.5 Complete amino acid sequence of NADK2. Green: putative plastidial transit peptide. Pink: putative CaM-binding site identified using CaM target database: (http://calcium.uhnres.utoronto.ca/ctdb/ctdb/sequence.html). Red: active NAD kinase domain.

```
PpNADK          QVEEFAKLVAVPENKPLYLHSQGGVGRACAMVSRWREYVLQLSGEGMR------------ 261
SmNADK          QVREFADIVSDAANRPVFLQSYAGVVRASAMVSRWREFVLR-------------------- 221
ZmNADK          QVQQFAALVSDGAKKPIYLYSKEGVSRTSAMVSRWKQYVTRSERLAVQ----------NH 368
SbNADK          QVQQFAALVSDGARKPIYLHSKEGVSRTSAMVSRWKQYVTRSERLAVQ----------NH 368
OsNADK          QVQRFAEIVSDSAKKPIYLHSQEGISRTSAMVSRWKQYVTRAERLATQ----------NR 373
HvNADK          QVQQFAALVSDGTKKPIYLHSKEGISRTSAMVSRWKQYATRAERLATK----------KR 370
BdNADK          QVQQFAALVSDGAKKPIYLHSKEGVGRTSAMVSRWKQYATRAERLATQ----------NR 369
AtNADK          QVELFASIVSDSSKRPIYVHSKEGVWRTSAMVSRWKQYMTRPITKEIP------------ 387
AlNADK          QVELFASIVSDSSKRPIYVHSKEGVWRTSAMVSRWKQYMTRPITKEIP------------ 387
JcNADK          HVEKFASLVSDCSKKPIYLHSKEGAWRTSAMISRWRQYMNRSASQFI-----TRSDSGPQ 395
RcNADK          QVVKFASLVSDSTKKPIYLHSKEGAWRTSAMISRWRQYMTRSVSQLF-----IPSDILPQ 382
PtNADK          QVEKFASLVSDSSKKPIYLHSKEGVRRTSAMVSRWRQ------------------------ 376
VvNADK          QVEKFASLVSDSSKKPIYLHSKEGAWRTSAMVSRWRQYMARSALQLVSNQPIVPNEILSR 402
GmNADK          QVVQFASFVSDCSKRPIYLHSKEGVLRTSAMVSRWRQYMARSSSQIVSNPPVTPYDMLLC 390
OlNADK          DVKRFIETVNDDKMRPILVHCKAGIGRTGSLVACWRVHQGMDVDEA-------------- 288
OtNADK          DVDRFIEAVNNESMRPVLVHCKAGIGRTGALVACWRVHQGMDVDEA-------------- 291
MpNADK          LVERFIEVANDRARRPMLVHCKAGIGRTGSMVSCWRISRGMDVDEARS------------ 274
                 *  *   .     :*: : .  *  *: :::: *:
```

Fig. 1.6 Alignment of the putative NADK2 CaM-binding site with other NADK sequences from plant and algae. Isoforms are indicated by the initials of the name of the species followed by "NADK". NCBI sequence codes are as follows. Ol: *Ostreococcus lucimarius* (XP_001421404); Ot: *Ostreococcus tauri* (XP_003083231); Mp: *Micromonas pusilla* (XP_003061343); Pp: *Physcomitrella patens* (XP_001755443); Sm: *Selaginella moellendorffii* (XP_002982512); Zm: *Zea mais* (AFW65483.1); Sb: *Sorghum bicolor* (XP_002449145); Os : *Oryza sativa* (NP_001067415); Hv: *Hordeum vulgaris* (BAJ87225.1); Bd: *Brachypodium distachium* (XP_003577753); At: *Arabidopsis thaliana* (NP_001185057); Al: *Arabidopsis lyrata* (XP_002890449); Jc: *Jatropa curcas* (BAJ53187.1); Rc: *Ricinus communis* (XP_002520312); Pt: *Populus trichocarpa* (XP_002302220); Vv: *Vitis vinifera* (XP_002284607); Gm: *Glycine max* (XP_003544706). Boxed sequence corresponds to the CaM-binding site identified using CaM target database. Well conserved hydrophobic amino acids highlighted in red could allow considering this CaM-binding as a 1-8-14 motif (see text and the introduction to this chapter).

2- Expression and purification of the *N*-terminal domain of NADK2 containing the CaM-binding site

NADK2 was reported to be rather unstable and not easy to purify up to homogeneity. Therefore, in order to investigate the CaM-binding properties of NADK2, we decided to produce and purify only the conserved *N*-terminal domain of unknown function that contains the CaM-binding site. We called this *N*-terminal version NADK2.1 (**Fig 1.7**). We designed our construct in order to keep a histidine-tag in frame at the *C*-terminus to allow affinity chromatography on a Nickel matrix.

NADK2.1 protein sequence:

```
  1- MAQLSEAFSPDLGLDSQAVKSRDTSNLPWIGPVPGDIAEVEAYCRIFRSAERLHGALMET
 61- LCNPVTGECRVPYDFSPEEKPLLEDKIVSVLGCILSLLNKGRKEILSGRSSSMNSFNLDD
121- VGVAEESLPPLAVFRGEMKRCCESLHIALENYLTPDDERSGIVWRKLQKLKNVCYDAGFP
181- RSDNYPCQTLFANWDPIYSSNTKEDIDSYESEIAFWRGGQVTQEGLKWLIENGFKTIVDL
241- RAEIVKDTFYQTALDDAISLGKITVVQIPIDVRMAPKAEQVELFASIVSDSSKRPIYVHS
301- KEGVWRTSAMVSRWKQYMTRPITKEIPVSEESKRREVSETKLGSNAVVSGKGVPTTTTRP
361- WLISDPNSSSVDKLAAALEHHHHHH
```

Fig. 1.7 NADK2 *N*-terminal domain (NADK2.1). In green an initiating Met inserted in place of R61 of the full-length sequence to produce the protein without its predicted plastidial transit peptide (*i.e.* in its mature form). In magenta, the identified CaM-binding site. In blue, the amino acid sequence coded by the pET30 vector that allows the protein to be in frame with a Histidine-tag at the *C*-terminus.

The protein was purified in two steps: Nickel affinity purification (**Fig. 1.8A**) followed by a CaM-affinity chromatography (**Fig 1.8B**). This second step not only allowed the protein purification and confirmed the CaM-binding properties of this protein region. The protein migrating at the correct size (45 kDa) was used to obtain specific antibodies against NADK2 (see Material and Methods section). Note the presence in **Fig. 1.8B** of a band co-eluting with NADK2.1 *N*-terminal domain but with a lower molecular weight. Subsequent western blot analyses revealed that this protein was a degradation product. To perform some assays of crystallization of this protein domain, David Cobessi (IBS, Grenoble) optimized the purification protocol, adding a Q-sepharose step after the Nickel affinity purification and a gel filtration step. Highly pure NADK2.1 protein could thus be obtained (**Fig.1.8C**), virtually free of any degradation product. This protein was used for the following biochemical assays.

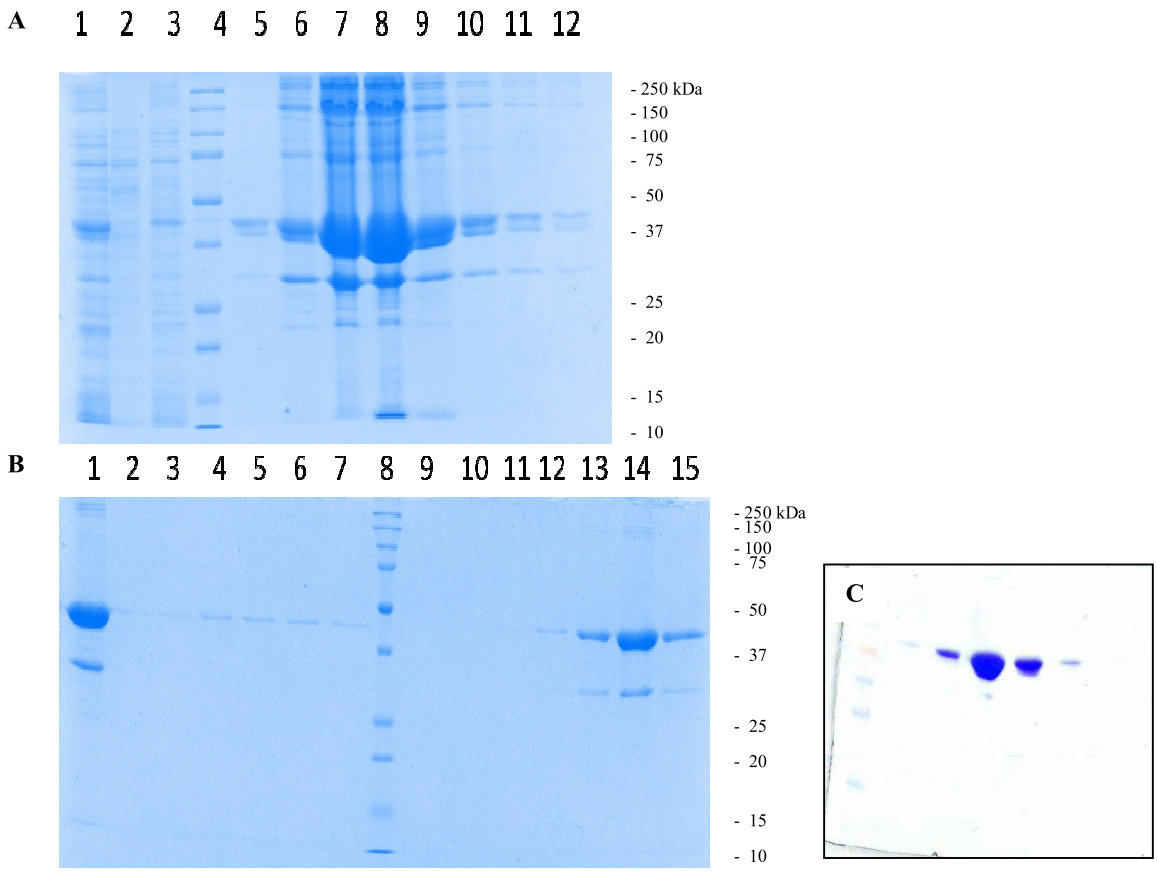

Fig. 1.8 SDS-PAGE documentation of the purification of NADK2.1. **A**. Nickel affinity chromatography. 1: soluble extract; 2-3: column washes; 4: molecular markers; 5-12: elutions with 250 mM imidazole **B.** CaM-affinity chromatography. 1: charge (pooled fractions of the Nickel affinity chromatography); 2-7: column washes; 8: molecular marker; 9-15: elutions with EGTA **C**. Purest NADK2.1 fractions eluted in the last purification step (gel filtration, see text).

3- Quantification of recombinant NADK2.1 affinity for CaM *in vitro* by fluorescence anisotropy

The CaM-affinity chromatography used as a purification step for NADK2.1 confirms that this domain is able to bind to CaM, so we used this *N*-terminal domain in order to develop a quantitative test to measure protein affinity for CaM.

3.1- Measure of the affinity of the NADK2.1 domain for CaM

In order to measure the affinity of NADK2.1 for CaM by fluorescence anisotropy, it was firstly necessary to label one of the two partners in order to make it fluorescent. We decided to label CaM because it was the smaller one, and also in order to use the same labeled protein to assess CaM interaction with other partners (see **Chapter 2**).

We took advantage of the presence of the unique cysteine in the sequence of AtCaM1 to label it with the probe C_5-maleimide-Alexa^{488}, which is excited at 488 nm and emits fluorescence at 522 nm.

AtCaM1-Alexa^{488} (200 nM) was incubated into a buffer containing 100 mM Hepes buffer pH 7.5, 200 mM salt (in order to avoid a-specific interactions), and in the presence of $CaCl_2$ (**Fig. 1.9**). The upper line represents fluorescence, which is measured every second and is stable during the whole time of the experiment (1500 seconds), a requirement for fluorescence anisotropy measurements. The bottom line represents the fluorescence anisotropy data of AtCaM1-Alexa^{488}. Fluorescence anisotropy is stable and does not change when NADK2.1 is added to the medium (at 100 seconds, as indicated by the arrow in **Fig. 1.9**). Fluorescence anisotropy increases after addition of 300 µM $CaCl_2$ (at 200 seconds), but this increase is slow and several minutes are necessary for the anisotropy value to stabilize. Addition of EGTA in excess over $CaCl_2$ (at approximately 1200 seconds) immediately restores the original level of fluorescence anisotropy, that increases again after addition of excess of $CaCl_2$, (1400 seconds), this time much more quickly.

The same experiment conducted with an excess of $MgCl_2$ up to 5 mM instead of $CaCl_2$ led to no variations in the fluorescence anisotropy of AtCaM1-Alexa^{488}, and, in another control experiment, the Alexa^{488} probe alone did not show any affinity for the target protein (not shown).

These results show the formation of a complex between NADK2.1 and AtCaM1-Alexa^{488}. This interaction is triggered by Ca^{2+}, but several minutes are needed to form this complex. This suggests that a slow conformational change of NADK2.1 is required before a stable NADK2.1-AtCaM1-Alexa^{488} complex is formed. Upon dissociation by EGTA, a subsequent and rapid addition of Ca^{2+} shows a much quicker increase in the fluorescence anisotropy, suggesting that the NADK2.1. domain does not

return to its initial conformation very quickly. This particular behavior would require further analyses and might be due to an unstable conformation of NADK2.1.

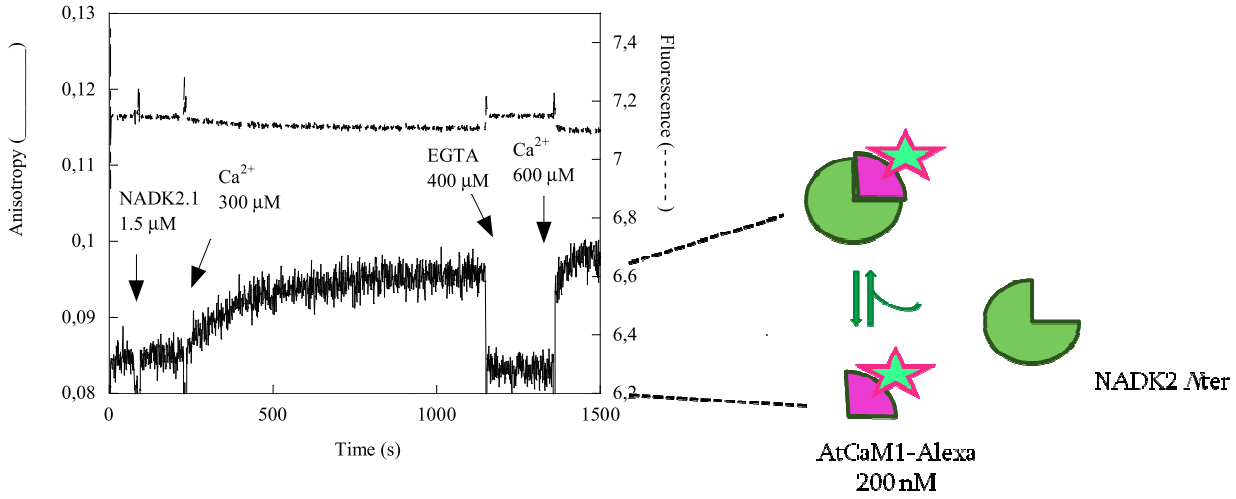

Fig. 1.9 Fluorescence anisotropy of AtCaM1-Alexa^{488} (200 nM) in the presence of $CaCl_2$/NADK2.1. After addition of NADK2.1 (1.5 µM) to **AtCaM1-Alexa^{488}** (at approximately 100 seconds, arrow) fluorescence anisotropy increases only when $CaCl_2$ is added (at approximately 200 seconds, arrow), but the complex formation is slow. Addition of EGTA in excess (400 µM, at approximately 1200 seconds immediately restores the original level of fluorescence anisotropy. Subsequent addition of $CaCl_2$ in excess (at approximately 1400 seconds) increases this value up to its maximum value but much quicker than previously. This behavior was repeatedly observed.

Once demonstrated that NADK2.1 binds to AtCaM1-Alexa^{488} in a Ca^{2+} dependent way, we quantified this binding affinity by progressively increasing the concentration of NADK2.1 in the medium (**Fig. 1.10**).

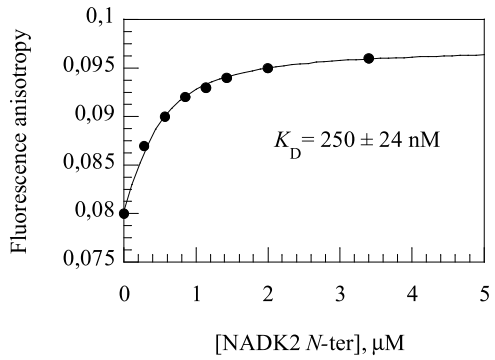

Fig. 1.10 NADK2.1 binding to AtCaM1-Alexa^{488} (0,2 µM) in the presence of 300 µM $CaCl_2$. Data points are the averaged steady-state (*i.e.* stabilized) fluorescence anisotropy values of three independent experiments. The curve represents the best fit obtained by non-linear regression analysis of the averaged data points using **Eqn. 1** in which "U" (unlabeled species) is NADK2.1 and "L" (labeled species) is AtCaM1-Alexa^{488}. Free AtCaM1-Alexa^{488} fluorescence anisotropy value was 0.084, maximal anisotropy value was 0.098 and K_D value was 250 nM (±24).

AtCaM1-Alexa^{488} anisotropy value reached a plateau for NADK2.1 concentration of approximately 4 µM.

To calculate the affinity of NADK2.1 for CaM, the amount of ligand (*i.e.* NADK2.1) bound to the receptor (*i.e.* AtCaM1-Alexa^{488}, 0.2 µM) is not negligible with respect to the total quantity of ligand (50 nM). Therefore, the K_D value was estimated using **Eqn.1** (see **Material and Methods**) which accounts for the amount of NADK2.1 bound to AtCaM1-Alexa^{488}. With this fit, a K_D value of NADK2.1 for AtCaM1-Alexa^{488} of 250 nM was calculated.

This value is in the range of high-affinity CaM-binding proteins and is for example similar to the one measured for plant CaM-activated glutamate decarboxylase (Gut et al, 2009).

3.2- Measure of the affinity of the NADK2 CaM-binding peptide for CaM

Since the labeling of AtCaM1 might affect its affinity for Ca^{2+} and/or for NADK2.1, we decided to design another test in which the labeling of the two partners is reversed.

We purchased a synthetic peptide corresponding to the 20 amino acids of the identified NADK2 CaM-binding site. This peptide was provided with a TaMRA fluorescent probe (a rhodamine molecule) at the *N*-terminus. We first checked that AtCaM1 did not bind to the free probe. Indeed when AtCaM1

was incubated in the presence of the free probe in the presence or the absence of Ca^{2+} no change in the anisotropy value could be observed.

Then, we made sure that the fluorescence anisotropy of the TamRa labeled peptide was stable during time and in the presence and absence of Ca^{2+} (**Fig. 1.11** upper line). The addition of 120 nM AtCaM1 (at 50 seconds) did not trigger any change in the fluorescence anisotropy of the peptide. When an excess of Ca^{2+} was added (110 seconds), a large and immediate increase in the fluorescence anisotropy was observed. Subsequent addition of EGTA in excess (160 seconds) restored the original fluorescence anisotropy level, which increased again after addition of Ca^{2+} (230 seconds). Then, we incubated the peptide with increasing amounts of unlabeled AtCaM1 obtaining a Ca^{2+}-dependent interaction (**Fig 1.12**).

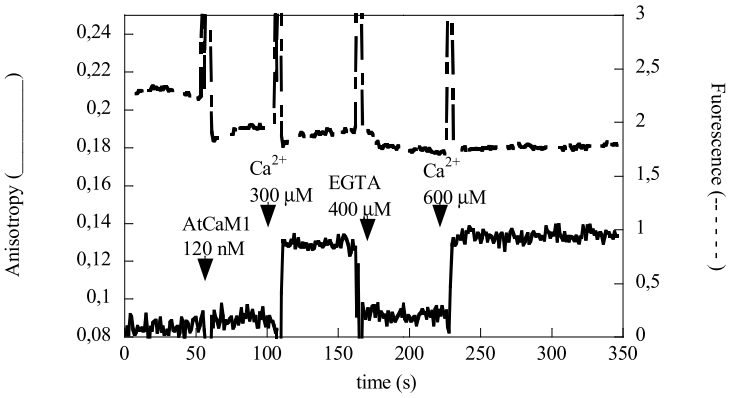

Fig. 1.11 Fluorescence and fluorescence anisotropy measurements using the NADK2.1 TamRa-labelled 20-aminoacid peptide corresponding to the NADK2 CaM-binding domain. The x-axis corresponds to the time of measurements**.** The upper line (right Y axis) corresponds to the fluorescence. The lower line (left Y axis) corresponds to the fluorescence anisotropy. TamRa-labeled peptide was used at a concentration of 50 nM; Following the addition of AtCaM1 (120 nM, at 50 seconds) the fluorescence remains stable during the entire measure which is a requirement of anisotropy measurement. The four "peaks" of fluorescence are caused by the agitation of the solution after each addition. Ca^{2+} (300 µM) was added at approximately 100 seconds; Excess of EGTA (400 µM) was added at 160 seconds; Excess Ca^{2+} (600 µM) was added at approximately 230 seconds.

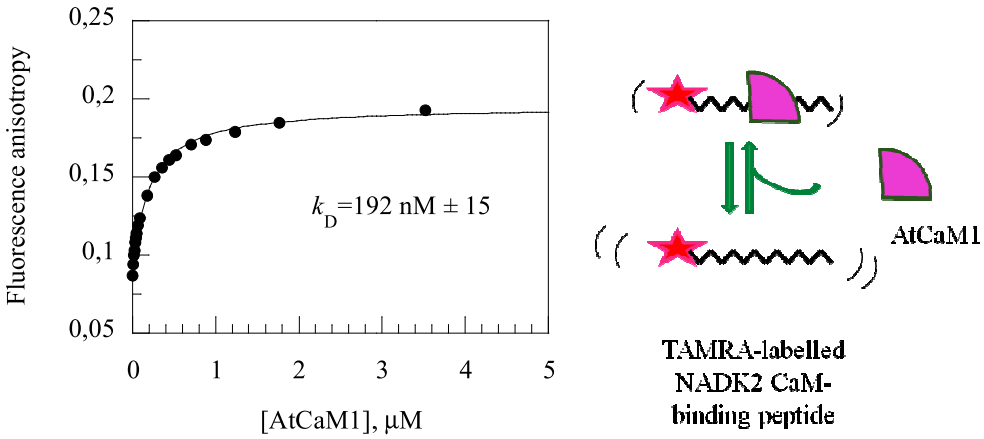

Fig. 1.12 AtCaM1 binding to the NADK2 peptide (50 nM) in the presence of 300 µM $CaCl_2$. Data points are the averaged fluorescence anisotropy values of three independent experiments. The curve represents the best fit obtained by non-linear regression analysis of the averaged data points using **Eqn. 1** in which "U" (unlabeled species) is AtCaM1 and "L" (labeled species) is the TamRa-labeled peptide. Free TamRa-labeled peptide fluorescence anisotropy value was 0.082, maximal anisotropy value was 0.195 and K_d value was 190 nM (± 15). Experimental conditions are the same as in **Fig. 1.11**.

As the concentration of AtCaM1 increased, the fluorescence anisotropy of the peptide increased too until a plateau was reached, at approximately 4 µM AtCaM1. The curve represents the best fit obtained by non-linear regression analysis of the averaged data points using **Eqn. 1**, for which a K_D value of 192 nM was calculated. This value is very close to the one previously calculated for the NADK2.1 domain/AtCaM1-Alexa^{488} (250 nM, **Fig. 1.10**), despite the very different nature of the CaM-binding material. Since both tests (NADK2.1 binding to AtCaM1-Alexa^{488} and AtCaM1 binding to the NADK2.1 peptide) gave similar results, we concluded that the affinity of NADK2.1 for CaM was close to 200 nM, and that this affinity was only due to the previously identified CaM-binding peptide (*i.e.* the rest of the domain does not contribute to the interaction).

We then tested the binding in different conditions. We showed that the presence of a mild detergent (LDAO) or variations in the salt concentration of the medium weakly influence the binding, although the presence of LDAO induced a shift in the maximum level of anisotropy. However, a lower buffer concentration drastically compromised the interaction (**Fig 1.13**).

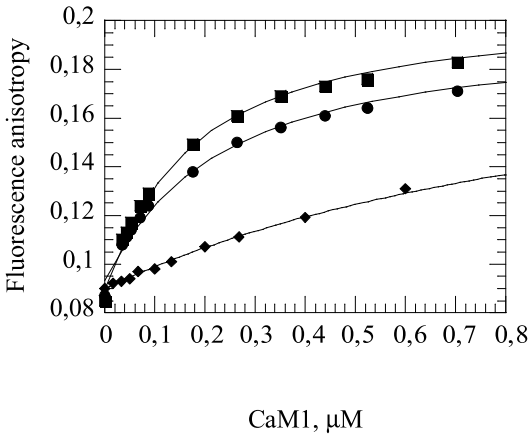

Fig. 1.13 Interaction of the NADK2 CaM-binding peptide with AtCaM1 in various conditions. (●) absence of LDAO and 200 mM Hepes-KOH pH 7.5; (■) presence of LDAO and 100 mM Hepes-KOH pH 7.5; (♦) absence of LDAO and 10 mM Hepes-KOH pH 7.5. In all cases, buffer was supplemented with 200 mM KCl.

These results suggested that the buffer composition can sometimes affect the binding properties and this must be taken into account. For these reasons, all other experiments in the following chpters were performed in the same conditions (*i.e.* 100 mM Hepes-KOH pH 7.5, 200 mM KCl).

Conclusions

Our quantitative tests applied to the NADK2 protein (*i.e.* binding of NADK2.1 to AtCaM1-Alexa^{488} or binding of AtCaM1 to the NADK2 CaM-binding peptide) led to calculate a K_D for AtCaM1 close to 200 nM, comparable to what previously obtained for another well characterized plant CaM partner, *i.e.* GAD (Gut et al, 2009).

As a first conclusion, the use of two quantitative tests to characterize the CaM interactions confirmed the high NADK2 affinity for CaM and the coherence of the results suggests that these tests can be applied to the identification of new CaM interactions as described in the following chapters. These tests might also give useful clues about the conformational state of the proteins. For example, the delay observed for the establishment of the complex NADK2.1-AtCaM1-Alexa^{488} might be due to conformational changes that could be further analyzed. This could simply be due to residual Nickel present in the buffer of the NADK2.1 protein entering into competition with Ca^{2+}. Another hypothesis is that in the absence of CaM this domain adopts a 3D conformation in which the CaM-binding site is not exposed, therefore deep and slow changes in the protein conformation are needed in order to form the complex. Further experiments are needed in order to better explain this behavior.

The obtained K_D of 200 nM, despite confirming its Ca^{2+}-dependent affinity of NADK2 for CaM, is suspicious if compared to the extremely high apparent affinity of CaM for the partially purified native NADK enzyme described several times in the literature ($K_{0.5}$ for the activation in the nanomolar or even subnanomolar range, see Delumeau et al, 1998, 2000). For this reason, we decided to analyze more deeply the NADK-AtCaM1 interaction (see **Chapter 6**).

Chapter 2:

A large-scale analysis of plastidial CaM-binding proteins and its validation

Introduction

In **Chapter 1**, we proposed a quantitative characterization of the interaction of NADK2 with CaM. Our results suggested that the NADK2 affinity for CaM is comparable to that of GAD2 and other well-characterized cytosolic CaM partners. These new data and the existence of few other previously identified CaM partners in the chloroplast prompted us to perform a large-scale analysis of plastidial CaM interactors, in order to obtain a broader picture of the Ca^{2+}/CaM-dependent regulation of this organelle.

In this chapter, we firstly discuss the presence of other potential CaM interactors in the chloroplast and the large-scale proteomic approach that was chosen and performed by my colleagues in collaboration with the EDyP laboratory of the CEA-Grenoble. We then critically analyze the proteomic results and describe the validation approaches that we adopted and optimized in order to confirm the new putative interactions.

- **Previous studies allowed the discovery of potential CaM partners in the chloroplast**

Besides NADK, whose regulation by CaM was discovered serendipitously long ago before the genomic era, few other plastidial proteins were proposed to interact with CaM. They were identified using different approaches, both targeted and untargeted. A list of all these proteins is provided below.

PSAN (At5g64040)

PsaN is a subunit of Photosystem I. By a phage-display survey, Reddy et al (2002) identified this protein as a potential CaM partner. Briefly, they generated several Arabidopsis and bean cDNA expression libraries from plants/cell cultures kept in different conditions. Colonies producing proteins able to interact, in the presence of $CaCl_2$, with ^{35}S-CaM (a mixture of AtCaM 2, 4 and 6) were isolated. The procedure was repeated three times and at the third selection round the experiment was performed also in the presence of EGTA. Corresponding cDNAs were then isolated from the phage colonies and the protein identity was deduced from the cDNA sequence by comparison to the Arabidopsis genome database. Seventy-seven proteins were identified by this approach and all of them bound to CaM only in the presence of $CaCl_2$. One of them was PsaN and another one the elongation factor 1-α.

EF1-α (At1g07920)

This protein is an elongation factor involved in protein translation. Durso and Cyr (1994) firstly demonstrated that a 50 kDa protein of carrot bound to tubulins by tubulin-affinity chromatography, then identified this protein as EF1-α by aminoacid sequencing. By CaM-affinity chromatography they showed that it was also able to bind to CaM in a Ca^{2+}-dependent manner. EF1-α was also detected by the phage-display analysis of Reddy et al cited above.

The localization of this protein in the chloroplast is however uncertain. The protein was detected by 68 spectral counts in the thylakoidal fractions used to build the AT_CHLORO database (Ferro et al, 2010), which is a reference of all known plastidial proteins of Arabidopsis. However, prediction programs state that this protein is more likely cytoplasmic or mitochondrial and its localization was never directly verified by GFP fusions or other *in vivo* techniques.

CPN21(At5g20720)

CPN21, also known as CPN10 is a functional homologue of the *E. coli* chaperone protein GroES. By a phage display screening similar to the one adopted by Reddy et al (2002), Yang and Poovaiah (2000) identified CPN21 as a Ca^{2+}-dependent CaM-binding protein. The authors confirmed the CaM interaction by a CaM-binding assay on blots (overlay assay, see below). They also demonstrated by truncations that the CaM-binding site is located at the *C*-terminal of the protein and that only one binding site per protein is present. Incubations of the blotted protein with ^{35}S CaM at different concentrations in the presence of Ca^{2+} also allowed deducing a K_D on the basis of the signal intensity estimated to be approximately 160 nM.

AAA+ ATPase (AFG1-like protein 1, At4g30490)

AAA+ ATPases are proteins associated with several functions. With the same procedure adopted for Tic32 (*i.e.*, CaM affinity chromatography of plastidial subfractions coupled with mass spectrometry, see **Introduction** and **Chapter 4**) the same authors isolated this other CaM-binding protein (Bussemer et al, 2009). By testing the CaM-binding of several deletion mutants they localized the CaM-binding site into the AAA+ domain. In the same work, the authors localized the protein in both chloroplasts and mitochondria by *in vitro* import experiments.

The literature on plastidial CaM-binding proteins summarized above shows that the role of CaM in the chloroplast is far from being understood. The CaM-binding site was not localized in all identified proteins and the plastidial localization of these proteins was not always confirmed. Even more importantly, the affinity of these proteins for CaM was only semi-quantitatively measured *in vitro*, and no data are available on the possible consequences of CaM on the protein activity. The only exceptions are native CaM-sensitive NADK, as discussed in **Chapter 1**, and Tic32, for which an inhibitory effect of its dehydrogenase activity in the presence of Ca^{2+}/CaM was reported. While providing support for the presence of Ca^{2+}/CaM control in the chloroplast, these studies do not give full understanding of this regulatory mechanism. For this reason, we decided to look at a larger scale.

- **Choice of the experimental system**

Large-scale studies on CaM-binding proteins were previously conducted in various organisms by several techniques. They allowed the identification of new potential CaM partners, frequently more than one hundred. Here we briefly summarize the techniques employed, their drawbacks and major findings.

<u>mRNA display</u>

Shen et al (2005 and 2008) used the mRNA display technique to identify CaM-binding proteins of human and *Caenorhabditis elegans*. This technique is based on *in vitro* synthesis of proteins linked to their mRNA sequence. Several selection cycles for CaM-binding proteins allow isolating proteins for the higher CaM affinity.

<u>Protein arrays</u>

Popescu et al (2007) used an Arabidopsis protein array of 1133 proteins (mostly kinases and transcription factors) expressed *in planta,* by transient protein expression in *Nicotiana benthamiana* leaves infiltrated with *Agrobacterium tumefaciens*. O'Connell et al (2010) used also a protein array - in this case of recombinant human proteins expressed in bacteria. They both verified the CaM-binding of their candidates by incubation with a labeled CaM: Alexa Fluor 488- or 546-conjugated S17C human CaM

in the case of O'Connell et al (2010), or several Alexa Fluor 647-conjugated CaM/CMLs isoforms in the case of Popescu et al (2007). In both cases, the set of tested proteins is limited and does not allow obtaining a complete coverage of the organism proteome. Moreover, especially in the case of recombinant proteins produced in bacteria, differences between the endogenous and the recombinant protein might exist, especially in their post-translational modifications.

Yeast two-hybrid

This approach was employed by Perochon et al (2010) who successfully identified PRR2 (pseudo-response regulator 2) as a target of Arabidopsis CML9. Previously, the same technique was employed in order to confirm *in vivo* the interaction between CaM and neurogranin (Prichard et al, 1999). A reverse approach (*i.e.* Y2H assay performed using the CaM partner as a bait) was used by O'Connor et al (1998).

CaM-affinity purifications combined with mass spectrometry

Other authors used CaM-affinity purification of tissue extracts combined with mass spectrometry analysis of the CaM-bound proteins: Berggård et al (2006) investigated mouse brain CaM-binding proteins, while Calábria et al (2008) focused on CaM targets of the brain of workers honeybees. The same strategy used *in planta* also allowed the successful detection of some plastidial CaM-binding proteins (Tic32 and AFG1-like, see above).

This last technique has the advantage to be performed on native proteins, therefore correctly assembled and processed. This is particularly important for plastidial proteins, since they are subjected to cleavage of the transit peptide, and sometimes phosphorylations, methylations, glycosylations or interactions with membranes. We therefore considered that this method was the most suitable to address our question.

A proteomic analysis of plastidial CaM-binding proteins was possible thanks to the high expertise of the LPCV laboratory in the purification of plastidial subcompartments and to collaboration with the EDyP laboratory for the liquid chromatography - mass spectrometry analysis. This collaboration previously allowed building the AT_CHLORO Database that gives a comprehensive view of the proteome

of the chloroplast and its subcompartments (stroma, thylakoids and envelope), with an indication of the relative abundance of each one on the basis of the spectral counts observed (Ferro et al, 2010).

In a CaM-affinity purification combined with mass spectrometry the relative abundance of proteins in cell extracts is extremely variable (approximately 3 mM for the large subunit of Rubisco to few nM for low abundant proteins). Proteins can also interact with each other forming tightly associated complexes and low-affinity or a-specific interactions with the CaM resin could determine the detection of certain proteins. In order to minimize these inconvenients, we started from highly pure protein samples from the different plastidial subcompartments, in order to ensure a good representation of all proteins and we established a validation protocol based on several techniques.

Previous large scale works not always reported the effort of confirming the newly identified potential CaM partners. When it was the case, several strategies were employed, with various protocols and controls. The most frequent techniques were co-immunoprecipitations, pull-down, Surface Plasmon Resonance (Biacore) and the overlay assay (an *in vitro* CaM-binding test performed with a radioactive or HRP-labeled CaM version). All these tests are rather qualitative, with the exception of the Biacore, for which a good estimation of the k_{on} is possible but not necessarily of the k_{off} (Nieba et al, 1996).

For our work, we decided to validate a subset of the detected proteins firstly with the overlay assay, since it is a widely accepted technique and easy to set up. This assay was reported to be quantitative (*i.e.* the signal corresponding to radiolabeled CaM bound to its target was proportional to the concentration of the CaM-partner, see Choi et al, 2005, for an example) and allowed the detection of several *bona fide* CaM-partners (Gayle et al, 1987). However, this test presents several drawbacks such as the denaturation of the protein during the SDS-PAGE and the subsequent fixation of the protein on a membrane (Oehler et al, 1999). In addition, we realized that the comparison of the binding properties of several proteins is not easy to achieve, and several parameters need to be considered while performing these tests on a heterogeneous set of proteins. We therefore optimized the experimental set up for the overlay assay and further validated a set of newly discovered proteins by CaM-affinity chromatography and a fluorescence anisotropy test developed for NADK2.

We will now explain the experimental procedure that allowed identifying the new CaM candidates. More details on the identified proteins and the validation procedure will be given in the Results section.

- CaM-affinity chromatography and mass spectrometry for the identification of plastidial CaM partners

CaM-affinity purification

The CaM-affinity purifications were performed by Daniel Salvi starting from Arabidopsis stroma and membrane fractions and from a fraction of spinach envelope/stroma. The spinach sample was used in order to start from more protein material, due to the difficulty in obtaining large amounts of highly pure envelope fractions from Arabidopsis chloroplasts. These chloroplast subfractions were obtained as illustrated in Dell'Aglio et al., 2013. All fractions were incubated with a CaM resin for two hours in the presence of $CaCl_2$ in excess (2 mM). The resin was then washed three times with the same $CaCl_2$ containing buffer and the proteins that stayed bound to the resin were then eluted by the addition of 2 mM EGTA-containing buffer. Wash and elution samples were collected and analyzed on SDS-PAGE gels colored by silver staining.

CaM-affinity purification steps were performed in the presence of salt (150 mM NaCl) and 0,1 % (v/v) Nonidet P40 (a nonionic, non-denaturing detergent), in order to minimize a-specific binding or contaminants with low affinity for the resin.

Samples were prepared for mass spectrometry analysis by loading the eluted fractions on a SDS-PAGE and stopping the migration when the proteins were concentrated between the stacking and the separating gels. Bands were manually excised and sent to mass spectrometry.

LC-Mass spectrometry analysis

The mass spectrometry analysis performed by the EDyP laboratory was preceded by a trypsic digestion of the protein samples. Then, peptides were subjected to liquid chromatography separation coupled with mass spectrometry. Collected data were processed automatically and protein identity was determined by comparison to the AGI protein database. For spinach samples, the SwissProt, TrEMBL and TAIR databases were interrogated in order to identify the Arabidopsis homolog of the retrieved peptides. Some peptides were manually checked in order to confirm the software predictions.

This approach allowed the identification of 210 proteins.

Results

1- General characteristics and properties of the plastidial CaM-binding candidates identified

Among the 210 CaM-binding candidates identified by mass-spectrometry, 96 were detected in Arabidopsis stroma, 147 in the Arabidopsis thylakoids and 27 in spinach fractions (stroma and envelope, **Fig. 2.1**).

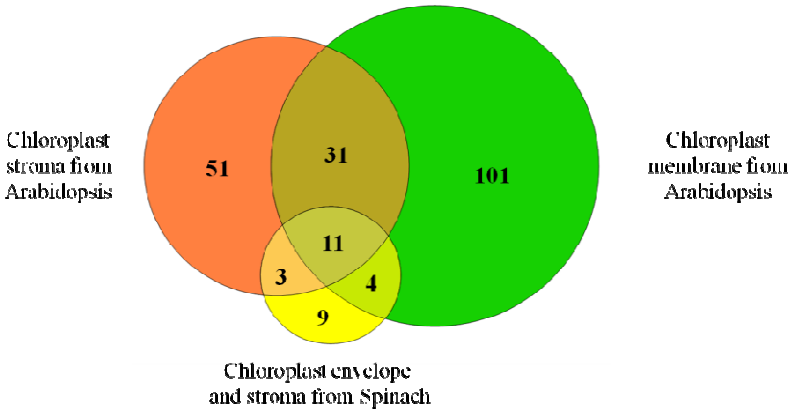

Fig. 2.1 Venn diagram illustrating the overlap between the proteins detected by mass spectrometry from the different chloroplast sub-fractions subjected to CaM-affinity chromatography (stroma, thylakoids and envelope).

As illustrated in **Fig. 2.1**, the most part of putative CaM-partners were detected in the membrane fractions of Arabidopsis (containing both thylakoids and envelope proteins). This high abundance of proteins with respect to the stroma fraction and the spinach sample is mainly due to the fact that large protein complexes (*i.e.* the photosynthetic complexes and the ATPase) were recovered in their integrity, a risk that was previously reported in literature (Reddy et al, 2004 and 2011). The low number of identified protein of the spinach sample is due to the fact that it was not always possible to identify with certainty which was the Arabidopsis homologue of each spinach peptide, since a protein data bank was not available for spinach.

It is noteworthy that 65 of the proteins detected were not present in the AT_CHLORO database. Some of them can be reasonably considered as contaminants with particular high CaM affinity (see below), while others likely represent low-abundant chloroplast proteins not previously detected that

were enriched during the affinity chromatography and can be integrated in the database. These proteins are listed in **Table 2.1**.

accession	Description	found in stroma	found in thylakoids	number of peptides
At5g17230	phytoene synthase	no	yes	3
At4g20760	short-chain dehydrogenase/reductase (SDR) family protein	no	yes	1
At1g26220	GCN5-related N-acetyltransferase (gNAT) family protein	no	yes	2
At4g00030	plastid-lipid associated protein PAP / fibrillin family protein	no	yes	3
At3g07670	SET domain-containing protein	no	yes	3
AtCg01020	chloroplast ribosomal protein L32	no	yes	1
At5g16130	40S ribosomal protein S7 (RPS7C)	no	yes	1
At2g24395	chaperone protein dnaJ-related	no	yes	1
At1g05385	photosystem II 11 kDa protein-related	no	yes	1
At5g63060	transporter	no	yes	2
At3g52920	unknown protein	no	yes	1
At1g64430	unknown protein	no	yes	1
At4g31530	binding / catalytic	no	yes	6
At1g01860	PFC1	yes	no	1
At1g59990	DEAD/DEAH box helicase, putative (RH22)	yes	no	6
At1g21640	NADK2	yes	yes	7
At1g06190	ATP binding / ATPase	yes	yes	10
AtCg00900	chloroplast ribosomal protein S7	yes	yes	5
At5g10860	CBS domain-containing protein	yes	yes	5
At3g23070	RNA binding	yes	no	1
At3g06980	DEAD/DEAH box helicase, putative	yes	no	2
At3g18390	EMB1865	yes	no	2
At5g10910	mraW methylase family protein	yes	no	4

Table 2.1 List of putative plastidial proteins detected by our proteomic analysis and not previously present in the AT_chloro database.

1.1- Many previously identified plastidial CaM-binding proteins were detected

Our list of candidates comprised most of the previously detected CaM-binding proteins of Arabidopsis chloroplasts. In particular, Tic32, NADK2, PsaN and the elongation factor (EF) 1-α were found in at least one plastidial subcompartment. It is interesting to notice that Tic32 (a minor membrane protein) was identified only thanks to the sample of spinach envelope and stroma, thus revealing the importance of subfractionation for the identification of low abundant proteins with high CaM affinity.

It is also interesting to underline that NADK2, whose plastidial localization was proven experimentally previously and by our results (see **Chapter 6**) was not present in the AT_CHLORO Database, probably for the low abundance of the protein in the stroma. However, our CaM-affinity chromatography allowed finding peptides for this protein, revealing once more enrichment in low abundant proteins resulting from the CaM-affinity chromatography.

AFG1-like and CPN21, previously identified as plastidial CaM partners, were not found in our samples. This absence might be due to a low abundance of these proteins, a low CaM affinity and/or physico-chemical properties of their peptides that limit their identification using mass spectrometry (size, charge, hydrophobicity).

1.2- Some highly probable contaminants are present

Contaminants of our set of plastidial CaM-binding candidates may include *i)* proteins that are not true CaM-binding proteins as well as *ii)* proteins not localized in the chloroplast.

i) The extreme different abundance of plastidial proteins and a-specific interaction of some proteins to the CaM resin might lead to the presence of untrue CaM-binding proteins in our list. Indeed, many protein complexes, such as ribosomes, the photosystems, and the ATP synthase were detected almost in their integrity. It is quite unlikely that all these proteins are true CaM-binding proteins and if CaM is implicated in the control of these complexes, this might reasonably be through only some of their subunits. The presence of all the proteins might therefore be due to several reasons: their high abundance, a-specific interactions with the resin and/or a "pull down" effect of the "true" CaM-binding subunit of these complexes. Since the number of spectral counts for all subunits is similar, it is difficult to predict which of these subunits might be those implicated in the interaction.

Not genuine CaM-binding proteins are difficult to identify without a direct CaM-binding assay. To make some predictions, a "score" was initially assigned to each protein on the basis of the number of spectral counts of each protein in the CaM affinity purification and AT-_CHLORO Database: (number of peptides detected/number of peptides in AT_CHLORO)*100. In principle, a high abundant protein such as Rubisco might probably bind the CaM resin only because its abundance increases a-specific interactions, but its score should be lower than the one of a low abundant protein with high CaM affin-

ity, therefore enriched in our study. However, this score was not applicable for proteins not present in AT_CHLORO database (such as NADK2) and might induce to exclude specific, high-affinity CaM partners that are highly abundant in the chloroplast.

The overlay assay that showed the interaction of Tic32 with CaM (Chigri et al, 2006) was performed in parallel also on other membrane proteins without obtaining any signal. Three of these proteins were also detected in our study and might therefore be considered as contaminants. These proteins were Tic110 (At1g06950), Toc64 (At3g17970) and Vipp1 (At1g65260). Among these three proteins, Vipp1 was chosen as a negative control for the validation procedure.

ii) a subset of proteins were not localized in the chloroplast.

Here again, it is difficult to make a comprehensive list of plastidial contaminants since the criteria to assign a protein to the chloroplast are not so strict. Plastidial proteins usually contain a cleavable transit sequence at their *N*-terminal that is required for their targeting to the chloroplast. However this is not always the case. For example, the protein ceQORH is addressed to the plastids thanks to an internal sequence not cleaved by proteases (Miras et al, 2002). Examples of *N*-terminal peptides that are not cleaved off are also known, *e.g.* the soluble chloroplast sensor kinase CSK (Puthiyaveetil et al, 2008). Plastidial transit sequences are not so different from the mitochondrial ones and it is difficult to assign subcellular localization to a protein only on the basis of predictions. In some cases, it has been proven experimentally that a protein is localized in both the mitochondria and in the chloroplast (Habib et al., 2007, Schleiff and Becker, 2010). Thirdly, proteomic projects such as AT_CHLORO Database (Ferro et al, 2010) give useful information about the chloroplast proteome but here again contaminants might be present.

The list of putative plastidial contaminants included in **Table 2.2** was realized considering different criteria. All these proteins are not coded by the plastidial genome, are not included in AT_CHLORO Database, do not contain a predicted plastidial transit peptide and/or their localization was experimentally proven to be outside the chloroplast.

Accession n°	Description	Found in (sample):			number of peptides
		Arabidopsis stroma	*Arabidopsis* thylakoids	Spinach envelope	
At2g20450	60S ribosomal protein L14	No	Yes	No	2
At5g16840	BPA1	Yes	Yes	No	6
At1g65960	GAD2	Yes	Yes	No	10
At5g63400	ADK1	No	Yes	No	6
At1g22530	PATL2	Yes	Yes	No	3
At4g18740	Transcription termination factor	Yes	No	No	2
At5g01730	ATSCAR4	Yes	No	No	1
At2g39920	Acid phosphatase class B family protein	No	Yes	No	1
At4g12880	Plastocyanin-like domain-containing protein	No	Yes	No	1
At1g76890	GT2; transcription factor	No	Yes	No	1
At3g07070	Protein kinase family protein	No	Yes	No	1
At1g72160	SEC14	No	Yes	No	1
At5g23760	Heavy-metal-associated protein	No	Yes	No	1
At1g61097	Expressed protein	No	Yes	No	1
At3g10860	Ubiquinone-binding protein, putative	No	Yes	No	1
At2g27730	Unknown protein	No	Yes	No	2
At2g21870	Unknown protein	No	Yes	No	3
At2g33040	ATP synthase gamma chain, mitochondria	No	Yes	No	5
At1g33240	AT-GTL1 (GT2-LIKE 1);	No	Yes	No	4
At2g22475	GEM (GL2-EXPRESSION MODULATOR)	No	Yes	No	3
At2g01050	Zinc ion binding	No	No	Yes	1
At3g20720	Unknown	No	No	Yes	1
At3g05970	LACS6 (long-chain acyl-CoA synthetase 6); long-chain-fatty-acid-CoA ligase	no	Yes	no	4
At4g20260	PCaP1 plasma membrane polypeptide family protein	no	Yes	no	4

Table 2.2 List of contaminants found in our proteomic survey of plastidial CaM-binding proteins.

Among these contaminants, we can observe the presence of GAD2 that, as stated above, is a high affinity CaM-binding protein located in the cytoplasm, on the basis of the localization of its activity (Breitkreuz and Shelp, 1995). This protein has no predicted transit peptide and is not present in the AT_CHLORO Database, suggesting that its detection in our study is due to the enrichment during the

CaM affinity purification. Indeed, two other proteins present in this list, the cytoplasmic proteins GT-2 (Xi et al, 2012) and the PCaP1 protein (Kato et al, 2010), were recently shown to bind CaM in the presence of $CaCl_2$.

All the other contaminants of this category are therefore good candidates as CaM-binding proteins, especially the most abundant one, *i.e.* the mitochondrial ATPC γ subunit. The investigation of their CaM-binding affinity is of high interest but goes beyond the aim of this work.

1.3- The new detected CaM-binding proteins belong to different categories and have different functions

If in general high-throughput surveys of CaM partners identified a high number of protein kinases, this is not the case for our study, where the only protein kinase identified is STN8, involved in the state transition process (Vainonen et al, 2005).

Fig. 2.2 is a schematic representation of all proteins detected and classified according to their function using MapManBin (Thimm et al, 2004). This representation shows that our list of candidates contains proteins involved in several chloroplastic processes, suggesting that Ca^{2+}/CaM control might target a wide variety of plastidial metabolic pathways and stress responses.

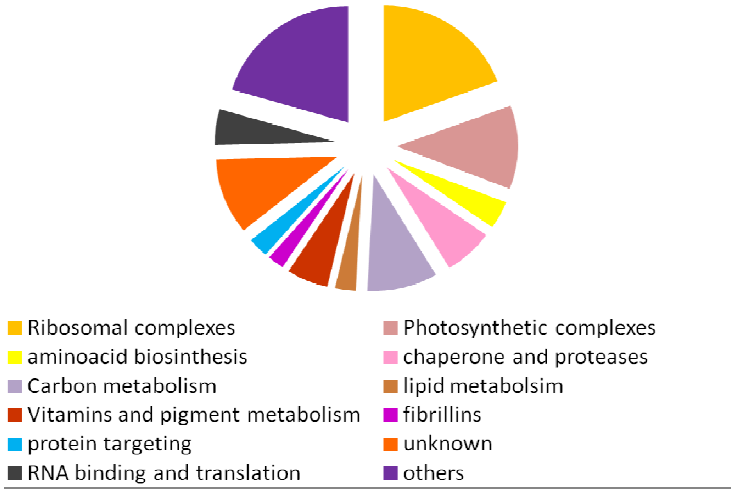

Fig. 2.2 Pie chart of the 210 identified proteins divided according to their function.

2- A subset of 20 detected proteins were validated by an optimized overlay assay

2.1- Choice of candidates

As described in the **Introduction** and the last paragraph, the CaM affinity purification performed to detect our candidates might hide false positives or proteins with a CaM affinity too low to be physiologically relevant.

We therefore selected a subset of 40 proteins for which the CaM-binding was to be validated and quantified. These proteins were implicated in different metabolic pathways and belonged to several protein categories (kinases, enzymes, Ca^{2+} binding proteins etc.). We avoided the choice of proteins belonging to large complexes, such as the ribosomes, the photosystems and the ATP synthase, since the probability of finding a genuine CaM-binding protein was estimated to be too low. We made an exception for the subunit γ of the ATP synthase complex because the mitochondrial isoform was also detected. This was considered as a clue for a possible CaM regulation of the activity of the ATP synthase in both organelles at the γ subunit.

Among the selected proteins, 17 were successfully expressed and purified in *E. coli* as His-tagged proteins. DAHPS3, ceQORH and TS2 were already available in the laboratory. An example of a successful purification is reported in **Fig 2.4** and profiles of purified proteins are reported in **Material and Methods**. All the tested proteins are represented as blue or red spots in **Fig. 2.3** and listed in **Table 2.3**.

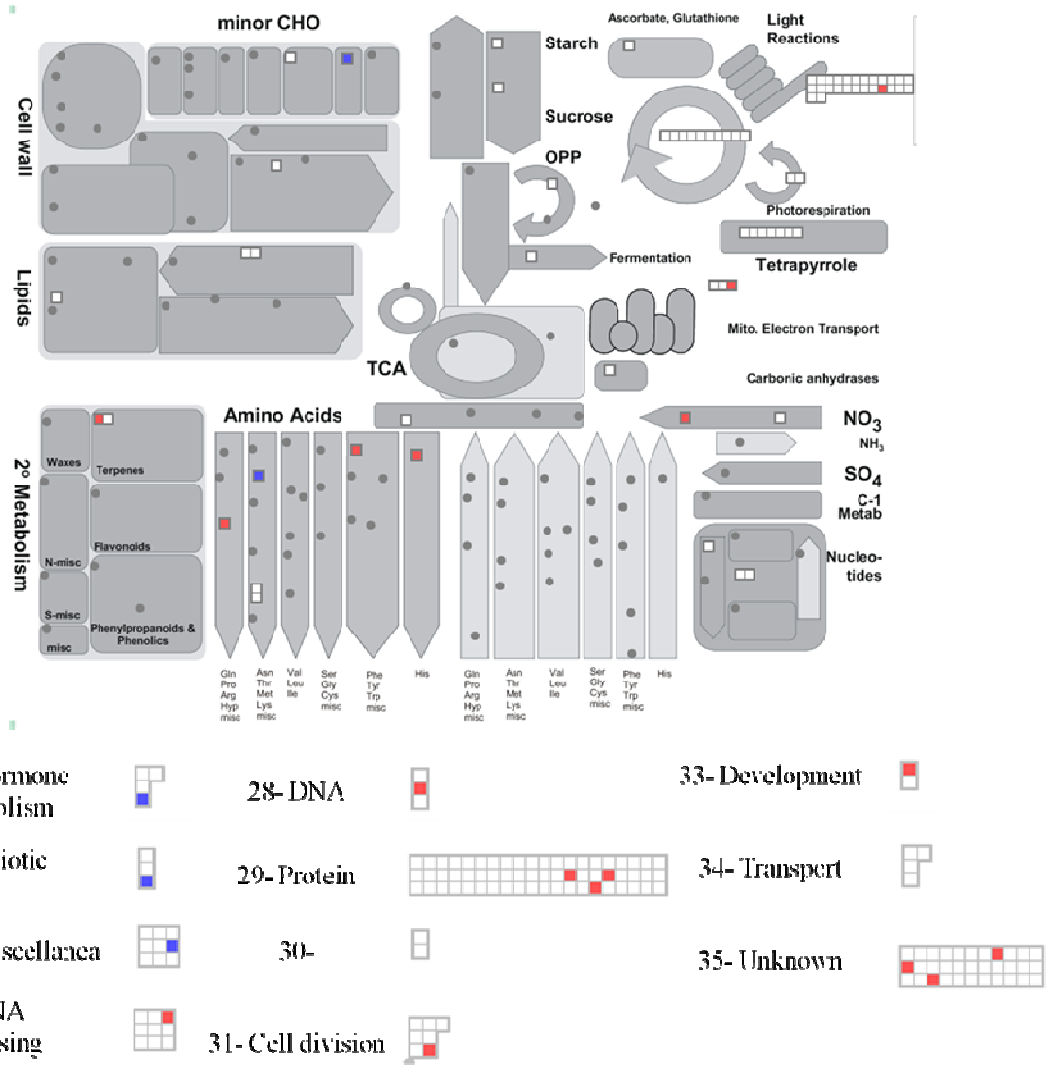

Fig. 2.3 Graphic representation of the CaM-binding candidate proteins detected by mass spectrometry during this work. Classification and representation was made using the MapMan tool. Each protein is represented by a square and located in the corresponding cellular pathway. Red squares represent proteins subsequently validated by the overlay assay. Blue squares represent proteins tested using also CaM-affinity chromatography and fluorescence anisotropy.

accession	Descrip-tion	#pep-tides in AT_STR	#pep-tides in AT_THY	#peptides in Spinach (ENV, STR)	Enrichment in stroma	Enrichment in thylakoids	Molecular weight (PPDB)	Isoelectric point (PPDB)
AT5G35630	GS2	2	0	0	0,3		47,41	6,42
AT1G17220	FUG1	10	0	0	50,0	-	109,74	7,14
AT1G59990	RH22	6	0	0	Only in CaM_STR	-	64,75	5,8
AT5G23060	CAS	0	1	0	-	0,7	41,28	9,41
AT5G10910	MraW	4	0	0	Only in CaM_STR		48,62	9,35
AT1G72810	TS2	1	0	0	12,5	-	56,92	8,23
AT2G21370	XK1-like	3	0	0	150,0		52,46	6,36
AT2G37500	ArgJ	1	5	0	4,3	60,9	48,71	6,21
AT5G01920	STN8	0	1	0	-	33,3	54,97	9,42
AT4G13010	ceQORH	0	8	6	-	131,3	34,43	9,04
At4g33510	DAHPS3	0	0	3	-		56,15	8,93
AT2G33040	ATPC mitoch.	0	5	0	-	Only in CaM_THY	35,45	9,01
AT5G63420	RNaseJ	8	6	0	100,0	87,5	100,55	8,42
AT4G01800	SecA	4	11	0	5,7	13,3	115,18	6,07
AT1G53280	DJ1	1	0	0	7,1	-	46,99	7,98
AT3G45140	LOX2	5	0	0	0,6		102,04	5,42
AT1G09795	PRT2	1	0	0	5,9	-	44,75	6,34
AT1G74470	GGR	0	2	0	-	1,3	51,83	9,03
AT1G80480	PTAC17	1	0	0	2,3	-	49,48	5,67
AT4G04640	ATPC1 plast.	0	16	0	-	16,2	40,91	8,13

Table 2.3 List of proteins selected for validation of their CaM-binding properties. The number of peptides per each analyzed sample (stroma, thylakoids or the spinach envelope) as well as the molecular weight and the theoretical pI of the full-length protein are reported.

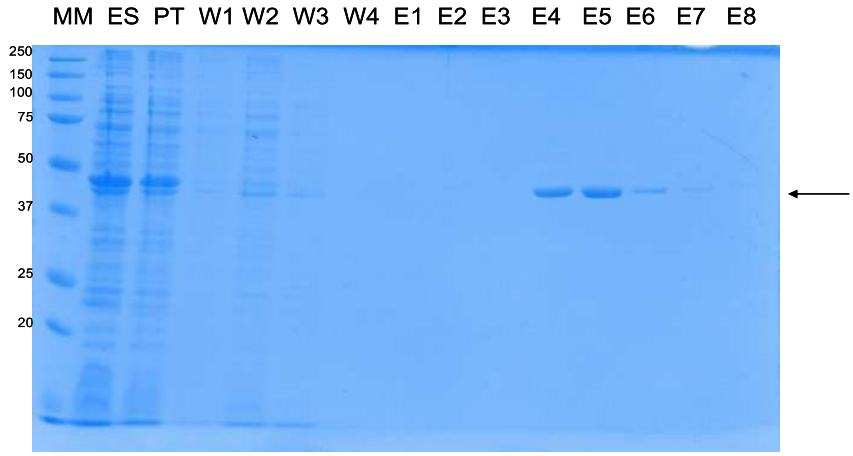

Fig 2.4 Example of a SDS-PAGE purification profile for a candidate protein (MraW). MM: molecular marker. SE: soluble extract. PT: pass-through. W: washing steps with 50 mM imidazole. E: elutions with 250 mM imidazole. The arrow indicates the expected protein size (see **Material and Methods** for the details concerning volumes and protein quantities).

2.2- Optimization of the overlay assay

One of the most common techniques used to confirm the CaM affinity and the Ca^{2+} dependence of the CaM interaction is the overlay assay (Gayle et al, 1987). Usually, the overlay assay consists in the following steps:

- SDS-PAGE of one or more candidates,
- Transfer of the protein to a nitrocellulose or PVDF membrane,
- Incubation of the membrane with an excess of radioactive CaM (^{135}I-CaM or ^{35}S-CAM) or with CaM crosslinked to Plus activated Horse radish peroxydase (HRP) in the presence of an excess of $CaCl_2$ or EGTA,
- Washes using $CaCl_2$ (or EGTA) containing buffer,
- Revelation of the signal (light, radioactivity) corresponding to CaM-binding proteins.

However, by running the technique on several proteins at the same time we noticed an extreme variability of the results. In particular we observed that:

- The larger the size of the protein, the less efficient its transfer on the membrane is. This leads to differences in the quantity of proteins that are actually incubated with CaM.
- When many proteins are transferred on the same membrane and incubated altogether with CaM, a competition for the binding to CaM can occur, thus resulting in different signals for the same protein depending on the others.
- The intensity of the overlay signal strongly depends on how long the films are revealed: at the beginning only some spots appear but the longer the waiting time is, the more proteins will give a positive signal. This is true for incubations both in the presence of $CaCl_2$ and EGTA. We indeed observed strong signals in the presence of EGTA with long incubation times.

These discrepancies were observed also for well-established CaM-binding proteins, *i.e.* NADK2 and Tic32 (see **Fig 2.5**).

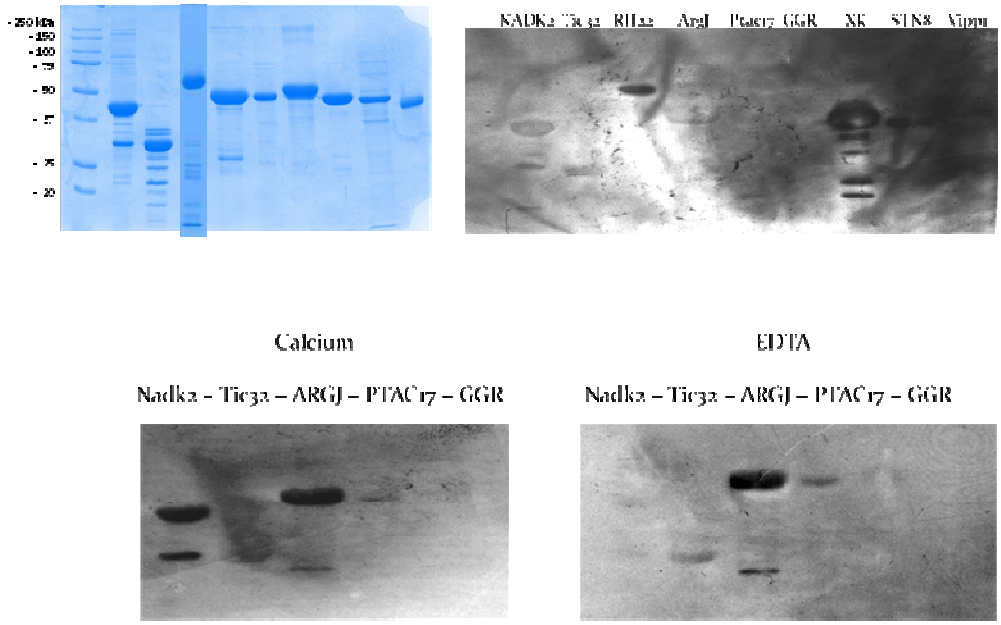

Fig. 2.5. **Examples of problems connected to the overlay assay setup.** Upper left panel: Coomassie staining of the proteins tested in overlay assay displayed on the upper right panel, showing that the same amount of each partially purified protein was loaded. In the upper right panel, it is possible to see that the signal of the positive controls is weaker than the one of some of the candidates (RH22 and XK1). However, in a similar experiment performed with fewer proteins (bottom left panel), the signal of NADK2 increases considerably as well as the one of ArgJ, but not the one of Tic32. Finally, in the presence of EDTA, Tic32 gives a weak signal and the signal for ArgJ is particularly strong. Note that the dark back-ground problem observed here was subsequently solved when Brij35 was introduced in the incubation media.

We therefore tried to improve the technique in order to gain more coherence and reliability to the results while testing many proteins at the same time. The final procedure consisted in:

- Spotting the same amount of protein (in nmol) directly on the membrane in order to avoid differences in the transfer efficiency,
- Cutting and incubating each spot independently with CaM-HRP (2.5 fold molar excess). For each protein, one spot was incubated with $CaCl_2$ and the other with EGTA.
- After washing, all the spots were again reassembled and the CaM signal was revealed on the same film. In order to calibrate the revelation, we included in each experiment the *N*-terminal domain of NADK2 as positive control and Vipp1 asa negative control. We also tested Tic32 as an additional positive control, and the plastidial prephenate aminotransferase (PAT: At2g22250, Graindorge et al, 2010) as an additional negative control, since this protein was not detected in our survey. The

revelation was stopped when a signal for NADK2 was visible only in the presence of $CaCl_2$ and not of EGTA, and when no signal was detectable for Vipp1 in any case.

A schematic representation of the procedure is illustrated in **Fig 2.6**. More technical details are provided in the **Material and Methods** section.

This optimized assay allowed testing many proteins in parallel in the same conditions and with the same CaM/candidate ratio. The comparison of the signals with two positive controls (*i.e.* proteins that bind to CaM only in the presence of $CaCl_2$, as reported in the literature and confirmed by our assays) and two negative controls (Vipp1 and PAT) allowed calibrating the experiment and avoided overexposure of the films.

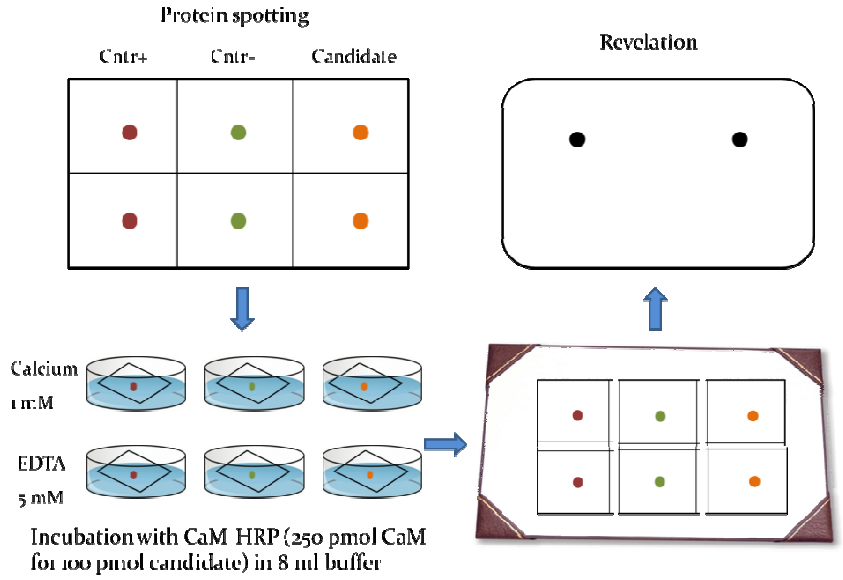

Fig. 2.6. Schematic representation of the revised procedure for the overlay assay. The buffer composition was as follows: 50 mM Tris–HCl, pH 7.5, 150 mM NaCl, 1% (w/v) BSA, and 1% (v/v) Brij35, either in the presence of 1 mM $CaCl_2$ or 5 mM EGTA.

2.3- The overlay assays confirm the binding of the 20 selected candidates but also reveal several possible modes of interaction with CaM

A first round of experiments was conducted by incubating the candidates with CaM for three hours, as normally done in similar studies in the past.

Representative spot signals obtained for positive controls in the presence of $CaCl_2$ and absence of signal for negative controls are shown in **Table 2.4**.

	Protein name	AGI	3 hours		15 minutes	
			Ca^{2+}	EGTA	Ca^{2+}	EGTA
Positive controls	NADK2 *Mer*	At1g21640	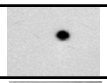	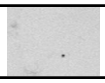		
	Tic32	At4g23430	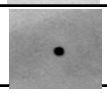	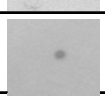		
Negative controls	Vipp1	At1g65260			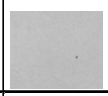	
	PAT	At2g22250	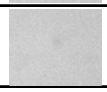			

Table 2.4 Positive and negative controls of the overlay assay.

Our optimized overlay assay showed then that all the selected candidates were able to bind to CaM in the presence of $CaCl_2$ and some of them also in the presence of EGTA. We compared the intensity of the signals with the one of NADK2 and divided the proteins in 4 groups

The first group (**Table 2.5**) contained proteins that bound CaM only in the presence of $CaCl_2$ and gave a strong signal, comparable to the one of NADK2. These proteins were the protein kinase STN8, the RNA helicase RH22, a xylulose kinase-like protein (XK-like 1), a translation initiator factor (Fug1), a nuclease (RNaseJ), the gamma subunit of the plastidial ATP synthase and the ceQORH protein (At4G13010, Miras et al 2002 & 2007, see **Chapter 3**).

	Protein name	AGI	3 hours		15 minutes	
			Ca^{2+}	EGTA	Ca^{2+}	EGTA
Group 1	STN8	At5g01920				
	RH22	At1g59990				
	XK-like1	At2g21370				
	Fug1	At1g17220				
	RNAseJ	At5g63420				
	ATPγC1	At4g04640				
	ceQORH	At4g13010				

Table 2.5 Overlay assays of the proteins belonging to Group 1. These proteins bind CaM only in the presence of Ca^{2+} and give a strong signal in comparison to NADK2.

The second group (**Table 2.6**) contained proteins for which the $CaCl_2$ signal was weak when compared to the one of NADK2. It included a protein translocase (SecA), a protein involved in the biosynthesis of histidine (PRT2), a geranyl geranyl reductase, a protein required for plastid gene expression (PTAC17) and an Arabidopsis homologue of animal DJ1, which protects cells from oxidative stress (Lin et al, 2011).

	Protein name	AGI	3 hours	
			Ca^{2+}	EGTA
Group 2	SecA	At4g01800		
	PRT2	At1g09795		
	GGR	At1g74470		
	Ptac17	At1g80480		
	DJ1	At1g53280		

Table 2.6 Overlay assays of the proteins belonging to Group 2. These proteins bind CaM only in the presence of Ca^{2+} but give a weaker signal when compared to the one obtained with NADK2.

Finally, the last two groups contained proteins able to bind to CaM even in the presence of EGTA, sometimes with a weak signal (group 3, **Table 2.7**) and sometimes with a signal comparable to what observed in the presence of $CaCl_2$ (group 4, **Table 2.8**). These proteins were a glutamine synthetase, a lipoxygenase, a protein involved in the biosynthesis of arginine, the gamma subunit of the mitochondrial ATP synthase, a 3-Deoxy-d-arabino-heptulosonate-7-phosphate synthase (DAHPS3), a protein methyltransferase (MraW), a threonine synthase (TS2), and the Ca^{2+} sensor CAS.

	Protein name	AGI	3 hours		15 minutes	
			Ca^{2+}	EGTA	Ca^{2+}	EGTA
Group 3	GS2	At5g35630				
	Lox2	At3g45140				
	ArgJ	At2g37500				
	ATPγM	At2g33040				
	DAHPS3	At1g22410				

Table 2.7 Overlay assays of the proteins belonging to Group 3. These proteins bind CaM even in the presence of EGTA, but give a weaker signal with respect to the one observed in the presence of Ca^{2+}.

	Protein name	AGI	3 hours		15 minutes	
			Ca^{2+}	EGTA	Ca^{2+}	EGTA
Group 4	MraW	At5g10910				
	CAS	At5g23060				
	TS2	At1g72810				

Table 2.8 Overlay assays of the proteins belonging to the Group 4. These proteins bind CaM even in the presence of EGTA, with a signal comparable to that observed in the presence of Ca^{2+}.

Another important parameter to consider is the time of incubation with CaM. The protocols reported in literature recommend incubations of proteins with CaM of several hours. However, since Ca^{2+} variations are normally transient and localized, CaM-partner interactions are supposed to be rapid and to occur in minutes or even seconds.

For all the cases in which we detected a strong signal after three hours of incubation with CaM, we therefore repeated the assay with a reduced incubation time of 15 minutes (**Tables 2.5-2.8**). The results obtained in these new conditions were heterogeneous. Indeed, some proteins that gave a strong signal in the presence of Ca^{2+} still showed a comparable signal after only 15 minutes (STN8, RNAseJ, XK1-like, RH2, ArgJ, ATPγM and TS2). However, the interaction with Fug1 was no more detected and the signal of ATPγC decreased drastically.

In general, the signals detected in the presence of EGTA were completely lost in all cases with the exception of ATPγM and TS2 that still showed a weak signal.

It is also important to underline that the signal of NADK2 was drastically reduced and no signal for Tic32 was visible in these new conditions (**Tables 2.4**).

2.4- Conclusions related to the overlay assays results

All in all, the overlay assay confirmed all the CaM affinity of all the studied proteins In the presence of Ca^{2+} and after 3 hours of incubation. However, variable signal intensities and behaviors in the presence of EGTA were observed, suggesting that for several proteins the interaction with CaM might not be Ca^{2+}-dependent. In addition, when the incubation time was decreased up to 15 minutes, several signals were lost or attenuated, even those of the positive controls. This might be due to several reasons. In particular, the way the protein interacts with the charged group of the membrane, the conformation adopted by the protein on the membrane and the conformational changes occurring after long incubations are hard to control in the overlay test and might generate artifacts that are difficult to estimate and avoid. A non-favorable conformation assumed by NADK2 and/or Tic32 might result in inaccessibility of the CaM-binding site when the incubation is not long enough to allow a conformational change, as previously reported for calcineurin (Hubbard and Klee, 1987). On the other hand, some EGTA signals

observed after 3 hours of incubation might be a-specific and due to alterations in protein structure due to the long incubation time.

3- Validation of a subset of proteins by CaM affinity chromatography and fluorescence anisotropy

To further investigate the newly discovered CaM interactions, some of the 20 candidates validated by the overlay assay were analyzed in more detail.

One important difference between the overlay assay and the CaM affinity purification previously performed is that, in the first case, the proteins were extracted from plant tissues while, in the second case, they were produced in *E. coli*. This implies that some differences (*e.g.* post-translational modifications) might be present and this might determine a different CaM affinity.

To ensure that these selected proteins maintained their CaM affinity in the conditions that allowed their initial binding on the CaM column, we performed CaM-affinity chromatography on soluble bacterial extracts overexpressing our candidates.

Not all proteins were easily analyzable by this technique, since some of them were not produced in a soluble form and required the presence of high urea concentrations to be maintained in solution. These were not compatible with the CaM-affinity chromatography and the fluorescence anisotropy technique that we established. This group included Vipp1, STN8, RNAse J, the two ATP gamma subunits, GGR, ArgJ, CAS and MraW.

Among the remaining proteins, we decided to focus on XK1-like, ceQORH, Lox2 and TS2. All these proteins showed strong overlay signals in the presence of Ca^{2+} after 3 hours of incubation. Lox2, ceQORH and TS2 were chosen because these are enzymes whose activity is known and easy to measure. It was therefore possible to confirm by enzymatic tests that the proteins were active In all cases, the activity of the proteins was measured in the presence and absence of AtCaM1, without detecting any difference (not shown). We however decided to pursue the analysis of these proteins, since the

binding to CaM can not only regulate the activity of its targets but also control its localization (see the **Introduction**). XK1-like was also added even if its activity has not yet been identified.

Soluble extracts of all these proteins were therefore applied to a CaM-column in the presence of $CaCl_2$. After extensive washing, elution was performed in the presence of EDTA in excess.

It is worth mentioning that, before loading on the gel the same volume of each sample, the pass-through, the wash and the elution were all concentrated up to the same volume (*i.e.* 0.75 mL). In this way, the SDS-PAGE of the same volume of each sample allowed an easy comparison of the amount of protein recovered at each step.

We then tested the affinity of these proteins for AtCaM1 labeled with the fluorophore $Alexa^{488}$, as previously done for NADK2 (see **Chapter 1**).

3.1- XK1-like

In the sequence of this protein, two putative CaM-binding sites are predicted by the Calmodulin Target Database (**Annex I**).

The CaM column SDS-PAGE profile (**Fig 2.7A**) shows that the recombinant XK1-like proteins was totally recovered in both the pass-through and the washing fractions, while no protein was recovered after addition of EGTA. This means that this protein had no affinity for the CaM-resin in our experimental conditions (that were the same used for NADK2.1 in **Chapter 1**).

We also performed fluorescence anisotropy measurements with AtCaM1-$Alexa^{488}$, in the same way as previously done for NADK2.1. Here again, and in the same experimental conditions (100 mM Hepes pH 7.5, 200 mM KCl and excess of $CaCl_2$) we incubated several amounts of XK1-like with AtCaM1-$Alexa^{488}$ and measured the fluorescence anisotropy of the AtCaM1-$Alexa^{488}$. As illustrated in **Fig. 2.7B**, incubation of AtCaM1-$Alexa^{488}$ with up to 6 µM XK1-like did not trigger any variation on the fluorescence anisotropy.

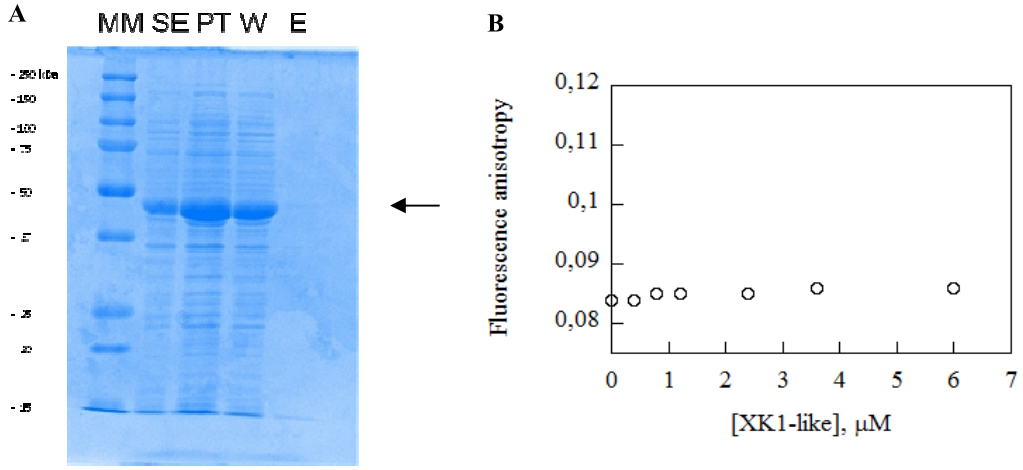

Fig 2.7 CaM-affinity chromatography and fluorescence anisotropy of XK1-like. A. CaM-affinity chromatography of XK1-like, showing that no Ca^{2+}-dependent CaM-binding is observed for this protein in these conditions. M: molecular marker; SE: soluble extract; PT: pass-through; W: washing in the presence of $CaCl_2$, E: elution with EGTA. XK1-like size is indicated by an arrow. **B**. AtCaM1-Alexa^{488} fluorescence anisotropy measurements at various XK1-like concentrations in the presence of $CaCl_2$.

In conclusion, both the CaM-affinity chromatography and the fluorescence anisotropy do not confirm the binding of XK1-like to calmodulin. These last findings are in disagreement with the detection of XK1-like in the high-throughput screening and the overlay assay.

3.2- Lox2

The same set of experiments performed for XK1-like was applied to Lox2.

According to the Calmodulin Target Database, Lox2 might contain a CaM-binding site between amino acids 533- and 542 (**Annex I**).

The SDS-PAGE profile of a CaM-affinity chromatography of recombinant Lox2 is reported in **Fig. 2.8A**. In the case of Lox2, we can observe that the protein was partially present in the pass-through of the column and partially (approximately half of the total amount on the basis of visual estimation) in the elution. No binding of LOX2 to AtCaM1-Alexa^{488} was observed in our fluorescence anisotropy test (**Fig. 2.8B**).

B

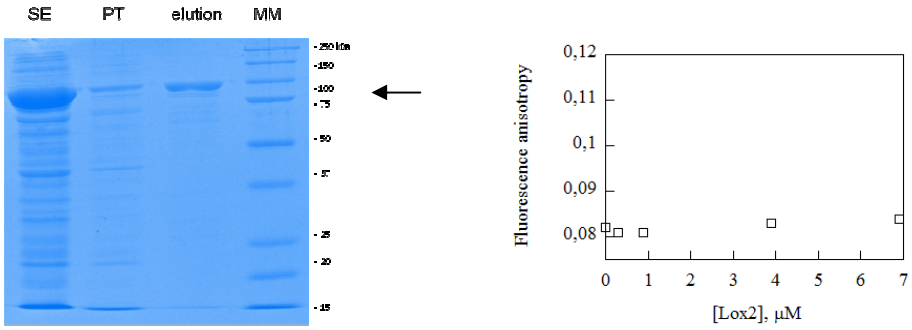

Fig. 2.8 CaM-affinity chromatography and fluorescence anisotropy measurements with Lox2. A. CaM-affinity chromatography of Lox2, showing that some Ca^{2+}-dependent CaM-binding is observable for this protein in these conditions. M: molecular marker; SE: soluble extract; PT: pass-through; E: elution. Lox2 size is indicated by an arrow. **B**. CaM-Alexa^{488} fluorescence anisotropy measured at various Lox2 concentrations in the presence of $CaCl_2$.

4. TS2

A putative CaM-binding site is localized at the *C*-terminus of the sequence (see **Annex I**), but TS2 protein was not able to bind to a CaM column **(Fig. 2.9A)**. Although it showed binding to AtCaM1-Alexa^{488} in our fluorescence anisotropy assay **(Fig. 2.9B)**, these new data reveal features of a-specific binding, since no saturation was reached even at high protein concentrations **(Fig. 2.9B)**. Moreover, the binding was not completely abolished by addition of EGTA (not shown).

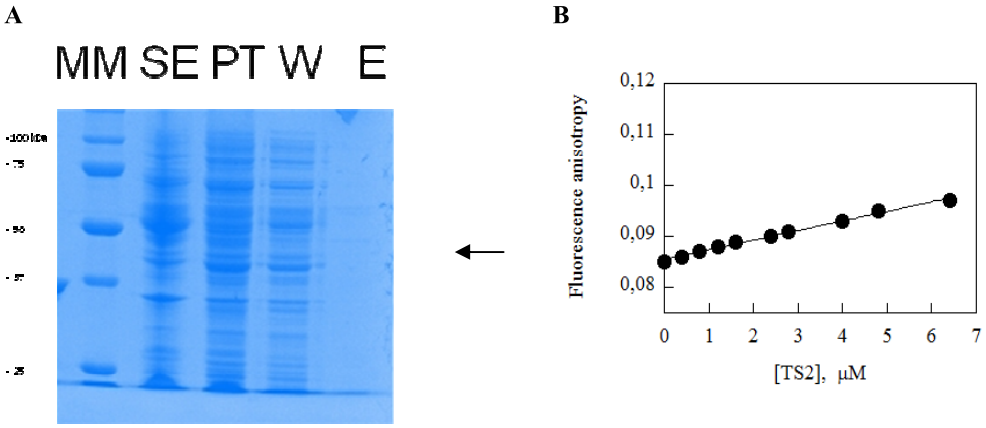

Fig. 2.9 CaM-affinity chromatography and fluorescence anisotropy measurements with TS2. A CaM-affinity chromatography of TS2, showing that no Ca^{2+}-dependent CaM-binding is observable for this protein in these conditions. M: molecular marker; SE: soluble extract; PT: pass-through; W: washing in the presence of $CaCl_2$; E: elution. TS2 size is indicated by an arrow. **B**. AtCaM1-Alexa^{488} fluorescence anisotropy measured at various TS2 concentrations in the presence of $CaCl_2$.

5. ceQORH

As for XK1-like, ceQORH also contains two putative CaM-binding sites, one at the center of the sequence and the other at the *C*-terminus (see **Annex II**).

Daniel Salvi and Lucas Moyet previously demonstrated that this protein is able to bind the CaM resin during a CaM-affinity chromatography and observed strong signals in overlay assays (see **Chapter 3** for the details of this discovery and the historical context).

Overlays (**Table 2.5**) and CaM affinity chromatography (**Fig 2.10A**) were reproduced and anisotropy measurements were carried out under conditions identical to that of the other proteins tested.

In the CaM-affinity chromatography the protein was found partly in the pass-through and partly in the eluted fractions. This might be due to overload of the column and/or to the rapidity of the passage on the CaM matrix. In the eluted fraction we can distinguish 2 additional bands of a lower molecular weight with respect to ceQORH (34 kDa). These might be degradation products of the entire protein or translational arrests, since they are not visible in all other CaM columns we performed.

A highly pure and active protein purified by Cécile Giustini was used in the anisotropy assay measurements. A strong increase in fluorescence anisotropy was observed and was exclusively observed in the presence of Ca^{2+}. The titration curve displayed in **Fig. 2.10B** allowed calculating a K_D of 0.8 µM. CaM-binding to ceQORH will be further characterized in the next chapter.

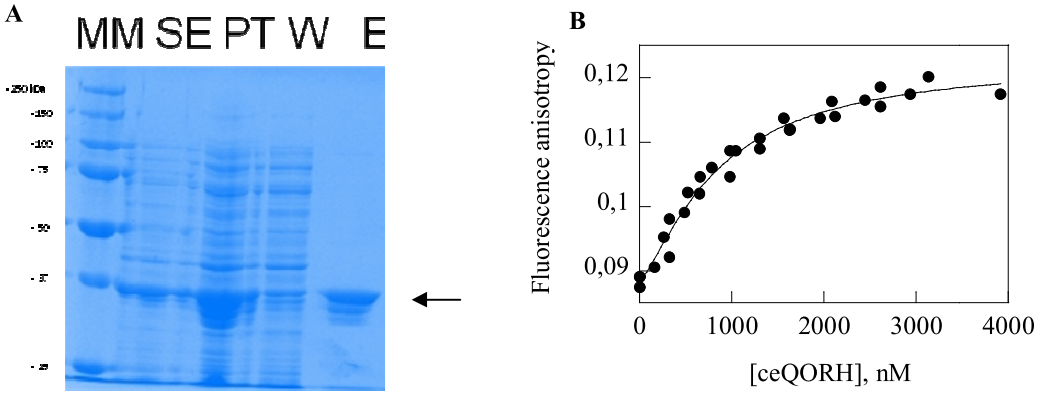

Fig. 2.10 CaM-affinity chromatography and fluorescence anisotropy measurements with ceQORH. A. CaM-affinity chromatography of ceQORH, showing Ca^{2+}-dependent CaM-binding. M: molecular marker; SE: soluble extract; PT: pass-through; W: washing in the presence of $CaCl_2$; E: elution. The additional bands at a lower molecular weight than ceQORH full-length protein and might be due to protein degradation or to translation arrest. ceQORH size is indicated by an arrow. **B**. CaM-Alexa^{488} fluorescence anisotropy measured at various ceQORH concentrations using highly pure protein in the presence of $CaCl_2$.

Discussion

We detected a conspicuous subset of new potential plastidial CaM partners. Even excluding the proteins belonging to large protein complexes (the photosystems, the ATP synthase or the ribosomes) our set of candidates comprises proteins involved in all plastidial processes, such as metabolism (sugar, amino acids, lipid, pigment biogenesis, photosynthesis), plastid division, transport, DNA replication, RNA translation and protein synthesis.

The detection of such a high number of candidates is similar to what obtained in previous analogous surveys on CaM partners and might suggest that, as for other cell subcompartments, CaM/Ca^{2+} plays an important role in orchestrating the metabolic and developmental activities of this organelle.

Since the effect of CaM-binding to a protein can lead to various effects on the protein activity or protein properties, we developed several tests in order to confirm and better characterize the new putative interactions.

The overlay assay is a simple and routine test in which the proteins are spotted and bound on a membrane and incubated with the HRP-labeled CaM in the presence of $CaCl_2$ or EGTA. Thanks to an optimized protocol that required the presence of positive and negative controls we were able to observe that, although all our 19 candidates bound to CaM, the signal intensities were variable and the Ca^{2+} dependence of the signal not always confirmed. The time of incubation of the two partners was also critical, since when reduced to 15 minutes many of the observed signals disappeared. In these conditions, the protein conformation is difficult to predict, and it was observed that, after some time, it is prone to change (Hubbard and Klee, 1987). This might explain the differences observed between the observations made at 3 hours of incubation or 15 minutes.

We then decided to investigate the binding of a subset of new CaM-binding candidates (TS2, Lox2, XK1-like and ceQORH) using other two other techniques, *i.e.* a CaM-affinity chromatography and a fluorescence anisotropy test previously performed on NADK2 and Tic32. With the exception of XK1-like, for which the activity is unknown, all others resulted to be active, therefore considered to be correctly folded.

The only protein who appeared to bind AtCaM1 with high affinity in all cases is ceQORH. Not only a strong, $CaCl_2$-dependent overlay signal was observed both after 3 hours and 15 minutes of incubation, but the protein was retained on the CaM-column and released by addition of EGTA in excess. Finally, binding experiments in fluorescence anisotropy showed that the protein had a strong affinity for AtCaM1-Alexa^{488}, with a calculated K_D of 800 nM.

For all other proteins we obtained different results according to the employed techniques.

In the case of TS2, both the overlay and the fluorescence anisotropy showed that the protein was able to bind to AtCaM1 but the binding was not Ca^{2+} specific. In addition, fluorescence anisotropy revealed that the K_D of TS2 for AtCaM1 is too high to be considered physiological and the binding observed is probably an artifact.

The cases of Lox2 and XK1-like are the most puzzling. Lox2 bound to AtCaM1 in the overlay (weak signal but Ca^{2+}-dependent) and was eluted with EGTA on the CaM-affinity chromatography. However, it was not able to bind CaM in fluorescence anisotropy assays. This suggests that this protein has a weak affinity for CaM, probably detectable only when the protein is in excess. XK-like1, on the contrary, gives a strong and Ca^{2+}-dependent overlay signal but is not retained on the CaM column and does not bind AtCaM1 in fluorescence anisotropy assays. The most likely explanation for this result is that the binding of this protein to CaM is possible only in some conformational states that are observed only when the protein is fixed on a solid support and in the presence of high salt concentrations and detergents.

The absence of binding or the low affinity interactions between TS2, XKlike1 and LOX2 and AtCaM1-Alexa^{488} might come from the labeling of AtCaM1. However competition tests (not shown) such as the one described in the next chapter on ceQORH did not allow detecting any strong interaction, suggesting that the labeling is not responsible for the absence of interaction observed.

In conclusion, despite the high number of proteins retrieved by the mass-spectrometry analysis, among the subset of proteins we tested the only one that was able to bind CaM in a Ca^{2+}-dependent way in all cases and with a low K_D for AtCaM1-Alexa^{488} is ceQORH. This both suggests the presence of other proteins with similar high CaM affinity in our initial list of CaM-binding candidates, but also

reveals that finding high-affinity CaM-binding proteins requires strong effort and the putative interactions need to be confirmed by several qualitative and quantitative techniques.

The case of the ceQORH-CaM interaction will be examined more in depth in the next chapter.

Part of the work described in this chapter constituted the material of a recent publication in Molecular BioSystems (Dell'Aglio et al, 2013, see **Annex III**).

Chapter 3

Advanced biochemical characterization of the interaction of the ceQORH protein with At-CaM1

Introduction

One of the proteins found as a potential CaM partner in the proteomic survey described in **Chapter 2** is ceQORH (chloroplast envelope Quinone Oxidoreductase Homolog).

The ceQORH protein is an NADPH oxidoreductase particularly active on 9-hydroxy-12-oxo-10(E) - octadecanoic acid (Gilles Curien, unpublished data). As this protein is highly abundant in the chloroplast envelope (2 % of the envelope protein on a protein mass basis), its *in vitro* activity suggests that the protein might be important for detoxification of lipid peroxidation products that are set free following oxidative stress.

Before discussing the *in vitro* results we obtained about the interaction of ceQORH with CaM by fluorescence anisotropy, we will briefly discuss the current available knowledge on this protein and its peculiar properties. ceQORH was indeed studied for many years prior to my arrival in the D-Phy-Chloro team of the PCV laboratory, lead to the issue of CaM/Ca^{2+} control of the chloroplast. For sake of clarity we delayed up to this chapter the presentation of ceQORH properties and the description of its interaction with CaM identified by Daniel Salvi and Stéphane Miras in the course of his PhD thesis.

- **Discovery of ceQORH as a plastidial protein without a classic *N*-terminal transit peptide**

With the exception of proteins of the outer envelope membrane and membrane proteins that pass through the ER and the Golgi apparatus, all plastidial proteins usually contain a *N*-terminal sequence of approximately 10-100 amino acids that is necessary for the correct targeting of the protein to the chloroplast. This sequence is normally cleaved after crossing of the envelope membranes. Thylakoid proteins sometimes contain two different cleavable sequences, the first to be successfully targeted to the stroma and the second to reach the membrane or the lumen of the thylakoids (see Jarvis et al, 2008, Albiniak et al, 2012 and Li and Chiu 2010 for reviews). This dogma was challenged in 2002 when Miras et al reported the existence of ceQORH, a protein localized at the inner envelope membrane but lacking a cleavable transit peptide.

The authors showed by western blot that the protein was enriched and highly abundant (1-2%) in the inner membrane of the chloroplast envelope though the protein primary sequence did not contain a pre-

dicted transit peptide. This lack of cleavable transit peptide was also demonstrated through the sequencing (mass spectrometry) of the native protein purified from chloroplast envelope proteins, and the demonstration that this protein is not mature after its import into the chloroplast (MS/MS-derived primary sequence of the protein corresponds to the *N*-terminus of the protein predicted from a 5'-RACE validated cDNA sequence). By alkaline treatment of the envelope fractions, they also showed that ceQORH is not a transmembrane protein but probably interacts with the lipid bilayer through electrostatic interactions (Miras et al, 2002).

In order to elucidate the mechanisms of transport of this protein into the chloroplast, the group adopted two additional strategies: *i)* co-immunoprecipitation of the protein from envelope fraction and analysis of the precipitate by mass spectrometry, and *ii)* GFP-fusions to assess the protein localization in Arabidopsis cells.

In order to elucidate the mechanism of plastidial localization of this protein, the authors repeated the localization experiments with truncated versions of ceQORH. These experiments confirmed again that the *N*-terminal sequence is not implicated in the protein localization, since the deletion of the first 60 amino acids did not disrupt the correct protein transport in the chloroplast. On the contrary, these experiments showed that amino-acids 60-100 are essential, but not sufficient, to drive the protein into the plastids (Miras et al, 2002). These results suggest that the information needed to successfully target ceQORH in the chloroplast comes not only from the sequence but also from the 3D protein conformation.

More recently, by *in vitro* chloroplast protein import experiments, the targeting of ceQORH to plastids was further confirmed. In addition, the authors showed that the transport of the protein is not due to the passage through the classic protein import machinery (TOC-dependent targeting machinery) but another pathway still to be characterized might be involved (Miras et al, 2007).

- **ceQORH interaction with CaM – preliminary data**

As previously shown by Miras et al (unpublished data) and as confirmed in the high-throughput proteomic analysis presented in the previous chapter, ceQORH is a Ca^{2+}-dependent CaM-binding protein with high CaM affinity. However, enzymatic tests performed by Gilles Curien in the presence and in the absence of CaM showed that CaM had no impact on the protein activity, suggesting that the interaction does not radically modify the conformation of the protein under the experimental conditions used.

In order to further analyze the interaction of ceQORH with CaM and gain more clues about its significance, a ceQORH CaM-binding site was identified thanks to the Calmodulin binding database (**Fig. 3.1A** and **B**). This site is neither a 1-8-14 nor a 1-5-10 CaM-binding sequence. It however resembles a 1-5-10 CaM-binding sequence in which at position 10 we find a methionine instead of the more classic phenylalanine, isoleucine, leucine, valine or tryptophan. A secondary structure prediction shows that, while the majority of CaM-binding sites are helices, only the first part of the region corresponding to the putative ceQORH CaM-binding site forms a helix, while the last amino acids are situated in a loop region (**Fig. 3.1A**).

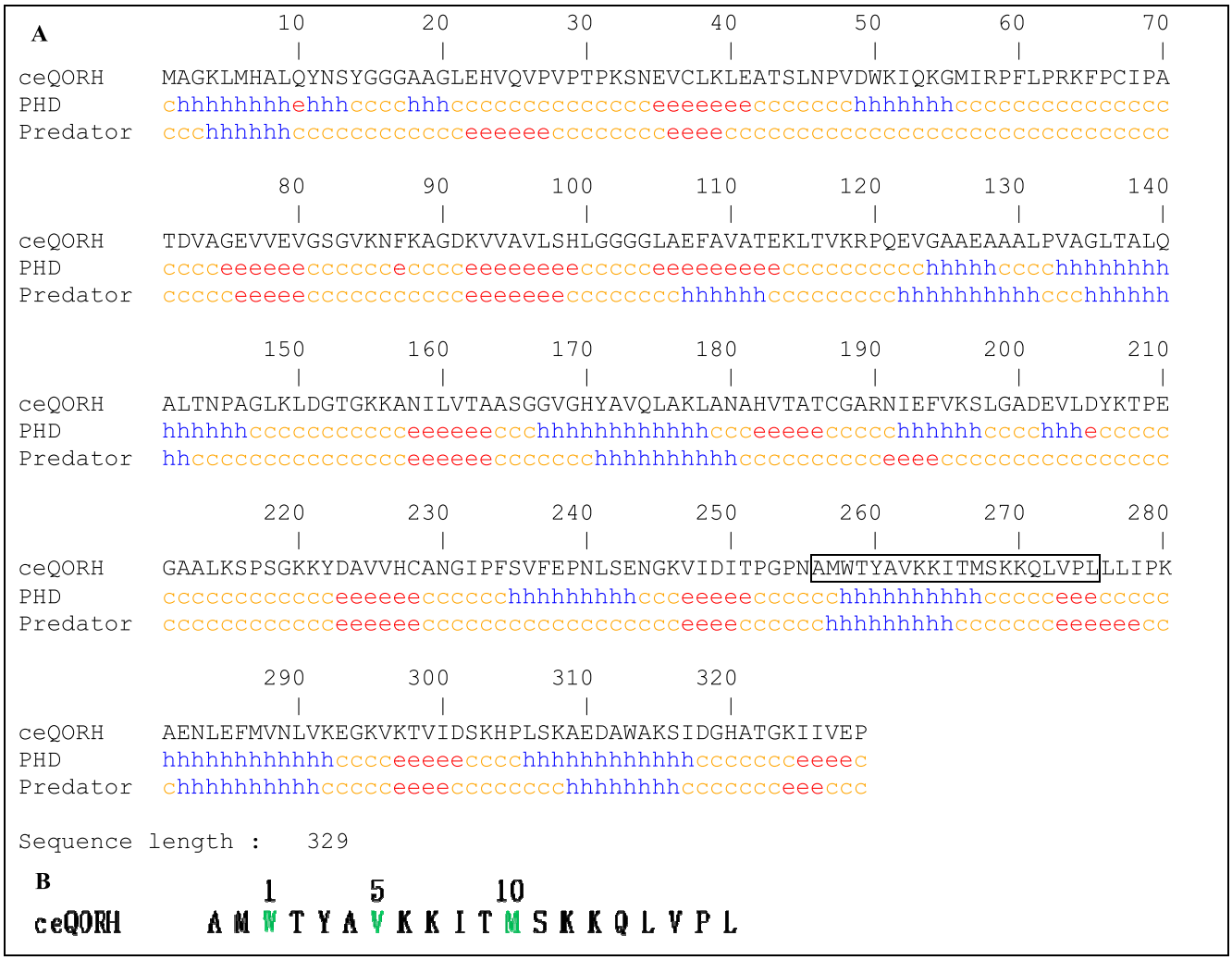

Fig. 3.1 Sequence and secondary structure of the predicted ceQORH CaM-binding site. A. Prediction of ceQORH secondary structure with the programs PHD (http://npsa-pbil.ibcp.fr/cgi-bin/npsa_automat.pl?page=/NPSA/npsa_phd.html) and Predator (http://www.programmableweb.com/api/predat

In order to better understand the role of ceQORH-CaM interaction, Daniel Salvi and Lucas Moyet produced a mutated recombinant version of the ceQORH protein where one hydrophobic and two charged amino acids of the predicted CaM-binding site are substituted by glycines or alanines (**Fig 3.2**).

	1					5					10							
ceQORH	A	M	W	T	Y	A	V	K	K	I	T	M	S	K	K	Q	L	V	P	L
Mutant	A	M	W	T	Y	A	V	K	K	I	T	G	S	A	A	Q	L	V	P	L

Fig. 3.2 Mutated version of the ceQORH CaM-binding site. Residues forming the 1-5-10 motif of the wild-type protein are in green. Mutated residues are underlined and displayed in red.

The mutated version of ceQORH ("ceQORH mut") was produced in *E. coli* and purified. Overlay assays performed on this protein showed a weaker signal with respect to WT ceQORH.

The wild-type and mutated proteins were compared with respect to their activity and their affinity for AtCaM1-Alexa^{488} by fluorescence anisotropy assays. The mutated version of ceQORH was nearly as active as the WT version, indicating that the mutation did not affect the conformation of the active site of the protein (Gilles Curien, unpublished). In contrast with the overlay assays that showed lower signal intensity for the mutated protein, the binding curves of the mutated and wild-type ceQORH were comparable (**Fig. 3.3**).

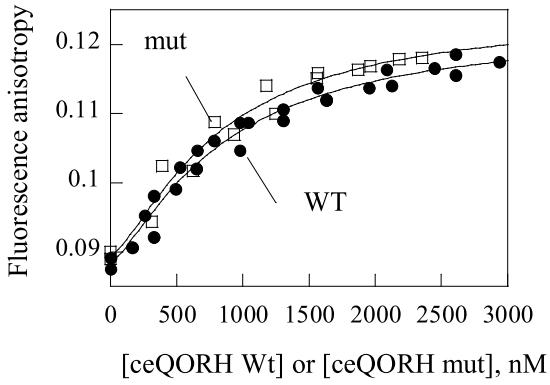

Fig. 3.3 Fluorescence anisotropy measurements of the interaction of AtCaM1-Alexa^{488} with ceQORH WT and ceQORH mutated in the CaM-binding site. Fluorescence anisotropy was measured as a function of the concentration of wild-type ceQORH (wt, black dots) and ceQORH mutated in the CaM-binding site ("mut", white squares) with 200 nM [AtCaM1-Alexa^{488}].

Previous experiments conducted by Gilles Curien pointed out an interesting property of ceQORH: this protein can be denatured in the presence of 8 M urea, but subsequent urea dilution (40 mM final concentration) allows the refolding of the protein to an active form and the same result was obtained when the same experiment was carried out in the presence of CaM but with EGTA (**Fig. 3.4A**). On the

contrary, in the presence of CaM and Ca^{2+} the recovery of activity of urea-denatured ceQORH was strongly compromised (see the 50-200 s part of the curve in **Fig 3.4B**). However, upon addition of an excess of EGTA (after 220 s), disrupting the ceQORH-CaM interaction, activity increases immediately. Note that a subsequent addition of an excess of Ca^{2+} (after 350 s) does not promote inhibition of the enzyme, a result in agreement with the fact that folded ceQORH is not inhibited by CaM. Increasing CaM concentration (**Fig. 3.4C**) decreases the residual ceQORH activity (**Fig. 3.4C**). It appears therefore that the protein renaturation is compromised by an excess of AtCaM1, in a Ca^{2+}-dependent way.

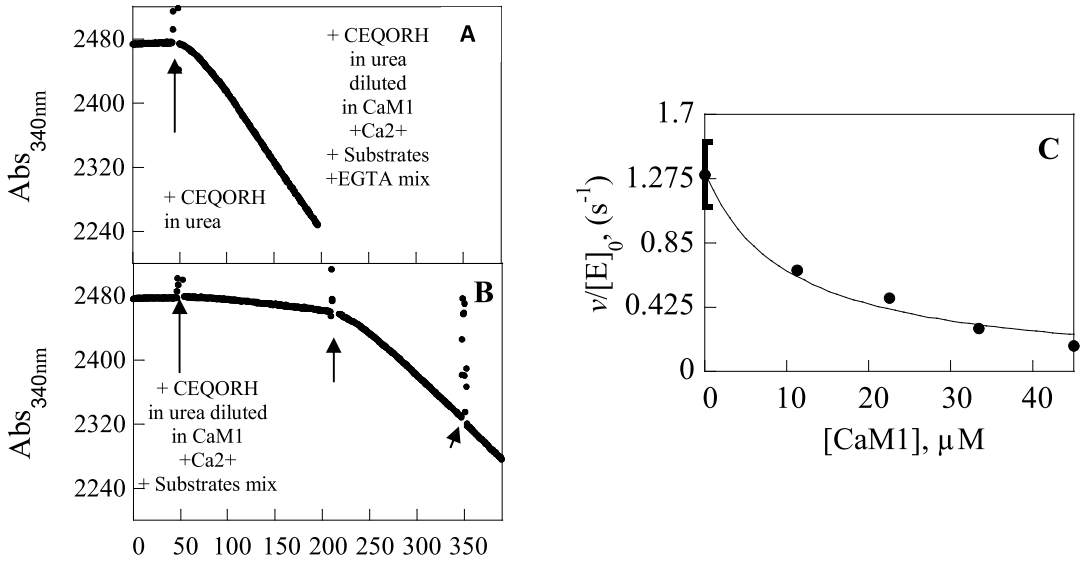

Fig. 3.4 Effect of AtCaM1-Ca^{2+} on ceQORH protein folding. The addition of AtCaM1 and Ca^{2+} to folded ceQORH does not affect ceQORH activity (not shown). When ceQORH is denatured in urea and the protein (and urea) are diluted in the presence of the substrates the protein folds and is catalytically active (not shown). When the same experiment is carried out in the presence of AtCaM1, Ca^{2+} (500 µM) and excess EGTA (2 mM) the enzyme also folds in a catalytically active form (see **Fig. 3.4A**). When EGTA is omitted (**B**) very little activity is detected. However, subsequent addition of EGTA reactivates the enzyme to similar level of activity as in **A**. Subsequent addition of an excess of Ca^{2+} does not reverse the effect. **C** shows that the AtCaM1 effect is concentration dependent. A large excess of AtCaM1 is required to prevent ceQORH folding into the active form. Experimental conditions: **A.** 12.5 µM urea denatured ceQORH mix was prepared by mixing equal volumes of native ceQORH (25 µM CeQORH, 1 mM DTT) with a 8 M urea-Tris 100 mM pH 8.0 solution. 0.5 µl denaturated ceQORH solution was added to the reaction mixture containing 100 µM Chalcone, 160 µM NADPH, 45 µM AtCaM1 and 500 µM Ca^{2+} with an excess EGTA (2 mM) (**A**) or in the absence of EGTA (**B**). In the experiment (**B**) an excess of EGTA (2 mM) was added after 200 s leading to ceQORH activation. An excess of Ca^{2+} (total concentration 5 mM) was added 150 s later. The experiment described in B was reproduced with increasing amounts of CaM. The curve was fitted with a hyperbola. Half decrease in activity occurred for 10 µM AtCaM1.

These results can be explained by the following model. In the denatured state the CaM-binding domain of ceQORH is accessible and binding of CaM in the presence of Ca^{2+} prevents the folding of the protein in an active state. In the active, folded state of ceQORH, CaM is still able to bind to ceQORH (**Fig. 3.3**), but without any effect on the protein activity. A role of CaM in preventing ceQORH folding is therefore proposed.

- **Aim of the work**

In summary, previous results revealed that CaM interaction has no effect on the protein activity of the WT and mutated ceQORH proteins. However, the mutated version gave a weaker overlay signal with respect to the WT protein.

We therefore decided to improve the characterization of the CaM interaction with ceQORH, by testing the affinity of the WT and mutated version of the identified CaM-binding peptide and by competition experiments.

Results

1- Characterization of the putative high-affinity CaM-binding site of ceQORH

1.1- Experimental setup

We purchased the TamRA-conjugated 20-amino acid peptides corresponding to the putative ceQORH CaM-binding domain and its mutated version (**Fig 3.5**). We then analyzed their binding to AtCaM1 by fluorescence anisotropy measurements as previously described for NADK2.

The fluorescence anisotropy of the peptides was measured with an excess of $CaCl_2$. Experimental conditions were the same used for NADK2 (see **Chapter 1**). However, we observed that, unlike the NADK2 TamRA-labeled peptides, fluorescence of these peptides was not stable during the experiments and led to variations of more than 20% of the starting value. In order to overcome this problem, we added a mild concentration of a non-ionic detergent (LDAO, 14 μM), observing no variations in the fluorescence anisotropy values but a stabilized fluorescence.

In these conditions, the ceQORH peptide was able to interact with CaM. The binding was instantaneous (*i.e.* shorter than the mixing time) after addition of CaM (as indicated by the arrow at 90 s in **Fig. 3.5**). Fluorescence anisotropy of the peptide-CaM complex was stable during time and returned to the basal level (free peptide) upon addition of EGTA (added at 330 s in **Fig. 3.6**), indicating reversible binding of the peptide to CaM. Subsequent addition of Ca^{2+} reproduced the increase in fluorescence anisotropy observed at the beginning of the experiment and addition of EGTA again allowed the fluorescence anisotropy to go back to the original level.

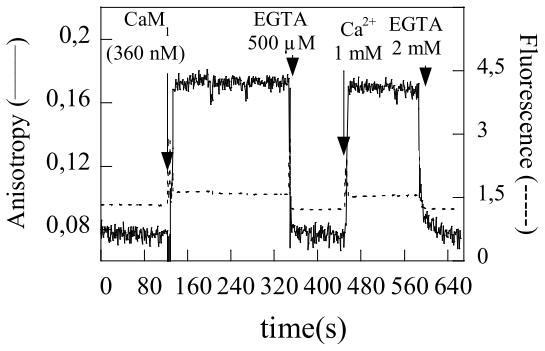

Fig. 3.5 Stability of fluorescence and fluorescence anisotropy of the ceQORH CaM-binding TamRa-labeled peptide. Addition of AtCaM1 (at 90 s), EGTA (at 350 s), $CaCl_2$ (at 450 s) and again EGTA (at 600 s) did not alter the fluorescence levels (dotted line, right Y axis) more than 20%. Fluorescence anisotropy (black line, left Y axis) instantaneously increased with addition of $CaCl_2$ in the presence of AtCaM1 and came back to the original levels with excess of EGTA.

1.2- Affinity of the CaM-binding peptide for AtCaM1

A binding curve for the ceQORH CaM-binding peptide was performed by incremental addition of small aliquots of concentrated unlabeled AtCaM1. Results displayed in **Fig. 3.6** show that binding of AtCaM1 to the CaM-binding peptide of ceQORH reaches saturation. Half saturation was reached at approximately 50 nM AtCaM1. As this value is close to the concentration of total peptide in solution (50 nM), these results indicate tight binding. Equation 1 (**Eqn. 1** in **Material and Methods**) was thus used to fit the data, as explained for NADK2 in **Chapter 1**. The apparent K_D we calculated (12 nM) was much lower if compared to the one previously measured for the entire protein (**Fig 3.3**) using At-CaM1-Alexa^{488}.

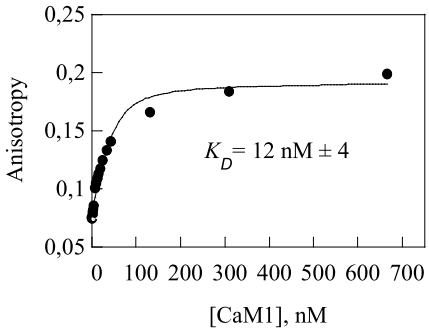

Fig. 3.6 Binding of the Tamra-labeled ceQORH wild-type CaM-binding peptide to AtCaM1. Measurements were done with 50 nM ceQORH peptide. The curve is the best fit obtained by non-linear regression analysis of the data using **Eqn.1** A K_D of 12 nM was calculated.

We performed the same binding experiment in the presence of 180 nM TamRa-peptide, *i.e.* more than 10 times the observed K_D. The corresponding binding profile shown in **Fig. 3.7** reveals a similar K_D value (9 nM) and allows deducing the stoichiometry of the binding. In these conditions (Stein et al, 2011), the curve can be separated in two linear segments. The value corresponding to the intersection point of these two segments gives the number of CaM molecules per peptide. We observed a 1:1 stoichiometry between AtCaM1 and the ceQORH peptide.

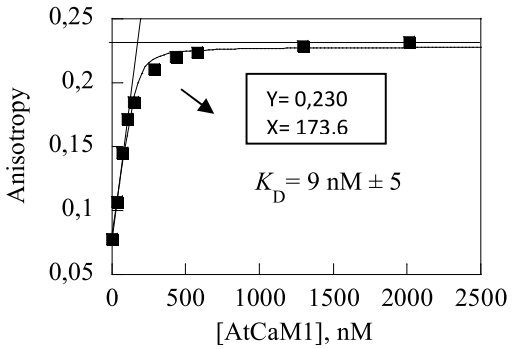

Fig. 3.7 Titration of the ceQORH (175 nM) peptide by AtCaM1. The abscissa of the intersection point between the tangent at the origin and the asymptotic line at the top corresponds to the amount of AtCaM1 needed in order to bind all the peptides present. The obtained value (*i.e.* 173 nM AtCaM1) for 180 nM TamRA labeled peptide suggests a 1:1 binding stoichiometry.

1.3- Ca^{2+}-dependence of the ceQORH CaM-binding peptide and CaM

In order to quantify the Ca^{2+} dependency of the interaction between the ceQORH CaM-binding sequence and CaM, we incubated the ceQORH peptide and CaM into a buffer depleted in residual Ca^{2+} by treatment with chelex resin (immobilized EDTA) at increasing [Ca^{2+}].

Fluorescence anisotropy measurements are reported in **Fig 3.8** and show a binding curve with a strong sigmoidicity. The data points were fitted by a Hill equation (**Eqn. 2**, see **Material and Methods**). The Hill number value (n_H=2.6±0.2) is in agreement with the presence of four Ca^{2+}-binding sites per CaM molecule and the cooperative nature of their binding previously described (Potter et al, 1983). The $K_{0.5}$ value for Ca^{2+} was in the micromolar range (1.4±0.05 µM), *i.e.* a concentration compatible with the plastidial concentration or the cytosolic concentration upon stress exposure.

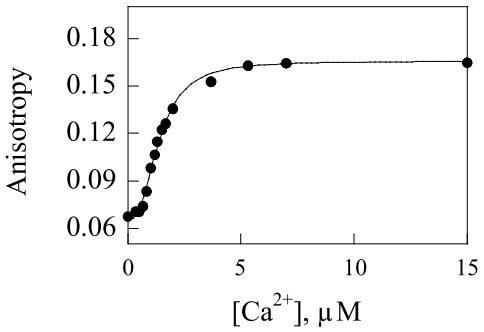

Fig. 3.8 Fluorescence anisotropy of ceQORH TamRA labeled CaM-binding peptide in the presence of AtCaM1 as a function of [Ca^{2+}]. [AtCaM1] = 360 nM; [ceQORH TamRA-labeled peptide] = 50 nM; Data points are the averaged anisotropy values of three independent experiments. The solid line is the best fit obtained by non-linear regression analysis of the data points using a Hill equation (**Eqn.2**). $K_{0.5}$ for Ca^{2+} = 1.4±0.05 µM, Hill number = 2.6±0.2.

1.4- Interaction of the mutated version of the peptide with AtCaM1

In order to confirm the role of this site in the interaction with AtCaM1, the experiment was repeated in the same conditions with the mutated version of this peptide (see **Fig. 3.2**). The measured anisotropy changes of this peptide (white dots in **Fig. 3.9**) were much different than those observed with the WT peptide (black dots in **Fig. 3.9**), even if still Ca^{2+} dependent (*i.e.*, the interaction was disrupted by addition of excess of EGTA, not shown). A value of approximately 300 nM could be obtained for the K_D of the mutant peptide by curve fitting of the data points using **Eqn. 1**, indicating that the affinity of the

mutated peptide for AtCaM1 was 30 times lower than for the wild-type version. As an additional control, we also tested an unrelated peptide (TKALGISYGRKKRRQRRRA). We observed a certain degree of binding (lower that what observed for the mutated site) that can be considered as a-specific, as it was not Ca^{2+} dependent (straight line, white squares in **Fig. 3.9**).

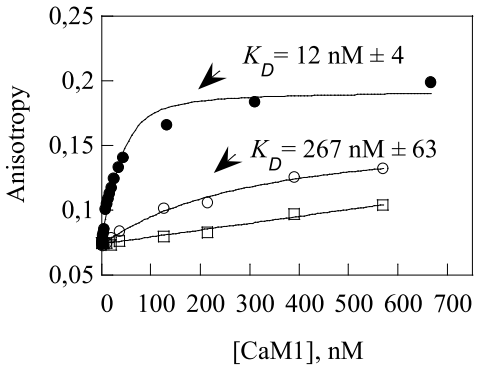

Fig. 3.9 Comparison of the CaM-affinity of wild-type ceQORH TamRa-labeled CaM-binding peptide (black dots), mutant ceQORH TamRa-labeled CaM-binding peptide (white dots) and an additional control TamRa-labeled peptide (white squares). All peptides were used at a concentration of 50 nM. The curve is the best fit obtained on the averaged data of three experiments (see text).

In conclusion, at physiological Ca^{2+} levels the ceQORH CaM-binding peptide displays high CaM affinity (approximately 10 nM) and a 1:1 binding stoichiometry. Few mutations are able to severely compromise this interaction.

The affinity measured for the WT peptide is approximately 70 times higher if compared with the results obtained with the full-length ceQORH protein (see **Fig. 3.3** in the introduction of this chapter). Measurements were repeated with new preparations of AtCAM1-Alexa^{488} and ceQORH with the same results. This large difference in the K_D of the entire protein measured with AtCaM-Alexa^{488} and the TamRa peptide can be explained in two ways: either the identified peptide is not suitable for measuring the CaM affinity of the entire protein, or the AtCaM1-Alexa^{488} labeling lowers the affinity of AtCaM1 for ceQORH. The first hypothesis might be supported by the fact that the identified peptide, despite its high CaM affinity, is not accessible once the protein is folded. Indeed, preliminary data about the ceQORH structure (Sarah Mas-y-Mas et al, unpublished) suggest that the protein is a monomer that could assemble in tetramers, and, in this particular assembly, the identified CaM-binding site might not be accessible for CaM. The second hypothesis is supported by the fact that the Alexa labeling is done

on a unique cysteine that is located in the first Ca^{2+}-binding site of AtCaM1 (see **Fig. I.9** in the **Introduction**) and this labeling could affect some interactions.

To test these two hypotheses, we developed an additional CaM-ceQORH binding test: a competition assay in which none of the partners is labeled.

2- Competition between ceQORH and its CaM-binding peptide or the NADK2 CaM-binding peptide. Comparison with the mutated ceQORH protein

2.1- ceQORH competes with its own CaM-binding peptide for binding AtCaM1

We started by forming the complex between the ceQORH peptide (50 nM) and AtCaM1 (360 nM). As expected, we observed a shift in the fluorescence anisotropy of the peptide from approximately 0.084 to 0.180. At this point, we added increasing amounts of ceQORH (**Fig. 3.10**). After each addition we observed a decrease in the detected fluorescence anisotropy of the peptide, a sign of the fact that the ceQORH peptide was set free by ceQORH protein, in agreement with the formation of the competing complex AtCaM1-ceQORH.

Such data can be analyzed by curve fitting (see Vinson et al, 1998) to deduce the K_D of the competing interaction of ceQORH with AtCaM1 (called K_{D2}), knowing the K_{D1} (for the interaction between the peptide and AtCaM1) as well as the concentration of free AtCaM1 (called $[AtCaM]_0$) just before the competitor ceQORH is added (*i.e.* for [ceQORH]= 0). K_{D1} (12 nM) is obtained by curve fitting of the data displayed in **Fig. 3.6**. The value of free AtCaM1 was obtained by calculation using **Eqn. 3**, knowing the total concentration of labeled peptide, K_{D1} and total AtCaM1 concentration used in the assay.

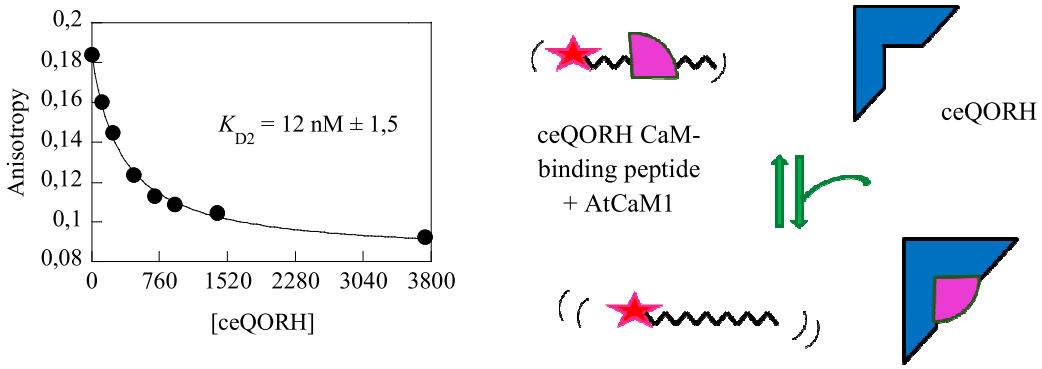

Fig. 3.10 Competition between the labeled CaM-binding peptide of ceQORH and ceQORH full length protein for AtCaM1. Increasing amounts of ceQORH were added to the complex AtCaM1-TamRA-labeled peptide of ceQORH, causing a decrease in the fluorescence anisotropy of the TamRA-labeled peptide. Total TamRA-labeled peptide concentration was 50 nM. Free AtCaM1 concentration ($[AtCaM1]_0$ = 312 nM) for $[AtCaM1]_{total}$ = 360 nM was obtained by calculation using **Eqn. 3**. The curve was obtained by non-linear regression analysis of the data point using **Eqn. 4**, with a K_{D1} value of 12 nM. The curve is the best fit obtained on the averaged data of three experiments.

We then used **Eqn. 4** to fit the experimental data. The apparent K_D (K_{D2}) was estimated of approximately 12 nM. This value corresponds to what previously observed for the isolated peptide (**Fig. 3.6**). However, it is much lower if compared to the value obtained for the entire protein with AtCaM1-Alexa^{488} (800 nM). This therefore suggests that the binding experiments with AtCaM1Alexa^{488} are affected by the labeling of AtCaM1 and suggest the importance of analyzing these interactions without the bias of fluorescent probes.

To give an idea of the precision of such indirect determination of K_D values we compared the experimental data with a set of theoretical curves generated by simulation (**Fig. 3.11**). These curves were generated assuming the experimental concentration of the peptide (50 nM) and that of free AtCaM1 (312 nM), for several values of ceQORH affinity for AtCaM1 (=K_{D2}). By superposing the experimental data with the simulation, it can be observed that the experimental curve matches the theoretical one obtained for K_{D2} = 10 nM (**Fig. 3.11**) and is clearly different from other values for K_{D2}.

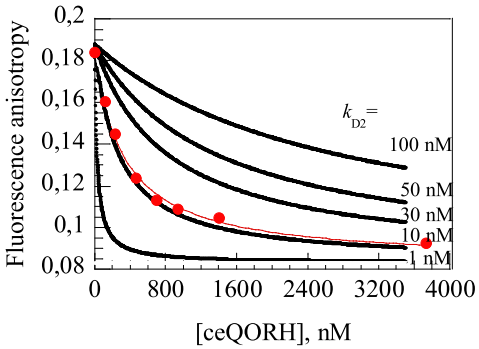

Fig. 3.11 Simulation of disruption of the complex AtCaM1-ceQORH peptide by the ceQORH protein for several values of K_{D2}. The experimental data (red dots) are from **Fig. 3.10**. Simulations were run for K_{D2} = 1, 10, 30, 50, and 100 nM.

2.2- ceQORH competes with the NADK2 CaM-binding peptide for binding AtCaM1

In principle, the competition assay described above can be done with any CaM interacting labeled peptide. In order to examine this, we established another competition test using this time the CaM-binding TamRA labeled peptide of NADK2 that we showed having a K_D for AtCaM1 of 190 nM (see **Chapter 1**), rather than the ceQORH peptide.

For this, we started by forming the complex between the NADK2 labeled peptide (50 nM) and At-CaM1 (200 nM). As expected, we observed a shift in the fluorescence anisotropy of the peptide from 0.100 to 0.145. At this point, we added increasing amounts of ceQORH (**Fig. 3.12**). After each addition we observed a decrease in the detected fluorescence anisotropy of the peptide, a sign of the fact that the NADK2 peptide was set free by ceQORH and in agreement with the formation of the competing complex AtCaM1- ceQORH.

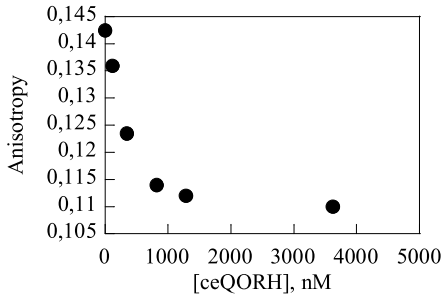

Fig. 3.12 Competition between the CaM-binding peptide of NADK2 and ceQORH for AtCaM1. Increasing amounts of ceQORH were added to the complex CaM-peptide NADK2 ([AtCaM1] = 200 nM, [NADK2 peptide] = 50 nM). The curve is the best fit obtained on the averaged data of three experiments.

In this case, however, the fluorescence anisotropy of the peptide did not reach the level of the peptide alone (*i.e.* approximately 0.100), but was stabilized at 0.11 and the original anisotropy value was not even reached with addition of EGTA in excess (not shown). This suggested Ca^{2+}-independent interferences between the NADK2-peptide and the ceQORH protein.

One explanation for these data is that the ceQORH protein might bind nonspecifically to the NADK2 peptide. To test this hypothesis, we performed a binding experiment by incubating the NADK2 peptide alone with increasing amounts of ceQORH. We indeed observed an increase of the NADK2 peptide fluorescence anisotropy, indicating that the NADK2 peptide was able to interact with ceQORH. Interestingly, we could deduce a K_D value of approximately 300 nM from these data (**Fig. 3.14**) indicating a rather strong affinity, though of no physiological meaning.

Competition assays require therefore checking that no interaction between the CaM-binding peptide and the CaM competitor occurs.

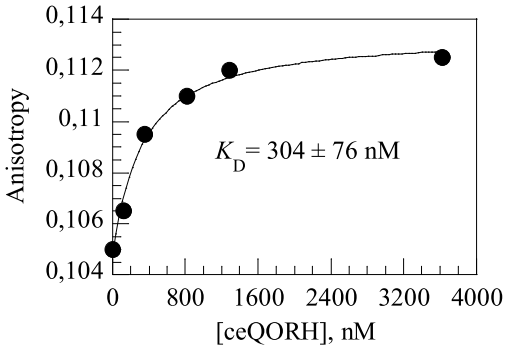

Fig. 3.14 A-specific binding of ceQORH to the NADK2 CaM-binding TamRa-labeled peptide. Measurements were performed in the same conditions as above. The measured K_D is of approximately 300 nM. The curve is the best fit obtained on the averaged data of two experiments using Eqn.1.

2.3 -Disruption of AtCaM1-ceQORH peptide interaction by mutant ceQORH

Since we discovered that the labeling of AtCaM1 with Alexa^{488} affects the interaction of ceQORH with AtCaM1, the comparison of ceQORH and ceQORH mutant interaction with AtCaM1- Alexa^{488} displayed in **Fig. 3.3** needed to be re-examined. We thus investigated again the CaM affinity of the ceQORH protein mutated in the identified CaM-binding site by our competition test with the ceQORH CaM-binding peptide.

To measure the affinity of the ceQORH mut protein for AtCaM1, we incubated AtCaM1 (360 nM) with the ceQORH peptide and added increasing amounts of ceQORH mut and compared the results with those obtained with ceQORH WT (**Fig. 3.15**).

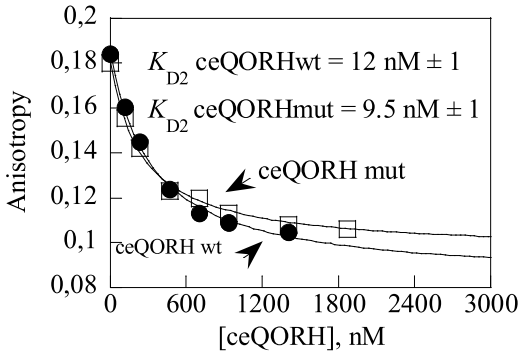

Fig. 3.15 Competition assay with wild-type ceQORH (black dots) and ceQORH mutated in the CaM-binding site (white squares). [AtCaM1] = 360 nM, [peptide] = 50 nM. Increasing amounts of ceQORH wt or ceQORH mut were added to the complex AtCaM1-Tamra labeled peptide of ceQORH, causing a decrease in the fluorescence anisotropy of the peptide. Free AtCaM1 concentration ($[AtCaM1]_0$= 316 nM) was obtained by calculation using **Eqn. 3** (see **Material and Methods**). Curves were obtained by non-linear regression analyses of the data point using **Eqn. 4**, a K_{D1} value of 12 nM, and $[AtCaM1]_0$ = 312 nM. The curve is the best fit obtained on the averaged data of three experiments.

It can be observed that the competition curve of the ceQORH mut is not different from that of the ceQORH WT and that both display a K_D for AtCaM1 of approximately 10 nM. This is reminiscent of what previously observed when the affinities of the wt and mutant ceQORH proteins for AtCaM1-Alexa^{488} were compared. In that case, both proteins showed the same K_D for AtCaM1, even if the value was much higher (*i.e.* 800 nM).

In conclusion, we observed again no difference on CaM affinity for the ceQORH wt and mutant forms. The higher value of K_D obtained with AtCaM1-Alexa^{488}, likely due to the Alexa labeling, since it occurs very near a Ca^{2+}-binding site. This hypothesis will need to be further verified, for example by other competition experiments in which the ceQORH-AtCaM1-Alexa^{488} complex will be disrupted by unlabeled AtCaM1. Preliminary results seem to confirm this hypothesis.

Conclusions and Perspectives

By our measurements on the ceQORH CaM-binding peptide and our competition experiments we showed that the ceQORH protein possesses a Ca^{2+}-dependent high affinity for AtCaM1. In addition, we showed that this 20-amino acids peptide is able to bind to AtCaM1 with high affinity and that this interaction can be 20 times lowered by the mutation of three residues.

These results are in agreement with the data obtained by Daniel Salvi that revealed that the ceQORH mutated protein gives a weaker overlay signal with respect to the wt protein.

In contrast, AtCaM1-Alexa^{488} binding experiments and competition tests showed that the wt and mutated ceQORH proteins do not display any difference in their binding affinity for AtCaM1. In both cases, the curves of the wt and mutant protein were perfectly comparable. These tests differed quantitatively, for the calculated K_D values, probably because of interference of the Alexa probe with calcium-binding or partner-binding, but not qualitatively.

As a difference between ceQORH wt and ceQORH mut is only observed with protein in the denatured state (peptide and probably overlay) this might suggest that *in vivo* binding to CaM occurs very early during the protein production, prior to its folding.

Normally, when synthesized, proteins are either bound to chaperones that help them to be correctly folded, or interact with the components of the various import machineries (the import indeed occurs when the protein is in its unfolded conformation). In this picture, CaM may play a role in preventing the protein folding in agreement with kinetic results (see **Fig. 3.4**) and interfere with its correct transport to the chloroplast. This hypothesis is supported by a different localization profile of ceQORH and its mutated form investigated by Daniel Salvi and Lucas Moyet. Plants stably expressing ceQORH-GFP show a dual plastidial and cytoplasmic localization of ceQORH. By contrast, when plants are transformed with the mutated form of ceQORH, only chloroplastic localization is observed. CaM might therefore sequester the protein in the cytoplasm. The details of this hypothetical mechanisms and its dependence on Ca^{2+} remain to be determined.

During this study we also designed a competition test for analyzing CaM interaction. This technique is particularly suitable because it can be performed without the need of labeling one of the two partners. A-specific interactions can sometimes lead to binding of the peptide to the target protein, but this can be easily monitored and the labeled peptide substituted with another one.

Chapter 4

Quantitative characterization Tic32 interaction with AtCaM1

Introduction

As illustrated in the **Introduction**, Tic32 (At4g23430) is a protein of the inner envelope membrane of plastids. The protein was proposed to be a NADPH-dependent dehydrogenase implicated in the regulation of plastidial protein import by interaction with members of the Tic/Toc translocon, in particular Tic110 (Chigri et al, 2006).

Its interaction with CaM was discovered thanks to approaches relying on mass spectrometry. The group of Prof. Jürgen Soll (München Universität) first demonstrated that targeting of proteins to the chloroplast was controlled by Ca^{2+} (Chigri et al, 2005). Starting from these observations, the aim of this group was to identify the targets of Ca^{2+} regulation within the chloroplast envelope. A protein extract from the chloroplast envelope was therefore incubated with CaM resin in the presence of $CaCl_2$ in excess (Chigri et al, 2006). After 16 hours incubation, proteins bound to the column were eluted with an excess of CaM and subjected to SDS-PAGE. One of the bands detected corresponded to Tic32, as assessed by mass spectrometry and by western blot with an antiserum raised against this protein. The interaction was subsequently verified by CaM-affinity chromatography of the recombinant protein expressed in *E. coli* and truncated versions of the protein allowed identifying the last 20 amino acids as crucial for the CaM interaction (**Fig. 4.1**). It is noteworthy that this identified CaM-binding site was not detected in the protein sequence by the Calmodulin Target database tool (see **Annex II**).

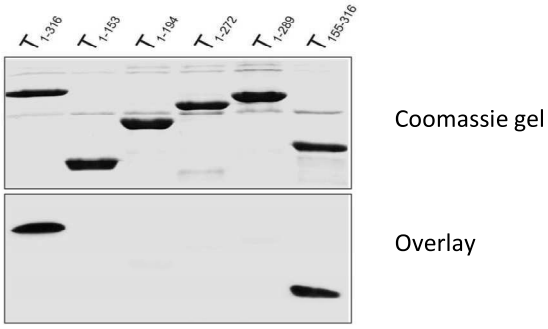

Fig. 4.1 CaM-binding to Tic32 and identification of the Tic32 CaM-binding site. Several truncations of Tic32 were produced and tested for their CaM-binding capacity (Chigri et al, 2006; see **Chapter 2** and **Material and Methods** for more details on the technique). Only the full-length protein containing the *C*-terminus (amino acids 290-316) was able to bind to CaM. Upper panel: coomassie gel of the different purified proteins. Lower panel: detection of HRP-CaM bound to Tic32 deletions.

Enzymatic assays showed also that the dehydrogenase activity of Tic32 was inhibited by CaM in the presence of Ca^{2+} when preincubated for 30 minutes before activity measurement.

For its ability to interact with CaM and its still discussed role in the regulation of protein import, a crystallization project of Tic32 is currently running between our Team, in the LPCV, and colleagues from the IBS (Sarah Mas-y-Mas and David Cobessi). In addition, it has recently been shown by Daniel Salvi that this protein, like ceQORH, is doubly localized in the cytoplasm and the chloroplast (unpublished results). This prompted us to better characterize this interaction with AtCaM1, by combining several fluorescence anisotropy measurements similarly to what previously illustrated for ceQORH (see **Chapter 3**).

Results

Pure recombinant Tic32 was already available in our lab (purified by Cécile Giustini in our team and Sarah Mas-y-Mas, IBS-Grenoble).

1- Quantification of recombinant Tic32 affinity for AtCaM1-Alexa^{488} *in vitro* by fluorescence anisotropy

We firstly measured the interaction of purified recombinant Tic32 (see Dell'Aglio et al, 2013 for details about the purification) with AtCaM1-Alexa^{488}. As displayed in **Fig. 4.2**, a saturation curve was obtained by incubating AtCaM1-Alexa^{488} with increasing amounts of Tic32. Curve fitting analysis using **Eqn. 1** (see **Material and Methods**) allowed obtaining a K_D value of 0.8 µM. The Ca^{2+} dependency of the interaction was also observed since the addition of EGTA in excess made the anisotropy go back to the original levels (not shown).

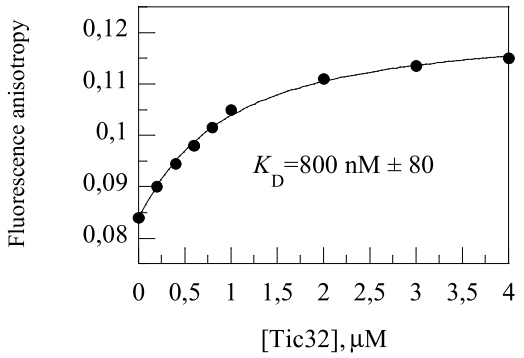

Fig. 4.2 Characterization of the CaM-binding affinity of Tic32 for AtCaM1-Alexa^{488}. Incubation of AtCaM1-Alexa^{488} (200 nM) with increasing amounts of Tic32. The curve is the best obtained by non-linear regression analysis of the data using **Eqn. 1**. The calculated K_D value of Tic32 for AtCaM1-Alexa^{488} is of approximately 800 nM.

2- Disruption of the Tic32-AtCaM1-Alexa^{488} by NADPH

It was previously reported (Chigri et al, 2006) that the binding of Tic32 to CaM is disrupted by NADPH, the cofactor of Tic32. The binding tests were performed with proteins bound to nitrocellulose membrane (overlay assays) and with long incubation times (three hours).

In order to further confirm this hypothesis with proteins in solution and in a short time scale, we tested the ability of NADPH to disrupt the Tic32-AtCaM1Alexa^{488} complex.

As shown in **Fig. 4.3**, addition of NADPH to the complex lowers the fluorescence anisotropy of At-CaM1-Alexa^{488} down to its free-state level thus strengthening the observations of Chigri et al (2006).

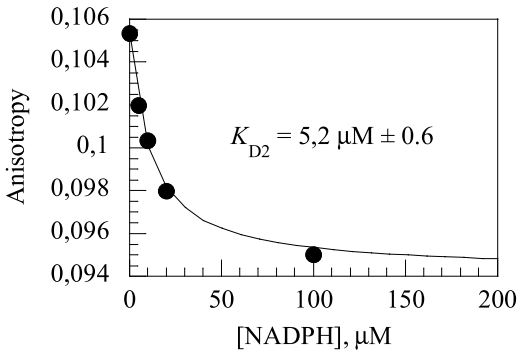

Fig. 4.3 Disruption of the interaction between Tic32 and AtCaM1-Alexa^{488} by NADPH. Increasing amounts of NADPH were added to the complex Tic32-AtCaM1-Alexa^{488}, causing a decrease in the fluorescence anisotropy of the fluorescent probe. The curve was obtained by non-linear regression analysis of the data points using **Eqn.4**, with [Tic32] total = 1 µM, $[Tic32]_0$ = 894 nM, a K_{D1} value of 800 nM and [AtCaM1-Alexa^{488}] = 200 nM. The curve is the best fit obtained on the averaged data of three experiments.

The curve was fit with **Eqn. 4**, as done in **Chapter 3** for all competition experiments. In this case, the competitor was the NADPH metabolite. The fit allowed estimating a K_D of Tic32 for NADPH of approximately 5 µM.

3- Competition between Tic32 and the ceQORH peptide

Since we previously observed with the ceQORH protein that the labeling of AtCaM1 might influence the CaM-partner interaction, we repeated the competition tests developed with ceQORH for Tic32.

Firstly, we established the complex between the ceQORH CaM-binding peptide (50 nM) and At-CaM1 (360 nM). Then, we added to the solution increasing amounts of Tic32 and we observed that the fluorescence anisotropy of the ceQORH peptide decreased with a hyperbolic profile. At the end of the experiments, anisotropy values almost reached the value of the free peptide. This allowed fitting the

data with a competition curve (**Eqn. 4, see Fig. 4.4**), as previously done for ceQORH in the **Chapter 3**. The measured K_{D2} for Tic32 binding to unlabeled AtCAM1 was estimated approximately 10 nM (7.0 nM ± 1).

This value is comparable to what previously measured for ceQORH (see **Chapter 3** and Insert in **Fig. 4.4**), suggesting that both proteins have the same affinity for AtCaM1.

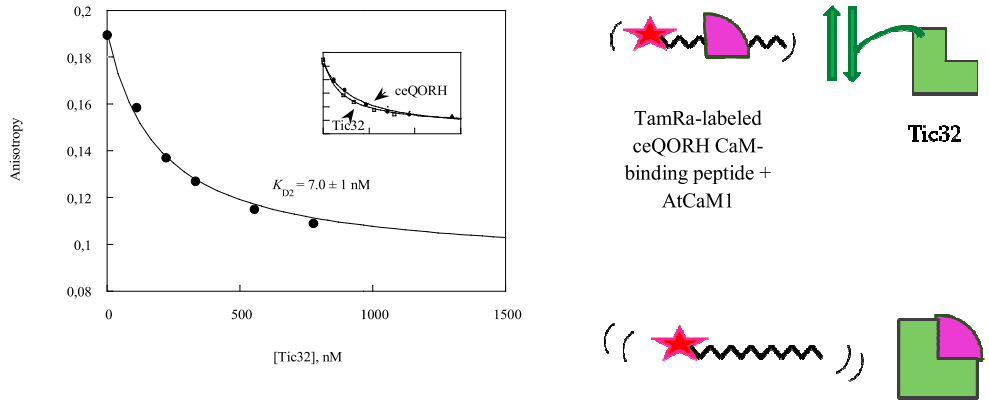

Fig. 4.4 Disruption of the AtCaM1-ceQORH CaM-binding peptide interaction by Tic32. [AtCaM1] = 360 nM, [peptide] = 50 nM. Conditions are the same as detailed for ceQORH in **Chapter 3**. The curve is the best fit obtained on the averaged data of three experiments using **Eqn. 1**. The calculated K_D is of approximately 10 nM. Insert: comparison of the competition curves obtained for Tic32 (white squares) and CeQORH (black squares).

4- Binding of the predicted Tic32 CaM-binding peptide to AtCaM1

In order to examine in more detail the interaction between Tic32 and AtCAM1, we designed and purchased a TamRa-labeled peptide corresponding to the *C*-terminus of the Tic32 sequence, which, according to the literature, contains amino acids that are important for the binding to CaM (**Fig. 4.5**). Indeed, a protein truncated of the last 26 amino acids proved not to bind CaM in an overlay assay (Chigri et al, 2006, see lane 5 in **Fig. 4.1**, above). We designed this peptide by aligning the *C*-terminal sequence of Tic32 of several plant species and eliminating the last amino acids that were not conserved and did not contain residues normally considered important in determining the CaM affinity.

```
Glycine          QVKGISGKYFSDSNLAKTTAQGTDSDLAKKLWDFSMDLTK-------- 313
Pisum            QVKGVSGEYFSDSNVYKTTPHGKDVDLAKKLWDFSINLVKQK------ 316
AtTic32          QVAGVSGEYFQDSNIAKPLPLVKDTELAKKVWDFSTKLTDSQSGESSS 322
Vitis            QVKGVSGEYFADSNIAKPSSKGKDAELGKKLWEFSISLTEPN------ 315
Populus          QVKGVSGEYFMDSNLSKASSLAKDEELAKKLWDFSLSLTNPK------ 315
Medicago         QVKGISGEYFTDSNKASPTSLAKDTKLAQKLWELSVSLSNTK------ 315
Zea              HVKGVSGKYFCDCNLYEPSANAKDMELAKRLWDFGVELIT-------- 316
Oryza            QVKGVSGKYFSDSNVNEASEKGNDMELAKRLWEYSIELIT-------- 316
                 :* *:**:** *.*  ..    .* .*.:::*: . .*
```

Fig. 4.5 Alignment of the *C*-terminal region of Tic32 homologs of several plant species. The amino acids identified by Chigri et al (2006) as important for CaM-binding are in red and the purchased peptide is squared. This protein region was compared to that of several plant species: *Glycime max* (NP_001242868.1), *Pisum sativum* (sp|Q6RVV4.1|TIC32_PEA), *Vitis vinifera* (XP_002274932.1), *Populus tricocharpa* (gb|ABK96367.1), *Medicago truncatula* (gb|ACJ84342.1), *Zea mays* (NP_001136855.1) and *Oryza sativa* (gb|EAZ10151.1).

We observed that the anisotropy of the peptide increased linearly in response to addition of AtCaM1 (**Fig. 4.6**) and to a very limited extent. As no sign of saturation could be observed even at high concentration (up to 7 µM AtCaM1) the interaction appears as a-specific. In addition the interaction was not Ca^{2+} dependent. Changes in the Hepes or salt concentrations did not modify the results.

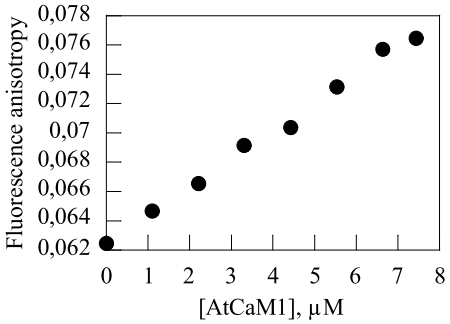

Fig. 4.6 Anisotropy of TamRa labeled *C*-terminus Tic32 peptide as a function of [AtCaM1]. The fluorescence anisotropy of the peptide increased slowly and linearly upon addition of increasing amounts of AtCaM1.

Conclusions

In this chapter, we used the fluorescence anisotropy measurements previously described for the study of the Tic32 interaction with AtCaM1.

Our results confirm the high CaM-affinity of Tic32. Indeed, the measured value is indeed of 800 nM if measured with AtCaM1-Alexa^{488}, but much lower (10 nM) if measured by the competition assay with the ceQORH peptide. These discrepancies, also observed for the ceQORH protein, again suggest that the labeling of AtCaM1 affects its binding properties to its partners and/or to Ca^{2+}.

As previously reported (Chigri et al, 2006) our competition tests performed with NADPH confirmed that the binding of Tic32 to CaM is disrupted by NADPH. Furthermore, the K_D of NADPH for Tic32 (5 µM) that we estimated suggests that, if the interaction between Tic32 and CaM is possible *in vivo*, this interaction should only occur in the presence of very low NADPH concentrations. These results also demonstrate that the fluorescence anisotropy-based technique that we developed during this work is particularly suitable, not only for the investigation of protein-protein interactions, but also to the formation of protein-metabolite complexes, such as the binding of a cofactor. Therefore, this technique could also be used for discovering or confirming new protein ligands such as inhibitors or other cofactors.

In addition, we showed that the region identified as the CaM-binding domain by Chigri et al. 2006 should be further investigated. Actually, the peptide we designed on the basis of these previous findings could not display the high CaM affinity we measured for the entire protein. This might be due *i)* to the fact that the protein needs to assume a particular 3D conformation in order to bind to AtCaM1, or *ii)* to the fact that the peptide should have been designed differently. Indeed, Chigri et al (2006) demonstrated the importance of these amino acids for CaM-binding but it is possible that some residues located upstream also participate to the CaM-trapping. The analysis of the Tic32 structure now in progress (Sarah Mas-y-Mas et al, unpublished) will hopefully help solving this question.

Chapter 5

A search for putative plastidial CaM-like proteins

Introduction

As previously reported in the general **Introduction**, several genes coding for CaM and CMLs isoforms are present in plant genomes. In Arabidopsis, seven genes were identified that code for "true" CaMs. In addition, plant genomes contain a high number of CaM-like (CML) proteins. In order to be classified as a CML, a protein must fulfill the following requirements: *i)* it must be composed mostly (or entirely) of EF-hand motifs, *ii)* it must not contain any additional domains and *iii)* must share at least 16% overall amino acid identity with CaM (Mc Cormack and Braams, 2003).

The Arabidopsis genome contains 50 genes coding for CMLs. All predicted proteins contain at least 2 EF-hand motifs with the exception of CML1 that contains only one Ca^{2+} binding domain (Mc Cormack and Braams, 2003).

Such a high variety of Ca^{2+} binding proteins is supposed to be associated to a fine control of cell responses to environmental stimuli. In this perspective, each CML should have different Ca^{2+} binding affinity and/or expression profile, bind specific target proteins and/or be targeted to various subcellular compartments. They are very similar and it is therefore complex to identify their specific partners and their biological functions. At present, only few CMLs were characterized in detail and a broad picture of their regulation and integration of their functions still needs to be acquired.

- **Biochemical properties**

Since they are composed mainly, if not completely, of Ca^{2+} binding sites, the biochemical properties of CMLs are supposed to be quite similar to those of CaM. This is proven by the fact that AtCML10 was reported to almost fully activate native plant NAD kinase, whereas AtCML 18, 39, 42, 43 and 47 were not (Turner et al, 2004). Even AtCaM2 showed a weaker activation effect on NADK with respect to AtCaM4 and 6 (Liao et al, 1996). The specificity of CMLs is however totally unknown for the moment. Lee et al (1997) tried to address the question by overlay assays on protein extracts from several plant tissues or from plants grown in various environmental conditions. They observed differences in the expression of two soybean CaM isoforms (SCaM-1 and -4), as well as differences in the affinity for the identified targets. They could not detect differences in their sets of targets, but this might be due to the

fact that the overlay assay cannot distinguish between specific and a-specific binding, nor properly compare the affinity of the two proteins.

At present, no 3D structures are available for CMLs with the exception of the human CML, that shares 85% sequence identity with the "true" human CaM (Han et al, 2002, PDB code: 1GGZ). However, the Ca^{2+} binding was confirmed for some of them by showing their different mobility on SDS-PAGE in the presence of $CaCl_2$ or EGTA, a common feature of Ca^{2+}-binding proteins. This mobility shift was observed for AtCaM7, 8, 37, 38 and 39, while it was less clear for AtCML9 (Zielinski 2002, Vanderbeld and Snedden, 2007).

- **Expression profiles**

Differential expression of CML genes is observed at various developmental stages (McCormalck et al, 2005), but also in response to a variety of stimuli such as heat stress (Al-Quraan et al, 2010), pathogen attacks (Chiasson et al, 2005; Takabatake et al, 2007), hormone treatments, chemical and abiotic stresses (Magnan et al, 2008; Vanderbeld and Snedden, 2007). In particular, AtCML24 was shown to be up-regulated by a wide variety of stimuli (Delk et al, 2005) and AtCML42 was closely associated to the regulation of trichome branching (Dobney et al, 2009).

- **Intracellular localization**

Some CMLs contain additional *N*-terminal of *C*-terminal extension sequences and are predicted to be located in specific cellular compartments such as the mitochondria, the ER or the chloroplast.

Some CMLs were indeed already localized in subcellular compartments other than the cytoplasm. In particular, several CaM isoforms were localized in the nucleus. This is the case for AtCaM7, which has been shown to bind to the promoter of light-responsive genes and regulate their activity (Kushwaha et al, 2008). Translocation of AtCML19 from the cytoplasm to the nucleus was also observed (Liang et al, 2006). Similarly, the Petunia PhCaM53, that contains a prenylation sequence at the *C*-terminus, is localized in the nucleus instead of the plasma membrane when its prenylation is abolished. The prenylation status of the protein was shown to be modulated *in vivo* by light/dark condition and sugar availability. A mutant form lacking the prenylation site gave a peculiar phenotype, thus confirming the importance of cor-

rect subcellular localization of this protein for a correct physiological regulation (Rodríguez-Concepción et al, 1999 and 2000). PhCaM53 is homologous to Arabidopsis AtCaM5 that also contains a predicted *C*-terminal prenylation site.

CaM-control of peroxisomal catalase activity was proposed (Yang and Poovaiah, 2002) and, more recently, AtCML3 was localized in this cell compartment (Chigri et al, 2012).

Calmodulin isoforms were also found in the mitochondria (AtCML30, Chigri et al, 2012), the extracellular space (Ma et al, 1999) and the vacuole, where AtCML18 (previously called AtCML15) was identified as a protein able to interact with the *C*-terminal region of AtNHX1, a vacuolar Na^+/H^+ antiporter (Yamaguchi et al, 2005).

- **Searching for CMLs in the chloroplast**

Although never directly observed, the presence of CaMs or CMLs in the chloroplast is supported by various observations:

- the fact that many CaM and CMLs were localized in many other cell compartments, such as the mitochondria, the vacuole and the nucleus;
- the presence of several CMLs containing *N*-terminal peptides that are predicted as putative plastidial transit sequences;
- the presence of plastidial CaM-binding proteins (such as NADK2, Tic32 and ceQORH and probably others, according to the high-throughput study illustrated in **Chapter 2**).

However, on the basis of our findings on the ceQORH protein illustrated in **Chapter 3**, the interaction between plastidial proteins and CaM/CMLs might also take place in the cytoplasm, before the protein import to its final destination.

These two mechanisms (*i.e.* CaM/CML-partner interaction in the chloroplast or in the cytoplasm) are both possible and not mutually exclusive.

In order to take advantage of the knowledge acquired by the proteomic approach and the potential of fluorescence anisotropy in testing the different interactions, it was therefore interesting to look for the presence of plastidial CMLs.

To do so, we first performed a proteomic analysis, searching for CaM or CMLs that are targeted to plastids. We also investigated the subcellular localization of four putative plastidial CMLs by localizing them in Arabidopsis protoplasts as GFP fusion proteins.

Results

1- A proteomic approach for the detection of plastidial CaM or CMLs from Arabidopsis

1.1- Establishment of a protocol for CaM purification

Calmodulins are little proteins that are known to be resistant to high temperatures. In addition, a protocol for CaM purification was previously established and used for the purification of several CaM isoforms (Lee et al, 1997). This procedure consists of binding the CaM protein to a phenyl-sepharose resin in the presence of an excess of $CaCl_2$. In these conditions, CaM is specifically retained on the column and can be subsequently released with addition of EGTA in excess.

In order to test the efficiency of this procedure, we focused firstly on AtCML41, a CML with a predicted plastidial localization. We cloned the cDNA of AtCML41, without the sequence corresponding to the predicted transit peptide, in an expression vector. **Fig. 5.1** illustrates the production of the recombinant protein in *E. coli* and its detection in crude extracts of bacterial proteins corresponding to total or soluble proteins.

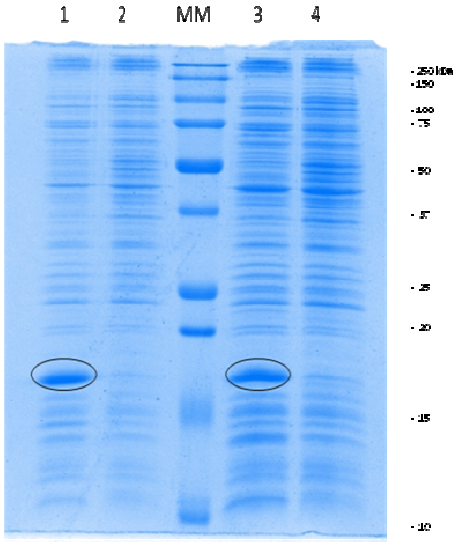

Fig 5.1 Production of recombinant AtCML41 without its putative plastidial transit peptide in *E. coli* Rosetta cells. In the total (1) and soluble (3) bacterial extracts of an induced culture an overexpressed protein is detected at the expected size (18 kDa). Such a band is not detected in non-induced total (2) and soluble (4) bacterial extracts. MM: molecular marker. The production of the protein was induced overnight at 20°C.

We then submitted the soluble bacterial extract containing the recombinant protein to a heat shock followed by centrifugation to remove all precipitated proteins (see **Material and Methods** for details). The supernatant contained a protein with the predicted size of the recombinant CML 41, suggesting that this CML, as true CaMs, was heat resistant. This fraction was then loaded on a phenyl sepharose resin equilibrated with a $CaCl_2$-containing buffer. Unbound proteins were washed from the column using the same buffer. Then, proteins bound to the matrix were eluted with an excess of EGTA. As shown in **Fig 5.2A** (lane 4) the eluted fraction contained a nearly homogeneous protein which migrated at the expected molecular weight.

A mobility-shift assay was performed **(Fig 5.2B)** and revealed a slightly faster migration of the protein in the presence of $CaCl_2$ versus EGTA as previously reported for true CaM or CML (Lee et al, 2000; Vanderbeld et al, 2007), strongly suggesting that the purified protein was indeed CML41.

In a typical soluble protein extract, CML41 represents approximately $1/20^{th}$ of the total proteins (*i.e.* approximately 100 mg/L of culture). After purification, approximately 45 mg of CML41/L of culture were recovered (*i.e.* 45% of the initial protein). It is important to underline that the protein was prone to precipitate during the final concentration step, which could explain the relatively low final yield.

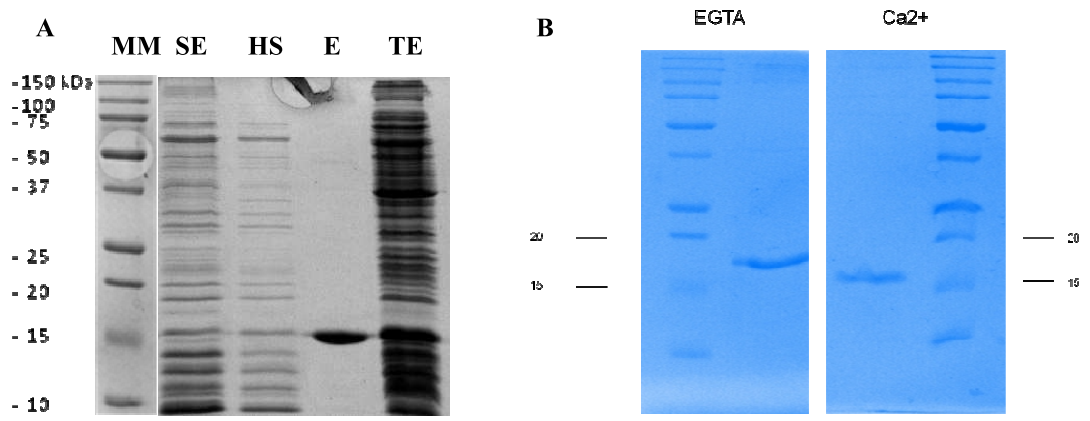

Fig 5.2 Purification of the recombinant AtCML41 in *E. coli* and Ca^{2+} binding test. SDS-PAGE profile of the purification of recombinant AtCML41. 20 µg of each protein extracts were loaded. MM: molecular weight markers. SE: soluble bacterial protein extract corresponding to a culture of bacteria in which protein expression was induced with IPTG (0.4 mM) overnight (note that the protein was less abundant than in the previous production assay, that was performed in a reduced culture volume: 100 mL against 1 L, **Fig. 5.1**, lane 3), HS: Soluble protein fraction following the heat shock (95°C, 2 min). E: protein fraction eluted from the phenyl sepharose column after the EGTA treatment. TE: total protein extract. **B**. Mobility shift assay of 10 µg of AtCML41 in the presence of 5 mM EGTA (left) or 1 mM $CaCl_2$ (right). The predicted molecular weight of recombinant AtCML41 (minus the predicted transit peptide) is 18 kDa.

1.2- Application of the CaM purification protocol to Arabidopsis chloroplast fractions

After validation of the efficiency of this powerful and easy protocol to purify CaM proteins, we decided to start from Arabidopsis chloroplast fractions in order to identify putative CML present in this cell compartment. We started with highly purified thylakoids and stroma samples from Arabidopsis chloroplasts and submitted these protein samples to the procedure used for CML41 (heat shock, binding of the soluble proteins on a phenyl sepharose column in the presence of $CaCl_2$, elution with EGTA and TCA precipitation).

The proteins that were specifically retained on the Phenyl sepharose column in the presence of $CaCl_2$ and eluted by EGTA were not visible on a standard coomassie gel, therefore a silver staining was performed (**Fig. 5.3**). Despite the virtual absence of protein at the size of CML41 (*i.e.* 18 kDa) the gel showed enrichment of specific bands that correspond to the size of calmodulins, *i.e.* between 15 and 25 kDa (**Fig 5.2**).

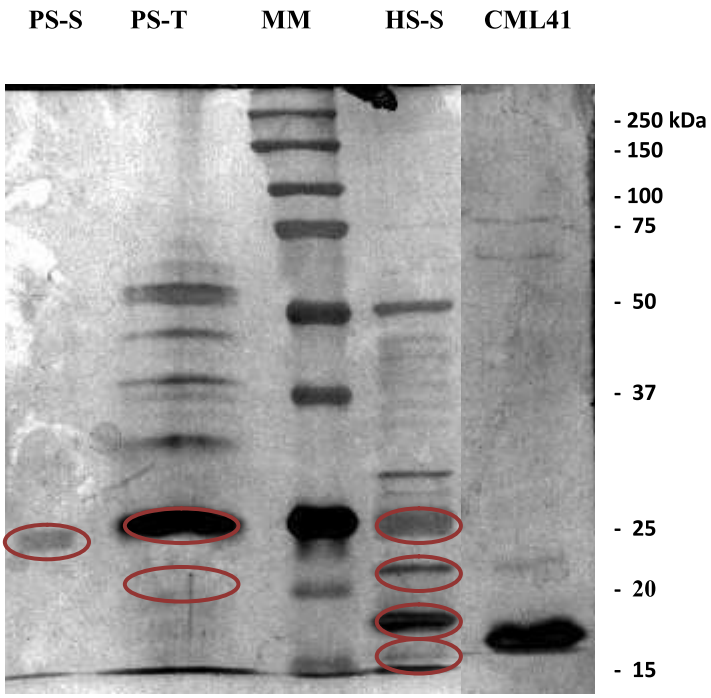

Fig 5.3 Silver staining gel of the SDS-PAGE of the proteins present in the last purification step (elution from the phenyl-sepharose column by EGTA) starting with Arabidopsis plastidial subfractions. For heat-shock extracts, 20 µg of protein were loaded. For phenyl sepharose purifications, 10 µL of each TCA precipitation were loaded. HS-S: stroma heat-shock; PS-S: stroma phenyl sepharose elution; PS-T: thylakoids phenyl sepharose elution. The thylakoid heat shock sample was not loaded since all the remaining sample was used for the mass spectrometry analysis. MM: molecular marker. CML41: pure CML41 (10 µg). Circles indicate the bands that were excised from a second identical gel and analyzed by mass spectrometry.

These bands were then excised from the gel and submitted to mass spectrometry at the EdyP laboratory (as described in **Material and Methods**) with the help of Alexandra Kraut. The same was done for the region comprised between 15 and 25 kDa of thylakoids and stroma heat shock samples, before the passage on the phenyl sepharose column. The samples corresponding to the phenyl sepharose elutions of stroma and thylakoids were also analyzed in their totality. In all samples, neither CaM nor CML proteins were identified. However, three peptides of a classic CaM were detected. Two of these peptides (VFDKDQNGFISAAELR and MKDTDSEEELKEAFR) are present in all seven AtCaMs, while one of them (ADQLTDDQISEFK) is present in five of them but absent in AtCaM1 and 4. This result might suggest the presence of true CaMs in the chloroplast and in particular at the level of the thylakoid membrane. However, the thylakoid fraction is known to contain 3% of envelope proteins (Ferro et al, 2010). Therefore, the presence of this protein might be simply explained as a contamination in the thylakoid fraction by a cytosolic CaM bound to the outer surface of the outer membrane of the chloroplast envelope. This second hypothesis ap-

pears to be the most probable. Indeed, since "true" CaMs lack any sort of transit sequence, an alternative import system should account for their localization in the chloroplast.

2- Localization of a subset of CMLs in Arabidopsis protoplasts

Since the proteomic analysis was not helpful, we decided to focus on the *in situ* localization of CMLs isoforms that are expected to be targeted to plastids. We started by investigating the putative intracellular localization of all CMLs by three subcellular targeting prediction programs. As reported in **Table 5.1**, several CMLs were predicted to contain a plastidial transit peptide by a least one prediction program. However, discrepancies existed between the three prediction systems. It has been reported several times that prediction programs show some limits in their ability to differentiate mitochondrial and plastidial transit peptides (Habib et al., 2007; Schleiff and Becker, 2010). For this reason, CMLs also predicted to contain mitochondrial transit peptides could be good candidates for a plastidial localization.

We could not test the all putative plastidial or mitochondrial CMLs for problems of time. We thus excluded AtCML25 and 42 since they were previously localized in the cytoplasm (Zhou et al, 2009 and Vadassery et al, 2012) and we focused on AtCML30, 35, 36 and 41 because: *i)* all these CMLs are predicted to contain four Ca^{2+} binding sites and are therefore supposed to be more similar to AtCaM1, which is able to activate plant NADK (see **Chapter 6**); *ii)* three of them (AtCML30, 35 and 36) were predicted to be plastidial or mitochondrial by at least two programs. AtCML41 was also selected since the Genevestigator profile showed that this protein is overexpressed in photosynthetic tissues (**Fig 5.4**).

The whole cDNA sequences corresponding to these four proteins were then cloned in the pUC vector, in frame with a GFP at the *C*-terminus, and under the control of a strong promoter (35S). Since in the meantime AtCML30 was localized in the mitochondrion by Chigri et al (2012), this CML was not further investigated. The all remaining constructs were used to transform Arabidopsis protoplasts (experiment performed by David Macherel, Université d'Angers).

All transformations were successful, even if for AtCML36 and 41 only few transformed protoplasts were obtained (**Fig 5.5)**. All tested constructs revealed a cytoplasmic localization. AtCML35 was also partially detected in the nucleus and AtCML41 in the ER (**Fig 5.5**). Control western blots (**Fig. 5.6)** performed on the transformed protoplasts showed that, despite the

presence of some GFP alone that could account for part of the fluorescence detected in the cytoplasm, all three fusion proteins were present (upper bands in **Fig. 5.6**). As no fluorescence signal could be detected in the chloroplast we can therefore conclude that none of our tested CMLs are localized in the chloroplast in our tested model system (*i.e.* Arabidopsis protoplasts).

CML	AGI	*N*-terminal extension	PSORT	YLOC	targetP
1	At3g59450	no	cytoplasm	cytoplasm	other
2	At4g12860	no	cytoplasm	nucleus	other
3	At3g07490	no	cytoplasm	cytoplasm	other
4	At3g59440	yes	plasma membrane	cytoplasm	secretory pathway
5	At2g43290	yes	endoplasmic reticulum	chloroplast	secretory pathway
6	At4g03290	no	cytoplasm	cytoplasm	other
7	At1g05990	no	cytoplasm	cytoplasm	other
8	At4g14640	no	cytoplasm	nucleus	other
9	At3g51920	no	peroxysomes	cytoplasm	other
10	At2g41090	no	peroxysomes	nucleus	other
11	At3g22930	no	cytoplasm	nucleus	other
12	At2g41100	yes	nucleus	nucleus	other
13	At1g12310	no	cytoplasm	cytoplasm	other
14	At1g62820	no	cytoplasm	cytoplasm	other
15	At1g18530	no	cytoplasm	cytoplasm	other
16	At3g25600	no	cytoplasm	cytoplasm	other
17	At1g32250	no	peroxysomes	cytoplasm	other
18	At3g03000	no	cytoplasm	cytoplasm	other
19	At4g37010	no	cytoplasm	nucleus	mitochondria
20	At3g50360	no	mitochondrial matrix	cytoplasm	mitochondria
21	At4g26470	yes	plasma membrane	nucleus	other
22	At3g24110	yes	chloroplast thylakoids	nucleus	other
23	At1g66400	yes	cytoplasm	cytoplasm	other
24	At5g37770	yes	cytoplasm	cytoplasm	other
25	At1g24620	yes	chloroplast stroma	nucleus	other
26	At1g73630	yes	cytoplasm	nucleus	other
27	At1g18210	yes	cytoplasm	cytoplasm	other
28	At3g03430	no	cytoplasm	cytoplasm	other
29	At5g17480	no	cytoplasm	cytoplasm	other
30	At2g15680	yes	chloroplast	cytoplasm	chloroplast
31	At2g36180	no	cytoplasm	cytoplasm	other
32	At5g17470	no	cytoplasm	cytoplasm	other
33	At3g03400	no	cytoplasm	cytoplasm	other
34	At3g03410	no	peroxysomes	cytoplasm	other
35	At2g41410	yes	mitochondrial matrix	chloroplast	chloroplast
36	At3g10190	yes	mitochondrial matrix	chloroplast	mitochondria
37	At5g42380	yes	chloroplast stroma	nucleus	chloroplast
38	At1g76650	yes	cytoplasm	nucleus	chloroplast
39	At1g76640	yes	nucleus	nucleus	other
40	At3g01830	yes	cytoplasm	nucleus	other
41	At3g50770	yes	cytoplasm	nucleus	chloroplast
42	At4g20780	no	chloroplast stroma	nucleus	other
43	At5g44460	no	chloroplast stroma	nucleus	mitochondria
44	At1g21550	no	mitochondrial matrix	cytoplasm	other
45	At3g29000	yes	endoplasmic reticulum	nucleus	secretory pathway
46	At5g39670	yes	plasma membrane	nucleus	other
47	At3g47480	no	endoplasmic reticulum	cytoplasm	secretory pathway
48	At2g27480	no	peroxysomes	chloroplast	other
49	At3g10300	yes	endoplasmic reticulum	nucleus	other
50	At5g04170	yes	plasma membrane	nucleus	other

Table 5.1 List of all Arabidopsis CMLs and their predicted localization using PSORT, YLOC and TargetP programs.

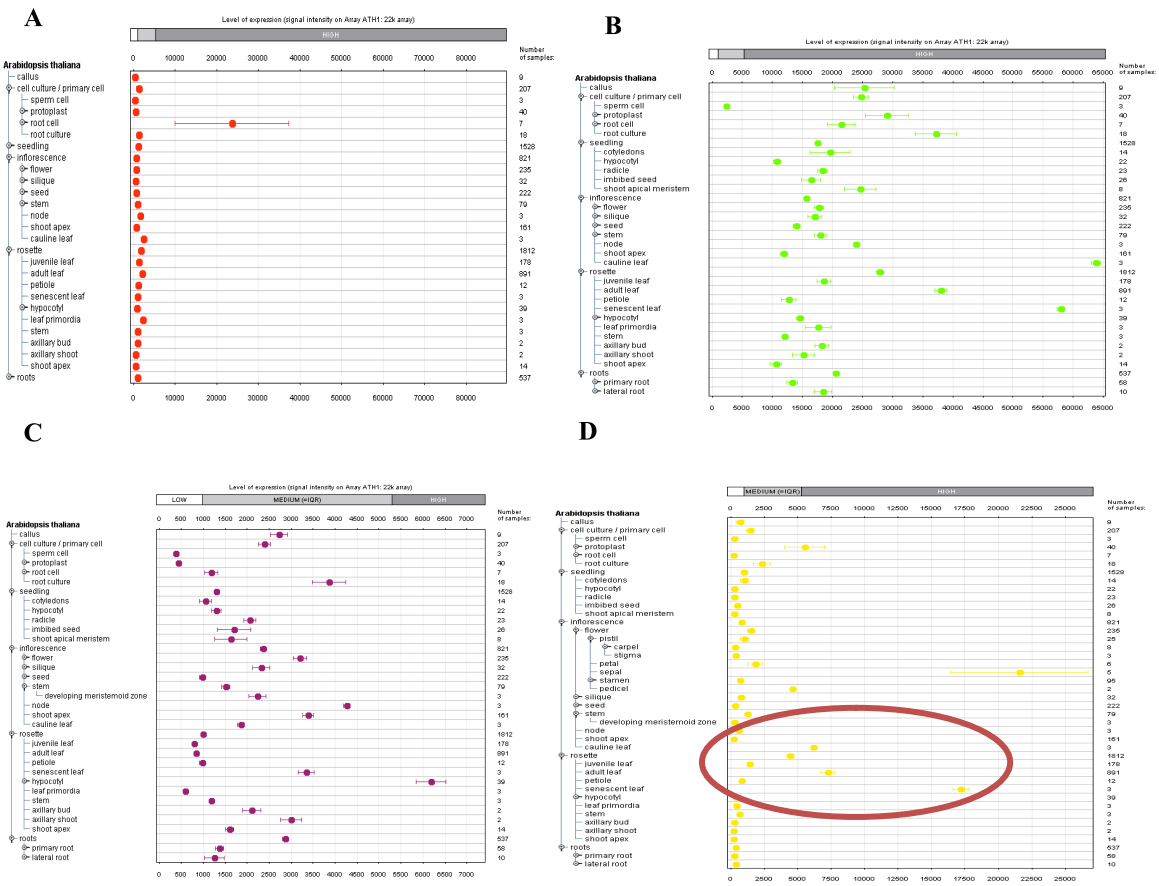

Fig 5.4 Gene expression profiles of the four selected CMLs. A. CML30 mRNA abundance, **B**. CML35 mRNA abundance; **C**. CML36 mRNA abundance; **D**. CML41 mRNA abundance. CML41 mRNAs appear to be particularly enriched in leaves and sepals.

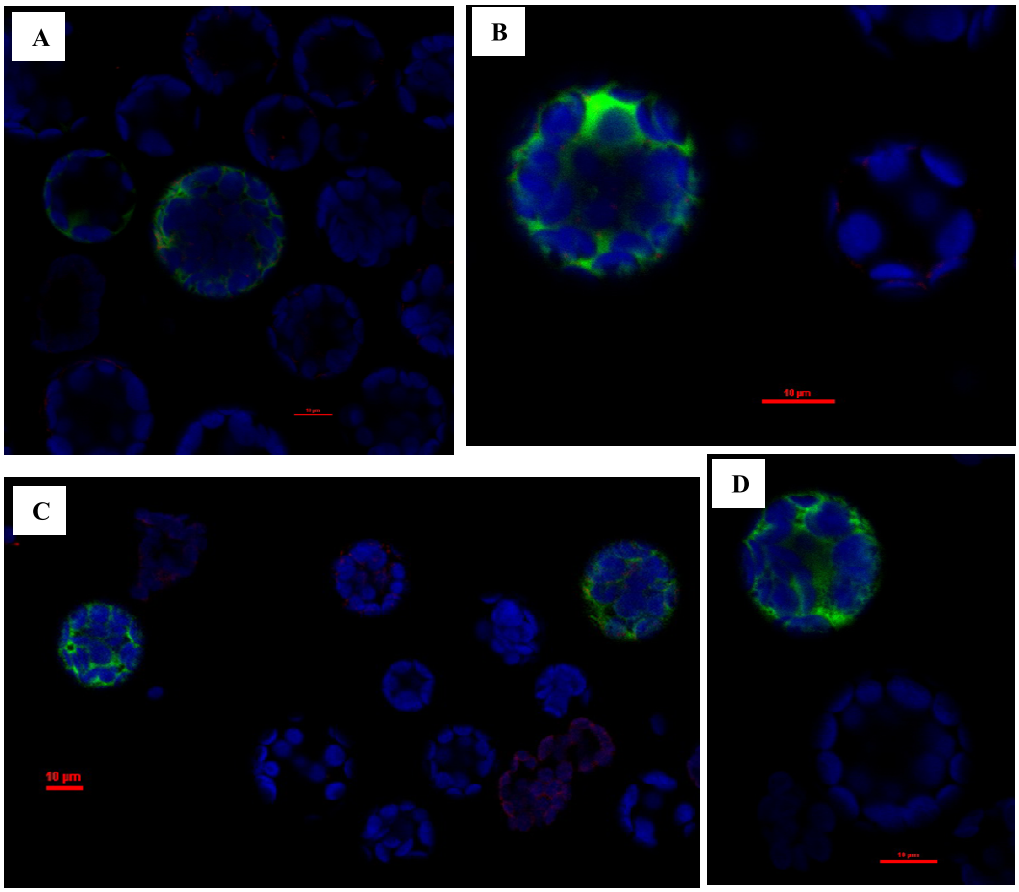

Fig 5.5 localization of CML 35, 36 and 41 fused to GFP in transformed Arabidopsis protoplast. **A**. Cytoplasmic control; **B**. CML35-GFP; **C**. CML36-GFP; **D**. CML41-GFP.

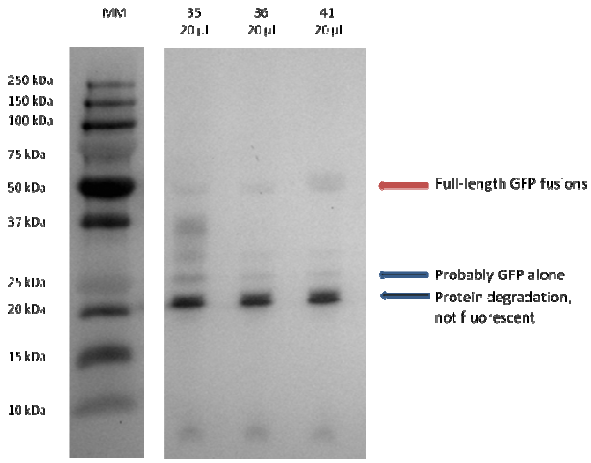

Fig 5.6 Western blot of the proteins extracted from the Arabidopsis protoplasts transformed with the different CML-GFP fusion proteins using an anti-GFP antibody. MM= molecular marker; The figures (35), (36) and (41) indicate the gel lanes loaded with proteins from protoplasts transformed with the plasmids coding for CML35-GFP, CML36-GFPCML41-GFP, respectively. The bands detected at approximately 50 kDa (red arrow) correspond to full-length fusion proteins; lower bands correspond to degradation and/or GFP alone (blue arrows).

Conclusions

In conclusion, our proteomic and localization approaches did not allow identifying plastidial CMLs. The only peptides detected from the proteomic analysis that belonged to a CaM were recognized as part of any of true CaMs and most probably due to cytosolic contaminations.

This might reflect the absence of such proteins in this cell compartment, or be due to technical reasons. In particular, identification of a protein by proteomics requires taht *i)* the protein is present in a sufficient amount to be detected *ii)* the presence of unique tryptic digested peptides that allow associating a protein with a unique amino acid sequence and *iii)* these peptides are sufficiently long to be analyzed by mass spectrometry and be recognized as specific for a protein or a set of few proteins. CaM and CMLs are very short and thus contain only few sites for tryptic digestion. The high similarity in their sequences challenges even more the possibility to find a specific peptide sequence allowing undoubtedly identification of a specific CaM or CML isoform. For example, in our case, the identified peptides in the thylakoid sample could not be attributed to a specific CaM isoform, since these peptides are present in five CaM isoforms with the exception of AtCaM1 and 4. On the other hand, these peptides are not present in any of the CMLs sequences. All these reasons could explain why the identification of CaMs in the chloroplast fractions during this analysis or during other previous proteomic studies targeted to chloroplast proteins did not allow retrieving any CML sequence.

Our *in situ* localization could not provide evidence for the plastidial localization of the 3 tested proteins. Since the localization was performed on protoplasts, this result do not exclude that some of these isoforms might be localized in the plastid in some particular cell types or during developmental-environmental specific conditions. In order to test this last hypothesis, stable plant expression is required and was not performed because it required longer time and we encountered problems in cloning the gene sequences in a suitable vector.

We were however able to determine the localization of these three proteins that appeared to be all cytoplasmic, with AtCML35 also found in the nucleus and AtCML41 also in the ER.

The presence of CaM or CMLs in the chloroplast is therefore still an open question. Since prediction programs are not reliable, the answer will require the investigation of the localization of all the other CMLs, starting with those containing an N-terminal extension as reported in **Table 5.1**.

Finally, it is worth mentioning that there are no structures yet available for CML proteins. The simple, rapid and efficient purification procedure for CML41 would easily allow developing crystallization projects for this protein or similar ones.

Chapter 6

Advanced characterization of recombinant NADK2 and plant NADK interaction with AtCaM1

Introduction

As illustrated in the **Introduction** and in **Chapter 1**, plant NAD kinase is the most studied plant enzyme able to interact with CaM. The importance of this enzyme in the photosynthetic process and our data about the interaction with CaM of its regulatory domain and its CaM-binding peptide prompted us to better investigate the relationship between plant NADK and CaM.

Here, we will briefly summarize literature data concerning the NADK2-CaM interaction, and then we will discuss our new findings.

NADP(H) (**Fig. 6.1**) is an essential cofactor of dehydrogenases found in all living organisms. While NAD(H) is primarily involved in catabolic reactions, NADP(H) participates in anabolic reactions and in defence against oxidative stress. Metabolic pathways that consume NADP include lipid biosynthesis, biosynthesis of many amino acids and the reduction of ribonucleotides to deoxyribonucleotides (Agledal et al, 2010 for a review of NADP functions).

NAD^+ is also as a substrate for mono- and poly-ADP ribosylation of proteins and DNA (Corda and Di Girolamo, 2003). Poly-ADP ribosylation has been implicated in the regulation of several processes, including DNA repair, transcription, and apoptosis.

In addition, NAADP, a derivative of NADP, is a potent intracellular Ca^{2+}-mobilizing messenger that triggers Ca^{2+} release from lysosomal Ca^{2+} stores in mammals (Guse et al, 2008). NAADP is considered the most potent Ca^{2+} mobilizing agent known so far.

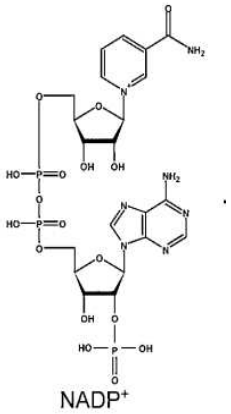

In plants, NADP has another peculiar role: it constitutes the final acceptor of electrons transported through the linear electron flow of the photosynthetic apparatus.

For all these reasons, understanding the regulatory mechanisms of NADP production and turnover is of particular interest, especially for plant biology.

Fig. 6.1 NADP: Nicotinamide Adenine Dinucleotide Phosphate

NAD kinase was identified and partially purified for the first time in 1950 from yeast (Kornberg, 1950), then also from bacteria and rat liver and heart. The subsequent years saw the establishment of better purification protocols from various sources; especially plants (see Yamamoto, 1966 for a review).

- **Control of NAD kinase activity in plants by Ca^{2+} and CaM**

In plants, NAD kinase activity was reported to be controlled by many factors, such as the physiological stage of the cell and light. In particular, it has been observed that NAD kinase activity is 17-fold more elevated in the root elongation region with respect to the root meristem (Allan and Trewavas, 1985). This high activity was mostly CaM/Ca^{2+} dependent.

Muto et al (1981) proposed a light control of NAD kinase activity. They showed that, in wheat leaves illuminated after dark overnight incubation, the cellular levels of NAD decreased and, vice versa, the NADP pool increased. The opposite conversion was observed when leaves were again put in dark after one hour of light exposure. These observations are in agreement with the activation of the photosynthetic machinery when leaves are exposed to light, and therefore an increase of the level of NADP is required. Indeed, cell subfractioning also allowed localizing NAD kinase activity in the chloroplast, with part of it located in the cytoplasm.

Right after that, the same authors (Muto et al, 1982) reported that plastidial calcium intake was induced by light exposure. They showed that this calcium accumulation lasts for approximately 5 minutes and that this transport is rather fast (*i.e.* up to 30 µmol Ca^{2+}/(h*mg chlorophyll). Measurements were performed as $^{45}Ca^{2+}$ intake and with Ca^{2+} sensitive electrodes.

One possible connection between light induced Ca^{2+} intake and NADK activity is that some sort of Ca^{2+}-dependent NADK modulator activates this enzyme in the presence of light. Indeed, in 1977 Muto and Miyachi demonstrated that NADK of pea was activated by a heat-stable proteinaceous factor present in the extract of various plants. They observed that their protein lost its activity after a passage through a DEAE cation exchange chromatography column, but incubation with some fractions of the DEAE elution pool, even after heat-shock treatment, was able to restore the enzyme activity (see also

Anderson et al, 1978). Some years later, in 1980, Anderson et al showed that this proteinaceous factor was calmodulin.

The work of Muto and Myiaki on several plant species showed that all plants contained NADK activator and that the NADK protein is generally localized in the chloroplast. In 1977, the authors also reported CaM activation was in pea, followed by spinach, Chinese cabbage, and rice. The activating effects of NADK from corn and Chlorella cells were very low.

In the following years, several authors also tried to identify the subcellular localization of this enzyme, with contrasting results.

Simon et al (1982) observed that, in chloroplasts of spinach leaves, NAD kinase was found both in the cytoplasm and in the chloroplast subfractions (stroma). They also showed that only the activity of the cytoplasmic fraction of the protein is enhanced 9-folds with calmodulin and Ca^{2+}, while the stromal NADK activity was not CaM-controlled. Later (Simon et al, 1984), they isolated two different NADK activities in the chloroplast: one localized at the outer envelope membrane, fully dependent on CaM/Ca^{2+}, and another, CaM-independent, localized in the stroma.

In contrast with what observed in spinach, Jarrett et al (1982) observed that, in pea, a chloroplast NADK isoform is Ca^{2+}/CaM dependent. They also reported that, in the chloroplast fraction, a calmodulin might be present.

The work of Dieter and Marmé (1984) also allowed observing CaM/Ca^{2+} dependent NAD kinase activity in the outer mitochondrial membrane of corn.

These discrepancies in the CaM-dependent NADK localization might be in part due to the different plants and plant tissues used and to different ways of isolating and analysing plant cell subcompartments.

Although mostly observed in plants, CaM/Ca^{2+} dependent NAD kinase activity was sometimes observed also in the animal kingdom. In 1985 the protein has been found into human neutrophils and here again modulated by Ca^{2+} and calmodulin (Williams, 1985). However, a complete characterization of

the human isoform expressed as a recombinant protein is in disagreement with CaM/Ca^{2+} stimulation (Lerner et al, 2001).

The activation of NAD kinase by Ca^{2+} and CaM has been demonstrated also for the NADK of sea urchin (Epel et al, 1982) and occurs during fertilization.

- **Biochemical data on NAD kinase activity**

NAD kinase activity can be measured by a 2 phase test: in the first step NADP is produced by NAD kinase; in the second, the NADP produced is quantified (see **Materials and Methods**).

Partial NAD kinase purification was attempted several times (Muto and Miyachi, 1977; Delumeau et al, 1998 and 2000; Turner et al, 2004). Despite the fact that different tissues and plant species were employed, there was generally high agreement about the enzyme activity and its properties.

In soluble extracts, CaM dependent activity was observed if the extracts were incubated in the presence of a CaM inhibitor or of excess of EGTA, otherwise the presence of endogenous CaM would result in measuring NADK activity even in the absence of an excess of CaM. The separation of NADK from endogenous CaM can be done by DEAE chromatography, since NADK is not retained on the resin, while CaM remains bound to the matrix and is eluted at higher salt concentrations. This procedure allowed obtaining NADK fractions totally dependent on exogenous CaM for activation (Delumeau et al, 1998).

NADK purification to homogeneity is hard to obtain since the enzyme is particularly unstable. The best purification was obtained by Delumeau et al (2000, **Fig. 6.2**). Their SDS-PAGE profile shows a clear enrichment of a polypeptide of approximately 56 kDa. Similar profiles were obtained previously (Dieter and Marmé 1980 on zucchini; Jarrett et al, 1982 on pea).

A

Table 1. Purification of NAD$^+$ kinase from 12 g of dry cells (260 g fresh of cells) from *L. pimpinellifolium*

	Total proteins (mg)	Total activity (μmol NADP$^+$ h^{-1})	Specific activity (μmol h^{-1} mg^{-1})	Yield (%)	Purification factor (fold)
Soluble proteins	758	118	0·16	100	1
HQ-HS (pH 6·5)	23	62	2·68	53	17
CaM-agarose	0·21	30	142	25	912
HQ (pH 7·5)	0·005	7·2	1440	6	9262

B

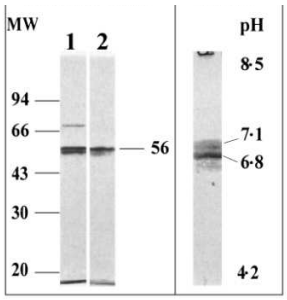

Fig. 6.2 Summary of the NADK purification from tomato root cell cultures and the corresponding gel profile from Delumeau et al (1998). **A**. SDS-PAGE of the two last purification steps. **B.** Isoelectrofocusing of the last purification step.

- **CaM isoforms are not interchangeable**

As illustrated in the introduction and more detailed in **Chapter 5**, plants possess a wide array of CaM isoforms. It is therefore interesting to see if they all have the same affinity for NADK and what are the elements important for the interaction.

In 1997, Lee et al tested two soybean calmodulins: a conserved SCaM1 and a more divergent SCaM4, and found that only the first isoform was able to activate pea NADK. A series of chimerae allowed understanding that the first Ca^{2+} binding domain of SCaM1 is crucial for the CaM-binding. In particular, this interaction is mediated by aminoacids K30 and E40, since substitution of these 2 aminoacids with E and D, respectively, completely disrupted the interaction.

Another comparative study (Karita et al, 2004) conducted on NtCAM 1, 3 and 13 clearly showed that different isoforms of CaM play different roles since, for example, the isoform 13 was not able to activate NADK from pea. In the same year, Turner et al (2004) identified the plastidial Arabidopsis NADK2 as the CaM-binding Arabidopsis NADK enzyme. They also showed that native CaM-activated NADK was activated by Petunia CaM81 or Arabidopsis CML47. A mild activation effect was detected

for Arabidopsis CML47 but almost no effect was detected with the Arabidopsis CMLs 2, 3, 18, 39, 42 and 43.

It was also established that the methylation of K115 compromised the activation of native plant NADK by CaM (Roberts et al, 1986).

- **NAD kinases from *Arabidopsis thaliana***

Several organisms, such as yeast, possess more than one isoform of NAD kinase. In the case of Arabidopsis, Turner et al (2004) reported the presence of two NAD-dependent NADK isoforms, one cytosolic and another plastidial. Some years later a third, NADH-dependent NAD kinase (NADK3) was identified (Turner et al, 2005).

The authors purified NADK2 from Arabidopsis seedlings, finding that the enzyme behaviour was similar to what observed by previous studies (*i.e.* separation of NADK2 from CaM by DEAE chromatography, high instability). However, the size of the enzyme was quite different with respect to what previously observed (110 kDa). In addition, the recombinant protein they produced in *E. coli* and purified, although able to bind to CaM in a CaM-affinity chromatography, was not activated by CaM (**Fig. 6.3**).

Table II. *Kinetic properties of Arabidopsis native and recombinant NADKs*

Partially purified CaM-dependent native NADK from 14-d-old seedlings grown in liquid culture or purified recombinant (Rec.) NADK expressed in *E. coli* were assayed as described in "Materials and Methods." Data represent mean ± SE.

Parameter	Native (CaM Dependent)	Rec. NADK1	Rec. NADK2
Optimum pH	8.0	7.9	7.9
$V_{max}^{Mg^{2+}\cdot ATP}$ (units mg^{-1} protein)	213 ± 7.2	11.1 ± 0.61	14.3 ± 0.30
K_m^{NAD}(mM)	0.20 ± 0.011	0.52 ± 0.030	0.43 ± 0.017
$K_m^{Mg^{2+}\cdot ATP}$(mM)	0.17 ± 0.014	0.73 ± 0.040	0.74 ± 0.012
$S_{0.5}^{Ca^{2+}}$(μM)	0.8 ± 0.07	12% inhibition at 0.2 mM Ca^{2+}	No effect
$S_{0.5}^{CaM}$(nM)	2.2 ± 0.079	No effect	No effect
I_{50}^{TFP}(μM)[b]	57 ± 2.90	No effect	No effect

[a]One unit of activity is defined as 1 μmol NADP h^{-1} mg^{-1} protein. [b]TFP, Trifluoperazine.

Fig. 6.3 Summary of the kinetic properties of the native (*i.e.* purified from *A. thaliana* plant) and recombinant NADK2 and NADK1 from the study of Turner et al (2004).

Through the expression of several truncated versions of the protein, the authors managed to identify a CaM-binding site in the *N*-terminal domain of the protein. The function of this plant specific *N*-terminal domain is unknown.

They also reported that the enzyme is present and active in young leaves and roots and that the activity in leaves strongly decreases with times. However, in another work (Waller et al, 2010), they showed that the gene is mainly expressed in leaf tissues, while NADK activity in roots should be mainly accounted to NADK1.

The plastidial NADK2 localization was further proved by Chai et al (2005) and by Waller et al (2010), using expression of NADK2-GFP constructs in Arabidopsis protoplasts.

The important role of NADK2 is accounted by the phenotypic characteristics of the *nadk2* mutant line characterized by Chai et al (2005) and Takahashi et al (2006). In particular, this line is characterized by a dwarf phenotype, chlorosis and impairment in photosynthesis.

- **Conclusions**

This rapid summary of current knowledge of NAD kinase and its interaction with CaM highlights that NADK is essential for all living organisms and that peculiar modulations of its activity take place in plants. In the case of Arabidopsis, CaM-dependent NADK activity has been associated to the NADK2 gene, which was localized in the chloroplast and with a key role in photosyhntesis. However, for the moment, no CaM isoforms have been localized in this cell compartment. In addition, the size of this enzyme (100 kDa) does not correspond to what previously observed (especially by Delumeau et al, 2000, *i.e.* 54 kDa), and the presence of CaM-dependent NADK activity in roots (where NADK2 is apparently not expressed) raise again the question of the importance and cellular localization of NADK regulation by CaM.

Even more questions arise from the results illustrated in **Chapter 1** about the affinity of NADK2 for AtCaM1. We observed that the affinity of the regulatory domain or the identified peptide for AtCaM1 are close to 200 nM. This value is not compatible with the high apparent affinity of CaM for plant NADK. These discrepancies might be due to several reasons: *i)* the affinity of AtCaM1 for NADK2 is

higher in the presence of enzyme substrates; *ii)* the affinity of the *N*-terminal domain was underestimated due to the fact that the Alexa probe lowers the affinity of the AtCaM1 for the *N*-terminal NADK2 domain, as previously observed for ceQORH (**Chapter 3**) and Tic32 (**Chapter 4**), and *iii)* the CaM-dependent plant NADK activity is due to another enzyme different from NADK2 or is constituted of a modified/shorter version of the same enzyme, that may be not localized in the chloroplast.

The N-terminal NADK2 domain was rather unstable and exhibited a slow binding to AtCaM1-Alexa^{488}. In addition, this protein does not contain its catalytic domain. Instead of repeating our competition experiments with the NADK2.1 protein, we decided to further characterize the activity and properties of the full-length NADK2 and the *in vivo* NADK CaM-dependent activity.

We also used *nadk2* plants to better characterize the role of NADK2 in photosynthesis (see **Annex IV**).

Results

1- Expression and activity of the entire NADK2 recombinant protein and its catalytic domain

1.1- Expression of the entire NADK2 and its catalytic domain

In order to investigate the activity of the NADK2 protein and its control by CaM, we produced two recombinant versions of this enzyme. The first one (named NADK2.2) represents the entire protein sequence without the putative plastidial transit peptide. The second (named NADK2.3) contained only the *C*-terminal catalytic region that, according to the protein alignments, corresponds to the sequence conserved among all NAD kinases (**Fig. 6.4**).

NADK2.2:

```
  1-MAQLSEAFSPDLGLDSQAVKSRDTSNLPWIGPVPGDIAEVEAYCRIFRSAERLHGALMET
 61-LCNPVTGECRVPYDFSPEEKPLLEDKIVSVLGCILSLLNKGRKEILSGRSSSMNSFNLDD
121-VGVAEESLPPLAVFRGEMKRCCESLHIALENYLTPDDERSGIVWRKLQKLKNVCYDAGFP
181-RSDNYPCQTLFANWDPIYSSNTKEDIDSYESEIAFWRGGQVTQEGLKWLIENGFKTIVDL
241-RAEIVKDTFYQTALDDAISLGKITVVQIPIDVRMAPKAEQVELFASIVSDSSKRPIYVHS
301-KEGVWRTSAMVSRWKQYMTRPITKEIPVSEESKRREVSETKLGSNAVVSGKGVPDEQTDK
361-VSEINEVDSRSASSQSKESGRFEGDTSASEFNMVSDPLKSQVPPGNIFSRKEMSKFLKSK
421-SIAPAGYLTNPSKILGTVPTPQFSYTGVTNGNQIVDKDSIRRLAETGNSNGTLLPTSSQS
481-LDFGNGKFSNGNVHASDNTNKSISDNRGNGFSAAPIAVPPSDNLSRAVGSHSVRESQTQR
541-NNSGSSSDSSDDEAGAIEGNMCASATGVVRVQSRKKAEMFLVRTDGVSCTREKVTESSLA
601-FTHPSTQQQMLLWKTTPKTVLLLKKLGQELMEEAKEAASFLYHQENMNVLVEPEVHDVFA
661-RIPGFGFVQTFYIQDTSDLHERVDFVACLGGDGVILHASNLFKGAVPPVVSFNLGSLGFL
721-TSHPFEDFRQDLKRVIHGNNTLDGVYITLRMRLRCEIYRKGKAMPGKVFDVLNEIVVDRG
781-SNPYLSKIECYEHDRLITKVQGDGVIVATPTGSTAYSTAAGGSMVHPNVPCMLFTPICPH
841-SLSFRPVILPDSAKLELKIPDDARSNAWVSFDGKRRQQLSRGDSVRIYMSQHPLPTVNKS
901-DQTGDWFRSLIRCLNWNERLDQKAL
```

NADK2.3:

```
  1-MAVGSHSVRESQTQRNNSGSSSDSSDDEAGAIEGNMCASATGVVRVQSRKKAEMFLVRTD
 61-GVSCTREKVTESSLAFTHPSTQQQMLLWKTTPKTVLLLKKLGQELMEEAKEAASFLYHQE
121-NMNVLVEPEVHDVFARIPGFGFVQTFYIQDTSDLHERVDFVACLGGDGVILHASNLFKGA
181-VPPVVSFNLGSLGFLTSHPFEDFRQDLKRVIHGNNTLDGVYITLRMRLRCEIYRKGKAMP
241-GKVFDVLNEIVVDRGSNPYLSKIECYEHDRLITKVQGDGVIVATPTGSTAYSTAAGGSMV
301-HPNVPCMLFTPICPHSLSFRPVILPDSAKLELKIPDDARSNAWVSFDGKRRQQLSRGDSV
361-RIYMSQHPLPTVNKSDQTGDWFRSLIRCLNWNERLDQKAL
```

Fig. 6.4 Sequence of the recombinant NADK2.2 (full-length, mature form) and NADK2.3 (active domain). In cyan, the added methionine for the production of the NADK2.2 mature protein (residues 61-999) or the NADK2.3 construct in *E. coli* (residues 609-999). In pink, the identified CaM-binding site, and, in red, the active NAD kinase domain.

These constructs were all expressed in *E. coli* and soluble extracts enriched in proteins of the expected size were obtained (**Fig 6.5**).

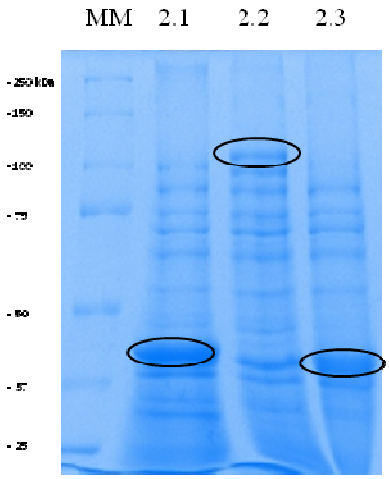

Fig. 6.5 Expression of recombinant NADK2 constructs. MM: molecular marker; 2.1: soluble protein extract of bacteria expressing NADK2.1 (*N*-terminal domain); 2.2: soluble protein extract of bacteria expressing NADK2.2 (full length protein); 2.3: soluble protein extract of bacteria expressing NADK2.3 (*C*-terminal catalytic domain).

1.2- NADK activity of the three constructs in crude bacterial protein extracts

In order to check that our recombinant proteins were active and compare the activities of our different NADK2 versions, we measured the NADK activity in the soluble bacterial extracts shown in **Fig. 6.5**. Measurements were conducted according to Turner et al (2004) and as detailed in **Materials and Methods.**

As negative control, an *E. coli* protein extract not expressing any of these constructs was used and, in this case, no NADP production was detected even after 30 minutes (not shown). We also tested, in parallel, the NADK activity of the NADK2.1 construct (NADK2 *N*-terminal domain) that we previously used to determine the affinity of NADK2 for AtCaM1 (see **Chapter 1**). Activity was measured at different time points in the presence or in the absence of 1 mM $CaCl_2$ and 300 nM AtCaM1 (**Fig. 6.6**).

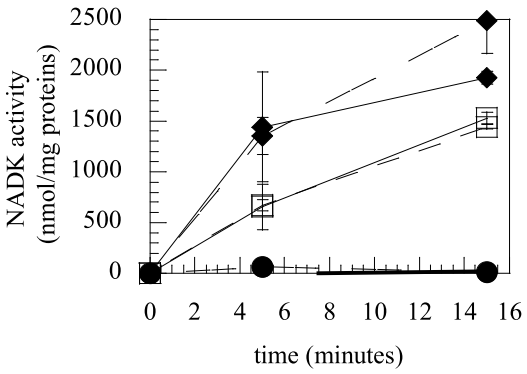

Fig. 6.4 Activity of NADK2.1, NADK2.2 and NADK2.3-expressing bacterial extracts as a function of time. For each measure, 5 µg or 20 µg of soluble extract were used in a final volume of 100 µL of buffer containing ATP, $MgCl_2$ and NAD and 300 nM AtCaM1. Measurements were conducted as detailed in Materials and Methods following the protocol of Turner et al (2004). Black dots: NADK2.1 bacterial extract; white squares: NADK2.2 bacterial extract; black diamonds: NADK2.3 bacterial extracts. Continuous lines represent measurements conducted in the presence of $CaCl_2$ and AtCaM1, dotted lines represents measurements conducted in the absence of $CaCl_2$ and AtCaM1.

As expected, **Fig. 6.6** shows that the bacterial extract expressing the NADK2.1 domain (NADK2 *N*-terminal domain) showed no detectable NAD kinase activity. On the contrary, both NADK2.2 and NADK2.3 extracts were able to produce NADP and the amount of NADP produced increased with the time. It can be observed that the NADK2.3-expressing soluble extract is approximately twice as active as the NADK2.2 one. This difference is likely due to the difference in the expression levels of the two proteins. Indeed, **Fig. 6.5** shows that NADK2.2 is less expressed than NADK2.3.

Fig. 6.6 also shows that no significant difference can be observed, for each construct, between the curved obtained in the absence and in the presence of $CaCl_2$ and 300 nM AtCaM1. Previously, it was also reported (Turner et al, 2004) that the activity of the recombinant NADK2 was not enhanced by the presence of Ca^{2+}/CaM, in contrast with the native NADK enzyme (*i.e.* the NADK CaM sensitive purified from plant).

Apart from confirming previous observations, our data show that the NADK2.2 (*i.e.* full-length recombinant protein without transit peptide) activity is comparable to that of the catalytic domain (NADK2.3). This suggests that, for the NADK2.2 recombinant protein, the *N*-terminal domain has no influence on the protein activity. In addition, the NADK2.2 recombinant form does not need CaM for

activity, in contrast to native CaM sensitive NADK that was shown to be inactive without CaM (Delumeau, 1998).

1.3- Activity of the pure recombinant NADK2

In order to obtain a better quantification of the activity and properties of the full-length recombinant protein, we purified this enzyme. We firstly precipitated the protein with ammonium sulfate (48%), then performed an ion exchange chromatography (DEAE), a gel filtration and another ion-exchange chromatography (Q-sepharose) (see **Fig. 6.7**), and we measured the activity of the protein in the presence and absence of Ca^{2+}/AtCaM1 after each purification step.

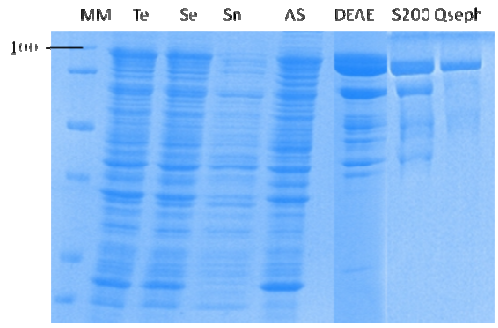

Fig. 6.7 Purification of NADK2.2 recombinant protein. MM: molecular marker; Te: total bacterial extract; Se: soluble bacterial extract; Sn: supernatant of the ammonium sulfate precipitation; AS: ammonium sulfate precipitate; DEAE: pool of the DEAE pass-through; S200: pool of the gel filtration chromatography; Qseph: pool of the Q-sepharose chromatography.

	Protein quantity (mg)	Specific activity (µmol NADP /(h*mg)	Yield (%)	Purification factor	Total activity (µmol NADP/h)
Soluble extract	1100	0,9	100	1	990
Solubilized ammonium sulfate precipitate	483	2,97	100	3,3	1000
Pool DEAE	72	4,31	31.41	4,79	311
Pool S200	0,820	63,21	5.23	70,23	51,84
Pool Q seph	0,059	14,03	0.083	15,56	0,828

Table 6.2 Purification table of recombinant NADK2.2 (full length mature protein) produced in E. coli.

As previously observed (Turner et al, 2004), the enzyme loses most of its activity in the steps following the ammonium sulfate precipitation (**Table 6.2**) and no Ca^{2+}/CaM control of this enzyme was detectable, *i.e.* measurements conducted in the presence of AtCaM1 and Ca^{2+} in excess were comparable to those conducted in their absence (not shown). Our results therefore confirm qualitatively what previously observed by Turner et al (2004).

From a quantitative point of view, Turner et al (2004) reported for NADK2 a specific activity of 10 µmol NADP/(h*mg). These calculations were made on the recombinant NADK2 after a step of CaM-affinity chromatography. We avoided this step because, in preliminary assays, we noticed that the yield was weak and the protein loses its activity after the step on the column, either for complicated interaction with the matrix or because right after the elution the protein is extremely diluted and prone to unfolding. In our case, we also observed an important loss of activity in the steps following the ammonium sulfate precipitation, so in order to properly estimate the specific activity of the protein we used the value obtained after the size-exclusion chromatography, because the gel profiles shows high enrichment in NADK2 protein and the highest specific activity was measured. The specific activity calculated at this step was 63 µmol NADP/(h*mg). We can estimate, on the basis of the SDS-PAGE profile, that NADK2 represents 25% of total proteins, the specific activity becomes approximately 240 µmol NADP/(h*mg). This value is 25 times higher than what calculated by Turner et al (2004). The apparent k_{cat} of the proteins is therefore of approximately 4 s^{-1}. This value is also comparable with what meas-

ured for other NADK enzymes, for example the one of *E. coli* , *Salmonella tiphium* and the human isoform (Kawai et al, 2001; Grose et al, 2006; Ohashi et al, 2011).

In conclusion, our measures on bacterial extracts and on the pure recombinant NADK2 confirm that Ca^{2+}/CaM have no effect on the protein activity, as previously reported. In addition, we provided a better estimation of the recombinant protein activity and observed that it is comparable to the one of other NADK enzymes previously characterized.

These data suggest that no CaM control is needed for the NADK2 protein, as its activity is perfectly comparable with that of the catalytic domain of other bacterial and eukaryotic NAD kinases. If this hypothesis is correct, the identification of NADK2 as the plant CaM-dependent NADK isoform should be revised, as also suggested by the SDS-PAGE profiles of highly enriched CaM-dependent NADK previously reported (see **Fig. 6.2**) showing a protein of approximately 50 KDa.

This observation prompted us to verify that, in Arabidopsis plant tissues, NADK activity can be enhanced by the presence of Ca^{2+}/AtCaM1 in excess with the objective to purify this protein, study its CaM affinity and check its identity.

2- Localization of NADK2 in plant tissues by western blot

2.1- Production of a polyclonal antibody specific for NADK2

Before studying the activity of the native NADK from plant tissues, we verified that NADK2 was expressed in our plant material and that it was localized in the chloroplast.

The purified NADK2.1 N-terminal domain described in **Chapter 1** is not present in NADK1 and 3 of Arabidopsis and therefore is specific for our protein of interest (NADK2). We took advantage of this in order to produce a NADK2-specific polyclonal antibody in guinea pig.

Fig. 6.6 shows the titration of the produced antibody. NADK2.1 pure protein (1 µg, 100 ng or 10 ng) was spotted on nitrocellulose and incubated in the presence of the antibody at different dilutions (1:2000, 1:3500 and 1:10,000, or the pre-immune serum). It can be observed that the protein is success-

fully detected down to 10 ng with a 10, 000th fold dilution of the antiserum. In contrast, the Guinea pig pre-immune serum was not able to recognize the protein.

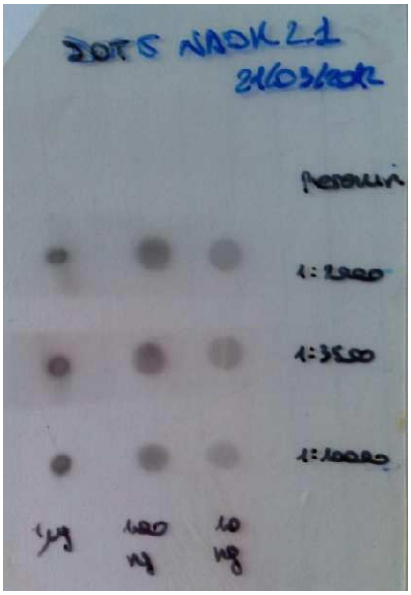

Fig. 6.6 titration of polyclonal antibodies against NADK2.1. Different amounts of purified NADK2.1 protein (1 µg, 100 ng or 10 ng) were spotted on nitrocellulose membrane and incubated with different amounts of anti-NADK2.1 serum. First column: 1 µg NADK2.1; second column: 100 ng; third column: 10 ng. First line: incubation with Guinea pig preimmune serum (no signal is detected); second-fourth line: incubation with anti- NADK2.1 serum at different dilutions: 1:2000; 1:3500 and 1:10,000, respectively. For subsequent WB analyses, the 1:3500 dilution was used.

2.2- Localization of NADK2 in subplastidial fractions and different plant tissues

Previous reports (Waller et al, 2010) showed that a NADK2-GFP fusion protein was localized in the stroma of Arabidopsis culture cells or protoplasts, and GUS staining revealed that the corresponding gene should be mainly expressed in leaf tissues. In order to confirm these results, we attempted to study the localization of NADK2 by western blots, in different tissues and in the plastidial compartments.

Firstly, we wanted to see if the expression of the protein in leaves was confirmed and if the protein was expressed in Arabidopsis cell cultures. We therefore extracted proteins from leaves of two different ages (two and four weeks old). In parallel, we also tested the presence of the enzyme in purified chloroplasts, stroma and thylakoids.

The western-blot analysis displayed in **Fig 6.7** shows that a band at the expected size of 100 kDa is detected in all the leaf extracts (2 or 4 weeks old, total and soluble protein samples, B, lanes 2 to 5). The weaker signal in the total extract of young leaves (B, lane 2) is due to the fact that the amount of protein loaded was only half of the other samples. **Fig. 6.7** also shows that the same band is present in the chloroplast (B, lane 6) and enriched in the stroma (lane 7), while barely present in the thylakoids (B, lane 8).

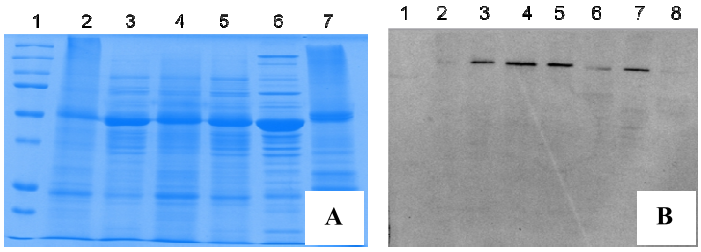

Fig. 6.7 SDS-PAGE (A) and Western blot (B) of total and soluble leaf extracts and plastidial subfractions using anti NADK2.1 antiserum. A. Molecular marker (1), total (2) and soluble (3) extracts from 4 weeks-old leaves; total (4) and soluble (5) extracts from 2 weeks-old leaves; stroma (6); thylakoids (7). **B**. Molecular marker (1), total (2) and soluble (3) extracts from 4 weeks-old leaves; total (4) and soluble (5) extracts from 2 weeks-old leaves; entire chloroplast (6); stroma (7); thylakoids (8).

These results therefore confirm that NADK2 is expressed in leaves, localized in the chloroplast, and soluble in the stroma.

We then investigated the enzyme expression in Arabidopsis cell culture extracts of 1 or 2 weeks. Here again (**Fig. 6.8**) we observed the presence of a band of 100 kDa, corresponding to the size of NADK2, in all cell extracts. We also loaded again our chloroplast, stroma and thylakoids protein extracts purified from leaves. Here again we noticed that the 100 kDa band was present in the stroma, and, while less visible, in the total chloroplast. Several bands of lower molecular weight are also observed especially in 2 weeks old cell extracts and might correspond to degradation of NADK2, shorter versions of the same protein, or cross-reacting proteins.

The same western blot analysis also confirms the stromal localization of the enzyme (**Fig. 6.8B**, lane 7).

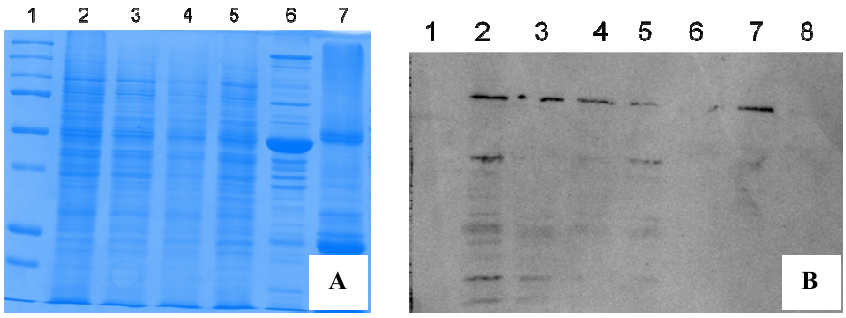

Fig. 6.8 SDS-PAGE (A) and Western blot (B) of total and soluble Arabidopsis cell protein extracts and plastidial subfractions. A. Molecular marker (1), total (2) and soluble (3) extracts from 2-weeks cells; total (4) and soluble (5) extracts from 1-week old cells; stroma (6); thylakoids (7). **B.** Molecular marker (1 and 9), total (2) and soluble (3) extracts from 2-weeks old cells; total (4) and soluble (5) extracts from 1-week-old cells; entire chloroplast (6); stroma (7); thylakoids (8).

3- Characterization of NADK activity in plant tissues

3.1- Native NADK from Arabidopsis is controlled by AtCaM1

We started by measuring NADK activity in protein extracts of Arabidopsis culture cells.

We first verified that the amount of NADP, produced by our cell extracts, increased linearly with time (**Fig. 6.10A**). Linearity was observed for 30 minutes of incubation. Measurements were also performed in the presence of Ca^{2+} and a CaM inhibitor (either W7 or TFP, at 50 µM). With W7, the rate was approximately 1/2 what observed with AtCaM1, while a stronger inhibition (6-fold reduction of NADP production rate) was observed with TFP.

We then measured the NADP produced by different amounts of cell extract (Fig. 6.10B). The NADP produced was proportional to the quantity of cell extract used (*i.e.* the NADK concentration).

We subsequently measured NADK activity in Arabidopsis cells of different ages. Cells were harvested at different time points and their activity measured in the presence of Ca^{2+} and AtCaM1 in excess. In our culture conditions, cells are known to reach the stationary phase at 5-6 days after inoculation. **Fig 6.11** shows that the levels of NADK activity in these cell extracts as a function of culture time follows a bell shaped curve with a maximum at day 3-5 (350 nmol NADP/(h*mg protein)), before cells enter a stationary phase.

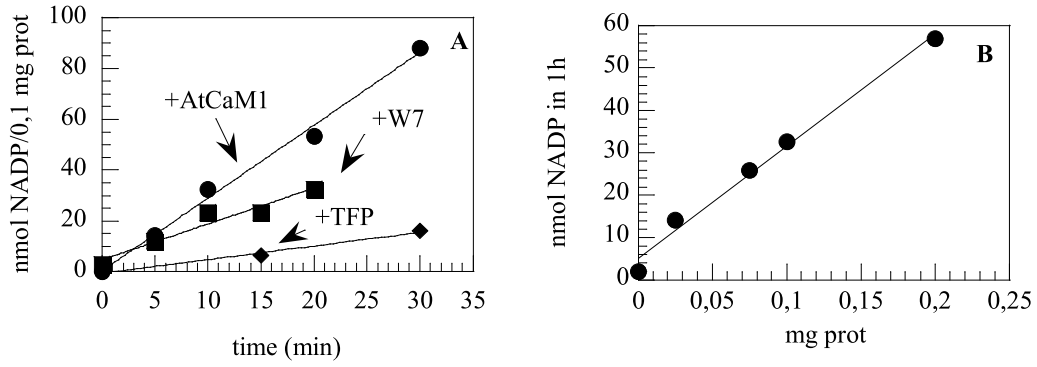

Fig. 6.10 NADK activity in Arabidopsis cells as a function of time (A) and protein concentration (B). Measurements were conducted as detailed in Material and Methods. In A, production of NADP was tested on 0.1 mg total protein extract supplemented with 1 mM $CaCl_2$ and 300 nM AtCaM1 (dots) the CaM inhibitor W7 (squares), or the CaM inhibitor TFP (diamonds. Both inhibitors were used at 50 µM).

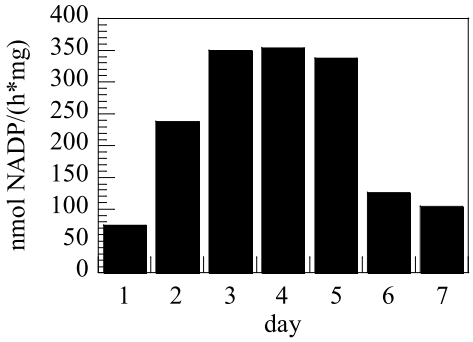

Fig 6.11 NADK activity measured in protein extracts prepared from Arabidopsis cell cultures of different ages. The abscissa indicates the day after the culture was placed in a new medium.

Our results showed that NADK activity was enhanced by the presence of AtCaM1, since the presence of two CaM inhibitors drastically reduced the measured activity. Control experiments showed that TFP and W7 have no effect on the coupling system.

In conclusion, Arabidopsis cells showed high NADK activity, which is higher when cells are in rapid division. This activity is mostly AtCaM1-dependent and, interestingly, two CaM-inhibitors acted differently, with TFP showing a stronger reduction of NADK activity with respect to W7.

4.1- NADK activity in different plant tissues.

After having assessed the NADK2 localization in plant tissues and its activity in crude cell extracts, we tried measuring NADK activity in leaf extracts, stroma and root extracts.

Despite several efforts, we could not manage to measure any activity from our leaf extracts, or from pure stromal preparations, whether CaM/Ca^{2+} was present or not and despite the fact that the protein was present in these samples on the basis of the western blots.

Activity in leaves and stroma may not be detected because of some components interfering with the test (pigments, extraction procedure) or with the protein. Secondly, NADK2 may be subjected to post-translational modifications leaving it inactive in our assay conditions. NADK activity was detected in root extract but the protein extraction protocol needs to be optimized n order to check the expression of NADK2 in these organs by western blot. In this respect it is interesting to note that the best activity reported in the literature was detected in tomato callus cultures from roots. According to Olivier Delumeau this was the tissue where the highest CaM-dependent NADK activity could be measured (personal communication).

3.2- NADK purification from plant cells

All past purifications of plant CaM-dependent NADK activity did not confirm the identity of the purified protein since the genes coding for NADK were not yet known. Our new results (*i.e.* lack of correlation between NADK activity and NADK2 expression level) might suggest the existence of a CaM-dependent NADK isoform different from NADK2 or a modified version of this protein. These hypotheses are also in agreement with the fact that SDS-PAGE profiles of pure CaM-dependent NADK report a polypeptide of approximately 56 kDa (Delumeau et al, 2000).

We therefore planned to purify the CaM dependent NADK activity and follow the purification process with the NADK2 specific antibody, in order to see if the CaM-dependent NADK activity and the NADK2 protein co-purify.

In order to do so, we started from Arabidopsis cell protein extracts. 400 mg of proteins were precipitated using ammonium sulfate as previously described by Delumeau et al (1998). In this fraction we

could measure a two-fold activation by AtCaM1 by comparing with activity measurements in the presence of W7 (CaM inhibitor) (**Table 6.2**). The precipitated proteins were dissolved as described in M&M to decrease ammonium sulfate concentration to approximately 100 mM and loaded on a DEAE column. The NADK activity was measured in 50 mL fractions corresponding to proteins not retained on the DEAE column, as CaM-dependent NADK was previously reported to be in the unbound fraction. NADK activity was detected only in the last two fractions reported in **Fig. 6.12A** and **B** (lanes 8 and 9). Proteins were then separated on a SDS-PAGE and a western blot was performed using anti-NADK2 antiserum. As shown in **Fig. 6.12B**, NADK2 protein was detected in the fraction were NADK activity was measured.

Fractions were pooled and concentrated and activity was measured in the presence of AtCaM1 or W7. Here again a 2-fold higher activity was measured when W7 was absent suggesting the presence of a CaM-sensitive NADK in this concentrated fraction. This fraction was then subjected to a CaM-affinity chromatography.

For CaM-affinity chromatography, the pool of the DEAE fractions containing CaM-dependent NADK activity was supplemented with $CaCl_2$ in excess (1 mM) and loaded three times on 3 mL CaM resin equilibrated in $CaCl_2$-containing buffer (see **Material and Methods** for further details). The pass-through was recovered and the column washed with 5 mL of the same buffer. Proteins retained on the column were then eluted with the same buffer containing EGTA in excess (5 mM). Eluted fractions were then concentrated up to 0.4 mg. **Fig. 6.12** (C and D) shows the SDS-PAGE profile of the purification and the associated western blot performed with NADK2 antiserum. It can be observed that the band at 100 kDa corresponding to the size of NADK2 is observed both in the pass through (**Fig. 6.12D** lane 3), in the second elution fraction (lane 6) and in the elution pool (lane 10). This is consistent with activity measurements reported in **Table 6.2** that shows NADK activity in both the pass through and the elution pool. Activity measurements reported in the same table show that 90% of the NADK activity was found in the pass-through of the CaM-column, and only 10% was retained on the resin.

The activation factor measured comparing the activity in the presence of AtCaM1 or W7 is constant during all the purification steps, without any observed enrichment in CaM-dependent activity. Note

however that in the pass-through of the CaM column, where NADK2 is detected (lane 3-4, in **Fig. 6.12D**) all the activity was CaM-independent (**Table 6.2**).

Sample	Protein quantity (mg)	Condition	Specific activity nmol/(h*mg)	Yield (%)	Total activity (nmol/h)	Purification factor	Activation factor
Soluble extract	400	CaM	111,72	100	44688	1	1,79
		W7	62,25	100	24900	1	
Ammonium sulfate precipitation	190	CaM	124,71	53,023	23694,9	1,11	2,58
		W7	48,33	36,8783	9182,7	0,77	
Pool DEAE	24	CaM	159,17	8,54834	3820,08	1,43	1,98
		W7	80,17	7,72723	1924,08	1,29	
Pass through CaM-column	22	CaM	109,09	5,37052	2399,98	0,98	1,09
		W7	100	8,83534	2200	1,61	
Elution CaM-column	0,389	CaM	455,01	0,39608	176,99889	4,09	2,07
		W7	218,51	0,34137	85,00039	3,51	

Table 6.2 Purification table of native CaM-activated NADK from protein extract prepared from Arabidopsis cell culture. AS: specific activity; AT: total activity.

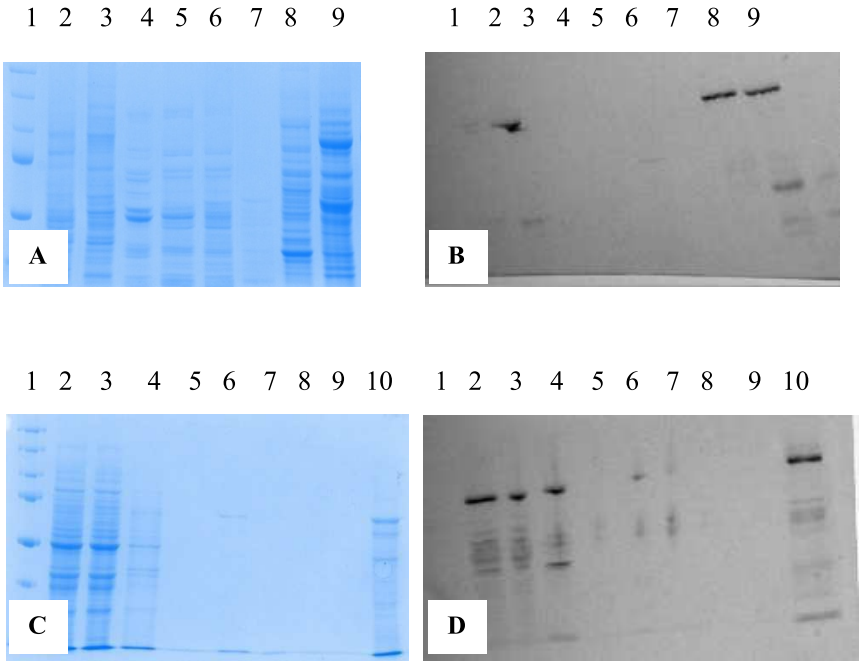

Fig. 6.12 Purification of CaM-dependent NADK from Arabidopsis cells: and D). A and C: SDS-PAGE profiles of the **DEAE (A) and CaM-affinity chromatography (C)**. B and D: corresponding western blots performed with the anti NADK2 serum. In panels A and B, 1 = molecular marker, 2 = soluble protein cell extract, 3 = ammonium sulfate precipitate resuspended and loaded on the DEAE column, 4 – 6: first fractions eluted from the DEAE column. In panels C and D, 1 = molecular marker, 2 = DEAE-containing fractions pooled, concentrated and loaded on the CaM-affinity column, 3 = pass-through of the CaM-affinity column, 4 = wash of the CaM-affinity column; 5-9 = EGTA elution fractions of the CaM affinity column; 10 = Pooled and concentrated eluted fractions of the CaM affinity column. 20 µg of proteins were loaded in each lane.

These results can be interpreted in different manners. If we assume that all the NADK activity detected is due to NADK2, then during the CaM-affinity purification its CaM-affinity and its CaM-sensibility were lost, as demonstrated by the fact that the majority of the activity is found in the pass-through and is no more CaM-dependent. In alternative, this CaM-dependent NADK activity could be ascribed to another NADK isoform or a different version of NADK2.

As indicated in the purification table, there is a dramatic loss of activity during the purification. This occurred despite great care in terms of the control of protein degradation (use of complete protease inhibitor mix), presence of high concentration of reductant and salt, protein manipulation at low temperature. This loss of activity has to be controlled and prevented to go further in the purification and to identify the CaM-sensitive NADK from plant.

Discussion

NADK2 was used as a positive control at the beginning of the work because of literature data indicating an extremely high apparent affinity of plant native NADK for CAM (in the sub-nanomolar range). We reported in **Chapter 1** that the affinity of the NADK2.1 domain and the NADK2 peptide for calmodulin is of approximately 200 nM. As the two tests gave similar values we did not hypothesized at that time that the labeling could affect the interaction. As the characterization of ceQORH and Tic32 interaction with AtCaM1-Alexa^{488} revealed that the affinity was lower for a labeled CaM than for unlabeled CaM we may have to reconsider the interaction between CaM and NADK2.1.

In addition, the absence of a band at 100 kDa in highly enriched CaM-dependent NADK fractions previously obtained (Delumeau et al, 2000) generated doubts on the identification of NADK2 as the CaM-regulated isoform and motivated the purification of native CaM-sensitive NADK.

We started by analyzing the activity of the NADK2 recombinant protein. We observed, as previously reported (Turner et al, 2004), that this enzyme is not subjected to CaM control but we also realized that its activity was comparable to that of the isolated NADK2.3 active domain and that of NADK from other organisms (bacteria and human). This indicated that the recombinant NADK2 is fully active. This explains why, though still able to bind CaM, no activating effect of this enzyme by CaM is observed. The reason why the enzyme is fully active despite the presence of its *N*-terminal regulatory domain is yet unknown.

We therefore decided to identify the nature of CaM-dependent NADK activity from Arabidopsis using cell cultures in which a high CaM-sensitive activity could be detected in a crude extract. The purification was carried out using a previously established protocol developed for the purification of the enzyme from tomato root cell culture. In parallel with activity measurements, we followed NADK2 protein using the antibody we produced against the *N*-terminal domain, in order to see whether the presence of NADK2 was correlated with the presence of CaM-sensitive NADK. We firstly confirmed NADK2 expression in Arabidopsis leaves and cells and its stromal localization. CaM-dependent NADK activity was also detected in cells, but not in the stroma and in leaves extracts.

The purification procedure we employed for CaM-dependent NADK from Arabidopsis cells was not satisfying since a lot of activity was lost at each purification step and because a clear separation of the CaM-dependent and independent NADK activity was not obtained, due to the extremely fragility of this protein that is known from the literature. Therefore, for the moment, no conclusions can be given for the molecular identity of the CaM-dependent NADK.

In order to gain more insights in this interaction and its control it is now required to improve the protocols of purification of the recombinant NADK2 and native CaM-sensitive NADK. The first purification will serve to better investigate the binding affinity of the recombinant protein, in case the presence of substrates is important for the CaM-binding. The second purification (from cell cultures) is necessary to confirm the identity of the CaM-dependent NADK enzyme.

Conclusions and Perspectives

Ca^{2+} dynamics into the cell and its sub-compartments were observed in response of a wide array of environmental stimuli and developmental events. How these Ca^{2+} fluxes influence the cell and orient its responses is however far from being elucidated.

The simpler, provoking explanation for Ca^{2+} movements is that they are just a protection for membranes and cell components that can be damaged after a stress. Even in the chloroplast, it might be concluded that the high amount of Ca^{2+} in this organelle only reflects the requirement of the photosynthetic machinery for Ca^{2+} and H^{+} ions when switched on by light (Plieth, 2001).

This argument is however not generally acceptable for several reasons. First of all, this hardly explains the differences between these Ca^{2+} fluxes in response to different stimuli. The shape, the duration and the spatial localization of these Ca^{2+} dynamics are indeed highly specific. An extensive variety of Ca^{2+} pumps, channels and regulatory systems evolved in order to control the limit and the extent of these signals.

Starting from bacteria up to animals, every species possesses a wide array of Ca^{2+}-binding proteins, each one different with respect to their Ca^{2+} affinity, their activity, expression levels in organs and tissues, and for their ability to interact with other proteins. Understanding Ca^{2+} signaling ideally consists in unraveling the network of protein-protein interactions that link every Ca^{2+}-binding protein to its effectors (for example, each Ca^{2+} dependent kinase to its substrate, each calmodulin to its partners), their regulatory mechanisms and their concentration in each cell type and in every developmental/environmental condition.

We are of course very far from obtaining such a picture, since in only few cases the key determinants of a particular Ca^{2+} response have been identified. In few cases, CaM and related proteins were associated to the direct modulation of the activity of their target enzymes but the series of events that, starting from the generation of a precise Ca^{2+} signal lead up to the cell response are still unclear. With the exception of the role of Ca^{2+} in the mechanics of muscle contraction, the well-elucidated example is the establishment of root symbiosis with bacteria and AM fungi (see Oldroyd, 2013 for a review). When the root perceives the presence of the symbiont (rhizobia bacteria or AM fungi) a signaling pathway still not completely characterized is activated at the level of the root cell plasma membrane. This leads to nuclear Ca^{2+} spiking at the level of the perinuclear membrane. This Ca^{2+} spiking is able to

activate a Ca^{2+}- and CaM- dependent kinase (CCaMK) that is normally auto-inhibited. CCaMK phosphorylates Cyclops, a protein of unknown function. Activation of CCaMK is necessary for both symbioses; therefore abolishment of Ca^{2+} spiking prevents the root nodule formation. *Vice versa*, mutant plants possessing a gain of function form of this enzyme (*i.e.* not autoinhibited) can overcome the absence of the Ca^{2+} signature, therefore producing nodules all the time, even in the absence of the symbiont. This elegant mechanism appears however to be more an exception than a rule. In addition, several aspects are still not well understood. For example, it is not clear how the root distinguishes between AM fungi and Rhizobia, therefore avoiding producing nodules all the time when CCaMK is activated.

In order to shed more light in the field, many approaches were employed. Since CaM partners are not easily predictable by bioinformatics tools, several high-throughput strategies were used to isolate new CaM interactors. Several structures of CaM bound to the CaM-binding domain of its targets and activity measurements were performed (see Tidow and Nissen, 2013). Many binding patterns were identified, revealing a wide variety of modes of interaction and no general rules on the mode of interaction and effect of CaM-binding. In addition, reverse genetics was employed to down-regulate expression of Ca^{2+}-binding proteins and see the effect of their lack *in planta* (Al-Quraan et al, 2010). Mutants of CaM-partners mutated in their CaM-binding site(s) were also performed *in vitro* (see Chigri et al, 2006, Turner et al, 2004) but never *in vivo*.

The slow advancement of the field might be certainly due to lack of simple and accessible ways of studying these protein-protein interactions. The case of CaM and CMLs is one of the most difficult. Indeed, lack of activity for this protein makes it difficult to study the effect of CaM-binding to a series of targets. The high similarity between CaM isoforms and CMLs in terms of size, amino acid conformation and protein sequence complicates the production of specific antibodies and other tools to identify these proteins, their localization in tissues and their abundance. In addition, the fact that, in the Ca^{2+} loaded form, CaM exposes hydrophobic regions, can result in a-specific binding to many substrates and this phenomenon is difficult to evaluate on a large scale.

This was evident in the evaluation of the high-throughput approach for the identification of plastidial CaM partners we employed and described in **Chapter 2**. The retrieved list of candidates was indeed very similar, in terms of number of putative candidates, to several other studies previously con-

ducted with various techniques (CaM-affinity chromatography, protein arrays or cDNA display). The majority of these works do not present ways to validate the newly-discovered putative interactions on a high number of candidates and that validations are rarely conducted in ways that allow quantitative measurement of the binding parameters and comparisons between proteins. In addition, with the exception of few cases (see Chigri et al, 2006, Perochon et al, 2010), these studies were not followed by the detailed characterization of some of the newly-discovered interactions. This suggests that going from the high-throughput approach to the identification of "real" key CaM partners is still a hard task. Rapid and versatile techniques to study the binding parameters are therefore strongly required.

For our project targeting CaM regulation in the chloroplast, we decided to combine classic validation procedures (overlay assays and CaM affinity chromatography) with several binding experiments using measurements of fluorescence anisotropy. The versatility of this last technique, in terms of controlled parameters (buffer composition, incubation time, Ca^{2+} concentration…) makes it very suitable to study these interactions, especially when activity tests are not easy to design. In addition, competition tests allow measuring the binding affinity of two partners without the inconvenient of a fluorescent labeling that could influence the observed binding.

We used these tests to study several plastidial proteins. Some of the studied proteins (Tic32 and NADK2) were CaM-partners already characterized during previous works. Our results support previous findings on the high CaM affinity of these proteins but raise also new questions about the importance of these interactions.

In particular, the high affinity of Tic32 for AtCaM1 was shown to be impaired at very low concentrations of NADPH. This leads to the question of the relevance of this interaction *in vivo*. In addition, we showed that the previously identified CaM-binding region is not able to bind AtCaM1 *per se*, and that additional amino acids located upstream of the previously identified site might be important for CaM-binding. The mechanism of CaM-binding of Tic32 needs therefore to be further investigated.

In the case of NADK2, the affinity measured for the putative NADK2 CaM-binding peptide (200 nM) is quite high if compared to the affinity of Tic32 and ceQORH. This might suggest that this is not the right anchoring point for CaM, or that other CaM-binding sites are present. The obtained K_D value for the *N*-terminal domain is probably overestimated due to the Alexa labeling of the AtCaM1 used for

these measurements and remains to be tested in competition as done for Tic32 and ceQORH. Since the recombinant NADK2 is probably fully active in the absence of CaM, these measurements might be important to confirm the identity of NADK2 as the CaM-regulated isoform. The problem of the lack of CaM control of this recombinant enzyme will however be solved only once characterized the native CaM-dependent NADK activity and its molecular identity.

For ceQORH, a high affinity (approximately 10 nM) of the entire protein and its identified CaM-binding site was measured. The comparison, *in vitro*, with a mutated version with similar activity and CaM affinity in the native state, combined with localization of wt and mutated version of the protein in experiments performed *in planta* (Daniel Salvi et al, unpublished) raise the hypothesis that, in this case, CaM controls the protein distribution between the cytoplasm and the chloroplast.

A double localization was also observed for Tic32 (Daniel Salvi et al, unpublished), suggesting that CaM might have a control in determining the localization of these proteins without transit peptides. Also the CaM-dependent NADK activity was found several times outside the plastids in many previous reports (Simon et al, 1982 and 1984; Dieter and Marmé, 1984) therefore even this enzyme might be differentially localized and CaM might be implicated in this process.

Further work will therefore consist in the generation of other ceQORH and Tic32 mutants in order to see the effect in their CaM-binding properties and their cellular localization. Structural data that provided by our collaborators at the IBS-Grenoble will be extremely useful in order to identify the CaM-binding region and decide where to mutate the proteins without affecting their conformation and their activity.

In the case of NADK2, the purification protocols of both the native and the recombinant protein need to be improved in order to allow a comparison between them. This is required first of all to confirm that the native CaM sensitive NADK is indeed NADK2. If this is the case, these pure proteins will be useful to compare them in terms of CaM affinity. NADK2 mutated versions in the CaM-biniding site will be produced and used to complement the *nadk2* mutant line, in parallel with the not-mutated NADK2 protein. This could give important clues about the importance of CaM in regulating the plastidial NADP pool.

Our tests also showed that not all the proteins identified by a high throughput study can be considered as physiological interactions. Indeed, TS2, Lox2 and XK1-like are all proteins that were not able to bind to CaM with high affinity when tested in fluorescence anisotropy and sometimes also on the CaM-affinity chromatography. Thanks to our binding tests, we could also show that sometimes the binding observed in the overlay assay is unspecific and takes place at CaM concentrations that are far from the physiological range. These tests coul be applied to all the other targets identified and not yet validated. Our measurements are not suitable for unsoluble proteins. Therefore, for these targets, the use of peptides corresponding to the most probable CaM-binding sites could be a way to obtain preliminary information on their CaM affinity.

Finally, since all these proteins are located in the chloroplast, an important question to answer is the presence of CaM and CMLs in this cell compartment. In the course of this study, we tried to answer this question by a high throughput approach and by the direct localization of some CMLs tagged with GFP. Our results do not support the presence of CMLs in this cell compartment, even if their existance cannot be excluded. Many putative plastidial CMLs still need to be localized before coming to a conclusion.

Perspectives

Unraveling Ca^{2+}/CaM signal transduction requires the integration of a high number of temporal, spatial, and quantitative parameters. For plants, the situation is even more complex because of the presence of the apoplast and the plastids and because of the high number of CaMs and CMLs that can be localized in several cell compartments.

A promising way of looking to Ca^{2+} signaling pathway is through modeling. This strategy was applied several times in the field of metabolism to identify key actors in enzyme pathways and key control steps in metabolic fluxes. The network of Ca^{2+} interactions and dynamics might be modeled and studied in a similar way and hopefully help obtaining interesting clues to orient further experimental work, as done by Selivanov et al (1998) for Ca^{2+} fluxes in animal mitochondria. However, to be useful, models have to be fed with a lot of quantitative data, for example the spatial and temporal extension of Ca^{2+} fluxes, the concentration of Ca^{2+} binding proteins in the cell compartments, the Ca^{2+} affinity of each of them, the abundance and affinity of their partners and so on. Many of these quantitative data are still not available in the literature and were never systematically investigated. Therefore, simulations of CaM-binding to partners are not possible and were only rarely tempted (Persechini and Stemmer, 2002, Dupont et al, 2003).

In our opinion, improving knowledge about Ca^{2+} signaling and its transduction through CaMs and related Ca^{2+} sensors implies two levels of analysis. Firstly, much more data are needed on the binding parameters of CaMs, CMLs and their distribution and concentration. These data are difficult to obtain, because of the high number of these proteins, their similarity and their lack of activity, so it might be useful to focus on simple models, i.e. unicellular organisms in particular cell conditions, or organisms containing few CaM and CMLs. The detection of CaM partners should be conducted by the combination of several techniques and stringent conditions in order to limit the detection of artifacts. Various and versatile techniques such as fluorescence anisotropy measurements need to be employed to calculate the CaM/partner affinities and their Ca^{2+} dependency. As a second, complementary step, these data can be used to simulate the CaM-binding to a wide population of partners at physiological concentrations and in response to different Ca^{2+} signatures. The construction of models encompassing spatial, temporal and biochemical quantitative data and simulations would facilitate the study of Ca^{2+} signaling and will help orienting further experimental work. Fourty-two years after the discovery of Calmodulin, we are still at the doorstep of its understanding.

Annex I

Localization of putative CaM-binding site in the sequence of NADK2, Tic32 and selected putative CaM partners here investigated using the Calmodulin Target database (http://calcium.uhnres.utoronto.ca/ctdb/ctdb/sequence.html). For each protein sequence, the numbers below (from 0 to 9) indicate the probability that they are part of a CaM-binding site. For every protein, the most likely predicted CaM-binding sites are squared. The regions of NADK2 and Tic32 that were previously identified as necessary for CaM-binding are in pink.

NADK2

```
....1 MFLCFCPCHV PIMSRLSPAT GISSRLRFSI GLSSDGRLIP FGFRFRRNDV PFKRRLRFVI RAQLSEAFSP DLGLDSQAVK
..... 0000000000 0000000000 0000000000 0000000000 0000000124 5555555555 5555555421 0000000000

...51 SRDTSNLPWI GPVPGDIAEV EAYCRIFRSA ERLHGALMET LCNPVTGECR VPYDFSPEEK PLLEDKIVSV LGCILSLLNK
..... 0000000000 0000000000 0000000000 0000000000 0000000000 0000000000 0000122457 8999999999

..151 GRKEILSGRS SSMNSFNLDD VGVAEESLPP LAVFRGEMKR CCESLHIALE NYLTPDDERS GIVWRKLQKL KNVCYDAGFP
..... 9999877542 1000000000 0000000000 0000000000 0000000000 0000000124 5788888888 8888888754

..201 RSDNYPCQTL FANWDPIYSS NTKEDIDSYE SEIAFWRGGQ VTQEGLKWLI ENGFKTIVDL RAEIVKDTFY QTALDDAISL
..... 2100000000 0000000000 0000000000 0000012222 2222222222 2222210000 0000000000 0000000000

..301 GKITVVQIPI DVRMAPKAEQ VELFASIVSD SSKRPIYVHS KEGVWRTSAM VSRWKQYMTR PITKEIPVSE ESKRREVSET
..... 0000000000 0000000000 0000000000 0000011111 1111111111 1111100000 0000000000 0012222222

..401 KLGSNAVVSG KGVPDEQTDK VSEINEVDSR SASSQSKESG RFEGDTSASE FNMVSDPLKS QVPPGNIFSR KEMSKFLKSK
..... 2222222222 2210000000 0000000000 0000000000 0000000000 0000000000 0000000111 1111111111

..451 SIAPAGYLTN PSKILGTVPT PQFSYTGVTN GNQIVDKDSI RRLAETGNSN GTLLPTSSQS LDFGNGKFSN GNVHASDNTN
..... 1111111000 0000000000 0000000000 0000000000 0000000000 0000000000 0000000000 0000000000

..551 KSISDNRGNG FSAAPIAVPP SDNLSRAVGS HSVRESQTQR NNSGSSSDSS DDEAGAIEGN MCASATGVVR VQSRKKAEMF
..... 0000000000 0000000000 0000000000 0000000000 0000000000 0000000000 0124577788 8888888888

..601 LVRTDGVSCT REKVTESSLA FTHPSTQQQM LLWKTTPKTV LLLKKLGQEL MEEAKEAASF LYHQENMNVL VEPEVHDVFA
..... 8754211100 0000000000 0000000000 0000000000 0000000000 0000000000 0000000000 0000000000

..701 RIPGFGFVQT FYIQDTSDLH ERVDFVACLG GDGVILHASN LFKGAVPPVV SFNLGSLGFL TSHPFEDFRQ DLKRVIHGNN
..... 0000000000 0000000000 0000000000 0000000000 0000000000 0000000000 0000000000 0000000000

..801 TLDGVYITLR MRLRCEIYRK GKAMPGKVFD VLNEIVVDRG SNPYLSKIEC YEHDRLITKV QGDGVIVATP TGSTAYSTAA
..... 0001111111 1111111111 1110000000 0000000000 0000000000 0000000000 0000000000 0000000000

..851 GGSMVHPNVP CMLFTPICPH SLSFRPVILP DSAKLELKIP DDARSNAWVS FDGKRRQQLS RGDSVRIYMS QHPLPTVNKS
..... 0000000000 0000000000 0000000000 0000000000 0000000122 2222222222 2222222100 0000000000

..951 DQTGDWFRSL IRCLNWNERL DQKAL
..... 0000011111 1111111111 11111
```

Tic32

```
....1 MWFFGSKGAS GFSSRSTAEE VTHGVDGTGL TAIVTGASSG IGVETARVLS LRGVHVVMAV RNTDSGAKVK EDIVKQVPGA
..... 0000000000 0000000000 0000000000 0000000000 0000000000 0000000000 0000000000 0000000000

...51 KLDVMELDLS SMQSVRKFAS EYKSTGLPLN LLINNAGIMA CPFMLSKDNI ELQFATNHLG HFLLTKLLLD TMKSTSRESK
..... 0000000000 0000000000 0000000000 0000000000 0000000000 0000000000 0000000000 0000000000

..151 REGRIVNLSS EAHRFSYPEG VRFDKINDKS SYSSMRAYGQ SKLCNVLHAN ELTKQLKEDG VNITANSLHP GAIMTNLGRY
..... 0000000000 0000000000 0000000000 0000000000 0000000000 0000000000 0000000000 0000000000

..201 FNPYLAVAVG AVAKYILKSV PQGAATTCYV ALNPQVAGVS GEYFQDSNIA KPLPLVKDTE LAKKVWDFST KLTDSQSGES
..... 0000000000 0000000000 0000000000 0000000000 0000000000 0000000000 0000000000 0000000000

..301 SS
..... 00
```

XK1-like

```
....1 MLILRQFQIS SFELFQSPKQ TGFYSSSRSV PLPRTRFYSD FRVMSGNKGT NYEKLYLGMD FGTSGGRFTV IDEQGEIKAQ
..... 0000000000 0000000000 0000000000 0000000000 0000000000 0000000000 0000000000 0000000000

...91 GKREYPPFMK EESMGWASSW KATLFSLLED IPVTVRSLVS SISLDGTSAT TLILNSESGE VLCQPYLYNQ SCPDALPEVK
..... 0000000000 0000000000 0000000000 0000000000 0000000000 0000000000 0000000000 0000000000

..171 SIAPANHTVC SGTSTLCKLV SWWNTEVPNR ESAVLLHQAD WLLWLLHGRL GVSDYNNALK VGYDPESESY PSWLLGQPYS
..... 0000000000 0000000000 0000000000 0000000000 0000000000 0000000000 0000000000 0000000000

..251 QLLPKVQAPG TSIGNLKESF TRQFGFPDDC IVCTGTTDSI AAFLAARATE PGKAVTSLGS TLAIKLLSTK RVDDARYGVY
..... 0000000000 0000000000 0000000000 0000000000 0000000000 0012223467 8888888888 8876664321

..331 SHRLDDKWLV GGASNTGGAI LRQLFSDEQL ERLSQEINPM VGSPLDYYPL QSSGERFPIA DPNLAPRLLP RPESDVEFLH
..... 0011111111 1111111111 1100000000 0000000000 0000000000 0000000000 0000000000 0000000011

..411 GILESIARIE GKGYKLLKEL GATEAEEVLT AGGGAKNDKW IKIRQRVLGL PVKKAVHTEA SYGASLLALK GAKQNSGL
..... 1111111111 1111111100 0000001234 6789999999 9999998764 4321111111 1111111111 00000000
```

Lox2

```
....1 MYCRESLSSL QTLNVAKSLS SLFPKQSALI NPISAGRRNN LPRPNLRRRC KVTASRANIE QEGNTVKEPI QNIKVKGYIT
..... 0000000000 0000000000 0000000000 0000000000 0000000000 0000000000 0000000000 0000000000

...91 AQEEFLEGIT WSRGLDDIAD IRGRSLLVEL ISAKTDQRIT VEDYAQRVWA EAPDEKYECE FEMPEDFGPV GAIKIQNQYH
..... 0000000000 0000000000 0000000000 0000000000 0000000000 0000000000 0000000000 0000000000

..171 RQLFLKGVEL KLPGGSITFT CESWVAPKSV DPTKRIFFSD KSYLPSQTPE PLKKYRKEEL ETLQGKNREE VGEFTKFERI
..... 0000000000 0000000000 0000000000 0000000000 0000000000 0000000000 0000000000 0000000000

..251 YDYDVYNDVG DPDNDPELAR PVIGGLTHPY PRRCKTGRKP CETDPSSEQR YGGEFYVPRD EEFSTAKGTS FTGKAVLAAL
..... 0000000000 0000000000 0000000000 0000000000 0000000000 0000000000 0000000000 0000000000

..331 PSIFPQIESV LLSPQEPFPH FKAIQNLFEE GIQLPKDAGL LPLLPRIIKA LGEAQDDILQ FDAPVLINRD RFSWLRDDEF
..... 0000000000 0000000000 0000000000 0000000000 0000000000 0000000000 0000000000 0000000000

..411 ARQTLAGLNP YSIQLVEEWP LISKLDPAVY GDPTSLITWE IVEREVKGNM TVDEALKNKR LFVLDYHDLL LPYVNKVREL
..... 0000000000 0000000000 0000000000 0000000000 0000000000 0000000000 0000000000 0000000000

..491 NNTTLYASRT LFFLSDDSTL RPVAIELTCP PNINKPQWKQ VFTPGYDATS CWLWNLAKTH AISHDAGYHQ LISHWLRTHA
..... 0000000000 0000000000 0000000000 0000000000 0000000000 0000000000 0000000000 0000000000

..571 CTEPYIIAAN RQLSAMHPIY RLLHPHFRYT MEINARARQS LVNGGGIIET CFWPGKYALE LSSAVYGKLW RFDQEGLPAD
..... 0000000000 0000000000 0000000000 0000000000 0000000000 0000000000 0099999999 9900000000

..651 LIKRGLAEED KTAEHGVRLT IPDYPFANDG LILWDAIKEW VTDYVKHYYP DEELITSDEE LQGWWSEVRN IGHGDKKDEP
..... 0000000000 0000000000 0000000000 0000000000 0000000000 0000000000 0000000000 0000000000

..731 WWPVLKTQDD LIGVVTTIAW VTSGHHAAVN FGQYGYGGYF PNRPTTTRIR MPTEDPTDEA LKEFYESPEK VLLKTYPSQK
..... 0000000000 0000000000 0000000000 0000000000 0000000000 0000000000 0000000000 0000000000

..811 QATLVMVTLD LLSTHSPDEE YIGEQQEASW ANEPVINAAF ERFKGKLQYL EGVIDERNVN ITLKNRAGAG VVKYELLKPT
..... 0000000000 0000000000 0000000000 0000000000 0000000000 0000000000 0000000000 0000000000

..891 SEHGVTGMGV PYSISI
..... 0000000000 000000
```

TS2

```
....1 MASFSLPHSA TYFPSHSETS LKPHSAASFT VRCTSASPAV PPQTPQKPRR SPDENIRDEA RRRPHQLQNL SARYVPFNAP
..... 0000000000 0000000000 0000000000 0000000000 0000000000 0000000000 0000000000 0000000000

...91 PSSTESYSLD EIVYRSQSGA LLDVQHDFAA LKRYDGEFWR NLFDSRVGKT NWPYGSGVWS KKEWVLPEID DDDIVSAFEG
..... 0000000000 0000000000 0000000000 0000000000 0000000000 0000000000 0000000000 0000000000

..171 NSNLFWAERF GKQYLQMNDL WVKHCGISHT GSFKDLGMSV LVSQVNRLRK MNKPVIGVGC ASTGDTSAAL SAYCASAGIP
..... 0001111111 1111111111 1110000000 1111111111 1111111111 0000000000 0000000000 0000000000

..251 SIVFLPADKI SMAQLVQPIA NGAFVLSIDT DFDGCMHLIR EVTAELPIYL ANSLNSLRLE GQKTAAIEIL QQFNWQVPDW
..... 0000000000 0000000000 0000000000 0000000000 0000000000 0000000000 0000000000 0000000000


..331 VIVPGGNLGN IYAFYKGFHM CKELGLVDRI PRLVCAQAAN ANPLYLHYKS GFKEDFNPLK ANTTFASAIQ IGDPVSIDRA
..... 0000000000 0000000000 0000000000 0000000000 0000000000 0000000000 0000000000 0000000000

..411 VYALKKSNGI VEEATEEELM DATALADSTG MFICPHTGVA LTAL[MKLRKS GVIGANDRTV] VVSTAHGLKF TQSKIDYHSK
..... 0000000000 0000000000 0000000000 0000000012 3456789999 9999999987 6543210000 0000000000

..491 NIKEMACRLA NPPVKVKAKF GSVMDVLKEY LKSNDK
..... 0000000000 0000111111 1111111111 111100
```

ceQORH

```
....1 MAGKLMHALQ YNSYGGGAAG LEHVQVPVPT PKSNEVCLKL EATSLNPVDW KIQKGMIRPF LPRKFPCIPA TDVAGEVVEV
..... 0000000000 0000000000 0000000000 0000000000 0000000000 0000000000 0000000000 0000000000

...91 GSGVKNFKAG DKVVAVLSHL GGGGLAEFAV ATEKLTVKRP QEVGAAEAAA LPVAGLTALQ ALTNPAGLKL DGTGKKANIL
..... 0000000000 0000000000 0000000000 0000000000 0000000000 0000000000 0000000000 0000000000

..171 VTAASGGVGH YAVQLA[KLAN AHVTATCGAR NIEFVK]SLGA DEVLDYKTPE GAALKSPSGK KYDAVVHCAN GIPFSVFEPN
..... 0000000000 0000003333 3333333333 3333330000 0000000000 0000000000 0000000000 0000000000

..251 LSENGKVIDI TPGPNAM[WTY AVKKITMSKK QLVPL]LLIPK AENLEFMVNL VKEGKVKTVI DSKHPLSKAE DAWAKSIDGH
..... 0000000000 0000036999 9999999999 9999963000 0000000000 0000000000 0000000000 0000000000

..331 ATGKIIVEP
..... 000000000
```

Annex II

Alignment of the NADK2 sequence with that of other NADKs of eukaryotes and prokaryotes.

1- Alignment of NADK2 with AtNADK1 (NP_188744.3, AT3G21070) and NADKs of *H. sapiens* (NM_001198993) and *E. coli* (NP_061441.1). The CaM-binding peptide of NADK2 is squared. This alignment shows the presence of a conserved C-terminal catalytic domain and the presence of a long additional N-terminal sequence in NADK2.

```
H.sapiens    ------------------------------------------------------------
NADK2        DLGLDSQAVKSRDTSNLPWIGPVPGDIAEVEAYCRIFRSAERLHGALMETLCNPVTGECR
NADK1        ------------------------------------------------------------
E.coli       ------------------------------------------------------------


H.sapiens    ------------------------------------------------------------
NADK2        VPYDFSPEEKPLLEDKIVSVLGCILSLLNKGRKEILSGRSSSMNSFNLDDVGVAEESLPP
NADK1        ------------------------------------------------------------
E.coli       ------------------------------------------------------------


H.sapiens    ------------------------------------------------------------
NADK2        LAVFRGEMKRCCESLHIALENYLTPDDERSGIVWRKLQKLKNVCYDAGFPRSDNYPCQTL
NADK1        ------------------------------------------------------------
E.coli       ------------------MSVTESKAKTERKSSRKPAKTQETVLSALLAQTEEVSVPLA


H.sapiens    ------------------------------------------------------------
NADK2        FANWDPIYSSNTKEDIDSYESEIAFWRGGQVTQEGLKWLIENGFKTIVDLRAEIVKDTFY
NADK1        ------------------------------------------------------------
E.coli       SLIKSPLNVRTVPYSAESVSELADSIKGVGLLQN----------LVVHALPGDRYGVAAG


H.sapiens    ------------------------------------------------------------
NADK2        QTALDDAISLGKITVVQIPIDVRMAPKAEQVELFASIVSDSSKRPIYVHSKEGVWRTSAM
NADK1        ------------------------MSSTYKLNHTDSFANGDAKSLLPNPENGFTHLTSL
E.coli       GRRLAALNMLAERDIIQVDWPVRVKVIPQELATAASMTENGHRRDMHPAEQIAGFRAMAQ


H.sapiens    ------------------------------------------------------------
NADK2        VSRWKQYMTRPITKEIPVSEESKRREVSETKLGSNAVVSGKGVPDEQTDKVSEINEVDSR
NADK1        AQSEKAVQELLLQQTPMQATDDHLVEFSEALR--TVAKALRGAAEGKALAQAEAAEWKRR
E.coli       EGKTPAQIGDLLGYSPRHVQRMLKLADLAPVILDALAEDRITTEHCQALALENDTARQVQ
```

```
H.sapiens     ------------------------------------MEMEQEKMTMNKELSPD-----
NADK2         SASSQSKESGRFEGDTSASEFNMVSDPLKSQVPPGNIFSRKEMSKFLKSKSIAPAGYLTN
NADK1         YELERSKNVELQHKELSN-----------------GVCADESNGQRMEHLAKSPR-----
E.coli        VFEAACQSGWGGKPDVRVIR---------------NLITESEVAVKDNTKFRFVG-----
                                                        .

H.sapiens     ---------AAAYCCSACHGDETWSYNHPIRGRAKS------------------------
NADK2         PSKILGTVPTPQFSYTGVTNGNQIVDKDSIRRLAETGNSNGTLLPTSSQSLDFGNGKFSN
NADK1         -----------LYAQEISSNGMETICSHEVLQDGGFN----------------------
E.coli        ---------ADAFSPDELRTDLFSDDEGGYVDCVALD----------------------
                           :.      .     .

H.sapiens     -----------RS--------------------LSASPALGSTKEFRRTRSLHGPCP---
NADK2         GNVHASDNTNKSISDNRGNGFSAAPIAVPPSDNLSRAVGSHSVRESQTQRNNSGSSSDSS
NADK1         ----------------------------------SFNNKLKRKASFKLSWGCKGMAN---
E.coli        ----------------------------------AALLEKLQAVAEHLREAEGWEWCAG--
                                                :       .         .

H.sapiens     --------------------------------VTTFGPKACVLQNPQTIMHIQDPASQR--
NADK2         DDEAGAIEGNMCASATGVVRVQSRKKAEMFLVRTDGVSCTREKVTESSLAFTHPSTQQQM
NADK1         --------------------------------DQHKKEIVSFE---RGNISTAERSSKQIS
E.coli        --------------------------------RMEPVG-ECRE----DSRAYRNLPEPEAV
                                                                  . .   .

H.sapiens     LTWNKSPKSVLVIKKMRDASLLQPFKELCTHLMEENMIVYVEKKVLEDPAIASDESFGAV
NADK2         LLWKTTPKTVLLLKKLG-QELMEEAKEEVHEKLLVFQICFQAASFLYHQENMNVLVEPEV
NADK1         LTWESDPQTVLIITKPNSTSVRVLSVDMVRWLRTQKGLNIYVEPRVKEELLSESSSFNFV
E.coli        LTEAEEERLNELMMRYDALENQCEESDLLAAEMKLIDCMAKVRAWTPEMRAGSGVVVSWR
              *       :   :: :    .      :                    .    .

H.sapiens     KKKFCTFR----------EDYDDISNQIDFIICLGGDGTLLYASSLFQGSVPPVMAFHLG
NADK2         HDVFARIPGFGFVQTFYIQDTSDLHERVDFVACLGGDGVILHASNLFKGAVPPVVSFNLG
NADK1         QTWEDVMIYD--AD----KEISLLHTKVDLLITLGGDGTVLWAASMFKGPVPPIVPFSMG
E.coli        YGNVCVQRG------VQLRSEDDVTDDADRTEQVQEKASVEEISLPLLTKMSSERTLAVQ
                            .. . :    *    :  .. :   :  :   :..  .: :

H.sapiens     SLGFLTP---FSFENFQSQVTQVIEG-NAAVVLRSRLKVRVVKELRGKKTAVHNGLGENG
NADK2         SLGFLTS---HPFEDFRQDLKRVIHGNNTLDGVYITLRMRLRCEIYRKGKAMPG------
NADK1         SLGFMTP---FHSEQYRDCLEAILKG-----PISITLRHRLQCHIIRDKATHEYE-----
E.coli        AALMQQPDKSLALLTWTLCLNVFGSG-----AYSKPAQISLECKHYSLTSDAPSG-----
              :  :  .        :   :  .  *          :  :  .

H.sapiens     SQAAGLDMDVGKQAMQYQVLNEVVIDRGPSSYLSNVDVYLDGHLITTVQGDGVIVSTPTG
NADK2         --------------KVFDVLNEIVVDRGSNPYLSKIECYEHDRLITKVQGDGVIVATPTG
NADK1         ------------PEETMLVLNEVTIDRGISSYLTNLECYCDNSFVTCVQGDGLILSTTSG
E.coli        --------------KEGAAFMALMAEKARLVVLLPEGWSRDMTTFLSLS-QEVLLSLLSF
                           .:  :  ::.    *       .   .  :. : ::::  :
```

```
H.sapiens     STAYAAAAGASMIHPNVPAIMITPICPHS-LSFRPIVVPAGVELKIMLSPE----ARNTA
NADK2         STAYSTAAGGSMVHPNVPCMLFTPICPHS-LSFRPVILPDSAKLELKIPDD----ARSNA
NADK1         STAYSLAAGGSMVHPQVPGILFTPICPHS-LSFRPLILPEHVTVRVQVPFN----SRSSA
E.coli        CTACSIHGVQTRECGHTSRSPLDPLETAIGFHMRDWWQPTKANFFGHLKKPQIIAALNEA
              .** :  .  :    :..   : *: .   : :*    *  . .   :       : . *

H.sapiens     WVSFDGRKRQEIRHGDSISITTSCYPLPSICVRDPVSDWFESLAQCLHWNVRKKQAHFEE
NADK2         WVSFDGKRRQQLSRGDSVRIYMSQHPLPTVNKSDQTGDWFRSLIRCLNWNERLDQKAL--
NADK1         WVSFDGKDRKQLEAGDALVCSMAPWPVSTACQVESTNDFLRSIHDGLHWNLRKTQSADGP
E.coli        GLSGAARDAEKMKKGD-----AAEHAEFHMKDNRWVPGWMCAPRPQTDATERTDNLADAA
               :*  .:  :::  **      :  .         . .:: :     . . *  :


H.sapiens     EEEEEEEG
NADK2         --------
NADK1         --------
E.coli        --------
```

2- Alignment of AtNADK2 with various plants and algae NADKs containing a similar N terminal extension. Conserved motifs important for catalysis (Shi et al, 2009) are highlighted in yellow. The long N-terminal extension can be observed in both plant and algal NADK isoforms. In addition, this domain can be divided in two regions, one conserved and one more variable.

Isoforms are indicated by the initials of the name of the species followed by "NADK". NCBI sequence codes are as follows. Ot: *Ostreococcus tauri* (XP_003083231); Mp: *Micromonas pusilla* (XP_003061343); Pp: *Physcomitrella patens* (XP_001755443); Sm: *Selaginella moellendorffii* (XP_002982512); Os : *Oryza sativa* (NP_001067415); (XP_003577753); At: *Arabidopsis thaliana* (NP_001185057); Pt: *Populus trichocarpa* (XP_002302220); Vv: *Vitis vinifera* (XP_002284607); Gm: *Glycine max* (XP_003544706).

```
Pt      MVLCLFHVP-VIMNRLSPVTGILSSCS--CSFKLN---NRDTKLVGFGFELQRK-ERLKR
Vv      MVACGFWVCRVVVVDMNPSYSSTTGVSNLTPYKLPPFFTSRSAVKLFGFGSQRK-SHLRR
Gm      -------------MAFSADMTAALSPSYQCFFKPP------PSGLGLGFEFQRKGRRLRR
At      MFLCFCPCHVPIMSRLSPATGISSRLR--FSIGLS----SDGRLIPFGFRFRRNDVPFKR
Os      ------------MLAVCARHGPAKLPP-----PPP----PLAGERAAAWVVGRWWWRPAA
Pp      ------------------------------------------------------------
Sm      ------------------------------------------------------------
Ot      ------------------------------------------------------------
Mp      ------------------------------------------------------------
```

```
Pt      KLKFVVSAELSKSFSVNLGLDSK--NISQSHDLSQLPWIGPVPGDIAEVEAYCRIFRAAE
Vv      RLKLVVSAELSKPFSLSFGLDS---QAFRSHDLSQLPWIGPVPGDIAEVEAYCRIFRAAE
Gm      HLNLVISAQLSNSFSLSFGLDSQNLNSFQSNDPSQLSWMGPVPGDIAEVEAFCRIFRNSE
At      RLRFVIRAQLSEAFSPDLGLDS---QAVKSRDTSNLPWIGPVPGDIAEVEAYCRIFRSAE
Os      AGRRGVVAARASFFSSRIGLDS---QNYHTRDLSQLLWVGPVPGDIAEIEAYCRIFRAAE
Pp      ------------------------------------------------------------
Sm      ------------------------------------------------------------
Ot      --------MFPSIDEDPMDADRDGDGVGRSREGACRSGRTPLP-------------QLAA
Mp      ------------------------------------------------------------

Pt      RLHAALMDTLCNPLTGECKISYDFPSEEKPLLEDKIVPVLGCILSLLNKGREDVLSGRSS
Vv      WLHCALMDTLCNPLTGECSVSYDFTSEEKPLLEDKIVSVLGCMLSLLNKGREDVLSGRSS
Gm      RLHSALMDALCNPLTGECSVSYEVPSDEKPQLEDKIVSVLGCMISLVNKGREDILSGRSS
At      RLHGALMETLCNPVTGECRVPYDFSPEEKPLLEDKIVSVLGCILSLLNKGRKEILSGRSS
Os      QLHTAVMSALCDPETGECPVRYDVQTEDLPVLEDKVAAVLGCMLALLNRGRKEVLSGRSG
Pp      ------MSSLRTLTLVQAGYANDR---DIPVLEEKVVAGLARIGAILQQGRLEVVGSRQ-
Sm      -------------------------------LEEKVVAGLGCIGATLHQGRLDILGG---
Ot      QLERAVLASFAEVLQTECEVDFDSGS-----WDECTGEVTEALGRVMVCASAAEVAGR--
Mp      -------MDFKDSMYDECVVDMTPFG-----IEECYGDVSNAVAEVCVSAHAAETAGN--
                                         ::        :      .     ..

Pt      IMNSFRVAEVSAMEGKLPPLAIFRSEMKRCCESLHVALENFLTPDDDRSLDVWRKLQRLK
Vv      IMSSFRVADVSAMEDKLPPLAIFRGEMKRCCESLHFALENYLTPDDDRSFDVWRKLQRLK
Gm      IINSFRAAEVSTTDDKLPPLALFRSEMKRCSESLHVALENYLIPDDDRSLNVWRKLQRLK
At      SMNSFNLDDVGVAEESLPPLAVFRGEMKRCCESLHIALENYLTPDDERSGIVWRKLQKLK
Os      VASAFQGSEDSTMD-KIPPLALFRGDLKRCCESMQVALASYLVPSEARGLDIWRKLQRLK
Pp      ----FVNMVNSPGF--VPPLARLRAELKESCESLQKALETCLYP-SLIPESIYRPLQRLH
Sm      ----YSNEEEER----LPRLARFRSKLRGCCSSLRTSLQSLLPAKGDQNLAVYRILHRLT
Ot      ----FSSRLKSKE------LKRLR----DALWDLRVKLESTCDQLGGCSVTIRHRFEALR
Mp      ----FNMALRRKE------LRRLR----AALWELRVTLERQSKDSGHCTLTVRHKLEALR
            :              *  :*     .  .::  *             : : :. *

Pt      NVCYDSGFH--RRDDYPCHMLFANWNAVYFSTS-----------REDIISKNS----EFA
Vv      NVCYDSGFP--RGDDYPSHMLFANWNPVYLSTS-----------KEDTESK------EAA
Gm      NVCYDSGFP--RGEGCPCHTLFANWNPVYLSAAS----------KDDSESKDT----EPA
At      NVCYDAGFP--RSDNYPCQTLFANWDPIYSSNT-----------KEDIDSYES----EIA
Os      NACYDAGFP--RADGHPCPTLFANWFPVYFSTV-----------PDDSLSDEL----EVA
Pp      NICYDAGFP--RLPGSPDHADIPNLAAVKLCPF-----------QGGNPNLNQN--EEIA
Sm      NVCLDAGFP--RPDGAPCYGHIPNFATVKL--------------QKGDENL-------VE
Ot      SASLDVVHEKRRAPNAPSGAAIPNLQVVP-----------------EIDN----ESRTA
Mp      SASLDVCHPQMRAANAPNATAIPNFQAVHQDFRVDALPDVFADSTEDSIDDDCEVEAEIA
        . . *  .   *  . *    :.*   :                      .
```

```
Pt      FWMGGQVTEEGLNWLLERGFKTIVDLRAEIIKDNFYKAAVDDAIAAGKVE---------L
Vv      FWSGGQVTEEGLKWLIDKGYKTIVDLRAENVKDIFYEAVVHDAVLSGKVE---------L
Gm      FWTGGQVTEEGLKWLLDKGYKTIIDLRAETVKDNFCQAALQDAISSGRIE---------L
At      FWRGGQVTQEGLKWLIENGFKTIVDLRAEIVKDTFYQTALDDAISLGKIT---------V
Os      FWRGGQVSEEGLEWLLLKGFKTIVDLREEDVKDDLYLSAIHEAVSLGKIE---------V
Pp      FWRGGQVTEEGVEWLLQQGFKVVVDMRAEQSGSPFVQSMLETAEKTGKLR---------I
Sm      FWRGGNINEEGLEWLLQREFKTIVDLRDEDPQNELAEAALMKAEASGRIR---------R
Ot      FYRGGQPTAEGRAWLVRNNFKTVIDLRGSDRDNQWLQAFGGGSGQGTYGP-----SALNI
Mp      FYRGGQPTAEGRAWLAERGFKTVIDLRFEDRDNQWTKPFGGGVGVGKRAPRLADDAGFEV
        *: **: . **  **  . :*.::*:* .   .    .

Pt      IKIAVEDGTAPSMEQVEKFASLVSDSSKKPIYLHSKEGVRRTSAMVSRWRQ---------
Vv      VKFPVEARTAPSMEQVEKFASLVSDSSKKPIYLHSKEGAWRTSAMVSRWRQYMARSALQL
Gm      VKIPVEVRTAPTMEQVVQFASFVSDCSKRPIYLHSKEGVLRTSAMVSRWRQYMARSSSQI
At      VQIPIDVRMAPKAEQVELFASIVSDSSKRPIYVHSKEGVWRTSAMVSRWKQYMTRP----
Os      VNLPVEIGTAPSAEQVQRFAEIVSDSAKKPIYLHSQEGISRTSAMVSRWKQYVTRAERLA
Pp      IKMPVPFRTAPTAEQVEEFAKLVAVPENKPLYLHSQGGVGRACAMVSRWREYVLQL----
Sm      VRIPVSVQTAPTMEQVREFADIVSDAANRPVFLQSYAGVVRASAMVSRWREFVLR-----
Ot      VHIPIHDMEPPTDEDVDRFIEAVNNESMRPVLVHCKAGIGRTGALVACWRVH--------
Mp      VHMPVTDMEPPTFELVERFIEVANDRARRPMLVHCKAGIGRTGSMVSCWRIS--------
        :.:.:    .*. * *  * . .     :*: ::.  *  *: ::*: *:

Pt      ------------------------------------QENGSLSETLNKRHSSNGLSNGAVS
Vv      VSNQPIVPNEILSRDPDGREELHVLSDVRESKSLKDETESLQQSSDIINSSNGVFHEQAS
Gm      VSNPPVTPYDMLLCNTNGSAKSWDSSMTAERSSLEKDINSLQESLNSTHNSVGTFDRSTS
At      ------ITKEIP---------------------VSEESKRREVSETKLGSNAVVSGKGVP
Os      TQNRSLNGNGKHVRN-----------DQTEQLTNSPGFSSEGSENGTPLESDRTMEGETC
Pp      ------SGEGMR-----------------NPTKGSLDSSNFSSDGNTSDDVGAALRFPTD
Sm      ------------------------------------GGLDR-NCTEPMCTVEDI---FLEETP
Ot      ------------------------------------QGMDVDEA-----------------
Mp      ------------------------------------RGMDVDEAR-SISHWS---------


Pt      -PKDENGQSINETYNVHASV----QDSIPLETVENK-VGSVANISMEADPLKAQVPPCNF
Vv      RVFDNKEESSNGAYNSHSS-----QGMASIKKIDNG-VGSQVSFCREIDPLKSQFPPCDV
Gm      QKKYNGKPQGTTAMSKVSTD----NRELSEATAAKE-ERSFPRNFSKINPLKAQVPPCDI
At      DEQTDKVSEINEVDSRSAS------SQSKESGRFEG-DTSASEFNMVSDPLKSQVPPGNI
Os      DIDIETARHNLEITNSLPSE----QSTEQGELHGTR-TELQSNFRLESNPLKAQFPSCDV
Pp      DSADEGASDYSNSRSLDAGDRDAKDSITPMEISSSGDEDDQRMITAVKSSFEAQRPGPNV
Sm      DKASE-------------------SSKVAAN-----------MLRTTSPFEAQMPGPDV
Ot      ------------------------------------------LSQENLVCDFGSIAQEA
Mp      --PYDRA-------------------------------------LALESLCCDFGSIAQET
                                                              .     :
```

```
Pt      FSKAEMSKFFRSKKFKPPAYSNYQLKGFEKL---------------HKVDGTDPESRFVE
Vv      FSKKEMSRFLRSKKITPPTYLNYQQKGFENLPVLGETYIGTRQR--SKTNGTGSASRLVE
Gm      FSKREMSKFLGSQKISPPSYVNYQSRRSECSPQPRNMNVTRLQGGVTVSTSDNLIPKIVG
At      FSRKEMSKFLKSKSIAPAGYLTNPSKILGTVPTPQFSYTGVTNG--NQIVDKDSIRRLAE
Os      FSKKGMTDFFRSKKVYPKSVLNPRRRSNSLLVSRRKQSLSAE----QNGAIDYEAAEFKV
Pp      FNKSSMSQFMKRRKTTPQGAGPVIGISDLAESTARRDQIG-------GIAGPAGQWRLAE
Sm      FSRMSMARFFKRKRTLPG--------------SARR------------------QRRTIY
Ot      YH----------------------------------------------------------
Mp      FVRSFADRLAKNKRNAAA-------------------------------------TIVE
        :

Pt      AKRSNGLVSGKMASSKPQSSPADSDKHLNGSSDASVGSGMGVFSGGERRFMTGNNVSTTV
Vv      TGGSNGSLSHSNVSPKAQSSAAANGALKNDDSCVSVGSTVNGFYKGERCSMTGSDGSSFV
Gm      SESSNGSARVDHPSRETQITVSDNWEVVNGSISSSVWTTVNGFSEQEMHYMTNANASNIV
At      TGNSNG----TLLPTSSQSLDFGNGKFSNGNVHASDNTNKS-ISDNRGNGFSAAPIAVPP
Os      LKSSNG------ASFDNDYILSVASGITNGKPSNNGASTSVEDREMETSVVTVDPRTSDT
Pp      PGIPRANA--GNDSLVTEPRGFPETSEENGRLNQQTGAHSDVAGEEIRNESSNGAAVDGE
Sm      S---RLD---------------PDENAQNGRFNAKVEVPSKPS----------GGSTNGR
Ot      --------------------------FIGNYETKEAEAVLG--------------------
Mp      SVIVKG-----------AGAAYEGAGFLDVAEAEEVDVIDARI--------ATPPPPPLM
                                    .     .

Pt      VENLTEHLACASIKDGGENNGVAYLSS--SDDDLCTIEGNMCASATGVVRVQSRRKAEMF
Vv      NNKLNKDATSTTVREDQKSHDKASIVS--GDDVLGQIEGNMCASTTGVVRVQSRKKAEMF
Gm      KDDFDNVTTNSQRIEDRMVKDRLALN----DDDMGSVEGDMCASSTGVVRVQSRKKAEMF
At      SDNLSRAVGSHSVRESQTQRNNSGSSSDSSDDEAGAIEGNMCASATGVVRVQSRKKAEMF
Os      SNSNGNAPLGSQ--KSAERNGSLYVE----REKSDHVDGNMCASATGVVRLQSRRKAEMF
Pp      VSSRSEQPVVRN--GGLVRVDPAESQGRSEVENAPIVEGDMCASTTGVVRVQSRRKAEMY
Sm      AGGRAK-----------------------EEDDNGAVQGDMCASKTGVVRLQSRKKAEMY
Ot      ------------------------------------------------EHSSLQDAPDMY
Mp      SGGEGM-----------------------GSGGVSAEAAAAAETQPAPASSLEQAPDMY
                                                          . .  .:*:

Pt      LVRTDGFSCTREQVTESSLAFTHPSTQQQMLMWKSMPKTVLLLKKLGQELLEEAK-----
Vv      LVRTDGFSCTREKVTESSLAFTHPSTQQQMLMWKSTPKTVLLLKKLGQALMEEAK-----
Gm      LVRTDGFSCTREKVTESSLAFTHPSTQQQMLMWKSMPKNVLLLKKLGEELMEEAK-----
At      LVRTDGVSCTREKVTESSLAFTHPSTQQQMLLWKTTPKTVLLLKKLGQELMEEAKEEVHE
Os      LVRTDGFSCTREKVTESSLAFTHPSTQQQMLMWKSPPKTVLLLKKLGDELMEEAK-----
Pp      LVRTDGFSCTRERVKESTLAFTHPSTQQQMLMWKTPPKTVLLLKKLGMELMDQAQ-----
Sm      LVRTDGYSCTRERVTESTLAFTHPSTQQQMLMWKTAPKTVLLLKKLGEELMEEAK-----
Ot      IIRTDGFSCTRELVEKRELKISHPSTQQLILVWRQQPRRVFIIKKIGHGLLPELIEVAHA
Mp      VIRTDGFTCTREEVEDGMLKISHPSTQQLVLVWRKPPKRILVLKKLGPALLPQLVEVSHA
        ::**** :**** * .  * ::****** :*:*:  *: ::::**:*  *: :
```

```
Pt      ---------EVASFLYHQEKMNVLVEPDVHDIFARIP-----------------------
Vv      ---------EIASFLFYQEKMNVLVEPEVHDIFARIP-----------------------
Gm      ---------MVASFLYHQEKMNVLVEPDVHDIFARIP-----------------------
At      KLLVFQICFQAASFLYHQENMNVLVEPEVHDVFARIP-----------------------
Os      ---------EVASFLHHQEKMNVLVEPDVHDIFARIP-----------------------
Pp      ---------TVASYLFHQEGMNVMVEPDVHDVFARIP-----------------------
Sm      ---------QVASFLYNHEGMNVMVEPDVHDRFARFP-----------------------
Ot      MMT------MGIRIVLDEDTMDELETADIGEDSIHR-------------------------
Mp      MLS------MGFEVVVEENVVGEMREEKAARDAARRSAAAGASGPGGADGAPGTSLGASA
                       :  .: :. :    .      :

Pt      --------------GFGFVQTFYSQDTSDLHEMVDFVACLGGDGVILHASNLFRGAFPPV
Vv      --------------GFGFVQTFYSQDTSDLHERVDFVACLGGDGVILHASNLFRDAVPPV
Gm      --------------GFGFVQTFYSQDTSDLHEKVDFVACLGGDGVILHASNLFRGAVPPI
At      --------------GFGFVQTFYIQDTSDLHERVDFVACLGGDGVILHASNLFKGAVPPV
Os      --------------GYGFVQTFYTQDTSDLHERVDFVACLGGDGVILHASNLFRTSVPPV
Pp      --------------GYGFVQTFYNQDTSELHEMVDFVVCLGGDGVILHASNLFREAVPPV
Sm      --------------GFGFIQTFYNHDIGELHERVDFVVCLGGDGVILHASNLFRSAVPPV
Ot      ---------ASVQRSAERVRKVDGQIPQEEWGTIDIVVCLGGDGVILYASKLFQGPVPPL
Mp      IRDLVLENVESVPDALARVIGTNATTP-TEYAGVDLIVCLGGDGVILHASKLFQGPVPPL
                       .   :              :*::.*********:**:**: ..**:

Pt      VSFNLGSLGFLTSHYFEDYRQDLRQVIHGNNTLDG-----VYITLRMRLRCEIFRN----
Vv      VSFNLGSLGFLTSHTFEDYRQDLRQIIHGNSTLDG-----VYITLRMRLRCEIFRN----
Gm      VSFNLGSLGFLTSHDFEDYKQDLRQVIRGNNTRDG-----VYITLRMRLRCEIFRK----
At      VSFNLGSLGFLTSHPFEDFRQDLKRVIHGNNTLDG-----VYITLRMRLRCEIYRK----
Os      VSFNLGSLGFLTSHNFEGFRQDLRAVIHGNNTLG------VYITLRMRLRCEIFRN----
Pp      ISFNLGSLGFLTSHAFEAFKGDLKSIIHG----SG-----VYITLRMRLRCELFRN----
Sm      VSFNLGSLGFLTAHPFEDFKQDLRAVIHGN-RIEG-----VYVTLRMRLRCEIVRD----
Ot      LGFHFGSLGFLTNHPSDEMAASLLQSIGRGKSVAN-IQGGVPITLRMRLECTLVKAKDTK
Mp      LGFHFGSMGFLTNHPPDHLAQSLLQSVGRGSNLAGGIKGGIPITLRMRLECSLVKANDSV
        :.*::**:**** *  :    .*   :             : :******.* : :

Pt      ---GKAVPGKVFDVLNEVVVDRGSNPYLSKIECYEHDRLITKVQGDGVIVATPTGSTAYS
Vv      ---GNAMPGKIFDVMNEIVVDRGSNPYLSKIECYEHDRLITKVQGDGVIVATPTGSTAYS
Gm      ---GKAMPGKVFDILNEVVVDRGSNPYLSKIECYEHDRLITKVQGDGVIVATPTGSTAYS
At      ---GKAMPGKVFDVLNEIVVDRGSNPYLSKIECYEHDRLITKVQGDGVIVATPTGSTAYS
Os      ---GKAMPGKVFDVLNEVVVDRGSNPYLSKIECYEHNHLITKVQGDGVIVATPTGSTAYS
Pp      ---GKPIPGKVFEVLNEVVVDRGSNPYLCKIECYERSRLITKVQADGVIVATPTGSTAYS
Sm      ---GQPVSGKVFEVLNEVVVDRGSNPYLCKIECYERNRLITKVQADGVLVATPTGSTAYS
Ot      RAGGTGQATKTVTVLNELLVDRGPSPYLSHIEAYDRGELITTIQADGVIVATATGSTAYS
Mp      RNGGDGAPSHAYAVLNEVLVDRGPSPFLSKIEAYDRGLFITTIQADGVMLATATGSTAYS
           *    . :   ::**::****..*:*.:**.*::. :**.:*.***::**.*******
```

```
Pt      TSAGGSMVHPNVPCMLFTPICPHSLSFRPVILPDSARLELKIPEDARSNAWVSFDGKRRQ
Vv      TAAGGSMVHPNVPCMLFTPICPHSLSFRPVILPDSARLELKIPKDARSNAWVSFDGKRRQ
Gm      TAAGGSMVHPNVPCILFTPICPHSLSFRPVILPDSAQLELKIPDDARSNAWVSFDGKRRQ
At      TAAGGSMVHPNVPCMLFTPICPHSLSFRPVILPDSAKLELKIPDDARSNAWVSFDGKRRQ
Os      TAAGGSMVHPNVPCMLFTPICPHSLSFRPVILPDSARLELKIPDDARSNAWVSFDGKRRQ
Pp      TAAGGSMVHPNVPCMLFTPICPHSLSFRPVILPDSALLELKVPDEARSNAWVSFDGKKRQ
Sm      TAAGGSMVHPNVPCMLFTPICPHSLSFRPVILPDSAILELKVPSDSRSNAWVSFDGKKRQ
Ot      VSAGGSMVHPNVPAILMTPICPHTLSFRPVVFPDSVELELRVASDARCSAWVSFDGRDRC
Mp      VSAGGSMVHPNVPAILMTPICPHTLSFRPVILPDSVEMELRVADDARCSAWVSFDGKERC
        .:***********.:*:******:******::***. :**::..::*..*******: *

Pt      QLSRGDSVRISMSQHPLPTVNKSDQTGDWFHSLVRCLNWNERLDQKAL------------
Vv      QLSRGDSVRISMSQHPLPTVNKSDQTGDWFHSLVRCLNWNERLDQKPFEASK--------
Gm      QLSRGDSVRISMSQHPLPTVNKFDQTGDWFSSLIRCLNWNERLDQKAL------------
At      QLSRGDSVRIYMSQHPLPTVNKSDQTGDWFRSLIRCLNWNERLDQKAL------------
Os      QLSRGDSVQISMSQHPLPTVNKSDQTGDWFRSLIRCLNWNERLDQKAL------------
Pp      QLCKGESMQISMSEYPMPTVNKLDQTEDWFASLSRCFGWNQRIEQRSITFYQE-------
Sm      QLTKGDLVRIHMGRNPMPTVNKSDQTSDWFRSLDRCFNWSARKEQMAL------------
Ot      ELESGDSVFVRMSEYPIPTINYADQTGDFISSLRRCLRWNERDIQHGFDTSQKEALRKIS
Mp      ELCAGDSIFVRMSECPVPTINYADQTGDFISSLRRCLRWNEREEQKPLDEKVTKKLRKMA
        :*  *: : : *.. *:**:*  *** *:: ** **: *. *  *  :

Pt      ------------------------
Vv      ------------------------
Gm      ------------------------
At      ------------------------
Os      ------------------------
Pp      ------------------------
Sm      ------------------------
Ot      ESSS--------------------
Mp      QGRVDLATVDLTMDESQDDATFV
```

Molecular BioSystems

RSC Publishing

PAPER

View Article Online
View Journal | View Issue

Cite this: *Mol. BioSyst.*, 2013, **9**, 1234

Complementary biochemical approaches applied to the identification of plastidial calmodulin-binding proteins†

Elisa Dell'Aglio,[abcd] Cécile Giustini,[abcd] Daniel Salvi,[abcd] Sabine Brugière,[abe] Faustine Delpierre,[abcd] Lucas Moyet,[abcd] Mathieu Baudet,[abe] Daphné Seigneurin-Berny,[abcd] Michel Matringe,[abcd] Myriam Ferro,[abe] Norbert Rolland*[abcd] and Gilles Curien[abcd]

Received 2nd January 2013,
Accepted 12th March 2013

DOI: 10.1039/c3mb00004d

www.rsc.org/molecularbiosystems

Ca^{2+}/Calmodulin (CaM)-dependent signaling pathways play a major role in the modulation of cell responses in eukaryotes. In the chloroplast, few proteins such as the NAD^+ kinase 2 have been previously shown to interact with CaM, but a general picture of the role of Ca^{2+}/CaM signaling in this organelle is still lacking. Using CaM-affinity chromatography and mass spectrometry, we identified 210 candidate CaM-binding proteins from different *Arabidopsis* and spinach chloroplast sub-fractions. A subset of these proteins was validated by an optimized *in vitro* CaM-binding assay. In addition, we designed two fluorescence anisotropy assays to quantitatively characterize the binding parameters and applied those assays to NAD^+ kinase 2 and selected candidate proteins. On the basis of our results, there might be many more plastidial CaM-binding proteins than previously estimated. In addition, we showed that an array of complementary biochemical techniques is necessary in order to characterize the mode of interaction of candidate proteins with CaM.

Introduction

CaM is one of the most versatile proteins of eukaryotic cells, as it is involved in several cellular signaling pathways and stress responses such as cell cycle,[1] metabolism,[2,3] and protein sorting.[4] Its versatility depends on its four high-affinity Ca^{2+} binding sites called EF-hands.[5] Ca^{2+} binding triggers a deep change in CaM conformation by the exposure of hydrophobic residues, thus modifying the affinity of CaM for its partners and differentially modulating their activity and properties.[6,7] Therefore, while lacking any sort of catalytic activity *per se*, CaM is one of the major transducers of Ca^{2+} signaling and a central node of cellular networks.[8,9]

In animals, several high-throughput studies have been recently conducted in order to obtain a broad picture of CaM partners using different approaches, such as protein arrays,[10] affinity chromatography coupled with mass spectrometry,[11] or mRNA display,[12,13] and in different model organisms such as mouse,[11] *Caenorhabditis elegans*[13] and humans.[10,12] All studies allowed the identification of a high number of new putative CaM-binding proteins, sometimes more than one hundred. In order to confirm the interactions retrieved by large-scale studies, several techniques were employed, *e.g.* pull-down,[12,13] overlay assay,[10] Biacore[10] or co-immuno-precipitation.[10,12,13] However, a standard validation pipeline has never been established and the estimation of the CaM-partner binding parameters is often difficult to determine, especially for proteins of unknown function or whose catalytic activity is difficult to measure.

In contrast to mammals or fungi, where only one or a few CaM isoforms are present, plant genomes contain several CaM genes, probably due to the constant need of plants to rapidly respond to local stress conditions.[14,15] In the model organism *Arabidopsis thaliana*, seven CaMs and fifty CaM-like proteins (CMLs) are present and localized in various organelles such as the nucleus,[16,17] the peroxisomes and the mitochondria.[18] CMLs are constituted mostly of a variable number of EF-hand

[a] *Université Joseph Fourier Grenoble 1, F-38054 Grenoble, France*
[b] *CEA, DSV, iRTSV, F-38054 Grenoble, France*
[c] *INRA, USC1359, 17 rue des Martyrs, F-38054 Grenoble, France*
[d] *CNRS, Laboratoire de Physiologie Cellulaire & Végétale, UMR 5168, 17 rue des Martyrs, F-38054 Grenoble, France. E-mail: norbert.rolland@cea.fr; Fax: +33 4 38 78 50 91; Tel: +33 4 38 78 49 86*
[e] *INSERM, U1038, Biologie à Grande Echelle, F-38054 Grenoble, France*

† Electronic supplementary information (ESI) available: Fig. S1 and Tables S1–S4. See DOI: 10.1039/c3mb00004d

motifs and share at least 16% overall amino acid identity with CaM.[15] They display partially different binding properties[19,20] and their expression changes according to cells, tissues and developmental stages.[21,22] The essential role of CaM in eukaryotes was demonstrated by the lethality of the knock-out of the CaM gene in yeast.[23] In plants, the high number of CaMs and CMLs makes it difficult to study their impact on plant physiology by reverse genetic approaches. Unraveling the details of the interactions of CaMs and CMLs with their targets at the biochemical level is therefore a major question in plant biology.

The chloroplast, the plant cell factory where photosynthesis and many plant metabolic pathways are located, was shown to respond in different ways to Ca^{2+} fluxes or Ca^{2+} oscillations.[24] For instance, a stromal Ca^{2+} spike induced by darkness has been associated with the sensing of light–dark transition and photoperiod.[25] More recently, the protein CAS (Calcium sensor, At5g23060), which is localized in the thylakoidal membrane,[26] has been related to the generation of external Ca^{2+}-induced cytosolic Ca^{2+} transients leading to stomatal closure in plants and photoacclimation in *Chlamydomonas reinhardtii.*[27] Some plant CMLs contain a putative plastidial transit peptide and therefore might be localized in the chloroplast and act as the transducers of Ca^{2+} signaling in this organelle.[28] A few plastidial proteins have been indeed shown to interact with CaM *in vitro* and a direct effect on their activity was demonstrated. The most well-known example is NADK2 (At1g21640), one of the three *Arabidopsis* NAD^+ kinase isoforms and the only one to be addressed to the chloroplast.[29] CaM–NADK2 interaction occurs only in the presence of Ca^{2+} and is required for native enzyme activity.[30] Other recently identified plastidial CaM targets are Tic32[28] (At4g23430), a component of the chloroplast protein import machinery, photosystem I PsaN subunit[31] (At5g64040), the elongation factor EF1-α[32](At1g07920), the heat shock protein CPN21[33] (At5g20720), and a AAA^+ ATPase (AFG1-like protein 1,[24] At4g30490). The majority of these CaM-binding proteins has been discovered in the course of targeted studies. Beside those studies, only two large-scale investigations on plant CaM-binding proteins were conducted so far. The first of these studies was based on a phage display approach and allowed the identification of PsaN as a CaM-binding protein,[31] while the second was conducted on an *Arabidopsis* protein array.[20] Neither of these studies was focused on the chloroplast. Therefore, the CaM-binding proteome of chloroplast is still an open question that needs to be addressed to better understand the physiology of this organelle and plant adaptation to stress and environmental conditions.[34]

In this study, we investigated the CaM-binding proteome of *Arabidopsis* plastidial sub-compartments (stroma, thylakoids and envelope), by a proteomic approach based on mass spectrometry combined with affinity chromatography. More than 200 proteins were identified. A subset of 19 candidates was chosen for further validation using *in vitro* CaM-binding (overlay) assays, which we optimized. We also designed two fluorescence anisotropy assays to measure the CaM-binding affinity in solution. This technique was applied to NADK2, Tic32 and a subset of new CaM-binding candidates.

Results

1. Searching for new plastidial CaM-binding proteins using affinity chromatography and mass spectrometry

The aim of this study was to investigate the CaM-binding proteome of the chloroplast. In order to get a better coverage of the plastidial CaM partners, we chose to combine (i) cell and chloroplast fractionation in order to retrieve low abundant CaM binding proteins, (ii) a CaM-affinity purification starting from the different plastidial sub-compartments (stroma, thylakoids and envelope), and (iii) a proteomic approach based on mass spectrometry. An overview of all steps of the procedure adopted is given in Fig. 1.

Stroma and membrane protein fractions were obtained by sub-fractionation of Percoll-purified *Arabidopsis* chloroplasts, in order to take advantage of the full-sequenced genome of this model plant. However, since the yield of envelope purification for *Arabidopsis* chloroplasts is very low and not compatible with subsequent CaM-affinity chromatography experiments, we also chose to use envelope fractions extracted from Percoll-purified spinach chloroplasts.

With the aim to reduce non-specific (low affinity) binding during the CaM-affinity chromatography, we adapted previously published protocols[35] to our protein samples. Chromatographic steps were thus performed in the presence of a low detergent concentration and of high salt concentrations (see Experimental procedures for buffers composition). After solubilisation of the proteins in the appropriate binding buffer, proteins were incubated with a calmodulin affinity matrix in the presence of 2 mM $CaCl_2$. After washing several times the affinity matrix with the same buffer, the CaM-binding proteins were recovered using an elution buffer in which Ca^{2+} was replaced by 2 mM EGTA, a Ca^{2+} chelator. Fig. 2 shows protein profiles obtained after solubilisation of the proteins, washing of the affinity matrix, and elution of the CaM-binding proteins. The profile of the eluted fractions (Fig. 2) was remarkably different when compared to the protein composition of the original samples or the washes, thus suggesting that the affinity chromatography resulted in the successful enrichment of specific proteins.

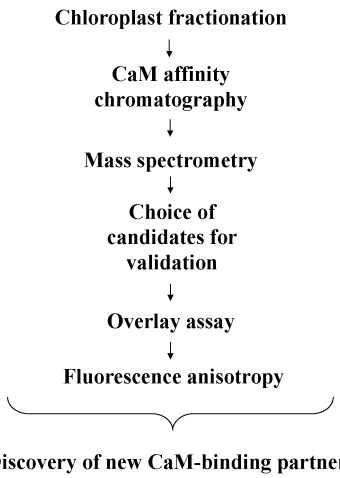

Fig. 1 Pipeline used to purify, identify and characterize new CaM–plastidial protein interactions.

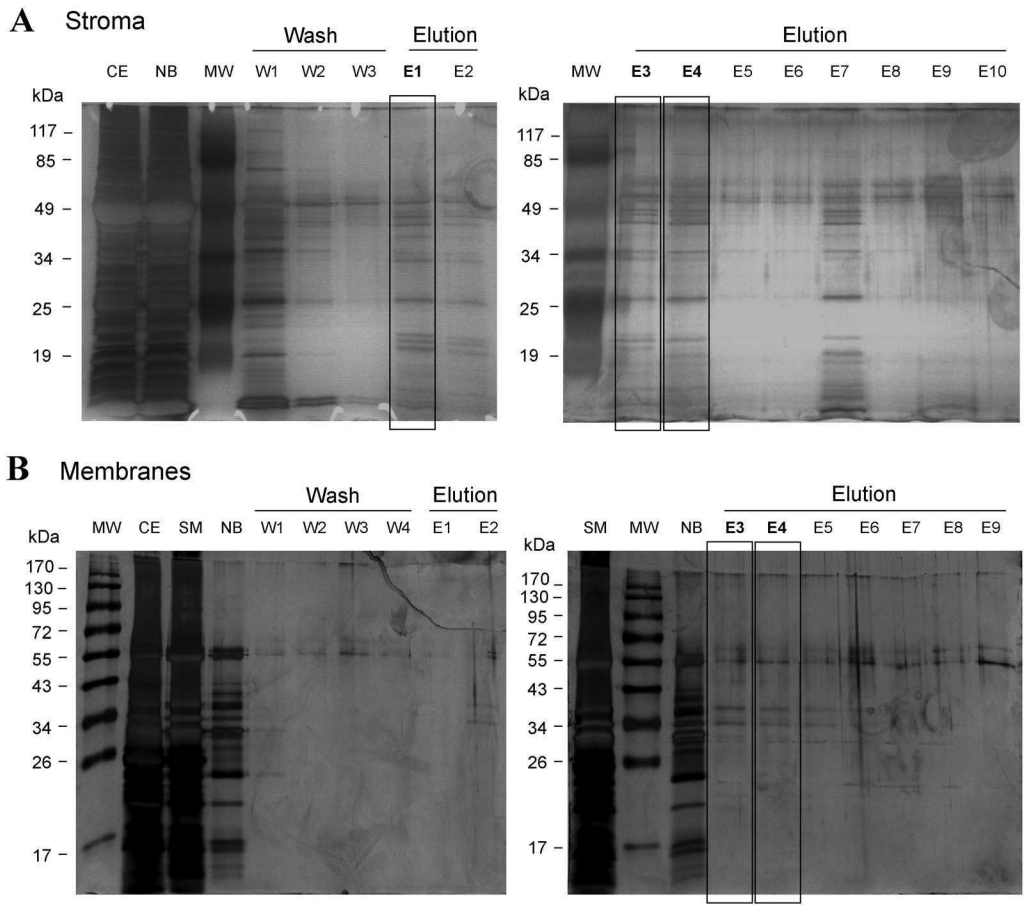

Fig. 2 Purification of CaM-binding proteins from chloroplast sub-fractions. (A) Affinity purification of CaM-binding proteins starting from stroma proteins (*Arabidopsis*). Proteins were separated on a SDS-PAGE (12% acrylamide). Proteins were detected using silver staining. MW: molecular weight markers. CE: 25 μL of stroma proteins (6 mg of stroma proteins at a 1 mg mL^{-1} concentration) in binding buffer (containing 2 mM $CaCl_2$). NB: 25 μL of proteins not bound to the CaM affinity resin (pass-through). W1 to W3: 25 μL of three successive washes of the CaM affinity resin using 1 mL of binding buffer (containing 2 mM $CaCl_2$). E1 to E10: 25 μL of ten successive washes of the CaM affinity resin using 100 μL of elution buffer (containing 2 mM EGTA). Fractions selected for further MS analyses were E1, E3 and E4. (B) Affinity purification of CaM-binding proteins starting from chloroplast membrane proteins (*Arabidopsis*). Proteins were separated on a SDS-PAGE (12% acrylamide). Proteins were detected using silver staining. MW: molecular weight markers. CE: 1 μL of membrane proteins (7 mg of membrane proteins at a 1.75 mg mL^{-1} concentration) in binding buffer (containing 2 mM $CaCl_2$). SM: 1 μL of membrane proteins soluble in binding buffer (containing 0.1% (v/v) NP40). NB: 1 μL of proteins not bound to the CaM affinity resin (pass-through). W1 to W4: 1 μL of four successive washes of the CaM affinity resin using 1 mL of binding buffer (containing 2 mM $CaCl_2$). E1 to E9: 25 μL of nine successive washes of the CaM affinity resin using 70 μL of elution buffer (containing 2 mM EGTA). Fractions selected for further MS analyses were E3 and E4. Similar profiles were obtained starting from envelope and stroma proteins purified from spinach chloroplasts.

Mass-spectrometry was then used to identify the CaM-binding proteins present in these eluted fractions (see Experimental procedures for full details). In order to get a comprehensive identification of these proteins, selected elution fractions (Fig. 2) were concentrated on a very thin band using a subsequent SDS-PAGE, as previously described.[36]

This proteomic approach allowed the identification of 210 CaM-binding candidates, 96 from the *Arabidopsis* stroma, 147 from the *Arabidopsis* thylakoids and 27 from spinach fractions (stroma and envelope) (Fig. 3 and Table S1, ESI†). The identified proteins are involved in several processes such as lipid metabolism, chlorophyll biosynthesis, protein biosynthesis and degradation (Fig. 4).

A short list of plastidial CaM-binding proteins was already available before our study and included NADK2, Tic32, Cpn21 and PsaN (Table 1). The absence of Cpn21 among the detected proteins suggests that our list is still not exhaustive. However, the present proteomic approach allowed the identification of NADK2, Tic32, PsaN and the elongation factor 1α (Table 1). The low abundance of NADK2 (not present in the AT_Chloro database)[37] and Tic32 (a minor membrane protein) indicates that enrichment in genuine CaM-binding proteins was actually obtained. In particular, Tic32 was only identified in the spinach envelope fraction, while it was not detected in the *Arabidopsis* membrane sample. This shows that sub-fractionation is essential in order to retrieve low abundant CaM-binding proteins.

2. Selection of candidates for validation of new plastidial CaM-binding partners

The use of detergent and excess of salt for affinity chromatography was supposed to minimize the non-specific interactions

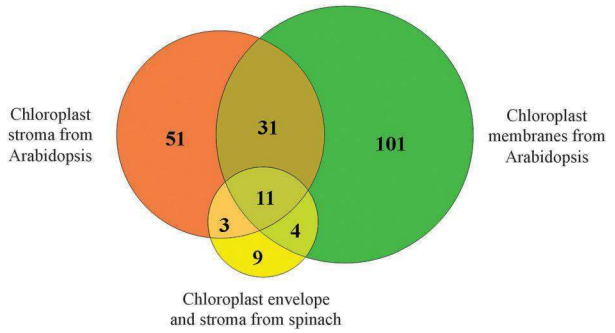

Fig. 3 Venn diagram illustrating the overlap between the proteins detected by mass spectrometry from the different chloroplast sub-fractions subjected to CaM-affinity chromatography (stroma, thylakoids and envelope).

with CaM. However, non-specific binding on the CaM matrix could still be due to the high abundance of some proteins or to strong protein–protein interactions, which could have caused the elution of protein complexes in their integrity. In order to verify the reliability of our proteomics approach, we therefore selected a list of 19 previously unidentified CaM-binding partners and validated them by an *in vitro* CaM-binding assay.

We excluded from this validation list the proteins that both did not contain a predicted transit peptide and were not detected in the AT_Chloro database,[37] thus being likely contaminants of our chloroplast fractions. We also excluded proteins previously localized in cell compartments other than the chloroplast. The low number of proteins (24 out of 210) and corresponding peptides belonging to this category is an indicator of the purity of our starting material (Table S2, ESI†). This list of putative contaminants contains GAD2[2] (At1g65960) and PCaP2[38] (At4g20260), two known CaM-binding proteins that are likely localized in the cytosol and the plasma membrane, respectively.

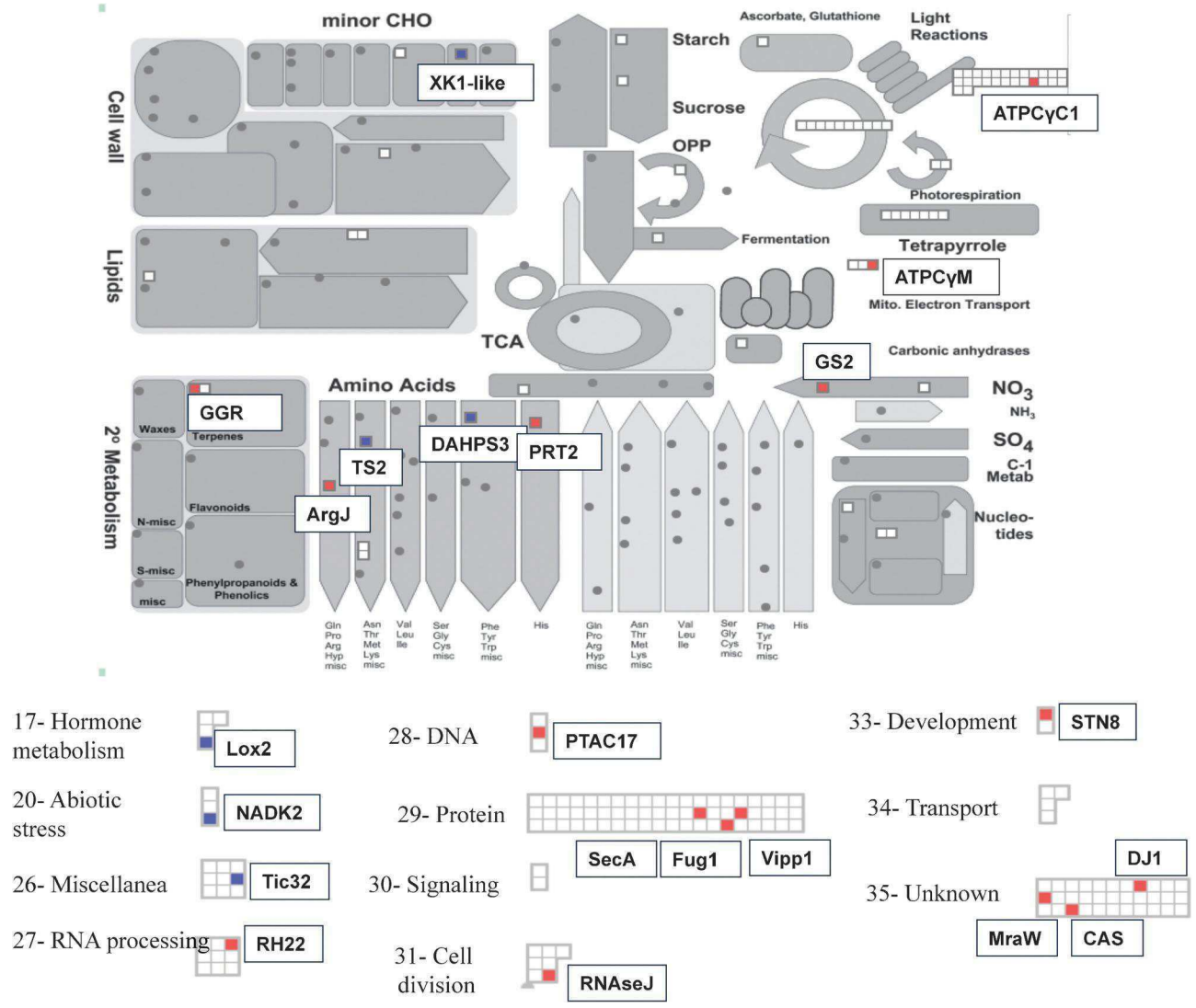

Fig. 4 Graphic representation of the CaM-binding candidate proteins detected by mass spectrometry during this work. Each protein is represented by a square and located in the corresponding cellular pathway. Red squares represent proteins subsequently validated by the overlay assay. Blue squares represent proteins tested using both overlay assays and fluorescence anisotropy.

Table 1 List of previously identified CaM-binding proteins also detected during this study

Accession no	Description	Found in (sample) *Arabidopsis* stroma	*Arabidopsis* thylakoids	Spinach envelope	Reference
At5g64040	PSAN	No	Yes	No	Reddy *et al.* 2002
At1g65960	GAD2	Yes	Yes	No	Zik *et al.* 1998
At1g07920	Elongation factor 1α	Yes	No	No	Durso and Cyr 1994
At4g23430	Tic32-like protein	No	No	Yes	Chigri *et al.* 2006
At4g20260	PCaP2	No	Yes	No	Kato *et al.* 2010
At1g21640	NAD^+ kinase 2	Yes	Yes	No	Turner *et al.* 2004

We noticed that our list of candidates contained almost all subunits of highly abundant protein supercomplexes, *i.e.* the ribosomes, the photosystems and the ATP synthase. This was probably due to the high abundance of the complexes and to the strong protein–protein interactions that take place between the different subunits. As it was difficult to estimate which, if any, of these subunits is a genuine CaM-binding partner, they were all excluded from the list of candidates to validate. However, we noticed that, among candidates, both the mitochondrial (ATPγM, At2g33040) and the plastidial (ATPγC1, At4g04640) gamma subunits of ATP synthase complexes were present. In particular, ATPγM was the only retrieved subunit of the mitochondrial F_1–ATP synthase complex and one of the only four mitochondrial contaminants, thus suggesting a high CaM-binding potential. On the basis of these observations, we decided to include both gamma subunits (the plastidial and the mitochondrial one) in our validation experiments.

Among the remaining proteins, candidates to validate were selected from several functional categories and were involved in different metabolic processes (Fig. 4).

3. *In vitro* validation of selected plastidial candidates by CaM-binding assays

To validate the CaM interaction for the selected subset of 19 candidates, we produced them as recombinant proteins in *E. coli* and performed a CaM-binding "overlay" assay (Fig. 5). In its classic form, the overlay assay relies on the detection of a protein transferred to a membrane by a radiolabelled CaM or a CaM coupled to the horseradish peroxidase (here $AtCaM_1$–HRP).

The overlay technique allows testing different proteins at the same time and was extensively used in several previously published studies aiming to identify CaM partners.[13,20,39] However, in the course of our study, preliminary experiments indicated that some critical parameters needed to be accurately tuned in order to obtain reliable results. In particular, when the assay is performed on many proteins on the same membrane with a low excess of $AtCaM_1$–HRP, a competition among the candidates occurs. The intensity of the signal for some proteins can therefore vary from one assay to the other. Moreover, a long exposure time of the films

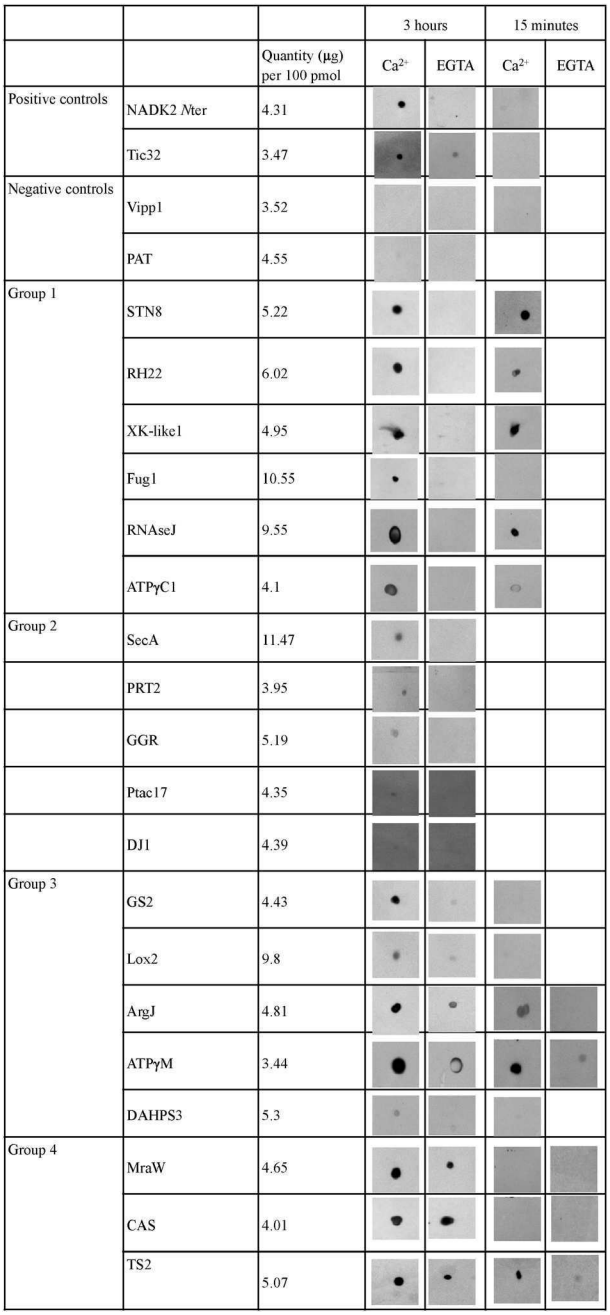

Fig. 5 *In vitro* $AtCaM_1$–HRP overlay assay performed on a subset of CaM-binding candidates. Proteins are classified according to the intensity of the signal detected under the different conditions tested after 3 h of incubation (third column). The intensity of the signal of each protein was compared to that of NADK2 (positive control). Group 1: proteins showing a strong Ca^{2+}-dependent signal. Group 2: proteins showing a weak signal in the presence of Ca^{2+}. Group 3: proteins still showing a weak signal in the presence of an excess of EGTA. Group 4: proteins showing a strong Ca^{2+}-independent signal. All proteins, which showed a strong signal after 3 h of incubation, were again tested with a reduced incubation time of 15 min (fourth column). Each experiment was performed twice.

can lead to the presence of a strong signal for every protein, even when the experiment is performed in the presence of an excess of EGTA, *i.e.* a calcium chelator. This is also true for the negative controls (see below). Finally, the transfer of proteins from the

SDS-PAGE gel to the membrane is more or less effective depending on the physico-chemical properties of proteins, thus leading to the transfer of different amounts of each candidate on the membrane (data not shown). We therefore decided to improve the procedure by spotting the proteins directly on the membrane and by incubating each candidate separately, with a 2.5-fold molar excess (30 nM) of $AtCaM_1$–HRP, for 3 hours, either in the presence of Ca^{2+} or EGTA. Revelations of all membranes, in the presence of Ca^{2+} or EGTA, were then performed in parallel.

In addition, since this interaction assay is semi-quantitative and since long film exposures led to a strong signal for every protein even in the absence of Ca^{2+}, we included, in the assay, two positive and two negative control proteins. Among the already established plastidial CaM-binding partners, NADK2 was already extensively characterized.[30,40] NADK2–CaM interaction was shown to be Ca^{2+} dependent and is required for the native enzyme activity.[40] The CaM-binding domain was recently identified and located in a putative regulatory region[29,30] at the N-terminal of the protein (Fig. 6A). The N-terminal part of NADK2, containing the CaM-binding site, was therefore selected as positive control, together with Tic32 which was previously demonstrated to interact with CaM.[28] As negative controls, we chose Vipp1 (At1g65260), a protein retrieved from our proteomic approach, but previously shown not to interact with bovine brain CaM–HRP in an *in vitro* assay,[28] and the plastidial prephenate aminotransferase (PAT,[41] At2g22250), which was not detected in our proteomic approach and therefore was expected not to interact with CaM.

Since the CaM–NADK2 interaction was shown to be Ca^{2+} dependent,[30] the film exposure was stopped when a positive signal was visible for NADK2 in the presence of Ca^{2+}, but still not detectable in the presence of EGTA. The signals obtained for each candidate to be tested was then compared to the one of the N-terminal region of NADK2, and a score was assigned according to its intensity. A schematic representation of the procedure can be found in Fig. S1 (ESI†).

We first tested the *in vitro* CaM-binding of each candidate after 3 hours of incubation with $AtCaM_1$–HRP (Fig. 5). Under these conditions, all tested proteins, except for the two negative controls (*i.e.* Vipp1 and PAT), were shown to interact with $AtCaM_1$–HRP in the presence of Ca^{2+}. The intensity of the signal varied extensively from one protein to another. A group of proteins (group 1 in Fig. 5: STN8-At5g01920, RH22-At1g59990, XK-like1-At2g21370, Fug1-At1g17220, RNAseJ-At5g63420 and ATPγC1) showed signal intensity similar to that of NADK2. For other proteins (group 2 in Fig. 5: SecA-At4g01800, PRT2-At1g09795, GGR-At1g74470, pTAC17-At1g80480, and DJ1-At1g53280), the detected signal was slightly weaker than that of NADK2.

In all cases mentioned above, the signals detected in the presence of Ca^{2+} were abolished in the presence of an excess of EGTA, consistent with the classic situation of CaM-controlled proteins. However, the situation was quite different for seven other candidates that showed an *in vitro* CaM-binding capacity even in the presence of an excess of EGTA. In some cases, the intensity of the signal was lower than the one detected in the presence of an excess of Ca^{2+} (Fig. 5, group 3: GS2-At5g35630, Lox2-At3g45140, ArgJ-At2g37500, ATPγM, and DAHPS3-At1g22410). Surprisingly, a weak signal was also detected for Tic32 even in the presence of EGTA. In three other cases (Fig. 5, group 4: MraW-At5g10910, CAS and TS2-At1g72810), the signal intensities were as high as the ones obtained in the presence of Ca^{2+}. CaM-binding in the absence of Ca^{2+} was previously reported for few proteins containing the so-called IQ-motifs, *i.e.* Ca^{2+} independent CaM-binding sites.[42] However, none of the above-cited candidates interacting with CaM in the presence of EGTA contained these IQ-motifs. One of the hypotheses, which could thus explain this behaviour, is that long incubation time (3 hours) with CaM–HRP increases the possibility of an non-specific binding with CaM.

In vivo CaM interaction is expected to be rapid (*i.e.* instantaneous or requiring few minutes to take place) in order to generate a rapid cell response. In order to lower the putative non-specific signals detected in the absence of Ca^{2+}, the 16 proteins which showed a positive signal in the overlay assay, as well as the negative control Vipp1, were therefore tested again for their ability to interact with $AtCaM_1$–HRP, but using a reduced (15 minutes) incubation time (Fig. 5, right column). Consistent with the hypothesis of an non-specific CaM-binding, the signal previously observed after incubation for 3 hours in the absence of Ca^{2+} was lost for most proteins under these new experimental conditions, or at least significantly decreased in the case of TS2 and ATPγM. However, in five cases, even the signals previously detected in the presence of Ca^{2+} were extremely reduced in these new conditions (GS2, MraW, CAS, Fug1, ATPγC1 and DAHPS3). This decrease in the signal intensity was even observed for the N-terminal domain of NADK2 or for Tic32, *i.e.* our two positive controls in these experiments. In contrast, for other proteins (STN8, RH22, XK-like1, RNAseJ, ArgJ, RNAseJ and ATPγM) the signal intensities remained similar to those detected after 3 hours of incubation with $AtCaM_1$–HRP, thus suggesting that the affinity of CaM for these candidates might be particularly strong.

In conclusion, our *in vitro* CaM-binding assays show that the whole subset of proteins chosen from the putative CaM-binding partners identified during this approach is able to interact with $AtCaM_1$–HRP in the presence of Ca^{2+}, provided that the incubation time is long enough (3 hours). However, depending on the protein, the incubation time and the presence of Ca^{2+}, we observed a wide variety of signal intensities. We therefore decided to go further into the characterization of the CaM-binding affinity of some proteins using additional techniques that would allow measuring the binding parameters in solution and under equilibrium conditions.

4. Quantitative measurement of CaM-affinity of plastidial candidates

In order to obtain more quantitative information about the binding affinity of the plastidial candidates, we developed two independent CaM-binding assays, based on fluorescence anisotropy (also called fluorescence polarization). Fluorescence anisotropy is a parameter that increases when the mobility of a fluorescent molecule decreases, for example due to the interaction of this fluorescent molecule with a partner.[43] This technique allows the determination of binding parameters for

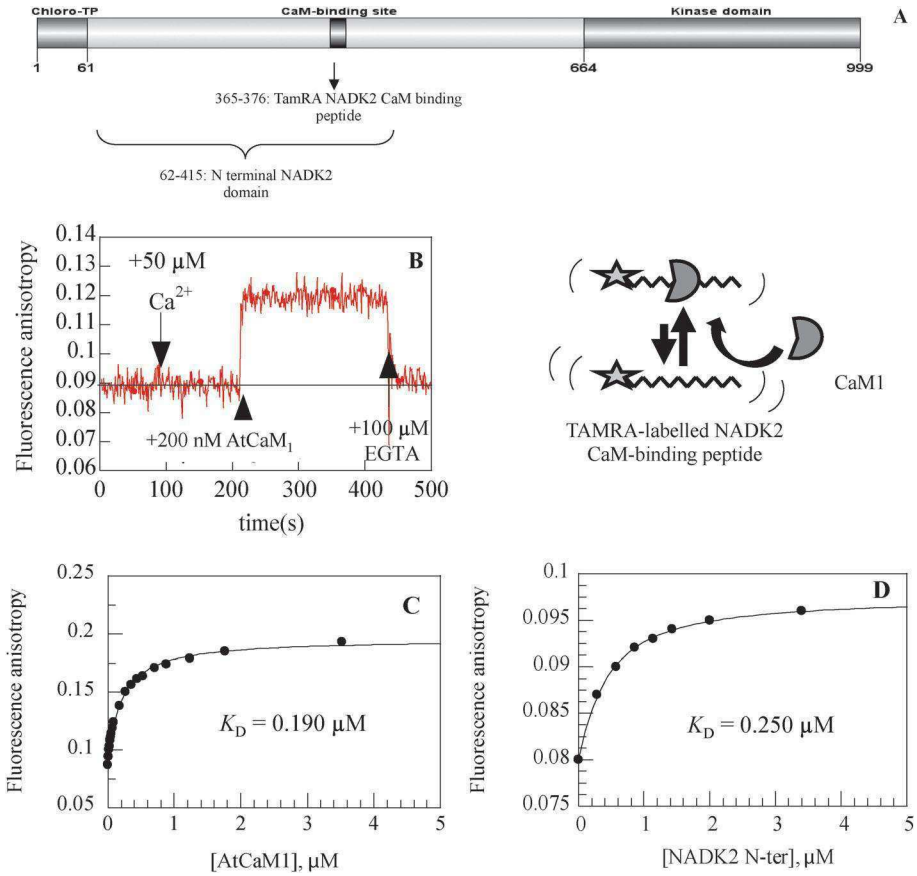

Fig. 6 Characterization of NADK2 CaM-binding affinity. (A) Schematic representation of the NADK2 protein, containing the plastidial transit peptide (amino acids 1–61), the CaM-binding site (amino acids 365–376) and the kinase domain (amino acids 664–999). For fluorescence anisotropy measurements, the CaM-binding site alone was labeled with the TAMRA fluorescent probe and used in combination with unlabeled $AtCaM_1$, while the N-terminal part of the protein containing the CaM-binding site (amino acids 62–415) was purified and used in combination with $AtCaM_1$-$Alexa^{488}$. (B) Direct measurement of the NADK2-TAMRA peptide fluorescence anisotropy as a function of time. The graph shows the changes in fluorescence anisotropy due to the complex formation of the peptide with $AtCaM_1$ in the presence of Ca^{2+} and the reversibility of the interaction upon Ca^{2+} chelation with an excess of EGTA. [NADK2 TAMRA peptide] = 50 nM, [$CaCl_2$] = 300 µM, [$AtCaM_1$] = 200 nM. (C) Direct measurement of the fluorescence anisotropy of the NADK2-TAMRA labelled peptide (50 nM) at different $AtCaM_1$ concentrations in the presence of 300 µM $CaCl_2$. (D) Direct measurements of the fluorescence anisotropy of $AtCaM_1$-$Alexa^{488}$ (200 nM) at different concentrations of the NADK2 N-terminal domain. Data points are the average fluorescence anisotropy values of three independent experiments. Experimental data were fitted using eqn (1). Data points are the average fluorescence anisotropy values of three independent experiments.

two interacting proteins without the need of a known and detectable enzymatic activity of any of the two partners.

First, we used the two assays to characterize the CaM-binding affinity of the NADK2 CaM-binding peptide alone or of the NADK2 N-terminal domain. For the first assay, we purchased a synthetic TAMRA-labeled peptide corresponding to the NADK2 CaM-binding sequence (IYVHSKEGVWRTSAMVSRWK) and measured the affinity of this labeled NADK2-peptide for unlabeled $AtCaM_1$ (Fig. 6B). For the second assay, we used a fluorescent version of $AtCaM_1$ ($AtCaM_1$-$Alexa^{488}$) and measured its binding affinity for the N-terminal part of NADK2 (which contains its CaM-binding domain).

In both assays, we first confirmed the interaction of NADK2 and $AtCaM_1$, since the fluorescence anisotropy increased following incubation of both partners. We also confirmed the requirement of Ca^{2+} for these interactions to occur, since the value of the fluorescence anisotropy returned to its original level in the presence of an excess of EGTA (Fig. 6B). The first assay (*i.e.* labeled NADK2-peptide incubated with $AtCaM_1$) allowed measuring a K_D value of 190 nM (Fig. 6C). The second assay (N-terminal part of NADK2 incubated with $AtCaM_1$-$Alexa^{488}$) allowed measuring a K_D value of 250 nM (Fig. 6D). These values are situated in the middle range of what is currently considered as a strong CaM-binding affinity (10 nM–1 µM).[10] This K_D value is also similar to the value of 100 nM measured for GAD2, a well characterized CaM-binding plant protein.[2] The good correspondence between the measurements performed with the CaM-binding peptide of NADK2 or the entire N-terminal domain of NADK2 indicates that the labeling of $AtCaM_1$ or of the NADK2 peptide has poor or no impact on the interaction.

Having validated the assays, we then performed similar $AtCaM_1$-$Alexa^{488}$ binding assays with a subset of plastidial candidates that showed various behavior in the overlay assays: Tic32, TS2, Lox2 and XK-like1 (Fig. 7).

Tic32, which was previously identified as a CaM-partner[28] and used as a positive control during this study, showed a K_D

value of 0.8 μM for CaM under our experimental conditions (Fig. 7A). In good agreement with what was previously reported, the interaction was completely disrupted by addition of EGTA in excess. This suggests that the weak overlay signal of Tic32 in the presence of EGTA after 3 hours of incubation with $AtCaM_1$–HRP was non-specific. In good agreement with the weak signal obtained in the overlay assay suggesting lack of interaction with $AtCaM_1$, Lox2 did not modify the AtCaM-Alexa^{488} anisotropy (Fig. 7B).

The results obtained for the other two proteins (TS2 and XK-like1) were surprising, especially in view of the strong signal observed in the overlay assays: TS2 was able to bind to CaM in the anisotropy assay, but the curve showed features of non-specific binding, not completely abolished by addition of EGTA (Fig. 7B). This was even more pronounced for XK-like1, which did not bind to $AtCaM_1$-Alexa^{488} (Fig. 7B).

A first explanation for the non-specific binding of TS2 and the absence of binding for Lox2 and XK-like1 to $AtCaM_1$-Alexa^{488} might be that Alexa^{488} bound on CaM hinders or prevents binding of TS2, Lox2 or XK-like1. We thus used competition experiments (not shown) using the NADK2-labelled peptide and unlabelled CaM as described in Fig. 6C. As no dissociation of the NADK2 peptide–CaM complex by an excess of TS2, Lox2 or XK-like1 could be observed we exclude that the non-specific binding (TS2) or absence of binding (Lox2 and XK-like1) displayed in Fig. 7B results from interference due to Alexa^{488} labeling of $AtCaM_1$. Strong overlay signals thus result either from non-specific interaction with $AtCaM_1$–HRP or from specific interaction requiring slow conformational changes (*i.e.* protein unfolding). These are features that have been overlooked in previous studies using CaM overlay assays.

In conclusion, the fluorescence anisotropy measurements showed a strong potential to obtain more quantitative information about the binding affinity of each candidate.

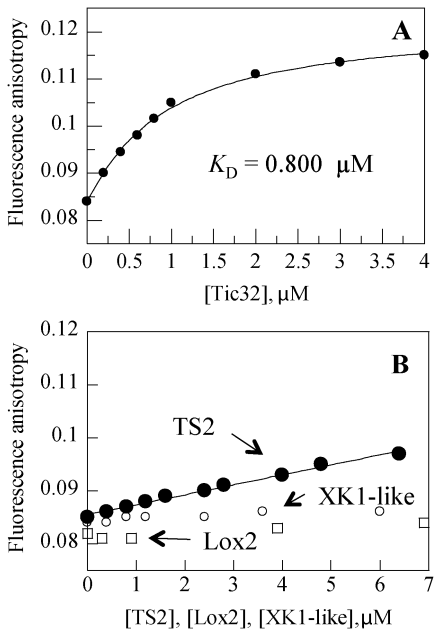

Fig. 7 Characterization of the CaM-binding affinity of some partners previously tested in the overlay assays: Tic32 (A), and TS2, Lox2 and XK1-like (B). Each protein was tested in the presence of $AtCaM_1$-Alexa^{488} (200 nM) and 300 μM $CaCl_2$. In the case of Tic32, the K_D is 0.8 μM, while TS2 shows non-specific binding features. All data points are the average fluorescence anisotropy values of two independent experiments. Experimental data were fitted using eqn (1).

Discussion

The chloroplast is essential for plant cell metabolism and functions, since it is the site where the photosynthetic reactions and the production of many metabolites such as lipids, pigments, hormones, amino acids and vitamins take place.[44] More and more evidence also indicates its contribution to cell defence mechanisms.[45,46] Understanding the signalling pathways associated with this cellular compartment is therefore a major objective of plant biology. One of the most important secondary messengers of eukaryotic cells is Ca^{2+}, whose signalling is transduced by many proteins and especially CaMs. The CaM family has been extensively duplicated in plants, thus making this network far more complex than in mammals.[19] Several CMLs contain N-terminal extensions.[15] According to prediction software, some of them might correspond to plastidial transit peptides, but high discrepancy is observed among the programs about the putative localization of these CMLs (Table S4, ESI†), and none of them has been experimentally proved to be addressed to the plastid. However, few plastidial proteins have been demonstrated to bind to at least one CaM isoform.[28,31,47] These findings have led to postulate a more general role of Ca^{2+}/CaM in controlling the chloroplast physiology.

In this work, we identified more than 200 putative CaM-binding partners using a proteomic approach based on affinity chromatography purifications and targeted to purified chloroplast subcompartments. Most of the CaM-binding partners retrieved from this study had never been shown to interact with CaM, and are involved in the main plastid functions, such as photosynthesis, amino acid synthesis, lipid and sugar metabolism, protein folding or DNA transcription. In order to validate a subset of these candidates, we optimized a standard semi-quantitative overlay assay and designed two fluorescence anisotropy assays to obtain quantitative data about the CaM-binding interaction even for proteins with yet unknown or with no catalytic activity.

The overlay assay[38,48] is a validation procedure commonly used in previously published studies on CaM-binding proteins.[10,28,31] With respect to other techniques such as Biacore, co-immunoprecipitation and pull-down, this test presents the advantage of being affordable and easy to perform. This technique was therefore chosen for a first validation step of a subset of 19 selected candidate proteins. A particular effort was made towards the optimization of the overlay technique in order to minimize the disadvantages due to protein transfer and the competition for CaM-binding among candidates. In particular, the semi-quantitative nature of the overlay approach required at least one positive (the N-terminal region of NADK2) and one negative control (Vipp1).

Our overlay assays confirmed the potential of the proteomics approach used during this work, as all the 19 tested candidates were shown to interact with CaM–HRP after 3 hours of incubation and in the presence of Ca^{2+}. However, a wide variety of signal intensities was observed under the different experimental conditions. This might indicate that the affinity for CaM of a protein linked to a solid support can vary according to the presence/absence of Ca^{2+} or the incubation time. The conformation of protein spotted on membranes is indeed difficult to predict, and protein conformational changes upon binding to membranes were previously reported.[49] These observations, and the semi-quantitative nature of the overlay assay, prompted us to use complementary techniques for direct measurements of the CaM-binding parameters for each candidate.

As great discrepancies between on and off rates measured using the Biacore instrument compared to values measured in solution were reported,[50] we designed fluorescence anisotropy assays for quantitative measurements. This technique not only allows following a complex formation–dissociation and the determination of K_Ds in solution, but also allows the testing of different conditions with any range of protein concentration, presence of substrates or inhibitors, and changes in buffer composition. Fluorescence anisotropy is therefore useful both for the validation of high through-put screening data and for the fine characterization of single protein–protein interactions.[51]

Fluorescence anisotropy has been firstly used in order to obtain the parameters of NADK2–CaM interaction. Two independent tests were designed. In the first case, the fluorescence anisotropy of the CaM-binding peptide of NADK2 conjugated with a TAMRA fluorescent probe was monitored upon binding to increasing concentrations of $AtCaM_1$. In the second case, we monitored the variations in the fluorescence anisotropy of $AtCaM_1$-$Alexa^{488}$ for the N-terminal region of NADK2, containing the CaM-binding peptide. Both measurements lead to calculate a Ca^{2+} dependent affinity of around 200 nM, thus confirming the reliability of the approach.

The same approach was subsequently used to investigate in more details some soluble candidates that showed different binding signals in the overlay assay. Quantitative information obtained using this technique appeared to be of great interest to understand the affinity of CaM for each candidate. In particular, a Ca^{2+}-dependent CaM affinity with a K_D value of around 1 μM was calculated for Tic32. In contrast, TS2 showed features of non-specific CaM-binding in solution, and this binding was not totally abolished by EGTA addition, as also observed in the overlay assay. No binding was observed for both Lox2 and XK-like, again despite the strong overlay signal of the latter.

On the basis of current knowledge, strong CaM-binding affinity is characterized by a K_D value ranging from 10 nM to 1 μM.[10] The K_D values obtained for Tic32 is within this range. This confirms the relevance of the Tic32–CaM interaction previously characterized.[28]

The overlay assay and the fluorescence anisotropy measurements were sometimes contradictory. A strong overlay signal was obtained for TS2 and XK-like1, but they did not bind to $AtCaM_1$-$Alexa^{488}$. These results suggest that, in the overlay assay, the protein interaction with the membrane might trigger changes in the protein conformation that might alter the CaM affinity of the protein with respect to the native protein state. Alternatively, specific conditions might be necessary to favour the complex formation in solution, such as the presence of the protein substrate, different pH or salt concentration. The flexibility of the fluorescence anisotropy measurements will allow more detailed studies on specific cases such as these ones or other candidates retrieved during our work.

Several membrane proteins gave a strong signal in the overlay assay. Among them, STN8[52] and CAS[26] are of great interest, because they both play a major role in the plant response to environmental stimuli[53–55] and because genetic and biochemical analysis using thylakoids suggests that CAS is phosphorylated by STN8.[56] The *in vitro* CaM-binding to STN8 and CAS suggests that a novel control level might exist in the regulation of main thylakoid functions (photo-acclimation and state transition). Another protein, RNAseJ, has recently been shown to be involved in RNA surveillance in the chloroplast.[57] Our data suggest that CaM might have a possible role in the control of transcription in this organelle. Finally, the strong binding of the mitochondrial ATPase γ subunit to $AtCaM_1$–HRP in the overlay assay is reminiscent of results obtained in yeast[58] showing that the F_0F_1ATP synthase inhibitor protein (IF1) binds to CaM and might therefore further support the role of CaM in the regulation of this protein complex. However, as all these recombinant proteins are insoluble, in depth quantitative characterization of their interaction with CaM will require the identification of the CaM-binding site prior to fluorescence anisotropy measurements using fluorescently labeled peptides, or the isolated and purified soluble domains containing the CaM-binding site, as performed during this study for NADK2.

From a methodological point of view, these results demonstrate that an optimized overlay screening is a useful technique for a preliminary validation of large-scale data of CaM partners. However, present results also show that the overlay signals may have different origins and hide a variety of different modes of interaction that need to be investigated one-by-one. Although fluorescence anisotropy is not widely exploited to investigate protein–protein interactions, this technique is highly valuable to get further insights into the characterization of protein–CaM interaction, thanks to its flexibility and versatility, and could be used to extend the validation proposed in this work to other candidates issued by this or other large-scale studies.

Conclusions

Our proteomic approach opens new perspectives on the control of Ca^{2+}/CaM in the chloroplast by the identification of more than 200 new CaM-binding candidates and the validation of a subset of them. We directly measured for the first time the affinity of NADK2 and Tic32 for CaM under soluble conditions. We also designed an optimized pipeline for the validation of CaM–candidate interactions by two different complementary strategies and established the fluorescence anisotropy as a

valuable technique for a quantitative investigation of protein–protein interactions.

Finally, the results presented here raise the question of the presence and identity of the CaM or CML isoforms that, in the chloroplast, control the targets identified during this work. Although several CMLs contain N-terminal extension similar to plastidial target sequences (Table S4, ESI†), up to now the presence of these proteins in higher plant chloroplasts was not reported.

Experimental procedures

Purification of chloroplasts and chloroplast envelope, stroma, and thylakoids from spinach and *Arabidopsis* leaves

Crude chloroplasts were obtained from 3–4 kg of spinach (*Spinacia oleracea* L) or 300–400 g of *Arabidopsis thaliana* leaves and purified by isopycnic centrifugation using Percoll gradients.[36,59] Purified intact chloroplasts were lysed in hypotonic medium, and envelope membranes were purified from the lysate by centrifugation in sucrose gradients. Spinach envelope enriched subfractions were obtained from purified intact spinach chloroplasts as previously described.[60]

Purification of CaM-binding proteins from *Arabidopsis* chloroplast sub-fractions

CaM-affinity purification was performed starting from *Arabidopsis* stroma and chloroplast membrane fractions (*i.e.* thylakoid and envelope membranes) or spinach envelope and stroma fractions.

For the stroma extract from *Arabidopsis* or spinach chloroplasts, 6 mg protein were solubilized in 6 mL of binding buffer (10 mM Tris–HCl pH 8, 150 mM NaCl, 1 mM Mg-acetate, 1 mM imidazole, 2 mM $CaCl_2$ and 0.1% (v/v) NP40) to reach a protein concentration of 1 mg mL^{-1}. This crude extract (fraction CE in Fig. 2A) was then incubated (rolling wheel) for two hours, at 4 °C, with 50 μL of CaM affinity resin (Stratagen) in the presence of 2 mM $CaCl_2$ (according to the manufacturer's instructions, 50 μL of CaM affinity resin has a binding capacity of 75–150 μg target proteins). After a centrifugation at 300*g* (2 minutes at 1800 rpm), the supernatant (fraction NB in Fig. 2A, *i.e.* proteins not bound to the matrix) was stored for further analyses. The matrix pellet was then washed three times (successive centrifugations at 300*g*) in 1 mL of binding buffer and corresponding supernatants were stored for further analyses (fractions W1 to W3 in Fig. 2A). Then, CaM-binding proteins were eluted from the matrix (fractions E1 to E10 in Fig. 2A, *i.e.* supernatants of successive centrifugations at 300*g*) in 10 fractions of 100 μL of elution buffer (10 mM Tris–HCl pH 8, 150 mM NaCl, 1 mM Mg-acetate, 1 mM imidazole, 2 mM EGTA and 0.1% (v/v) NP40). Each fraction (25 μL) was analyzed on an SDS-PAGE (12% acrylamide). Proteins were detected using silver staining. For the stroma extracts, fractions selected for further MS analyses were E1, E3 and E4 (Fig. 2A).

For the membrane extract from *Arabidopsis* chloroplasts or from the spinach envelope, 7 mg of chloroplast membrane proteins were solubilized (rolling wheel), for 45 minutes, at 4 °C in 4 mL of binding buffer (10 mM Tris–HCl pH 8.0, 150 mM NaCl, 1 mM Mg-acetate, 1 mM imidazole, 2 mM $CaCl_2$ and 0.1% (v/v) NP40) to reach a protein concentration of 1.75 mg mL^{-1} (fraction CE in Fig. 2B). This crude extract was then centrifuged, at 4 °C, for 1 hour at 50 000 rpm using a SW55 Ti rotor (300 000*g*). The supernatant (fraction SM in Fig. 2B, *i.e.* solubilized membrane proteins using 0.1% (v/v) NP40) was then incubated (rolling wheel), for two hours, at 4 °C, with 50 μL of calmodulin affinity resin (Stratagen) in the presence of 2 mM $CaCl_2$. After a centrifugation at 300*g* (2 minutes at 1800 rpm), the supernatant (fraction NB in Fig. 2B, *i.e.* proteins not bound to the matrix) was stored for further analyses. The matrix pellet was then washed four times (fraction W1 to W4 in Fig. 2B, *i.e.* supernatants of successive centrifugations at 300*g*) in 1 mL of binding buffer. Then, CaM-binding proteins were eluted from the matrix (fractions E1 to E9 in Fig. 2B, *i.e.* supernatants of successive centrifugations at 300*g*) in 9 fractions of 70 μL of elution buffer (10 mM Tris–HCl pH 8.0, 150 mM NaCl, 1 mM Mg-acetate, 1 mM imidazole, 2 mM EGTA and 0.1% (v/v) NP40). Each fraction (1 μL for CE, SM, NB and W1 to W4, and 25 μL for E1 to E9) was analyzed on an SDS-PAGE (12% acrylamide). Proteins were detected using silver staining. For the membrane extracts, fractions selected for further MS analyses were E3 and E4 (Fig. 2B).

Sample preparation for mass spectrometry analysis

Before mass spectrometry analyses, elution fractions (25 μL of fractions E1, E3 and E4 for the stroma and 10 μL of fractions E3 and E4 for the membranes) were loaded on a SDS-PAGE, and migration was stopped just between the stacking and the separating gels according to a previously described protocol[36] so that proteins were concentrated on a very thin band for further analyses. These discrete bands, containing all the proteins present in the eluted fractions, were detected in the SDS-PAGE gels using Coomassie blue staining. These protein bands were manually excised from the gels and washed several times by incubation in 25 mM NH_4HCO_3 for 15 min and then in 50% (v/v) acetonitrile containing 25 mM NH_4HCO_3 for 15 min. Gel pieces were then dehydrated with 100% acetonitrile and then incubated with 7% (v/v) H_2O_2/7% (v/v) formic acid for 15 min before being washed again with the destaining solutions described above. Modified trypsin (0.15 μg, Promega, sequencing grade) in 25 mM NH_4HCO_3 was added to the dehydrated gel bands for an overnight incubation at 37 °C. Peptides were then extracted from gel bands in three 15 min sequential extraction steps in 30 μL of 50% (v/v) acetonitrile, 30 μL of 5% (v/v) formic acid and finally 30 μL of 100% acetonitrile. The pooled supernatants were then dried under vacuum.

Mass spectrometry analysis and protein identification

For spinach samples the peptides were injected into a LC-Packings (Dionex) nanoLC system and first preconcentrated on a 300 μm × 5 mm PepMap C18 precolumn. The peptides were then eluted onto a C18 column (75 μm × 150 mm). The chromatographic separation used a gradient from solution A (5% (v/v) acetonitrile : 95% (v/v)

water : 0.1% (v/v) formic acid) to solution B (5% (v/v) acetonitrile : 95% (v/v) water : 0.1% (v/v) formic acid) over 60 min at a flow rate of 200 nL min^{-1}. The LC system was directly coupled to a QTOF Ultima mass spectrometer (Waters). MS and MS/MS data were acquired and processed automatically using MassLynx 3.5 software. Database searching was carried out using the MASCOT 2.3.01 program. Two protein databases were used: an updated compilation of SwissProt and Trembl (July 2010 version; 11 627 486 sequences) and the AGI protein database (TAIR V9; 30,899 sequences). Peptides showing a score higher than 40 were validated without any manual validation, and so were the proteins they identified. Peptides with scores higher than 20 and lower than 40 were checked manually. The remaining unassigned peptides were interpreted manually and internet MS-Pattern (http://prospector.ucsf.edu/) and Blast (http://www.ncbi.nlm.nih.gov/BLAST/) were used for protein identification.

For *Arabidopsis* samples the dried extracted peptides were resuspended in 5% (v/v) acetonitrile and 0.1% (v/v) trifluoroacetic acid and analysed by online nanoLC-MS/MS (Ultimate 3000, Dionex and LTQ-Orbitrap XL or VELOS Fischer Scientific). Peptide mixtures were loaded and desalted online in a reverse phase precolumn (Acclaim PepMap 100 C18, 5 μm bead size, 100 Å pore size, 5 mm × 300 μm) from LC Packings. They were resolved on a C18 column (Acclaim PepMap 100 C18, 3 μm bead size, 100 Å pore size, 15 cm × 75 μm). Peptides were separated using a 40 or 90 min-gradient with aqueous solvent A (2% ACN, 0.1% HCOOH) and solvent B (20% ACN, 0.1% HCOOH) developed as follows: 4–50% B in respectively 30 or 60 min, 50–90% B in 5 min, 90% B for 5 min, 90–4% B in 1 min and 4% B for 10 or 15 min. The full-scan mass spectra were measured from *m*/*z* 400 or 450 to 1600 or 1800. The LTQ-Orbitrap XL mass spectrometer was operated in the data-dependent mode. Briefly, a scan cycle was initiated with a full scan resolution set to 60 000 in the Orbitrap analyzer that was followed by MS/MS spectra of the most abundant ion for a period of 30 s and then excluding this ion for the followed fragmentations for the next 180 s. The activation type used was CID with a standard normalized collision energy set of 35%.

MS and MS/MS data were acquired using Xcalibur (Thermo Fischer Scientific) and processed automatically using Mascot Daemon software (version 2.3, Matrix Science). Consecutive searches against the TAIR V9 database were performed for each sample using Mascot 2.3.01 (Matrix Science). ESI-TRAP was chosen as the instrument, trypsin/P as the enzyme, and 2 missed cleavages were allowed. Precursor and fragment mass error tolerances were set, respectively, at 10 ppm and 0.8 Da. Peptide variable modifications allowed during the search were: acetyl (N-ter), dioxidation (M), oxidation (M) and trioxidation (C). The IRMa software[61] was used to filter the results: query homology threshold $p < 0.05$ and ion score cut-off 20. The filtered results were downloaded into a mass spectrometry identification database and a homemade tool was used for the compilation, grouping and comparison of the proteins from the different samples.

cDNA cloning

cDNA sequences of selected proteins were downloaded from the TAIR database (http://www.arabidopsis.org/) and transit peptide cleavage sites were identified using the ChloroP tool and by sequence comparison between homologous genes of other plant species with the BLAST tool of NCBI. The cDNA sequences corresponding to the mature proteins were cloned into pET15b, pET20b, pET28 or pET30 expression vectors (Novagen, Darmstadt, Germany). Proteins lacking a measurable catalytic activity were expressed with a Histidine tag which was not subsequently cleaved. All other proteins were expressed in their native form without the predicted chloroplast transit peptide sequence. Primer sequences, restriction enzymes used, the presence of the Histidine tag and the final sequence of each cloned protein are reported in Table S3 (ESI†). For NADK2, only the N-terminal region containing the CaM-binding sequence was cloned (amino acids 61–411). cDNAs were either amplified from an *Arabidopsis* cDNA library in pYES[62] or from a previously described *Arabidopsis* cDNA library.[63] Sequences of cloned cDNAs were verified by direct sequencing using T7 primers.

Protein expression

Colonies of transformed BL21 (DE3) Rosetta2 bacteria (Novagen, Darmstadt, Germany) grown on selective LB agar medium were transferred into 5 mL of LB medium supplemented with appropriate antibiotics and grown at 37 °C under agitation. Saturated cultures were transferred into 100 mL of the same medium and growth was continued until A_{600nm} reached 0.8. Protein expression was induced by addition of IPTG (0.4 mM) and growth was continued for 18 h at 20 °C. Pelleted bacteria were re-suspended in 3 mL of sonication buffer (20 mM Tris pH 8.0, 5 mM β-mercaptoethanol, 0.5 M NaCl, 5% (v/v) glycerol, 5 mM ε-aminocaproic acid and 1 mM benzamidine), and sonicated for 5 min at 4 °C on a Benson sonifier. Streptomycin sulfate (0.1% (w/v)) was added to precipitate DNA and the solution was centrifuged for 30 min at 30 000*g* at 4 °C. Protein expression and solubility were checked on Coomassie stained 12% acrylamide gels. Proteins were quantified by the method of Bradford[64] or, for pure proteins, by measuring protein absorbance at 280 nm using a Nanodrop 2000 (Thermo Scientific).

Protein purification of His-tagged soluble and insoluble proteins

Purification steps were carried out at room temperature on 2 mL of NiNTA resin (Quiagen). The column was equilibrated with 8 column volumes of buffer A (25 mM Tris pH 8.0, 0.5 M NaCl, 25 mM Imidazole). After loading the sample, the column was washed with 8 mL of buffer A followed by 8 mL of buffer B (25 mM Tris pH 8.0, 0.5 M NaCl, 50 mM imidazole). Elution was performed with 6 mL of buffer C (25 mM Tris pH 8.0, 0.5 M NaCl, 250 mM imidazole). Fractions containing the purified protein were pooled and dialyzed overnight at 4 °C in dialysis buffer (25 mM Tris pH 8.0, 1 mM DTT, 5% (v/v) glycerol). Prior to purification, insoluble proteins were solubilized in a urea-containing buffer as follows. Bacterial pellet was re-suspended

in 4 mL solubilization buffer (25 mM Tris pH 8.0, 0.5 M NaCl, 10 mM DTT, 5 mM ε-aminocaproic acid, 1 mM benzamidine), sonicated 5 min and centrifuged for 20 min at 14 000*g*. The pellet was washed three times in 4 mL of Triton buffer (25 mM Tris pH 8.0, 0.5 M NaCl, 1% (v/v) Triton X-100, 2 M urea) and, each time, centrifuged 10 min at 14 000*g*. The final pellet was resuspended in 5 mL of urea buffer (25 mM Tris pH 8.0, 0.5 M NaCl, 1% (v/v) Triton X-100, 8 M urea and 5 mM β-mercaptoethanol) and kept under agitation for 1 h before centrifugation for 20 min at 14 000*g* and recovery of the supernatant. For NiNTA purification, buffers B and C and dialysis buffer were supplemented with 5 mM β-mercaptoethanol and 6 M urea.

Purification of TS2

TS2 purification was carried out as previously described (Curien *et al.* 2009, Supplementary data).[65]

Purification of DAHPS3

The position of the transit peptide cleavage site of DAHPS3 (At1g22410) was defined by analogy with the N-terminus of potato DAHPS validated by N-terminal sequencing.[66] The codon corresponding to Ser51 in the predicted sequence of the full-length protein was replaced by an initiating methionine. The cDNA sequence corresponding to the predicted mature protein was amplified by PCR using an *Arabidopsis thaliana* cDNA library[62] (see Table S3, ESI†). Transformed bacteria were plated on LB agar supplemented with carbenicillin (100 μg mL^{-1}) and chloramphenicol (34 μg mL^{-1}) and grown overnight at 37 °C. Colonies were transferred into 15 mL of LB media supplemented with the antibiotics and growth was carried out at 37 °C. Saturated cultures were transferred into 800 mL LB media supplemented with the antibiotics and growth was continued for 3 hours at 37 °C. IPTG was added (0.4 mM) when $A_{600\ nm}$ of the culture reached 0.6. Growth was continued for 18 hours at 20 °C. Bacteria were collected by centrifugation (15 minutes, 2000*g*, 4 °C), re-suspended in a lysis buffer (50 mM Hepes–KOH pH 7.5, 3 mM $MnCl_2$, 1 mM DTT, 20% (v/v) glycerol, 5 mM aminocaproic acid and 1 mM benzamidine, 10 mL per litre culture). Bacteria were sonicated for 20 minutes at 4 °C on a Vibracell disruptor. Streptomycin sulfate (0.1% (w/v)) was added to the sonicator in order to precipitate DNA and the solution was centrifuged for 35 minutes at 30 000*g* at 4 °C. Purification steps were carried out at room temperature. The supernatant (600 mg) was loaded on an anion exchange resin (DEAE EMD 650(M) column, 26 × 260 mm^2) equilibrated in 50 mM Hepes–KOH, pH 7.5, 3 mM $MnCl_2$, 1 mM DTT, 20% (v/v) glycerol. DAHPS3 was eluted by a linear gradient of KCl in the same buffer (elution at 150 mM KCl). The protein was concentrated on a 30 K Amicon Ultra centrifugal filter (Millipore). Concentrated DAHPS fraction was loaded on a HiPrep 16/60 Sephacryl S-200 column (Pharmacia) equilibrated with 20 mM KPi, pH 7.5, 100 mM KCl, 1 mM DTT and 10% (v/v) glycerol. Pure protein in the elution buffer was concentrated using centricon devices up to 50–200 μM (on a monomer basis), aliquoted, quickly frozen in N_2 and stored at −80 °C for several months without any loss of activity.

DAHPS activity (30 nM protein) was measured at 25 °C in a quartz cuvette (150 μL) in the presence of Hepes–KOH, pH 8.0, 500 μM $MnCl_2$ and 10% (v/v) glycerol with the substrates phosphoenolpyruvate (0–300 μM) and erythrose 4-phosphate (0–300 μM). The reaction was initiated by the addition of erythrose 4-phosphate and followed by measuring the decrease in absorbance at 232 nm due to phosphoenolpyruvate consumption.

Purification of Tic32

The Tic32 cDNA sequence was cloned into the pET20b vector and the recombinant protein produced without a tag (see Table S3, ESI† for the primer sequence and other cloning details). Tic32 activity was followed by measuring formazan formation at 550 nm in the presence of 10 mM Tris, pH 8.0, 10 μg lysophosphatidyl choline, 100 μM NADPH and 100 μM nitroblue tetrazolium.[28] The protein extract from induced BL21(DE3)Rosetta2 bacteria was prepared as indicated above from a 4L-culture and purification was carried out at room temperature. The protein extract (0.6 g) was loaded on 130 mL of DEAE EMD 650(M) resin (Merk, Darmstadt, Germany) in a XK 26 column (Amersham Pharmacia) equilibrated with 50 mM Hepes, pH 7.5, 1 mM DTT, 1 mM EDTA, 10% (v/v) glycerol. Tic32 protein eluted in the pass through (60 mg) was loaded on a 10 mL column containing SP Sepharose high performance resin equilibrated in the same buffer. Proteins were eluted with a KCl gradient (0 to 0.5 M KCl, 300 mL). Tic32 containing fractions eluted at 250 mM KCl (36 mS) were concentrated on a 10 K Amicon Ultra centrifugal filter (Millipore) and loaded (20 mg) on a HiPrep 16/60 Sephacryl S-200 column (Pharmacia) equilibrated with 20 mM Hepes, pH 7.5, 200 mM KCl and 10% (v/v) glycerol. Pure protein was concentrated on a 10 K Amicon Ultra centrifugal filter (Millipore).

Purification of $AtCaM_1$

The $AtCaM_1$ (At5g37780) cDNA sequence was cloned into the pET15b expression vector without a tag (see Table S3, ESI† for the primer sequence and other cloning details). The protein extract from induced recombinant bacteria was loaded on 130 mL of DEAE EMD 650(M) resin (Merk, Darmstadt, Germany) in a XK 26 column (Amersham Pharmacia) equilibrated with 50 mM Hepes, pH 7.5, 1 mM EDTA, and 1 mM DTT. Proteins were eluted with a linear gradient of KCl buffer. $AtCaM_1$ containing fractions were pooled and loaded on a HiPrep 16/60 Sephacryl S-200 column (Amersham Pharmacia) equilibrated with 20 mM Hepes, pH 7.5, 100 mM KCl, 1 mM DTT. $AtCaM_1$ containing fractions were pooled and concentrated on a 3K concentrator (Amicon Ultra centrifugal filters, Millipore), and stored as aliquots at −80 °C.

HRP and $Alexa^{488}$ conjugations

HRP conjugation was carried out on 1 mg of purified $AtCaM_1$ by using the EZ-Link Plus Activated Conjugation Kit Peroxidase (ThermoScientific, Rockford, IL) at pH 7.2 following the manufacturer's instructions. We took advantage of the presence of a single Cys in $AtCAM_1$ to label the protein with a C5-maleimide $Alexa^{488}$ fluorescent probe. Labeling of 8 nmol of $AtCaM_1$ was performed by incubating the protein with a 7-fold

molar excess of C5-maleimide-Alexa^{488} from a 20 mM stock in dimethyl sulfoxyde (Molecular probes®, Invitrogen) for 45 min at room temperature in 10 mM Hepes, pH 7.5, 250 μM Tris(2-carboxyethyl)phosphine and 1 mM EDTA in a final volume of 200 μL. The labeled protein was separated from the free probe by gel filtration chromatography (G25 (M) resin, 1 × 30 cm^2) equilibrated with a buffer containing 10 mM Hepes, pH 7.5, 200 mM KCl and 1 mM EDTA and concentrated up to 40 μM in the same buffer.

CaM-binding assay

100 pmol of each purified candidate protein were spotted onto Whatman Protran nitrocellulose blotting membranes dried and independently incubated for 1 h in 8 mL of assay buffer (50 mM Tris–HCl, pH 7.5, 150 mM NaCl, 1% (w/v) BSA, 1% (v/v) Brij35) either in the presence of 1 mM $CaCl_2$ or 5 mM EGTA. $AtCaM_1$–HRP (250 pmol, of $AtCaM_1$–HRP (30 nM)) was added and incubation was extended for either 3 h or 15 min. After three washes with the assay buffer (10 min each), bound $AtCaM_1$–HRP was visualized using an ECL detection system according to the manufacturer's instructions (GE Healthcare Life Sciences, Pittsburgh, PA). For each candidate CaM-binding protein, the intensity of the signal was compared to that of NADK2 (positive control) and Vipp1 (negative control) either in the presence of Ca^{2+} or EGTA.

Fluorescence anisotropy measurements

Assays were carried out using a MOS-450 spectrometer (BioLogic, Inc.) in a 150 μL quartz cuvette, under controlled temperature (25 °C). Assay conditions were: 10 mM Hepes, pH 7.5, 200 mM KCl, and 300 μM $CaCl_2$.

Interaction of $AtCaM_1$-Alexa^{488} (200 nM) with an unlabeled NADK2 N-terminal domain (Nter-NADK2) was followed by the increase in fluorescence anisotropy with excitation at 488 nm and emission at 522 nm. Nter-NADK2 concentration was increased by incremental addition of small volumes of concentrated solutions.

Interaction of the NADK2 TAMRA labeled CaM-binding peptide (IYVHSKEGVWRTSAMVSRWK, 50 nM, Peptide Specialty laboratories, GmbH, Heidelberg) with unlabeled $AtCaM_1$ was followed by the increase in fluorescence anisotropy with excitation at 546 nm and emission at 579 nm. TAMRA-peptide powder was diluted in water with 30% (v/v) dimethylformamide to a final concentration of 3.6 mM and stored at −20 °C. Before use, stock solutions were diluted to a concentration of 5 μM in 100 mM Hepes, pH 7.5 and 200 mM KCl, supplemented with 5% (v/v) dimethylformamide. Peptide concentration was measured spectrophotometrically (ε_{540nm} = 55 000 M^{-1} cm^{-1}). Unlabeled $AtCaM_1$ concentration was increased progressively by addition of small volumes of concentrated solutions. In a control assay, the TAMRA probe alone did not show any affinity for $AtCaM_1$.

Under our experimental conditions, the concentration of complexes formed is significant as compared with the total protein concentration, a fact that needs to be accounted for during data analysis. Assuming the simple reaction:

$$CaM/Ca^{2+} + Protein \Leftrightarrow CaM/Ca^{2+} - Protein,$$

the relation between anisotropy, K_d and labeled and unlabeled protein concentrations is given by eqn (1).[67] In all experiments the curves were analyzed using Kaleidagraph software (Synergy Software, Reading, PA) and fitted according to eqn (1).

$$r = r_f + (r_b - r_f)\left(\frac{(K_D + [L] + [U]) - \sqrt{(K_D + [L] + [U])^2 - 4[L][U]}}{2[L]}\right) \quad (1)$$

Where r is the anisotropy, r_f is the anisotropy of the free labeled $AtCaM_1$-Alexa^{488} or free TAMRA labeled peptide, r_b is the maximal anisotropy of the bound labeled protein (or peptide), K_D is the dissociation constant, $[L]$ is the total concentration of labeled species and $[U]$ the total concentration of unlabeled species.

List of abbreviations

CaM	calmodulin
CML	CaM-like
NADK2	NAD kinase 2

Acknowledgements

This study received financial support from the French National Research Agency (ANR-2010-BLAN-1610-01 Chloro-Pro) and by the Labex GRAL (Alliance Grenobloise pour la Biologie Structurale et Cellulaire Intégrées: ANR-10-LABEX-04). E.D.A. was funded by a PhD fellowship from the CEA DSV (IRTELIS International Program). L.M. was funded by the Labex GRAL.

References

1 K. A. Skelding, J. A. Rostas and N. M. Verrills, *Cell Cycle*, 2011, **10**, 631–639.
2 M. Zik, T. Arazi, W. A. Snedden and H. Fromm, *Plant Mol. Biol.*, 1998, **37**, 967–975.
3 M. Sola-Penna, D. Da Silva, W. S. Coelho, M. M. Marinho-Carvalho and P. Zancan, *IUBMB Life*, 2010, **62**, 791–796.
4 S. Shao and R. S. Hegde, *Cell*, 2011, **147**, 1576–1588.
5 R. H. Kretsinger and C. E. Nockolds, *J. Biol. Chem.*, 1973, **248**, 3313–3326.
6 P. Cohen, *Annu. Rev. Biochem.*, 1989, **58**, 453–508.
7 R. K. Sharma, S. B. Das, A. Lakshmikuttyamma, P. Selvakumar and A. Shrivastav, *Int. J. Mol. Med.*, 2006, **18**, 95–105.
8 J. Haiech, E. Audran, M. Fève, R. Ranjeva and M.-C. Kilhoffer, *Biochimie*, 2011, **93**, 2029–2037.
9 M. Mikhaylova, J. Hradsky and M. R. Kreutz, *J. Neurochem.*, 2011, **118**, 695–713.
10 D. J. O'Connell, M. C. Bauer, J. O'Brien, W. M. Johnson, C. A. Divizio, S. L. O'Kane, T. Berggard, A. Merino, K. S. Akerfeldt, S. Linse and D. J. Cahill, *Mol. Cell. Proteomics*, 2010, **9**, 1118–1132.
11 T. Berggard, G. Arrigoni, O. Olsson, M. Fex, S. Linse and P. James, *J. Proteome Res.*, 2006, **5**, 669–687.

12 X. Shen, C. A. Valencia, J. Szostak, B. Dong and R. Liu, *Proc. Natl. Acad. Sci. U. S. A.*, 2005, **102**, 5969–5974.
13 X. Shen, C. A. Valencia, W. Gao, S. W. Cotten, B. Dong, B.-c. Huang and R. Liu, *Cell Calcium*, 2008, **43**, 444–456.
14 I. S. Day, V. S. Reddy, G. Shad Ali and A. S. Reddy, *Genome Biol.*, 2002, **3**, 1-0056.
15 E. McCormack and J. Braam, *New Phytol.*, 2003, **159**, 585–598.
16 R. Kushwaha, A. Singh and S. Chattopadhyay, *Plant Cell*, 2008, **20**, 1747–1759.
17 L. Liang, S. Flury, V. Kalck, B. Hohn and J. Molinier, *Plant Mol. Biol.*, 2006, **61**, 345–356.
18 F. Chigri, S. Flosdorff, S. Pilz, E. Koelle, E. Dolze, C. Gietl and U. C. Vothknecht, *Plant Mol. Biol.*, 2012, **78**, 211–222.
19 A. Perochon, D. Aldon, J. P. Galaud and B. Ranty, *Biochimie*, 2011, **93**, 2048–2053.
20 S. C. Popescu, G. V. Popescu, S. Bachan, Z. Zhang, M. Seay, M. Gerstein, M. Snyder and S. P. Dinesh-Kumar, *Proc. Natl. Acad. Sci. U. S. A.*, 2007, **104**, 4730–4735.
21 G. S. Ali, V. S. Reddy, P. B. Lindgren, J. L. Jakobek and A. S. N. Reddy, *Plant Mol. Biol.*, 2003, **51**, 803–815.
22 N. A. Al-Quraan, R. D. Locy and N. K. Singh, *Plant Physiol. Biochem.*, 2010, **48**, 697–702.
23 T. N. Davis, M. S. Urdea, F. R. Masiarz and J. Thorner, *Cell*, 1986, **47**, 423–431.
24 J. Bussemer, F. Chigri and U. C. Vothknecht, *FEBS J.*, 2009, **276**, 4294–4304.
25 J. Q. Sai and C. H. Johnson, *Plant Cell*, 2002, **14**, 1279–1291.
26 S. Weinl, K. Held, K. Schlucking, L. Steinhorst, S. Kuhlgert, M. Hippler and J. Kudla, *New Phytol.*, 2008, **179**, 675–686.
27 D. Petroutsos, A. Busch, I. Janssen, K. Trompelt, S. V. Bergner, S. Weinl, M. Holtkamp, U. Karst, J. Kudla and M. Hippler, *Plant Cell*, 2011, **23**, 2950–2963.
28 F. Chigri, F. Hormann, A. Stamp, D. K. Stammers, B. Bolter, J. Soll and U. C. Vothknecht, *Proc. Natl. Acad. Sci. U. S. A.*, 2006, **103**, 16051–16056.
29 M. F. Chai, Q. J. Chen, R. An, Y. M. Chen, J. Chen and X. C. Wang, *Plant Mol. Biol.*, 2005, **59**, 553–564.
30 W. L. Turner, J. C. Waller, B. Vanderbeld and W. A. Snedden, *Plant Physiol.*, 2004, **135**, 1243–1255.
31 V. S. Reddy, G. S. Ali and A. S. N. Reddy, *J. Biol. Chem.*, 2002, **277**, 9840–9852.
32 N. A. Durso and R. J. Cyr, *Plant Cell*, 1994, **6**, 893–905.
33 T. B. Yang and B. W. Poovaiah, *Biochem. Biophys. Res. Commun.*, 2000, **275**, 601–607.
34 V. S. Reddy and A. S. N. Reddy, *Phytochemistry*, 2004, **65**, 1745–1776.
35 B. Seraphin, E. Puig, E. Bouveret, B. Rutz and F. Caspary, in *Protein–Protein interactions: a molecular cloning manual*, ed. E. Golemis, Cold Spring Harbor, NY, 2002, pp. 313–328.
36 M. Ferro, D. Salvi, S. Brugiere, S. Miras, S. Kowalski, M. Louwagie, J. Garin, J. Joyard and N. Rolland, *Mol. Cell. Proteomics*, 2003, **2**, 325–345.
37 M. Ferro, S. Brugiere, D. Salvi, D. Seigneurin-Berny, M. Court, L. Moyet, C. Ramus, S. Miras, M. Mellal, S. Le Gall, S. Kieffer-Jaquinod, C. Bruley, J. Garin, J. Joyard, C. Masselon and N. Rolland, *Mol. Cell. Proteomics*, 2010, **9**, 1063–1084.
38 M. Kato, N. Nagasaki-Takeuchi, Y. Ide and M. Maeshima, *Plant Cell Physiol.*, 2010, **51**, 366–379.
39 D. H. O'Day, *Cell. Signalling*, 2003, **15**, 347–354.
40 O. Delumeau, M. Renard and F. Montrichard, *Plant, Cell Environ.*, 2000, **23**, 1267–1273.
41 M. Graindorge, C. Giustini, A. C. Jacomin, A. Kraut, G. Curien and M. Matringe, *FEBS Lett.*, 2010, **584**, 4357–4360.
42 S. Abel, T. Savchenko and M. Levy, *BMC Evol. Biol.*, 2005, **5**, 72.
43 J. R. Lakowicz, in *Principles of fluorescence spectroscopy*, ed. S. Science, New york, 2006, ch. 10–12.
44 N. Rolland, G. Curien, G. Finazzi, R. Kuntz, E. Maréchal, M. Matringe, S. Ravanel and D. Seigneurin-Berny, *Annu. Rev. Genet.*, 2012, **46**, 233–264.
45 M. Sierla, M. Rahikainen, J. Salojarvi, J. Kangasjarvi and S. Kangasjarvi, *Antioxid. Redox Signaling*, 2013, DOI: 10.1089/ars.2012.5016.
46 S. Kangasjarvi, J. Neukermans, S. Li, E. M. Aro and G. Noctor, *J. Exp. Bot.*, 2012, **63**, 1619–1636.
47 J. M. Anderson and M. J. Cormier, *Biochem. Biophys. Res. Commun.*, 1978, **84**, 595–602.
48 G. R. Slaughter and A. R. Means, in *Methods Enzymol*, ed. P. M. C. Anthony and R. Means, Academic Press, 1987, vol. 139, pp. 433–444.
49 M. J. Hubbard and C. B. Klee, *J. Biol. Chem.*, 1987, **262**, 15062–15070.
50 L. Nieba, A. Krebber and A. Pluckthun, *Anal. Biochem.*, 1996, **234**, 155–165.
51 R. Dagher, S. Peng, S. Gioria, M. Fève, M. Zeniou, M. Zimmermann, C. Pigault, J. Haiech and M.-C. Kilhoffer, *Biochim. Biophys. Acta*, 2011, **1813**, 1059–1067.
52 V. Bonardi, P. Pesaresi, T. Becker, E. Schleiff, R. Wagner, T. Pfannschmidt, P. Jahns and D. Leister, *Nature*, 2005, **437**, 1179–1182.
53 S. Reiland, G. Finazzi, A. Endler, A. Willig, K. Baerenfaller, J. Grossmann, B. Gerrits, D. Rutishauser, W. Gruissem, J. D. Rochaix and S. Baginsky, *Proc. Natl. Acad. Sci. U. S. A.*, 2011, **108**, 12955–12960.
54 H. Nomura, T. Komori, S. Uemura, Y. Kanda, K. Shimotani, K. Nakai, T. Furuichi, K. Takebayashi, T. Sugimoto, S. Sano, I. N. Suwastika, E. Fukusaki, H. Yoshioka, Y. Nakahira and T. Shiina, *Nat. Commun.*, 2012, **3**, 926.
55 M. Terashima, D. Petroutsos, M. Hudig, I. Tolstygina, K. Trompelt, P. Gabelein, C. Fufezan, J. Kudla, S. Weinl, G. Finazzi and M. Hippler, *Proc. Natl. Acad. Sci. U. S. A.*, 2012, **109**, 17717–17722.
56 J. P. Vainonen, Y. Sakuragi, S. Stael, M. Tikkanen, Y. Allahverdiyeva, V. Paakkarinen, E. Aro, M. Suorsa, H. V. Scheller, A. V. Vener and E. M. Aro, *FEBS J.*, 2008, **275**, 1767–1777.
57 R. E. Sharwood, M. Halpert, S. Luro, G. Schuster and D. B. Stern, *RNA*, 2011, **17**, 2165–2176.
58 S. Contessi, F. Haraux, I. Mavelli and G. Lippe, *J. Bioenerg. Biomembr.*, 2005, **37**, 317–326.

59 R. Douce and J. Joyard, in *Methods in Chloroplast Molecular Biology*, Elsevier, Amsterdam, 1982, pp. 239–256.
60 M. A. Block, A. J. Dorne, J. Joyard and R. Douce, *J. Biol. Chem.*, 1983, **258**, 3273–3280.
61 V. Dupierris, C. Masselon, M. Court, S. Kieffer-Jaquinod and C. Bruley, *Bioinformatics*, 2009, **25**, 1980–1981.
62 S. J. Elledge, J. T. Mulligan, S. W. Ramer, M. Spottswood and R. W. Davis, *Proc. Natl. Acad. Sci. U. S. A.*, 1991, **88**, 1731–1735.
63 S. Miras, D. Salvi, M. Ferro, D. Grunwald, J. Garin, J. Joyard and N. Rolland, *J. Biol. Chem.*, 2002, **277**, 47770–47778.
64 M. M. Bradford, *Anal. Biochem.*, 1976, **72**, 248–254.
65 G. Curien, O. Bastien, M. Robert-Genthon, A. Cornish-Bowden, M. L. Cardenas and R. Dumas, *Mol. Syst. Biol.*, 2009, **5**, 271.
66 J. Zhao, L. M. Weaver and K. M. Herrmann, *Planta*, 2002, **1**, 180–186.
67 L. Blanchoin and T. D. Pollard, *J. Biol. Chem.*, 1999, **274**, 15538–15546.

Annex IV

Advanced characterization of the mutant line Salk_122250

A.1- *nadk2* mutant line: genotyping and phenotyping

The T-DNA mutant nadk2 line "Salk_122250" was purchased from the SALK institute. Chai et al (2005) previously verified by southern blot that the insertion is located on a unique locus in the second exon of the gene At1g21640. The phenotypical analysis of this mutant revealed that it was viable but chlorotic and smaller with respect to wt plants. They produced few seeds and leaves and a shorter shoots. Chlorophyll content was reduced and impairment in other pigments was observed. Takahashi et al (2006) reported also that the non-photochemical quenching of this line was higher than in the WT at 50 µE.

We seeded them directly on soil and harvested the new generation of seeds that was supposed to contain $1/4^{th}$ of homozygous mutant plants.

Our first assays of growing these mutant plants revealed that they are extremely weak and prone to die during the first days. In order to maximize the chances of survival, the pool of seeds containing WT, heterozygous and mutant plants was seeded on MS-medium supplemented with sucrose, then transferred on soil after two weeks, in short day (8:16 light/dark period) and low light intensity (40 µE).

To identify mutant plants at an early stage (2-4 leaves), we compared their F_v/F_m parameter with that of WT plants, thanks to a camera device that allows *in vivo* measurements. When chlorophyll is excited by light, part of the absorbed energy is re-emitted as red fluorescence when the chlorophyll electron goes back to its fundamental level. By applying a saturating flash of actinic (photosynthetic) light to dark-adapted plants, the fluorescence emitted by PSII goes from its basal level (F_0) to its maximum (F_m). The ratio F_v/F_m, *i.e.* $(F_m-F_0)/F_m$ gives therefore the value of the maximal quantum efficiency of the photosystem II (PSII) in the observed plant/leaf. In general, for all plant species this value is approximately 0.8 (Maxwell and Johnson, 2000). A lower value denotes photoinhibition, due to damages on the photosynthetic apparatus. The observation of our two-week old plants allowed identifying some plants with a F_v/F_m value of approximately 0.6. A low F_v/F_m value for homozygous nadk2 plants was also previously reported (Takahashi et al, 2006) and was therefore used as a screening method

for the isolation of mutant plants (**Fig. A.1**). These plants were transferred on soil after two more weeks with some WT plants kept as control. A high number of these putative mutant plants died soon after the transfer.

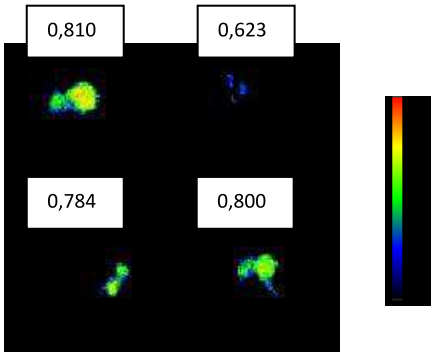

Fig. A.1 Four plants at the cotyledon stage observed for their F_v/F_m value with an *in vivo* camera device. The upper left plants showed a F_v/F_m value denoting low chlorophyll fluorescence and was selected as a putative mutant plant.

At four weeks, the remaining putative mutant plants were extremely small and chlorotic with respect to WT plants. **Fig. A.2** shows the phenotype of 6 weeks-old wt and mutant plants. Even if mutant plants were able to develop new leaves, their number was drastically reduced with respect to wt plants and also their size was compromised. The radical apparatus of these mutants was also remarkably underdeveloped (not shown). None of them was able to produce seeds or flowers.

Fig. A.2 Six weeks old WT (left) and nadk2 (right) Arabidopsis plants grown in low light conditions (40 µE, 8L/16D light cycle).

F_v/F_m measurements were repeated several times during the growth of the plant and spectroscopic observations were performed on 4 week-old plants. In order to confirm the mutant homozygous genotype of these plants, DNA was extracted from the remaining leaves and two

control PCRs were performed (**Fig. A.3**; see **Materials and Methods** for further detail about the primers and the PCR conditions).

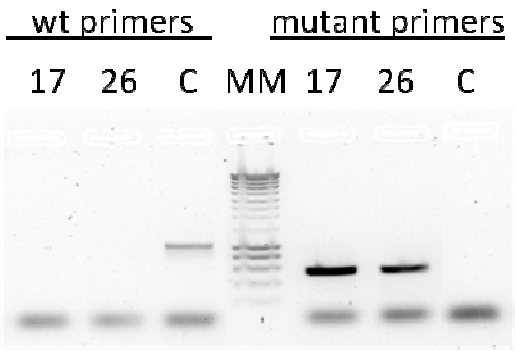

Fig. A.3 Genotyping by PCR of nadk2 plants. 17 and 26 are the number of two muntant plants. C is a control, WT plant.

A.2- Fluorescence induction curves show a block of linear electron transfer downstream PSI

Six-weeks old plants grown on soil were used for spectroscopic and fluorescence experiments, following the protocol described in Trouillard et al, 2012.

Firstly, we observed the fluorescence induction curve of nadk2 and WT plants. To do so, we observed the variation of red fluorescence emitted by dark-adapted leaves as a function of time during a series of light pluses. **Fig. A.4** represents what can be observed in a WT leaf in normal conditions. The saturation curve can be divided in three parts. The first part (in pink in the image) represents a delay that is attributed to the reduction of PSI acceptors (Ferredoxin and NADP). The second part of the curve (in green in **Fig. A.4**) reflects the reduction of the PSII acceptors (the plastoquinon pool). Finally, an additional saturating pulse is applied, in order to reach the F_m value that will be used to calculate the F_v/F_m parameter (Maxwell and Johnson, 2000).

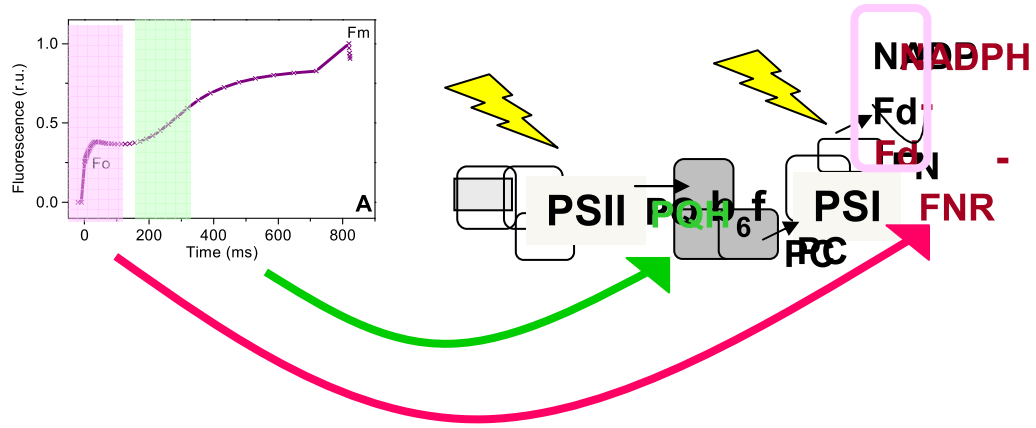

Fig. A.4 Schematic representation of the fluorescence induction curve of a WT leaf (Breyton et al, 2006). The first (pink) part of the curve reflects the delay due to the reduction of the acceptors of PSI; the second (green) is due to reduction of the PSII acceptors.

Fig. A.5 displays the evolution of the F_v/F_m parameter for wt and nadk2 leaves as a function of time during the fluorescence induction kinetics. WT plants reach the maximum fluorescence level (F_m) after approximately 350 ms after illumination. For nadk2 plants, this level is reached earlier, at approximately 200 ms. In addition, the delay phase observed in wt plants at approximately 50-100 ms is almost abolished in mutant plants. The absence of this plateau can be ascribed to a faster reduction of its electron acceptors due to a block of the linear electron flow downstream PSI.

These results suggest impairment in the photosynthetic apparatus of dark-adapted mutant plants with a partial block located downstream PSI.

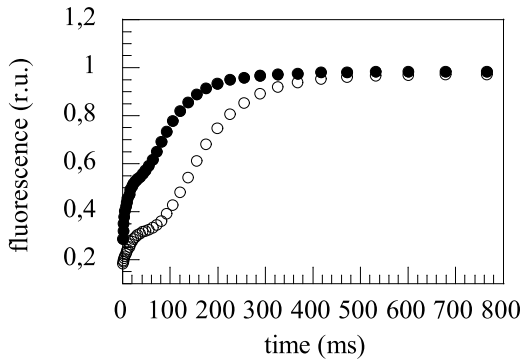

Fig. A.5 Fluorescence induction curve of nadk2 (balck dots) and WT (white dots) leaf measured at 40 µE.

A.3- Comparison of the electron transfer rate of PSII in WT and mutant plants

The electron transfer rate of PSII measures the number of electrons that pass through PSII per second at a certain light intensity. It can be calculated as the quantum yield of PSII (Φ_{PSII}) multiplied by the PSII photochemical rate constant.

To calculate Φ_{PSII}, we performed several fluorescence kinetics of nadk2 and WT dark-adapted leaves at different light intensities. Kinetics were similar to that reported in the scheme of **Fig. A6** and consisted of a series of illuminations of dark-adapted leaves with a series of saturation light pulses during continuous actinic light illumination. The Φ_{PSII} parameter was then calculated as $(F_m'-F_t)/F_m'$, and divided by the photochemical rate constant (*i.e.* the time necessary to reduce 2/3 of the PSII acceptors, Maxwell and Johnson, 2000).

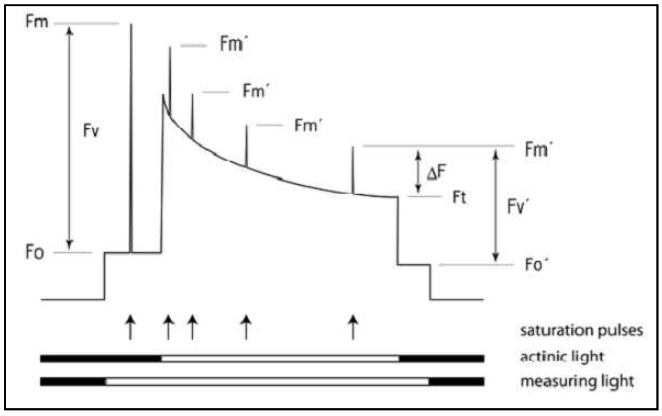

Fig. A6 Schematic representation of the fluorescence curves obtained to calculate Φ_{PSII}. From Minagawa, 2005. Schematic representation of the fluorescence measurements performed to study the PSII quantum efficiency. F_0: minimum fluorescence value in dark-adapted leaves; F_m: maximum fluorescence value in dark-adapted leaves; F_v: F_m-F_0; F_m': maximum fluorescence value in the presence of actinic (photosynthetic) light; F_0': minimum fluorescence value in the presence of actinic light; F_t: steady-state yield of fluorescence in the light; F_v': F_m'-F_0'.

The ETR values calculated at several light intensities are reported in **Fig. A7**. It can be observed that ETR increases by increasing the light intensity, up to reaching a plateau at approximately 12/s. Mutant leaves display a completely different phenotype, as the ETR is always extremely lower and at approximately 1/s at all light intensities tested.

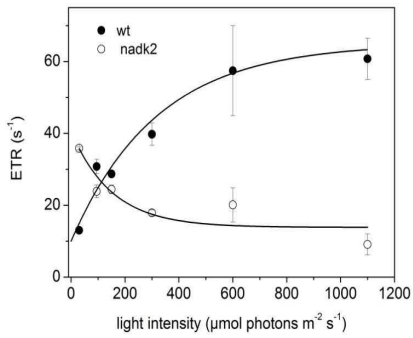

Fig. A7 ETR of PSII of WT (white dots) and nadk2 (black dots) leaves at several light intensities.

A.3- Cyclic electron flow of WT and nadk2 plants

Electrons that are introduced in the photosynthetic machinery can have two different fates: either they pass through the linear path and are transferred to NADP, to be then used for metabolic reducing reactions, or they are deviated from PSI back to Cyt-b_6f. This second pathway is called cyclic electron flow (CEF, see scheme of **Fig. A8**) and allows generating additional proton gradient that can increase the ATP production, without providing additional NADPH.

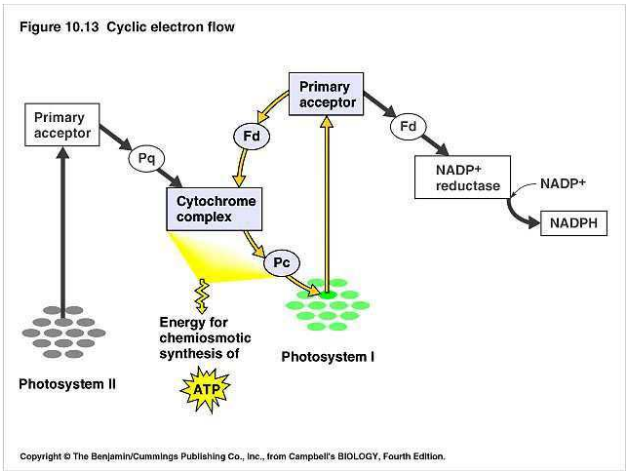

Fig. A8 Schematic representation of the linear (gray arrows) and cyclic (yellow arrows) electron flow of photosynthesis. Pq: plastoquinon pool; Pc: plastocyanine; Fd: ferredoxin.

To evaluate the contribution of CEF in WT with respect to mutant plants, we observed the variation in the oxidation state of P700, the primary acceptor of PSI, as previously described (Joliot and Joliot, 2006, Breyton et al, 2006).

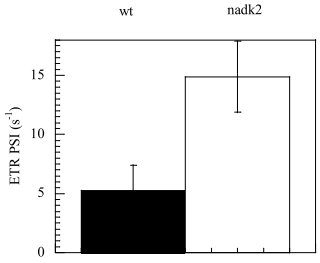

Fig. A.9 Electron transfer rate of PSI due to CEF in several conditions for wt (white bars) and mutant (black bars) leaves. Dark: dark-adapted leaves upon illumination with a far-red source, fr: leaves preflashed with far red light and then kept in dark for 1 minute, pulse: leaves pre-illuminated with green light for five minutes and then kept in the dark for one additional minute.

If compared to WT plants, it can be observed (**Fig. A.9**) that nadk2 plants displayed higher values of CEF. These results are consistent with a higher passage of electrons between PSI and cyt-b_6f due to cyclic electron flow that might be induced by lack of NADP.

A.4- Non-photochemical quenching

Plant adaptation mechanisms that are used to cope with high light stress conditions include: *i)* state transition (*i.e.* the transfer of PSII antenna complex to PSI, in order to minimize the linear electron flow, named qE), *ii)* thermal inactivation of the PSII antenna complex (qT) and *iii)* photoinhibition due to dismantling of the PSII (qI). These mechanisms are overall known as non-photochemical quenching (NPQ). NPQ can be measured as fluorescence kinetics as the one illustrated in **Fig. A.10**. In the presence of only weak measuring light the minimal fluorescence (F_0) is seen. When a saturating light pulse is given, the photosynthetic light reactions are saturated and fluorescence reaches its maximum level (F_m'). Upon continuous illumination with moderately excess light (750 µmol photons m^2 s^{-1}; growth light was 130 mmol photons m^2 s^{-1}), a combination of qP (photochemical quelching) and NPQ lowers the fluorescence yield. NPQ (qE + qT + qI) can be can be defined as (F_m°-F_m')/F_m'. After switching off the light, recovery of F_m within a few minutes reflects relaxation of the qE component of NPQ (Maxwell and Johnson, 2000).

NPQ of nadk2 leaves were performed before by Takahashi et al (2006), but only at 50 µE. Here, the same measurements were conducted at several light intensities and compared with wt plants. It can be observed that nadk2 leaves exhibit higher levels of NPQ at weak light intensities. NPQ levels are however similar for higher lights intensities. This is coherent with

the hypothesis that the photosynthetic apparatus of mutant leaves is more stressed, leading to higher NPQ levels in order to minimize the linear electron flow.

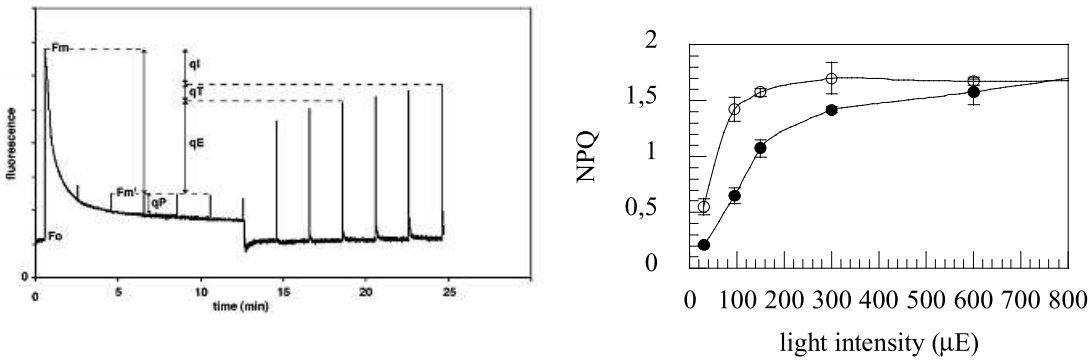

Fig. A.10 NPQ measurements on wt and nadk2 leaves. Left panel: schematic representation of the fluorescence kinetics used to measure NPQ components (from Müller et al, 2001); Right panel: NPQ levels in wt (black dots) and nadk2 (white dots) leaves at different light intensities.

Conclusions

Our analyses of the nadk2 mutant line confirm the photosynthesis deficiency of these mutants and the higher NPQ levels. In addition, we provided evidence of the impairment of linear electron flow and increasing in the cyclic electron flow of these mutants.

The total contribution of PSI plus PSII to the two pools still needs to be determined experimentally as well as NADP levels and NADK activity in mutant plants.

Since these plants normally lack plastidial source of NADP in important question that arises is why they can manage to survive (although with severl impairment in growth and development). Transport of NADP from cytosol to chloroplast might be possible through a NAD channel (Palmieri et al, 2009) that was seen to be able to transport a little amount of NADP. This hypothesis needs to be tested by the production of a double mutant for the NADK2 gene and this transporter.

References

Agledal, L., M. Niere and M. Ziegler (2010). *The phosphate makes a difference: cellular functions of NADP*. Redox Report **15**(1): 2-10.

Al-Quraan, N. A., R. D. Locy and N. K. Singh (2010). *Expression of calmodulin genes in wild type and calmodulin mutants of Arabidopsis thaliana under heat stress*. Plant Physiology and Biochemistry **48**(8): 697-702.

Albiniak, A. M., J. Baglieri and C. Robinson (2012). *Targeting of lumenal proteins across the thylakoid membrane*. Journal of Experimental Botany **63**(4): 1689-1698.

Alexander, K., B. Cimler, K. Meier and D. Storm (1987). *Regulation of calmodulin binding to P-57. A neurospecific calmodulin binding protein*. The Journal of Biological Chemistry **262**(13): 6108-6113.

Allan, E. and A. Trewavas (1985). *Quantitative changes in calmodulin and NAD kinase during early cell development in the root apex of* Pisum sativum L. Planta **165**(4): 493-501.

Allen, G. J. and D. Sanders (1995). *Release of Ca^{2+} from individual plant vacuoles by both InsP3 and cyclic ADP-ribose*. Science **268**(5211): 735-737.

Anagli, J., F. Hofmann, M. Quadroni, T. Vorherr and E. Carafoli (1995). *The Calmodulin-binding domain of the inducible (macrophage) nitric oxide synthase*. European Journal of Biochemistry **233**(3): 701-708.

Anderson, J. M. and M. J. Cormier (1978). *Calcium-dependent regulator of NAD kinase in higher plants*. Biochemical and Biophysical Research Communications **84**(3): 595-602.

Au, T. K. and P. C. Leung (1998). *Identification of the binding and inhibition sites in the calmodulin molecule for ophiobolin A by site-directed mutagenesis*. Plant Physiology **118**(3): 965-973.

Audran, E., R. Dagher, S. Gioria, P. O. Tsvetkov, A. A. Kulikova, B. Didier, P. Villa, A. A. Makarov, M.-C. Kilhoffer and J. Haiech (2013). *A general framework to characterize inhibitors of calmodulin: Use of calmodulin inhibitors to study the interaction between calmodulin and its calmodulin binding domains*. Biochimica et Biophysica Acta (BBA) – Molecular Cell Research **1833**(7): 1720-1731.

Babu, A., S. Pemrick and J. Gulati (1986). *Ca^{2+} activation of troponin C-extracted vertebrate striated fast-twitch muscle fibers*. FEBS Letters **203**(1): 20-24.

Bækgaard, L., A. T. Fuglsang and M. G. Palmgren (2005). *Regulation of plant plasma membrane H^{+}-and Ca^{2+}-ATPases by terminal domains.* Journal of Bioenergetics and Biomembranes **37**(6): 369-374.

Balsera, M., T. A. Goetze, E. Kovács-Bogdán, P. Schürmann, R. Wagner, B. B. Buchanan, J. Soll and B. Bölter (2009). *Characterization of Tic110, a channel-forming protein at the inner envelope membrane of chloroplasts, unveils a response to Ca^{2+} and a stromal regulatory disulfide bridge*. The Journal of Biological Chemistry **284**(5): 2603-2616.

Barry, B. A., C. Hicks, A. De Riso and D. L. Jenson (2005). *Calcium ligation in photosystem II under inhibiting conditions*. Biophysical Journal **89**(1): 393-401.

Batistič, O. and J. Kudla (2012). *Analysis of calcium signaling pathways in plants*. Biochimica et Biophysica Acta (BBA)-General Subjects **1820**(8): 1283-1293.

Bayley, P., W. Findlay and S. Martin (1996). *Target recognition by calmodulin: Dissecting the kinetics and affinity of interaction using short peptide sequences*. Protein Science **5**(7): 1215-1228.

Becker, D. W. and J. J. Brand (1985). *Anacystis nidulans demonstrates a photosystem II cation requirement satisfied only by Ca^{2+} or Na^{+}*. Plant Physiology **79**(2): 552-558.

Benlloch, R., M. C. Kim, C. Sayou, E. Thévenon, F. Parcy and O. Nilsson (2011). *Integrating long-day flowering signals: a LEAFY binding site is essential for proper photoperiodic activation of APETALA1*. Plant Journal **67**(6): 1094-1102.

Berggård, T., G. Arrigoni, O. Olsson, M. Fex, S. Linse and P. James (2006). *140 Mouse brain proteins identified by Ca^{2+}-calmodulin affinity chromatography and tandem mass spectrometry*. Journal of Proteome Research **5**(3): 669-687.

Bhattacharya, S., C. G. Bunick, and W. J. Chazin (2004). *Target selectivity in EF-hand calcium binding proteins.* Biochimica et Biophysica Acta (BBA)-Molecular Cell Research **1742**(1): 69-79.

Black, D., Q.-K. Tran and A. Persechini (2004). *Monitoring the total available calmodulin concentration in intact cells over the physiological range in free Ca^{2+}.* Cell Calcium **35**(5): 415-425.

Blanchoin, L. and T. D. Pollard (1998). *Interaction of actin monomers with* Acanthamoeba actophorin *(ADF/cofilin) and profilin*. The Journal of Biological Chemistry **273**(39): 25106-25111.

Bligny, R. and J.-J. Leguay (1987). *Techniques of cell suspension culture*. Methods in Enzymology **148**: 3-16.

Block, M. A., A.-J. Dorne, J. Joyard and R. Douce (1983). *Preparation and characterization of membrane fractions enriched in outer and inner envelope membranes from spinach chloroplasts. II. Biochemical characterization.* The Journal of Biological Chemistry **258**(21): 13281-13286.

Bolger, R., T. E. Wiese, K. Ervin, S. Nestich and W. Checovich (1998). *Rapid screening of environmental chemicals for estrogen receptor binding capacity.* Environmental health perspectives **106**(9): 551.

Boursiac, Y. and J. F. Harper (2007). *The origin and function of calmodulin regulated Ca^{2+} pumps in plants*. Journal of bioenergetics and biomembranes **39**(5-6): 409-414.

Breitkreuz, K. E. and B. J. Shelp (1995). *Subcellular compartmentation of the 4-aminobutyrate shunt in protoplasts from developing soybean cotyledons*. Plant Physiology **108**(1): 99-103.

Breyton, C., B. Nandha, G. N. Johnson, P. Joliot and G. Finazzi (2006). *Redox modulation of cyclic electron flow around photosystem I in C3 plants.* Biochemistry **45**(45): 13465-13475.

Brière, C., T. C. Xiong, C. Mazars and R. Ranjeva (2006). *Autonomous regulation of free Ca^{2+} concentrations in isolated plant cell nuclei: A mathematical analysis*. Cell Calcium **39**(4): 293-303.

Buschmeier, B., H. E. Meyer, H.-H. Kiltz, L. M. Heilmeyer Jr and G. W. Mayr (1987). *The sites of interaction of calmodulin with phosphofructokinase*. Signal Transduction and Protein Phosphorylation, Springer US. 259-263.

Bussemer, J., F. Chigri and U. C. Vothknecht (2009). *Arabidopsis ATPase family gene 1-like protein 1 is a calmodulin-binding AAA(+)-ATPase with a dual localization in chloroplasts and mitochondria.* FEBS Journal **276**(14): 4294-4304.

Calábria, L. K., L. Garcia Hernandez, R. R. Teixeira, M. Valle de Sousa and F. S. Espindola (2008). *Identification of calmodulin-binding proteins in brain of worker honeybees*. Comparative Biochemistry and Physiology Part B: Biochemistry and Molecular Biology **151**(1): 41-45.

Chai, M. F., Q. J. Chen, R. An, Y. M. Chen, J. Chen and X. C. Wang (2005). *NADK2, an Arabidopsis chloroplastic NAD kinase, plays a vital role in both chlorophyll synthesis and chloroplast protection*. Plant Molecular Biology **59**(4): 553-564.

Charles, S. A. and B. Halliwell (1980). *Action of calcium ions on spinach (Spinacia oleracea) chloroplast fructose bisphosphatase and other enzymes of the Calvin cycle*. Biochemical Journal **188**(3): 775.

Chen, C.-H. and A. L. Lehninger (1973). *Ca^{2+} transport activity in mitochondria from some plant tissues*. Archives of Biochemistry and Biophysics **157**(1): 183-196.

Cheney, R. E. and M. S. Mooseker (1992). *Unconventional myosins*. Current Opinion in Cell Biology **4**(1): 27-35.

Cheng, N.-H., J. K. Pittman, T. Shigaki, J. Lachmansingh, S. LeClere, B. Lahner, D. E. Salt and K. D. Hirschi (2005). *Functional association of Arabidopsis CAX1 and CAX3 is required for normal growth and ion homeostasis*. Plant Physiology **138**(4): 2048-2060.

Cheong, Y. H., K.-N. Kim, G. K. Pandey, R. Gupta, J. J. Grant and S. Luan (2003). *CBL1, a calcium sensor that differentially regulates salt, drought, and cold responses in Arabidopsis*. The Plant Cell **15**(8): 1833-1845.

Cheung, W. (1970). *Calcium-binding protein*. Biochemical and Biophysical Research Communications **38**: 533-538.

Chiasson, D., S. K. Ekengren, G. B. Martin, S. L. Dobney and W. A. Snedden (2005). *Calmodulin-like proteins from Arabidopsis and tomato are involved in host defense against* Pseudomonas syringae *pv. tomato*. Plant Molecular Biology **58**(6): 887-897.

Chigri, F., S. Flosdorff, S. Pilz, E. Koelle, E. Dolze, C. Gietl and U. C. Vothknecht (2012). *The Arabidopsis calmodulin-like proteins AtCML30 and AtCML3 are targeted to mitochondria and peroxisomes, respectively*. Plant Molecular Biology **78**(3): 211-222.

Chigri, F., F. Hoermann, A. Stamp, D. K. Stammers, B. Boelter, J. Soll and U. C. Vothknecht (2006). *Calcium regulation of chloroplast protein translocation is mediated by calmodulin binding to Tic32*. Proceedings of the National Academy of Sciences of the United States of America **103**(43): 16051-16056.

Chigri, F., J. Soll and U. C. Vothknecht (2005). *Calcium regulation of chloroplast protein import*. Plant Journal **42**(6): 821-831.

Choi, M. S., M. C. Kim, J. H. Yoo, B. C. Moon, S. C. Koo, B. O. Park, J. H. Lee, Y. D. Koo, H. J. Han, S. Y. Lee, W. S. Chung, C. O. Lim, and M. J. Cho (2005). *Isolation of a calmodulin-binding transcription factor from rice (*Oryza sativa L.*).* The Journal of Biological Chemistry, **280**(49), 40820-4083

Clark, G. B. and S. J. Roux (1995). *Annexins of plant cells*. Plant physiology **109**(4): 1133-1139.

Coe, H. and M. Michalak (2009). *Calcium binding chaperones of the endoplasmic reticulum*. General Physiology Biophysics **28**: F96-F103.

Cohen, P. (1988). Calmodulin, in Molecular aspect of cellular regulation, Vol. 5 (Cohen, P., ed.), Elsevier, Amsterdam.

Conn, S. J., M. Gilliham, A. Athman, A. W. Schreiber, U. Baumann, I. Moller, N.-H. Cheng, M. A. Stancombe, K. D. Hirschi and A. A. Webb (2011). *Cell-specific vacuolar calcium storage mediated by CAX1 regulates apoplastic calcium concentration, gas exchange, and plant productivity in Arabidopsis*. The Plant Cell **23**(1): 240-257.

Corbett, E. F., K. M. Michalak, K. Oikawa, S. Johnson, I. D. Campbell, P. Eggleton, C. Kay and M. Michalak (2000). *The conformation of calreticulin is influenced by the endoplasmic reticulum luminal environment*. The Journal of Biological Chemistry **275**(35): 27177-27185.

Corda, D., and M. Di Girolamo, (2003). *Functional aspects of protein mono-ADP-ribosylation.* The EMBO journal **22**(9): 1953-1958.

Corti, C., E. LeClerc L'Hostis, M. Quadroni, H. Schmid, I. Durussel, J. Cox, P. Dainese Hatt, P. James and E. Carafoli (1999). *Tyrosine phosphorylation modulates the interaction of calmodulin with its target proteins*. European Journal of Biochemistry **262**(3): 790-802.

Costa, A., I. Drago, S. Behera, M. Zottini, P. Pizzo, J. I. Schroeder, T. Pozzan and F. L. Schiavo (2010). *H_2O_2 in plant peroxisomes: an in vivo analysis uncovers a Ca^{2+}-dependent scavenging system*. Plant Journal **62**(5): 760-772.

Crivici, A. and M. Ikura (1995). *Molecular and structural basis of target recognition by calmodulin*. Annual Review of Biophysics and Biomolecular Structure **24**(1): 85-116.

Czempinski, K., S. Zimmermann, T. Ehrhardt and B. Müller-Röber (1997). *New structure and function in plant K^+ channels: KCO1, an outward rectifier with a steep Ca^{2+} dependency*. The EMBO journal **16**(10): 2565-2575.

Davis, T. N., M. S. Urdea, F. R. Masiarz and J. Thorner (1986). *Isolation of the yeast calmodulin gene: calmodulin is an essential protein.* Cell **47**(3): 423-431.

Day, I. S., V. S. Reddy, G. Shad Ali and A. S. Reddy (2002). *Analysis of EF-hand-containing proteins in Arabidopsis.* Genome Biology **3**(10): RESEARCH0056.

Delk, N. A., K. A. Johnson, N. I. Chowdhury and J. Braam (2005). *CML24, regulated in expression by diverse stimuli, encodes a potential Ca^{2+} sensor that functions in responses to abscisic acid, daylength, and ion stress*. Plant Physiology **139**(1): 240-253.

Dell'Aglio, E., C. Giustini, D. Salvi, S. Brugière, F. Delpierre, L. Moyet, M. Baudet, D. Seigneurin-Berny, M. Matringe, M. Ferro, N. Rolland and G. Curien (2013). *Complementary biochemical approaches applied to the identification of plastidial calmodulin-binding proteins*. Molecular Biosystems **9**(6): 1234-1248.

Delumeau, O., F. Montrichard and D. L. Laval-Martin (1998). *NAD^+ kinase activity, calmodulin levels during the growth of isolated cells from* Lycopersicon pimpinellifolium *and kinetic constants of the calmodulin-dependent NAD^+ kinase*. Plant Science **138**(1): 43-52.

Delumeau, O., M. Renard and F. Montrichard (2000). *Characterization and possible redox regulation of the purified calmodulin-dependent NAD(+) kinase from* Lycopersicon pimpinellifolium. Plant Cell and Environment **23**(11): 1267-1273.

Demidchik, V., R. J. Davenport and M. Tester (2002). *Nonselective cation channels in plants*. Annual Review of Plant Biology **53**(1): 67-107.

Dennison, K. L. and E. P. Spalding (2000). *Glutamate-gated calcium fluxes in Arabidopsis*. Plant Physiology **124**(4): 1511-1514.

Dieter, Peter, and D. Marmé (1980) *Partial purification of plant NAD kinase by calmodulin-Sepharose affinity chromatography.* Cell Calcium **1**(5): 279-286.

Dieter, P. and D. Marme (1984). *A Ca^{2+}, Calmodulin-dependent NAD kinase from corn is located in the outer mitochondrial membrane*. The Journal of Biological Chemistry **259**(1): 184-189.

Dobney, S., D. Chiasson, P. Lam, S. P. Smith and W. A. Snedden (2009). *The Calmodulin-related calcium sensor CML42 plays a role in trichome branching.* The Journal of Biological Chemistry **284**(46): 31647-31657.

Dodd, A. N., J. Kudla and D. Sanders (2010). *The language of calcium signaling*. Annual Review of Plant Biology **61**: 593-620.

Dominguez, D. C. (2004). *Calcium signalling in bacteria*. Molecular Microbiology **54**(2): 291-297.

Douce, R., J. Joyard, A.-J. Dorne and M. A. Block (1985). *Origin of the plastid envelope membranes*. Recent Advances in Biological Membrane Studies, Springer**:** 179-203.

Downie, L., J. Priddle, C. Hawes and D. E. Evans (1998). *A calcium pump at the higher plant nuclear envelope?* FEBS Letters **429**(1): 44-48.

Drago, I., M. Giacomello, P. Pizzo and T. Pozzan (2008). *Calcium dynamics in the peroxisomal lumen of living cells.* The Journal of Biological Chemistry **283**(21): 14384-14390.

Drakenberg, T. n., S. Forsén and H. Lilja (1983). *^{43}Ca NMR studies of calcium binding to proteins: Interpretation of experimental data by bandshape analysis*. Journal of Magnetic Resonance (1969) **53**(3): 412-422.

Dupont, G., G. Houart and P. De Koninck (2003). *Sensitivity of CaM kinase II to the frequency of Ca^{2+} oscillations: a simple model.* Cell Calcium **34**(6): 485-497.

Durso, N. A. and R. J. Cyr (1994). *A calmodulin-sensitive interaction between microtubules and a higher plant homolog of elongation factor-1 alpha*. The Plant Cell **6**(6): 893-905.

Edwards, K., C. Johnstone and C. Thompson (1991). *A simple and rapid method for the preparation of plant genomic DNA for PCR analysis.* Nucleic Acids Research **19**(6): 1349.

Elledge, S. J., J. T. Mulligan, S. W. Ramer, M. Spottswood and R. W. Davis (1991). *Lambda-yes- A multifunctional cDNA expression vector for the isolation of genes by complementation of yeast and* Escherichia coli *mutations.* Proceedings of the National Academy of Sciences of the United States of America **88**(5): 1731-1735.

Epel, D. (1982). *The cascade of events initiated by rises in cytosolic Ca^{2+} and pH following fertilization in sea urchin eggs*. In Ions, Cell Proliferation, and Cancer. A. Boyonton, W. McKeehan, and J. Whietfield (eds.): pp 327-339. Academic Press, New York.

Ettinger, W. F., A. M. Clear, K. J. Fanning and M. L. Peck (1999). *Identification of a Ca^{2+}/H^{+} antiport in the plant chloroplast thylakoid membrane*. Plant Physiology **119**(4): 1379-1386.

Fallon, J. L. and F. A. Quiocho (2003). *A closed compact structure of native Ca^{2+}-calmodulin*. Structure **11**(10): 1303-1307.

Felle, H. (1988). *Auxin causes oscillations of cytosolic free calcium and pH in* Zea mays *coleoptiles*. Planta **174**(4): 495-499.

Ferro, M., S. Brugiere, D. Salvi, D. Seigneurin-Berny, M. Court, L. Moyet, C. Ramus, S. Miras, M. Mellal, S. Le Gall, S. Kieffer-Jaquinod, C. Bruley, J. Garin, J. Joyard, C. Masselon and N. Rolland (2010). *AT_CHLORO, a comprehensive chloroplast proteome database with subplastidial localization and curated information on envelope proteins*. Molecular & Cellular Proteomics **9**(6): 1063-1084.

Fisher D.D., S. Gilroy and R. J. Cyr (1996). *Evidence for opposing effects of calmodulin on cortical microtubules*. Plant Physiology **112**(3):1079–1087

Furuichi, T., K. W. Cunningham and S. Muto (2001). *A putative two pore channel AtTPC1 mediates Ca^{2+} flux in Arabidopsis leaf cells.* Plant and Cell Physiology **42**(9): 900-905.

Furuyama, T. and V. A. Dzelzkalns (1999). *A novel calcium-binding protein is expressed in* Brassica pistils *and anthers late in flower development.* Plant Molecular Biology **39**(4): 729-737.

Galon, Y., A. Finkler and H. Fromm (2010). *Calcium-regulated transcription in plants*. Molecular Plant **3**(4): 653-669.

Gayle, R., R. Slaughter and A.R. Means (1987). *Use of the ^{125}I-labeled protein gel overaly technique to study calmodulin-binding proteins*. Methods in Enzymology **139**(35): 433-444.

Geisler, M., N. Frangne, E. Gomès, E. Martinoia and M. G. Palmgren (2000). *The ACA4 gene of Arabidopsis encodes a vacuolar membrane calcium pump that improves salt tolerance in yeast*. Plant Physiology **124**(4): 1814-1827.

Ghanotakis, D. F., G. T. Babcock and C. F. Yocum (1984). *Calcium reconstitutes high rates of oxygen evolution in polypeptide depleted photosystem II preparations*. FEBS Letters **167**(1): 127-130.

Grabarek, Z. (2011). *Insights into modulation of calcium signaling by magnesium in calmodulin, troponin C and related EF-hand proteins*. Biochimica et Biophysica Acta (BBA)-Molecular Cell Research **1813**(5): 913-921.

Graindorge, M., C. Giustini, A. C. Jacomin, A. Kraut, G. Curien and M. Matringe (2010). *Identification of a plant gene encoding glutamate/aspartate-prephenate aminotransferase: The last homeless enzyme of aromatic amino acids biosynthesis*. FEBS Letters **584**(20): 4357-4360.

Grose, J. H., L. Joss, S. F. Velick and J. R. Roth (2006). *Evidence that feedback inhibition of NAD kinase controls responses to oxidative stress.* Proceedings of the National Academy of Sciences of the United States of America **103**(20): 7601-7606.

Guo, H., T. Mockler, H. Duong and C. Lin (2001). *SUB1, an Arabidopsis Ca^{2+}-binding protein involved in cryptochrome and phytochrome coaction.* Science **291**(5503): 487-490.

Guse, A. H. and H. C. Lee (2008). *NAADP: a universal Ca^{2+} trigger*. Science Signaling **1**(44): re10.

Gut, H., P. Dominici, S. Pilati, A. Astegno, M. V. Petoukhov, D. I. Svergun, M. G. Grütter and G. Capitani (2009). *A common structural basis for pH-and calmodulin-mediated regulation in plant glutamate decarboxylase*. Journal of Molecular Biology **392**(2): 334-351.

Habib, S. J., W. Neupert and D. Rapaport (2007). *Analysis and prediction of mitochondrial targeting signals*. Methods in Cell Biology **80**: 761-781.

Han, B.-G., M. Han, H. Sui, P. Yaswen, P. J. Walian and B. K. Jap (2002). *Crystal structure of human calmodulin-like protein: insights into its functional role.* FEBS Letters **521**(1): 24-30.

Han, S., R. Tang, L. K. Anderson, T. E. Woerner and Z.-M. Pei (2003). *A cell surface receptor mediates extracellular Ca^{2+} sensing in guard cells*. Nature **425**(6954): 196-200.

Harper, J. F., G. Breton, and A. Harmon (2004). *Decoding Ca^{2+} signals through plant protein kinases*. Annual Review of Plant Biology **55**: 263-288.

Harper, J. F., and A. Harmon (2005). *Plants, symbiosis and parasites: a calcium signalling connection*. Nature Reviews Molecular Cell Biology **6**(7): 555-566.

Hirschi, K. D., R.-G. Zhen, K. W. Cunningham, P. A. Rea and G. R. Fink (1996). *CAX1, an H^+/Ca^{2+} antiporter from Arabidopsis.* Proceedings of the National Academy of Sciences of the United States of America **93**(16): 8782-8786.

Hirschi, K. D. (1999). *Expression of Arabidopsis CAX1 in tobacco: altered calcium homeostasis and increased stress sensitivity.* The Plant Cell **11**(11): 2113-2122.

Holleman, A. F. and E. Wiberg, (2001). Inorganic Chemistry, San Diego: Academic Press.

Hormann, F., M. Kuchler, D. Sveshnikov, U. Oppermann, Y. Li and J. Soll (2009). *Tic32, an essential component in chloroplast biogenesis*. (vol 279, pg 34756, 2004). The Journal of Biological Chemistry. **284**(42): 29240-29240.

Huang, L. Q., T. Berkelman, A. E. Franklin and N. E. Hoffman (1993). *Characterization of a gene encoding a Ca^{2+}-Atpase-like protein in the plastid envelope.* Proceedings of the National Academy of Sciences of the United States of America **90**(21): 10066-10070.

Hubbard, M. J. and C. B. Klee (1987). *Calmodulin binding to calcineurin – ligand – induced renaturation of protein immobilized on nitrocellulose*. The Journal of Biological Chemistry **262**(31): 15062-15070.

Ikura, M., G. M. Clore, A. M. Gronenborn, G. Zhu, C. B. Klee and A. Bax (1992). *Solution structure of a calmodulin-target peptide complex by multidimensional NMR*. Science **256**(5057): 632-638.

Islam, M. M., M. A. Hossain, R. Jannat, S. Munemasa, Y. Nakamura, I. C. Mori and Y. Murata (2010). *Cytosolic alkalization and cytosolic calcium oscillation in Arabidopsis guard cells response to ABA and MeJA*. Plant and Cell Physiology **51**(10): 1721-1730.

Jami, S. K., G. B. Clark, B. T. Ayele, P. Ashe and P. B. Kirti (2012). *Genome-wide comparative analysis of annexin superfamily in plants*. PloS one **7**(11): e47801.

Jarrett, H. W., C. J. Brown, C. C. Black and M. J. Cormier (1982). *Evidence that calmodulin is in the chloroplast of peas and serves a regulatory role in photosynthesis*. The Journal of Biological Chemistry **257**(22): 3795-3804.

Jarrett, H. W. and J. L. Foster (1995). *Alternate binding of actin and calmodulin to multiple sites on dystrophin*. The Journal of Biological Chemistry **270**(10): 5578-5586.

Jarvis, P. (2008). *Targeting of nucleus-encoded proteins to chloroplasts in plants*. New Phytologist **179**(2): 257-285.

Johnson, C. H., M. R. Knight, T. Kondo, P. Masson, J. Sedbrook, A. Haley and A. Trewavas (1995). *Circadian oscillations of cytosolic and chloroplastic free calcium in plants*. Science **269**(5232): 1863-1865.

Johnson, J. D., C. Snyder, M. Walsh and M. Flynn (1996). *Effects of myosin light chain kinase and peptides on Ca^{2+} exchange with the N-and C-terminal Ca^{2+} binding sites of calmodulin*. The Journal of Biological Chemistry **271**(2): 761-767.

Johnson C. H., R. Shingles and W. F. Ettinger. (2006). *Regulation and role of calcium fluxes in the chloroplast.* In: Wise RR, Hoober J, eds. *The structure and function of plastids*. The Netherlands: Springer, 403–416.

Joliot, P. and A. Joliot (2006). *Cyclic electron flow in C3 plants*. Biochimica et Biophysica Acta (BBA)-Bioenergetics **1757**(5): 362-368.

Kakiuchi, S. and R. Yamazaki (1970). *Calcium dependent phosphodiesterase activity and its activating factor (PAF) from brain: studies on cyclic 3', 5'-nucleotide phosphodiesterase (III)*. Biochemical and Biophysical Research Communications **41**(5): 1104-1110.

Karita, E., H. Yamakawa, I. Mitsuhara, K. Kuchitsu and Y. Ohashi (2004). *Three types of tobacco calmodulins characteristically activate plant NAD kinase at different Ca^{2+} concentrations and pHs*. Plant and Cell Physiology **45**(10): 1371-1379.

Kato, M., N. Nagasaki-Takeuchi, Y. Ide and M. Maeshima (2010). *An Arabidopsis hydrophilic Ca^{2+}-binding protein with a PEVK-rich domain, PCaP2, is associated with the plasma membrane and interacts with calmodulin and phosphatidylinositol phosphates*. Plant and Cell Physiology **51**(3): 366-379.

Kawai, S., S. Mori, T. Mukai, W. Hashimoto and K. Murata (2001). *Molecular characterization of* Escherichia coli *NAD kinase.* European Journal of Biochemistry **268**(15): 4359-4365.

Kawasaki, H., S. Nakayama and R. Kretsinger (1998). *Classification and evolution of EF-hand proteins*. Biometals **11**(4): 277-295.

Keller, T., H. G. Damude, D. Werner, P. Doerner, R. A. Dixon and C. Lamb (1998). *A plant homolog of the neutrophil NADPH oxidase gp91phox subunit gene encodes a plasma membrane protein with Ca^{2+} binding motifs*. The Plant Cell **10**(2): 255-266.

Kim, Y. Y., H. Choi, S. Segami, H. T. Cho, E. Martinoia, M. Maeshima and Y. Lee (2009). *AtHMA1 contributes to the detoxification of excess Zn(II) in Arabidopsis*. Plant Journal **58**(5): 737-753.

Klimecka, M. and G. Muszynska (2007). *Structure and functions of plant calcium-dependent protein kinases*. Acta Biochimica Polonica-English Edition- **54**(2): 219.

Klüsener, B., G. Boheim and E. W. Weiler (1997). *Modulation of the ER Ca^{2+} channel BCC1 from tendrils of* Bryonia dioica *by divalent cations, protons and H_2O_2*. FEBS Letters **407**(2): 230-234.

Knight, M. R., A. K. Campbell, S. M. Smith and A. J. Trewavas (1991). *Recombinant aequorin as a probe for cytosolic free Ca^{2+} in* Escherichia coli. FEBS Letters **282**(2): 405-408.

Kornberg, A. (1950). *Enzymatic synthesis of triphosphopyridine nucleotide*. The Journal of Biological Chemistry **182**(2): 805-813.

Kosuta, S., S. Hazledine, J. Sun, H. Miwa, R. J. Morris, J. A. Downie and G. E. Oldroyd (2008). *Differential and chaotic calcium signatures in the symbiosis signaling pathway of legumes*. Proceedings of the National Academy of Sciences of the Unites States of America **105**(28): 9823-9828.

Kreimer, G., M. Melkonian, J. Holtum and E. Latzko (1985). *Characterization of calcium fluxes across the envelope of intact spinach chloroplasts.* Planta **166**(4): 515-523.

Kreimer, G., B. Surek, I. E. Woodrow and E. Latzko (1987). *Calcium binding by spinach stromal proteins*. Planta **171**(2): 259-265.

Kretsinger, R. H. and C. E. Nockolds (1973). *Carp muscle calcium-binding protein. II. Structure determination and general description.* The Journal of Biological Chemistry **248**(9): 3313-3326.

Kudla, J., O. Batistič and K. Hashimoto (2010). *Calcium signals: the lead currency of plant information processing*. The Plant Cell **22**(3): 541-563.

Kuhn, S., J. Bussemer, F. Chigri and U. C. Vothknecht (2009). *Calcium depletion and calmodulin inhibition affect the import of nuclear-encoded proteins into plant mitochondria*. Plant Journal **58**(4): 694-705.

Kumar, V., V. P. R. Chichili, X. Tang and J. Sivaraman (2013). *A Novel Trans Conformation of Ligand-Free Calmodulin.* PloS one **8**(1): e54834.

Kushwaha, R., A. Singh and S. Chattopadhyay (2008). *Calmodulin7 plays an important role as transcriptional regulator in Arabidopsis seedling development*. The Plant Cell **20**(7): 1747-1759.

Lasorsa, F. M., P. Pinton, L. Palmieri, P. Scarcia, H. Rottensteiner, R. Rizzuto and F. Palmieri (2008). *Peroxisomes as novel players in cell calcium homeostasis.* The Journal of Biological Chemistry **283**(22): 15300-15308.

Lau, A., A. McLaughlin, and S. McLaughlin. (1981). *The adsorption of divalent cations to phosphatidylglycerol bilayer membranes.* Biochimica et Biophysica Acta (BBA)- Biomembranes. **645**(2):279-292

Leclerc, E., C. Corti, H. Schmid, S. Vetter, P. James and E. Carafoli (1999). *Serine/threonine phosphorylation of calmodulin modulates its interaction with the binding domains of target enzymes*. Biochemical Journal **344**: 403-411.

Lee, S. H., H. Y. Seo, J. C. Kim, W. Do Heo, W. S. Chung, K. J. Lee, M. C. Kim, Y. H. Cheong, J. Y. Choi and C. O. Lim (1997). *Differential activation of NAD kinase by plant calmodulin isoforms: the critical role of domain 1*. The Journal of Biological Chemistry **272**(14): 9252-9259.

Lee, S.H., J. D. Johnson, M. P. Walsh, J. E. Van Lierop, C. Sutherland, A. Xu, W. A. Snedden, D. Kosk-Kosicka, H. Frommm, N. Narayanan and M. J. Cho (2000). *Differential regulation of Ca2+/calmodulin-dependent enzymes by plant calmodulin isoforms and free Ca^{2+} concentration*. Biochemical Journal, **350**: 299-306.

Lerner, F., M. Niere, A. Ludwig and M. Ziegler (2001). *Structural and functional characterization of human NAD kinase*. Biochemical and Biophysical Research Communications **288**(1): 69-74.

Leung, J., M. Bouvier-Durand, P.-C. Morris, D. Guerrier, F. Chefdor and J. Giraudat (1994). *Arabidopsis ABA response gene ABI1: features of a calcium-modulated protein phosphatase*. Science **264**(5164): 1448-1452.

Levin, R. M. and B. Weiss (1977). *Binding of trifluoperazine to the calcium-dependent activator of cyclic nucleotide phosphodiesterase*. Molecular Pharmacology **13**(4): 690-697.

Lewit-Bentley, A. and S. Réty (2000). *EF-hand calcium-binding proteins.* Current Opinion in Structural Biology **10**(6): 637-643.

Li, Y., G.-X. Wang, M. Xin, H.-M. Yang, X.-J. Wu and T. Li (2004). *The parameters of guard cell calcium oscillation encodes stomatal oscillation and closure in* Vicia faba*.* Plant Science **166**(2): 415-421.

Li, H.-m. and C.-C. Chiu (2010). *Protein transport into chloroplasts*. Annual Review of Plant Biology **61**: 157-180.

Liang, L., S. Flury, V. Kalck, B. Hohn and J. Molinier (2006). *CENTRIN2 interacts with the arabidopsis homolog of the human XPC protein (AtRAD4) and contributes to efficient synthesis-dependent repair of bulky DNA lesions.* Plant Molecular Biology **61**(1-2): 345-356.

Liao, B., M. C. Gawienowski and R. E. Zielinski (1996). *Differential stimulation of NAD kinase and binding of peptide substrates by wild-type and mutant plant calmodulin isoforms*. Archives of Biochemistry and Biophysics **327**(1): 53-60.

Lin, J., T. J. Nazarenus, J. L. Frey, X. Liang, M. A. Wilson and J. M. Stone (2011). *A plant DJ-1 homolog is essential for* Arabidopsis thaliana *chloroplast development*. PloS One **6**(8): e23731.

Logan, D. C. and M. R. Knight (2003). *Mitochondrial and cytosolic calcium dynamics are differentially regulated in plants*. Plant Physiology **133**(1): 21-24.

Lundblad, J. R., M. Laurance and R. H. Goodman (1996). *Fluorescence polarization analysis of protein-DNA and protein-protein interactions.* Molecular Endocrinology **10**(6): 607-612.

Ma, L., X. Xu, S. Cui and D. Sun (1999). *The presence of a heterotrimeric G protein and its role in signal transduction of extracellular calmodulin in pollen germination and tube growth*. The Plant Cell **11**(7): 1351-1363.

Magnan, F., B. Ranty, M. Charpenteau, B. Sotta, J. P. Galaud and D. Aldon (2008). *Mutations in AtCML9, a calmodulin-like protein from* Arabidopsis thaliana*, alter plant responses to abiotic stress and abscisic acid*. Plant Journal **56**(4): 575-589.

Magnani, R., L. M. Dirk, R. C. Trievel and R. L. Houtz (2010). *Calmodulin methyltransferase is an evolutionarily conserved enzyme that trimethylates Lys-115 in calmodulin.* Nature Communications **1**: 43.

Malhó, R. (1998). *Spatial characteristics to calcium signalling; the calcium wave as a basic unit in plant cell calcium signalling.* Philosophical Transactions of the Royal Society of London. Series B: Biological Sciences **353**(1374): 1463-1473.

Malmendal, A., J. Evenäs, E. Thulin, G. P. Gippert, T. Drakenberg and S. Forsén (1998). *When size is important accommodation of magnesium in a calcium binding regulatory domain*. The Journal of Biological Chemistry **273**(44): 28994-29001.

Martin, S. R., A. Andersson Teleman, P. M. Bayley, T. Drakenberg and S. Forsen (1985). *Kinetics of calcium dissociation from calmodulin and its tryptic fragments.* European Journal of Biochemistry **151**(3): 543-550.

Mazars, C., C. Brière, S. Bourque and P. Thuleau (2011). *Nuclear calcium signaling: an emerging topic in plants*. Biochimie **93**(12): 2068-2074.

Maxwell, K., and G. N. Johnson (2000) *Chlorophyll fluorescence—a practical guide*. Journal of Experimental Botany **51**(345): 659-668.

McCombs, J. E. and A. E. Palmer (2008). *Measuring calcium dynamics in living cells with genetically encodable calcium indicators.* Methods **46**(3): 152-159.

McCormack, E. and J. Braam (2003). *Calmodulins and related potential calcium sensors of Arabidopsis*. New Phytologist **159**(3): 585-598.

McCormack, E., Y.-C. Tsai and J. Braam (2005). *Handling calcium signaling: Arabidopsis CaMs and CMLs.* Trends in Plant Science **10**(8): 383-389.

McNamara, V. P. and K. Gounaris (1995). *Granal photosystem II complexes contain only the high redox potential form of cytochrome b-559 which is stabilised by the ligation of calcium*. Biochimica et Biophysica Acta (BBA)-Bioenergetics **1231**(3): 289-296.

McNeil, S., T. Lakey and S. Tomlinson (1985). *Calmodulin regulation of adenylate cyclase activity*. Cell Calcium **6**(3): 213-226.

Meador, W. E., A. R. Means and F. A. Quiocho (1992). *Target enzyme recognition by calmodulin: 2.4 Å structure of a calmodulin-peptide complex.* Science **257**(5074): 1251-1255.

Meyer, K., M. P. Leube and E. Grill (1994). *A protein phosphatase 2C involved in ABA signal transduction in* Arabidopsis thaliana*.* Science **264**(5164): 1452-1455.

Miller, A. F. and G. W. Brudvig (1989). *Manganese and calcium requirements for reconstitution of oxygen-evolution activity in manganese-depleted photosystem II membranes*. Biochemistry **28**(20): 8181-8190.

Miller, A. J. and D. Sanders (1987). *Depletion of cytosolic free calcium induced by photosynthesis*. Nature **326**(6111): 397-400.

Minagawa, J. (2005). *Chlorophyll fluorescence of photosynthetic organisms*. Bio/Chemiluminescence and its Applications to Photosynthesis, N. Wada and M. Mimuro (eds.): 149-174.

Miras, S., D. Salvi, M. Ferro, D. Grunwald, J. Garin, J. Joyard and N. Rolland (2002). *Non-canonical transit peptide for import into the chloroplast.* The Journal of Biological Chemistry **277**(49): 47770-47778.

Miras, S., D. Salvi, L. Piette, D. Seigneurin-Berny, D. Grunwald, C. Reinbothe, J. Joyard, S. Reinbothe and N. Rolland (2007). *Toc159- and Toc75-independent import of a transit sequence-less precursor into the inner envelope of chloroplasts*. The Journal of Biological Chemistry **282**(40): 29482-29492.

Miyawaki, A., J. Llopis, R. Heim, J. M. McCaffery, J. A. Adams, M. Ikura and R. Y. Tsien (1997). *Fluorescent indicators for Ca^{2+} based on green fluorescent proteins and calmodulin.* Nature **388**(6645): 882-887.

Monshausen, G. B., T. N. Bibikova, M. H. Weisenseel and S. Gilroy (2009). *Ca^{2+} regulates reactive oxygen species production and pH during mechanosensing in Arabidopsis roots*. The Plant Cell **21**(8): 2341-2356.

Moreno, I., L. Norambuena, D. Maturana, M. Toro, C. Vergara, A. Orellana, A. Zurita-Silva and V. R. Ordenes (2008). *AtHMA1 is a thapsigargin-sensitive Ca^{2+}/heavy metal pump*. The Journal of Biological Chemistry **283**(15): 9633-9641.

Muir, S. R. and D. Sanders (1997). *Inositol 1, 4, 5-trisphosphate-sensitive Ca^{2+} release across nonvacuolar membranes in cauliflower.* Plant Physiology **114**(4): 1511-1521.

Müller, P., X.-P. Li and K. K. Niyogi (2001). *Non-photochemical quenching. A response to excess light energy*. Plant Physiology **125**(4): 1558-1566.

Murashige, T. and F. Skoog (1962). *A revised medium for rapid growth and bio assays with tobacco tissue cultures*. Physiologia Plantarum **15**(3): 473-497.

Muto, S. and S. Miyachi (1977). *Properties of a protein activator of NAD kinase from plants.* Plant Physiology **59**(1): 55-60.

Muto, S., S. Miyachi, H. Usuda, G. E. Edwards and J. A. Bassham (1981). *Light-induced conversion of nicotinamide adenine dinucleotide to nicotinamide adenine dinucleotide phosphate in higher plant leaves*. Plant Physiology **68**(2): 324-328.

Muto, S., S. Izawa and S. Miyachi (1982). *Light-induced Ca^{2+} uptake by intact chloroplasts*. FEBS Letters **139**(2): 250-254.

Næsted, H., G. I. Frandsen, G.-Y. Jauh, I. Hernandez-Pinzon, H. B. Nielsen, D. J. Murphy, J. C. Rogers and J. Mundy (2000). *Caleosins: Ca^{2+}-binding proteins associated with lipid bodies*. Plant Molecular Biology **44**(4): 463-476.

Nakayama, S., H. Kawasaki and R. Kretsinger (2000). *Evolution of EF-hand proteins*. Calcium Homeostasis, 23(**1**)**:** 29-58.

Nauseef, W. M., S. J. McCormick and R. A. Clark (1995). *Calreticulin functions as a molecular chaperone in the biosynthesis of myeloperoxidase*. The Journal of Biological Chemistry **270**(9): 4741-4747.

Navazio, L., M. A. Bewell, A. Siddiqua, G. D. Dickinson, A. Galione and D. Sanders (2000). *Calcium release from the endoplasmic reticulum of higher plants elicited by the NADP metabolite nicotinic acid adenine dinucleotide phosphate*. Proceedings of the National Academy of Sciences of the United States of America **97**(15): 8693-8698.

Navazio, L., P. Mariani and D. Sanders (2001). *Mobilization of Ca^{2+} by cyclic ADP-ribose from the endoplasmic reticulum of cauliflower florets*. Plant Physiology **125**(4): 2129-2138.

Nelson, M. R. and C. E. Creutz (1995). *Combinatorial mutagenesis of the four domains of annexin IV: effects on chromaffin granule binding and aggregating activities*. Biochemistry **34**(9): 3121-3132.

Nieba, L., A. Krebber and A. Pluckthun (1996). *Competition BIAcore for measuring true affinities: Large differences from values determined from binding kinetics*. Analytical Biochemistry **234**(2): 155-165.

Nobel, P. S. (1969). *Light-induced changes in the ionic content of chloroplasts in* Pisum sativum. Biochimica et Biophysica Acta (BBA)-Bioenergetics **172**(1): 134-143.

Nomura, H., T. Komori, S. Uemura, Y. Kanda, K. Shimotani, K. Nakai, T. Furuichi, K. Takebayashi, T. Sugimoto, S. Sano, I. N. Suwastika, E. Fukusaki, H. Yoshioka, Y. Nakahira and T. Shiina (2012). *Chloroplast-mediated activation of plant immune signalling in Arabidopsis*. Nature Communications **3**: 926.

O'Connell, D. J., M. C. Bauer, J. O'Brien, W. M. Johnson, C. A. Divizio, S. L. O'Kane, T. Berggard, A. Merino, K. S. Akerfeldt, S. Linse and D. J. Cahill (2010). *Integrated protein array Screening and high throughput validation of 70 novel neural calmodulin-binding proteins*. Molecular and Cellular Proteomics **9**(6): 1118-1132.

O'Neil, K. T. and W. F. DeGrado (1990). *How calmodulin binds its targets: sequence independent recognition of amphiphilic α-helices.* Trends in Biochemical Sciences **15**(2): 59-64.

O'Connor, M. B. and C. M. O'Connor (1998). *Complex interactions of the protein L-isoaspartyl methyltransferase and calmodulin revealed with the yeast two-hybrid system*. The Journal of Biological Chemistry **273**(21): 12909-12913.

Oehler, S., Alex, R., and Barker, A. (1999). *Is nitrocellulose filter binding really a universal assay for protein–DNA interactions?* Analytical Biochemistry, **268**(2): 330-336.

Ogawa, Y., and M. Tanokura (1984). Calcium binding to calmodulin: effects of ionic strength, Mg^{2+}, pH and temperature. Journal of Biochemistry **95**(1): 19-28.

Ohashi, K., S. Kawai, M. Koshimizu and K. Murata (2011). *NADPH regulates human NAD kinase, a $NADP^{+}$-biosynthetic enzyme*. Molecular and Cellular Biochemistry **355**(1-2): 57-64.

Oldroyd, G. E. (2013). *Speak, friend, and enter: signalling systems that promote beneficial symbiotic associations in plants.* Nature Reviews Microbiology **11**(4): 252-263.

Osawa, M., M. B. Swindells, J. Tanikawa, T. Tanaka, T. Mase, T. Furuya and M. Ikura (1998). *Solution structure of calmodulin-W-7 complex: the basis of diversity in molecular recognition*. Journal of Molecular Biology **276**(1): 165-176.

Osawa, M., H. Tokumitsu, M. B. Swindells, H. Kurihara, M. Orita, T. Shibanuma, T. Furuya and M. Ikura (1999). *A novel target recognition revealed by calmodulin in complex with Ca^{2+}-calmodulin-dependent kinase kinase*. Nature Structural and Molecular Biology **6**(9): 819-824.

Otterhag, L., M. Sommarin and C. Pical (2001). *N-terminal EF-hand-like domain is required for phosphoinositide-specific phospholipase C activity in* Arabidopsis thaliana. FEBS Letters **497**(2): 165-170.

Ozers, M. S., J. J. Hill, K. Ervin, J. R. Wood, A. M. Nardulli, C. A. Royer and J. Gorski (1997). *Equilibrium binding of estrogen receptor with DNA using fluorescence anisotropy.* The Journal of Biological Chemistry **272**(48): 30405-30411.

Palmieri, F., B. Rieder, A. Ventrella, E. Blanco, P. T. Do, A. Nunes-Nesi, A. U. Trauth, G. Fiermonte, J. Tjaden and G. Agrimi (2009). *Molecular identification and functional characterization of Arabidopsis thaliana mitochondrial and chloroplastic NAD^{+} carrier proteins*. The Journal of Biological Chemistry **284**(45): 31249-31259.

Pandey, G. K., J. J. Grant, Y. H. Cheong, B.-G. Kim and S. Luan (2008). *Calcineurin-B-like protein CBL9 interacts with target kinase CIPK3 in the regulation of ABA response in seed germination*. Molecular Plant **1**(2): 238-248.

Parker, G. J., T. L. Law, F. J. Lenoch and R. E. Bolger (2000). *Development of high throughput screening assays using fluorescence polarization: nuclear receptor-ligand-binding and kinase/phosphatase assays*. Journal of Biomolecular Screening **5**(2): 77-88.

Peiter, E., F. J. Maathuis, L. N. Mills, H. Knight, J. Pelloux, A. M. Hetherington and D. Sanders (2005). *The vacuolar Ca^{2+}-activated channel TPC1 regulates germination and stomatal movement*. Nature **434**(7031): 404-408.

Perochon, A., S. Dieterle, C. Pouzet, D. Aldon, J.-P. Galaud and B. Ranty (2010). *Interaction of a plant pseudo-response regulator with a calmodulin-like protein.* Biochemical and Biophysical Research Communications **398**(4): 747-751.

Persechini, A. and P. M. Stemmer (2002). *Calmodulin is a limiting factor in the cell*. Trends in Cardiovascular Medicine **12**(1): 32-37.

Persson, S., S. E. Wyatt, J. Love, W. F. Thompson, D. Robertson and W. F. Boss (2001). *The Ca^{2+} status of the endoplasmic reticulum is altered by induction of calreticulin expression in transgenic plants*. Plant Physiology **126**(3): 1092-1104.

Petroutsos, D., A. Busch, I. Janssen, K. Trompelt, S. V. Bergner, S. Weinl, M. Holtkamp, U. Karst, J. Kudla and M. Hippler (2011). *The chloroplast calcium sensor CAS is required for photoacclimation in* Chlamydomonas reinhardtii. The Plant Cell **23**(8): 2950-2963.

Phizicky, E. M., and Fields, S. (1995). *Protein-protein interactions: methods for detection and analysis.* Microbiological Reviews, **59**(1) : 94-123.

Plieth, C. (2001). *Plant calcium signaling and monitoring: pros and cons and recent experimental approaches*. Protoplasma **218**(1-2): 1-23.

Popescu, S. C., G. V. Popescu, S. Bachan, Z. M. Zhang, M. Seay, M. Gerstein, M. Snyder and S. P. Dinesh-Kumar (2007). *Differential binding of calmodulin-related proteins to their targets revealed through high-density Arabidopsis protein microarrays*. Proceedings of the National Academy of Sciences of the United States of America **104**(11): 4730-4735.

Portis Jr, A. R. and H. W. Heldt (1976). *Light-dependent changes of the Mg^{2+} concentration in the stroma in relation to the Mg^{2+} dependency of CO_2 fixation in intact chloroplasts.* Biochimica et Biophysica Acta (BBA)-Bioenergetics **449**(3): 434-446.

Post, J. A. and G. A. Langer (1992). *Sarcolemmal calcium binding sites in heart: I. Molecular origin in gas-dissected sarcolemma*. The Journal of Membrane Biology **129**(1): 49-57.

Potter, J. D., P. Strang-Brown, P. L. Walker and S. Iida (1983). *Ca^{2+} binding to calmodulin*. Methods in Enzymology **102**: 135-143.

Prichard, L., J. C. Deloulme and D. R. Storm (1999). *Interactions between neurogranin and calmodulin* in vivo. The Journal of Biological Chemistry **274**(12): 7689-7694.

Puthiyaveetil, S., T. A. Kavanagh, P. Cain, J. A. Sullivan, C. A. Newell, J. C. Gray, C. Robinson, M. van der Giezen, M. B. Rogers and J. F. Allen (2008). *The ancestral symbiont sensor kinase CSK links photosynthesis with gene expression in chloroplasts.* Proceedings of the National Academy of Sciences of the United States of America **105**(29): 10061-10066.

Qin, N., R. Olcese, M. Bransby, T. Lin, and L. Birnbaumer (1999). *Ca^{2+}-induced inhibition of the cardiac Ca^{2+}-channel depends on calmodulin.* Proceedings of the National Academy of Sciences of the United States of America **96** (5): 2435–2438.

*Raaflaub J. (1956). Applications of metal buffers and metal indicators in biochemistry. Methods of Biochemical Analysis **3**:301–325.*

Racker, E. and E. Schroeder (1958). *The reductive pentose phosphate cycle. II. Specific C-1 phosphatases for fructose 1, 6-diphosphate and sedoheptulose 1, 7-diphosphate*. Archives of Biochemistry and Biophysics **74**(2): 326-344.

Reddy, A. S. (2001). *Calcium: silver bullet in signaling*. Plant Science **160**(3): 381-404.

Reddy, V. S., G. S. Ali and A. S. N. Reddy (2002). *Genes encoding calmodulin-binding proteins in the Arabidopsis genome*. The Journal of Biological Chemistry **277**(12): 9840-9852.

Reddy, V. S., Ali, G. S., and Reddy, A. S. N. (2003). *Characterization of a pathogen-induced calmodulin-binding protein: mapping of four Ca^{2+}-dependent calmodulin-binding domains*. Plant Molecular Biology, **52**(1): 143-159.

Reddy, V. S. and A. S. N. Reddy (2004). *Proteomics of calcium-signaling components in plants*. Phytochemistry **65**(12): 1745-1776.

Reddy, A. S. N., Ben-Hur, A., & Day, I. S. (2011). *Experimental and computational approaches for the study of calmodulin interactions*. Phytochemistry, **72**(10): 1007-1019.

Reid, R. and F. Smith (1992). *Measurement of calcium fluxes in plants using ^{45}Ca*. Planta **186**(4): 558-566.

Rhoads, A. R. and F. Friedberg (1997). *Sequence motifs for calmodulin recognition*. The FASEB Journal **11**(5): 331-340.

Rigden, D. J., M. J. Jedrzejas and M. Y. Galperin (2003). *An extracellular calcium-binding domain in bacteria with a distant relationship to EF-hands*. FEMS Microbiology Letters **221**(1): 103-110.

Rigden, D. J., D. D. Woodhead, P. W. Wong and M. Y. Galperin (2011). *New structural and functional contexts of the Dx [DN] xDG linear motif: insights into evolution of calcium-binding proteins*. PloS One **6**(6): e21507.

Rizo, J. and T. C. Südhof (1998). *C2-domains, structure and function of a universal Ca^{2+}-binding domain*. The Journal of Biological Chemistry **273**(26): 15879-15882.

Roberti, M. J., T. M. Jovin and E. Jares-Erijman (2011). *Confocal fluorescence anisotropy and FRAP imaging of α-synuclein amyloid aggregates in living cells*. PloS One **6**(8): e23338.

Roberts, D., P. Rowe, F. Siegel, T. Lukas and D. Watterson (1986). *Trimethyllysine and protein function. Effect of methylation and mutagenesis of lysine 115 of calmodulin on NAD kinase activation*. The Journal of Biological Chemistry **261**(4): 1491-1494.

Roberts, D. M., L. Besl, S.-H. Oh, R. V. Masterson, J. Schell and G. Stacey (1992). *Expression of a calmodulin methylation mutant affects the growth and development of transgenic tobacco plants*. Proceedings of the National Academy of Sciences of the United States of America **89**(17): 8394-8398.

Rodríguez-Concepción, M., S. Yalovsky, M. Zik, H. Fromm and W. Gruissem (1999). *The prenylation status of a novel plant calmodulin directs plasma membrane or nuclear localization of the protein*. The EMBO Journal **18**(7): 1996-2007.

Rodríguez-Concepción, M., G. Toledo-Ortiz, S. Yalovsky, D. Caldelari and W. Gruissem (2000). *Carboxyl-methylation of prenylated calmodulin CaM53 is required for efficient plasma membrane targeting of the protein*. Plant Journal **24**(6): 775-784.

Roh, M. H., R. Shingles, M. J. Cleveland and R. E. McCarty (1998). *Direct measurement of calcium transport across chloroplast inner-envelope vesicles*. Plant Physiology **118**(4): 1447-1454.

Roux, S. J., K. McEntire, R. D. Slocum, T. E. Cedel and C. C. Hale (1981). *Phytochrome induces photoreversible calcium fluxes in a purified mitochondrial fraction from oats*. Proceedings of the National Academy of Sciences of the United States of America **78**(1): 283-287.

Rusnak, F. and P. Mertz (2000). *Calcineurin: form and function*. Physiological Reviews **80**(4): 1483-1521.

Sai, J. Q. and C. H. Johnson (2002). *Dark-stimulated calcium ion fluxes in the chloroplast stroma and cytosol*. The Plant Cell **14**(6): 1279-1291.

Sanders, D., J. Pelloux, C. Brownlee and J. F. Harper (2002). *Calcium at the crossroads of signaling.* The Plant Cell **14**(suppl 1): S401-S417.

Sato, M., K. Takahashi, Y. Ochiai, T. Hosaka, K. Ochi and K. Nabeta (2009). *Bacterial alarmone, guanosine 5'-diphosphate 3'-diphosphate (ppGpp), predominantly binds the β' subunit of plastid-encoded plastid RNA polymerase in chloroplasts.* Chembiochem **10**(7): 1227-1233.

Schleiff, E. and T. Becker (2010). *Common ground for protein translocation: access control for mitochondria and chloroplasts*. Nature Reviews Molecular Cell Biology **12**(1): 48-59.

Seigneurin-Berny, D., A. Gravot, P. Auroy, C. Mazard, A. Kraut, G. Finazzi, D. Grunwald, F. Rappaport, A. Vavasseur, J. Joyard, P. Richaud and N. Rolland (2006). *HMA1, a new Cu-ATPase of the chloroplast envelope, is essential for growth under adverse light conditions.* The Journal of Biological Chemistry **281**(5): 2882-2892.

Selivanov, V. A., F. Ichas, E. L. Holmuhamedov, L. S. Jouaville, Y. V. Evtodienko and J.-P. Mazat (1998). *A model of mitochondrial Ca^{2+}-induced Ca^{2+} release simulating the Ca^{2+} oscillations and spikes generated by mitochondria*. Biophysical Chemistry **72**(1): 111-121.

Shao, S. and Ramanujan S. Hegde (2011). *A calmodulin-dependent translocation pathway for small secretory proteins*. Cell **147**(7): 1576-1588.

Shen, X., C. A. Valencia, J. Szostak, B. Dong and R. Liu (2005). *Scanning the human proteome for calmodulin-binding proteins*. Proceedings of the National Academy of Sciences of the United States of America **102**(17): 5969-5974.

Shen, X., C. A. Valencia, W. Gao, S. W. Cotten, B. Dong, B.-c. Huang and R. Liu (2008). *Ca^{2+}/Calmodulin-binding proteins from the C. elegans proteome.* Cell Calcium **43**(5): 444-456.

Shi, F., Y. Li, , Y. Li and X. Wang (2009). *Molecular properties, functions and potential applications of NAD kinases*. Acta Biochimica et Biophysica Sinica **41**(5):352-261.

Simon, P., P. Dieter, M. Bonzon, H. Greppin and D. Marmé (1982). *Calmodulin-dependent and independent NAD kinase activities from cytoplasmic and chloroplastic fractions of spinach (*Spinacia oleracea L.*)*. The Plant Cell Reports **1**(3): 119-122.

Simon, P., M. Bonzon, H. Greppin and D. Marme (1984). *Subchloroplastic localization of Nad kinase-activity - evidence for a Ca^{2+}, calmodulin-dependent activity at the envelope and for a Ca^{2+}, calmodulin-independent activity in the stroma of pea-chloroplasts.* Febs Letters **167**(2): 332-338.

Slemmon, J. R., J. I. Morgan, S. M. Fullerton, W. Danho, B. S. Hilbush and T. M. Wengenack (1996). *Camstatins are peptide antagonists of calmodulin based upon a conserved structural motif in PEP-19, neurogranin, and neuromodulin*. The Journal of Biological Chemistry **271**(27): 15911-15917.

Snedden, W. A., N. Koutsia, G. Baum and H. Fromm (1996). *Activation of a recombinant Petunia glutamate decarboxylase by calcium/calmodulin or by a monoclonal antibody which recognizes the calmodulin binding domain.* The Journal of Biological Chemistry **271**(8): 4148-4153.

Stael, S., A. G. Rocha, T. Wimberger, D. Anrather, U. C. Vothknecht and M. Teige (2012a). *Cross-talk between calcium signalling and protein phosphorylation at the thylakoid.* Journal of Experimental Botany **63**(4): 1725-1733.

Stael, S., B. Wurzinger, A. Mair, N. Mehlmer, U. C. Vothknecht and M. Teige (2012b). *Plant organellar calcium signalling: an emerging field.* Journal of Experimental Botany **63**(4): 1525-1542.

Stein, R. L. (2011). *Kinetics of enzyme action: essential principles for drug hunters.* Hoboken, N.J.: John Wiley.

Stepanyuk, G. A., S. Golz, S. V. Markova, L. A. Frank, J. Lee and E. S. Vysotski (2005). *Interchange of aequorin and obelin bioluminescence color is determined by substitution of one active site residue of each photoprotein*. FEBS Letters **579**(5): 1008-1014.

Takabatake, R., E. Karita, S. Seo, I. Mitsuhara, K. Kuchitsu and Y. Ohashi (2007). *Pathogen-induced calmodulin isoforms in basal resistance against bacterial and fungal pathogens in tobacco*. Plant and Cell Physiology **48**(3): 414-423.

Takahashi, A., P. Camacho, J. D. Lechleiter and B. Herman (1999). *Measurement of intracellular calcium*. Physiological Reviews **79**(4): 1089-1125.

Takahashi, K., K. Kasai and K. Ochi (2004). *Identification of the bacterial alarmone guanosine 5'-diphosphate 3'-diphosphate (ppGpp) in plants.* Proceedings of the National Academy of Sciences of the United States of America **101**(12): 4320-4324.

Takahashi, H., A. Watanabe, A. Tanaka, S. N. Hashida, M. Kawai-Yamada, K. Sonoike and H. Uchimiya (2006). *Chloroplast NAD kinase is essential for energy transduction through the xanthophyll cycle in photosynthesis*. Plant and Cell Physiology. **47**(12): 1678-1682.

Thimm, O., O. Bläsing, Y. Gibon, A. Nagel, S. Meyer, P. Krüger, J. Selbig, L. A. Müller, S. Y. Rhee and M. Stitt (2004). *Mapman: a user-driven tool to display genomics data sets onto diagrams of metabolic pathways and other biological processes*. Plant Journal **37**(6): 914-939.

Tidow, H., L. R. Poulsen, A. Andreeva, M. Knudsen, K. L. Hein, C. Wiuf, M. G. Palmgren and P. Nissen

(2012). *A bimodular mechanism of calcium control in eukaryotes. Nature **491**: 468–472.*

Tidow, H. and P. Nissen (2013). *Structural diversity of calmodulin binding to its target sites*. FEBS Journal. doi: 10.1111/febs.12296.

Tiwari, B. S., B. Belenghi and A. Levine (2002). *Oxidative stress increased respiration and generation of reactive oxygen species, resulting in ATP depletion, opening of mitochondrial permeability transition, and programmed cell death*. Plant Physiology **128**(4): 1271-1281.

Trewavas, A. (1999). *Le calcium, c'est la vie: calcium makes waves*. Plant Physiology **120**(1): 1-6.

Tricoire, L., K. Tsuzuki, O. Courjean, N. Gibelin, G. Bourout, J. Rossier and B. Lambolez (2006). *Calcium dependence of aequorin bioluminescence dissected by random mutagenesis.* Proceedings of the National Academy of Sciences of the United States of America **103**(25): 9500-9505.

Trouillard, M., M. Shahbazi, L. Moyet, F. Rappaport, P. Joliot, M. Kuntz and G. Finazzi (2012). *Kinetic properties and physiological role of the plastoquinone terminal oxidase (PTOX) in a vascular plant*. Biochimica et Biophysica Acta (BBA)-Bioenergetics **181**7(12):2140-2148.

Tsai, M. D., T. Drakenberg, E. Thulin and S. Forsén (1987). *Is the binding of magnesium (II) to calmodulin significant? An investigation by magnesium-25 nuclear magnetic resonance*. Biochemistry **26**(12): 3635-3643.

Turano, F. J., S. S. Thakkar, T. Fang and J. M. Weisemann (1997). *Characterization and expression of NAD (H)-dependent glutamate dehydrogenase genes in Arabidopsis*. Plant Physiology **113**(4): 1329-1341.

Turner, W. L., J. C. Waller, B. Vanderbeld and W. A. Snedden (2004). *Cloning and characterization of two NAD kinases from Arabidopsis. Identification of a calmodulin binding isoform.* Plant Physiology **135**(3): 1243-1255.

Turner, W. L., J. C. Waller and W. A. Snedden (2005). *Identification, molecular cloning and functional characterization of a novel NADH kinase from Arabidopsis thaliana (thale cress)*. Biochemical Journal **385**: 217-223.

Vadassery, J., M. Reichelt, B. Hause, J. Gershenzon, W. Boland and A. Mithöfer (2012). *CML42-mediated calcium signaling coordinates responses to Spodoptera herbivory and abiotic stresses in Arabidopsis*. Plant Physiology **159**(3): 1159-1175.

Vainonen, J. P., M. Hansson and A. V. Vener (2005). *STN8 protein kinase in Arabidopsis thaliana is specific in phosphorylation of photosystem II core proteins*. The Journal of Biological Chemistry **280**(39): 33679-33686.

Vainonen, J. P., Y. Sakuragi, S. Stael, M. Tikkanen, Y. Allahverdiyeva, V. Paakkarinen, E. Aro, M. Suorsa, H. V. Scheller, A. V. Vener and E. M. Aro (2008). *Light regulation of CaS, a novel phosphoprotein in the thylakoid membrane of* Arabidopsis thaliana. FEBS Journal **275**(8): 1767-1777.

van der Luit, A. H., C. Olivari, A. Haley, M. R. Knight and A. J. Trewavas (1999). *Distinct calcium signaling pathways regulate calmodulin gene expression in tobacco*. Plant Physiology **121**(3): 705-714.

Van der Spoel, D., B. L. D. Groot, S. Hayward, H. J. Berendsen and H. J. Vogel (1996). *Bending of the calmodulin central helix: a theoretical study*. Protein Science **5**(10): 2044-2053.

Vanderbeld, B. and W. A. Snedden (2007). *Developmental and stimulus-induced expression patterns of Arabidopsis calmodulin-like genes CML37, CML38 and CML39*. Plant Molecular Biology **64**(6): 683-697.

Vandonselaar, M., R. A. Hickie, W. Quail and L. T. Delbaere (1994). *Trifluoperazine-induced conformational change in Ca^{2+}-calmodulin.* Nature Structural and Molecular Biology **1**(11): 795-801.

Vinson, V. K., E. M. De La Cruz, H. N. Higgs and T. D. Pollard (1998). *Interactions of Acanthamoeba profilin with actin and nucleotides bound to actin.* Biochemistry **37**(31): 10871-10880.

Virgin, I., Ghanotakis, D. F., and Andersson, B. (1990). *Light-induced D1-protein degradation in isolated Photosystem II core complexes.* FEBS letters **269**(1): 45-48.

Virolainen, E., O. Blokhina and K. Fagerstedt (2002). *Ca^{2+}-induced high amplitude swelling and cytochrome c release from wheat (*Triticum aestivum L.*) mitochondria under anoxic stress.* Annals of Botany **90**(4): 509-516.

Vishwasrao, H. D., P. Trifilieff and E. R. Kandel (2012). In vivo *imaging of the actin polymerization state with two-photon fluorescence anisotropy*. Biophysical Journal **102**(5): 1204-1214.

Waller, J. C., P. K. Dhanoa, U. Schumann, R. T. Mullen and W. A. Snedden (2010). *Subcellular and tissue localization of NAD kinases from Arabidopsis: compartmentalization of de novo NADP biosynthesis*. Planta **231**(2): 305-317.

Weinl, S. and J. Kudla (2009). *The CBL–CIPK Ca^{2+}-decoding signaling network: function and perspectives*. New Phytologist **184**(3): 517-528.

Weinstein, H. and E. L. Mehler (1994). *Ca^{2+}-binding and structural dynamics in the functions of calmodulin*. Annual Review of Physiology **56**(1): 213-236.

Williams, M. B. and H. P. Jones (1985). *Calmodulin-dependent NAD kinase of human neutrophils*. Archives of Biochemistry and Biophysics **237**(1): 80-87.

Wilson, M. A. and A. T. Brunger (2000). *The 1.0 Å crystal structure of Ca^{2+}-bound calmodulin: an analysis of disorder and implications for functionally relevant plasticity*. Journal of Molecular Biology **301**(5): 1237-1256.

Wilson, M. E., G. S. Jensen and E. S. Haswell (2011). *Two mechanosensitive channel homologs influence division ring placement in Arabidopsis chloroplasts*. The Plant Cell **23**(8): 2939-2949.

Wolenski, J. S. (1995). *Regulation of calmodulin-binding myosins*. Trends in Cell Biology **5**(8): 310-316.

Wu, P., M. Brasseur and U. Schindler (1997). *A high-throughput STAT binding assay using fluorescence polarization.* Analytical Biochemistry **249**(1): 29-36.

Wylie, D. C. and T. C. Vanaman (1988). *Structure and evolution of the calmodulin family of calcium regulatory proteins*. Calmodulin **5**: 1-15.

Xi, J., Y. Qiu, L. Du and B. Poovaiah (2012). *Plant-specific trihelix transcription factor AtGT2L interacts with calcium/calmodulin and responds to cold and salt stresses*. Plant Science **185**: 274-280.

Xiong, T. C., A. Jauneau, R. Ranjeva and C. Mazars (2004). *Isolated plant nuclei as mechanical and thermal sensors involved in calcium signalling*. Plant Journal **40**(1): 12-21.

Yamaguchi, T., G. S. Aharon, J. B. Sottosanto and E. Blumwald (2005). *Vacuolar Na^+/H^+ antiporter cation selectivity is regulated by calmodulin from within the vacuole in a Ca^{2+}- and pH-dependent manner*. Proceedings of the National Academy of Sciences of the United States of America **102**(44): 16107-16112.

Yamamoto, Y. (1966). *NAD kinase in higher plants*. Plant Physiology **41**(3): 523.

Yang, T. B. and B. W. Poovaiah (2000). *Arabidopsis chloroplast chaperonin 10 is a calmodulin-binding protein*. Biochemical and Biophysical Research Communications **275**(2): 601-607.

Yap, K. L., J. Kim, K. Truong, M. Sherman, T. Yuan and M. Ikura (2000). *Calmodulin target database*. Journal of Structural and Functional Genomics **1**(1): 8-14.

Yap, K. L., T. Yuan, T. K. Mal, H. J. Vogel and M. Ikura (2003). *Structural basis for simultaneous binding of two carboxy-terminal peptides of plant glutamate decarboxylase to calmodulin*. Journal of Molecular Biology **328**(1): 193-204.

Yazawa, M., M. Ikura, K. Hikichi, L. Ying and K. Yagi (1987). *Communication between two globular domains of calmodulin in the presence of mastoparan or caldesmon fragment. Ca^{2+} binding and ^1H NMR*. The Journal of Biological Chemistry **262**(23): 10951-10954.

Yuan, T. and H. J. Vogel (1998). *Calcium-calmodulin-induced dimerization of the carboxyl-terminal domain from petunia glutamate decarboxylase. A novel calmodulin-peptide interaction motif.* The Journal of Biological Chemistry **273**(46): 30328-30335.

Zakharov, S. D., R. G. Ewy and R. A. Dilley (1993). *Subunit III of the chloroplast ATP-synthase can form a Ca^{2+}-binding site on the lumenal side of the thylakoid membrane*. FEBS Letters **336**(1): 95-99.

Zhang, M., T. Tanaka and M. Ikura (1995). *Calcium-induced conformational transition revealed by the solution structure of apo calmodulin*. Nature Structural & Molecular Biology **2**(9): 758-767.

Zhou, L., Y. Fu and Z. Yang (2009). *A genome-wide functional characterization of arabidopsis regulatory calcium sensors in pollen tubes*. Journal of Integrative Plant Biology **51**(8): 751-761.

Ziegenhagen, R. and H. Jennissen (1990). *Plant and fungus calmodulins are polyubiquitinated at a single site in a Ca^{2+}-dependent manner*. FEBS Letters **273**(1): 253-256.

Zielinski, R. E. (1998). *Calmodulin and calmodulin-binding proteins in plants*. Annual Review of Plant Biology **49**(1): 697-725.

Zielinski, R. E. (2002). *Characterization of three new members of the* Arabidopsis thaliana *calmodulin gene family: conserved and highly diverged members of the gene family functionally complement a yeast calmodulin null.* Planta **214**(3): 446-455.

Résumé de thèse en Français

INTRODUCTION

Le rôle du calcium dans la signalisation des eucaryotes. Le calcium est un facteur de signalisation de première importance pour les organismes eucaryotes, car les ions calciques interviennent dans la réponse des cellules à de nombreux stimuli. Dans des conditions standards, la concentration du calcium cytosolique est très faible (environ 100 nM) grâce à l'activité de pompes et transporteurs qui excrètent le calcium en excès dans l'apoplaste ou le stockent dans des organites tels que le réticulum endoplasmique, la vacuole et la mitochondrie. La différence entre la concentration calcique dans le cytosol et les organelles de stockage ou l'apoplaste permet des changements rapides de la concentration en calcium cytosolique grâce à l'ouverture de canaux à calcium situés sur les membranes des organelles de stockage ou sur la membrane plasmique. Ces changements ont été observés en réponse à plusieurs facteurs de type biotique, abiotique ou développementaux. Le paradigme de la « réponse calcique » affirme que, suite à certains stimuli environnementaux ou certaines conditions de stress, la concentration de calcium dans le cytosol passe de l'ordre du nanomolaire au micromolaire, avec un pattern spatial et temporel spécifique souvent appelé « signature calcique ». Le calcium en excès est tamponné par de nombreuses « Calcium-binding proteins » (CBPs), qui constituent des senseurs de calcium. A leur tour, les CBPs pourraient interagir avec d'autres composants cellulaires et d'autres protéines (notamment enzymes, canaux et facteur de transcription) qui permettraient à la cellule de s'adapter à des nouvelles conditions. Ce principe est valable pour tous les eucaryotes ; toutefois, des différences importantes sont à signaler entre les cellules animales et végétales en ce qui concerne la variété des senseurs et des fluxes de calcium.

Les « vagues de calcium » qui en résultent doivent pouvoir être finement modulées afin de générer des réponses cellulaires très différentes. Les transporteurs calciques, ainsi que les CBP, se sont donc énormément dupliqués et spécialisés, de sorte que chaque tissu ou type cellulaire est capable de générer des « signatures calciques » différentes selon les conditions, et d'y répondre de manière spécifique.

Des fluctuations calciques ont été observées non seulement au niveau du cytosol mais aussi dans la plupart des organites cellulaires végétaux, à savoir le réticulum endoplasmique, l'apoplaste, la mitochondrie, la vacuole, le noyau, les peroxysomes et les chloroplastes.

Les CBPs végétales. De nombreuses protéines végétales ont été étudiées pour leur propriété à lier le calcium. Elles sont réparties en trois classes principales : les annexines, les protéines à domaine C2 et les protéines à domaine EF-hand. Ces dernières sont les plus répandues chez les végétaux et les eucaryotes en général. Le domaine EF-hand est constitué de 29 acides aminés qui forment deux hélices autour d'une boucle (structure « helix-loop-helix »). La première hélice est appelée E et la deuxième est appelée F. Le calcium est lié dans la boucle située entre les deux hélices.

Une étude bioinformatique à grande échelle du génome d'*Arabidopsis thaliana* a récemment montré que le nombre des protéines présentant au moins un domaine de liaison au calcium de type EF-hand s'élève à plus de 250. Celles-ci peuvent être classées en 6 groupes. Le nombre de ces domaines est variable (entre 1 et 6), et dans la plupart des cas ils sont organisés en pairs, ce qui faciliterait la liaison au calcium par des effets de synergie entre les différents domaines.

La calmoduline (CaM). Dans cette classification, les calmodulines (CaMs) et les protéines dites "CaM-like" (CMLs) appartiennent au groupe 4. Grâce à un senseur fluorescent exprimé de façon stable pour la détection à la fois de la CaM libre (apo-CaM) et de celle liée au calcium, une concentration intracellulaire de CaM de 8.8 ±2.2 µM a été mesurée dans les cellules de rein humain. Des résultats similaires ont été obtenus dans des cellules végétales de *Daucus carota* et de *Vicia faba*.

Chez les animaux, la CaM est une petite protéine d'environ 150 acides aminés formée de quatre domaines EF-hand, deux en région N-ter et deux en région C-ter. L'affinité de la CaM pour le calcium a été estimée à environ 1-10 nM. L'affinité de la région N-ter et C-ter n'est d'ailleurs pas la même (le domaine C-ter serait dix fois plus affin pour le calcium que le domaine N-ter) et un effet synergique facilite très probablement la liaison au calcium au niveau deux lobes.

Les couples d'EF-hand sont séparés par une longue hélice très flexible. La liaison du calcium ne confère à la CaM aucune activité catalytique ; cependant, le calcium déclenche un réarrangement structural important de la protéine. Ceci conduit généralement à une augmentation de l'affinité de la CaM pour d'autres protéines, appelées « protéines cibles ». Lorsque la CaM acquière la capacité de se lier à ses cibles en présence d'un excès de calcium, elle modifie leurs propriétés. Ces variations dépendent de la cible considérée, ce qui ne permet pas de

donner des règles générales sur les effets de la CaM. Parmi les effets les plus observés on retrouve l'activation de kinases et autres classes d'enzymes, l'activation de pompes de calcium et le contrôle de la sécrétion de petites protéines.

Le nombre des protéines considérées comme des cibles de la CaM est extrêmement élevé. Cependant, l'étude des interactions CaM-cibles est compliquée, car les domaines de liaison à la CaM ne peuvent être identifiés avec certitude par la seule analyse de leur séquence primaire. Une analyse biochimique approfondie est donc nécessaire pour chaque interaction, premièrement pour déterminer la force de l'interaction (mesure d'affinité) et dans un second temps pour en évaluer le rôle physiologique.

Le calcium et le chloroplaste. Si la concentration du calcium dans le stroma est comparable à celle du cytosol (environ 200 nM), la concentration mesurée dans les thylakoïdes est beaucoup plus élevée. Les thylakoides peuvent, par conséquent, être considérés comme un site de stockage du calcium dans le chloroplaste. Le transport du calcium dans le chloroplaste demeure encore assez mystérieux, car à l'heure actuelle aucun transporteur situé sur l'enveloppe ou au niveau de la membrane des thylakoides n'a été caractérisé. Cependant, le calcium pourrait avoir une fonction régulatrice très importante dans cette organelle, en particulier pour les variations physiologiques qui accompagnent la transition jour/nuit et pour l'adressage dans le chloroplaste des protéines sans peptide signal. A ce jour, ni CaM ni CMLs n'ont pu être détectées dans le chloroplaste. Cependant, un petit nombre de protéines cibles de la CaM (notamment la NAD kinase 2 et Tic32) sont censées se situer dans cette organelle.

Objectif du travail. L'objectif de cette thèse a été de mettre en place des méthodes biochimiques quantitatives pour l'analyse des interactions protéine-protéine et de les appliquer à l'étude des interactions CaM-cibles chloroplastiques d'*Arabidopsis thaliana*, afin de mieux comprendre le rôle de la calmoduline dans le chloroplaste.

RÉSULTATS

Chapitre 1

Afin d'étudier les interactions CaM-cibles, nous avons mis en place différents essais quantitatifs reposant sur la technique de l'anisotropie de fluorescence. Cette technique permet d'étudier les interactions protéiques en solution et dans de nombreuses conditions expérimen-

tales. Elle requière la présence d'une sonde flourescente sur une des deux protéines, afin de pouvoir mesurer son degré d'anisotropie par spectrométrie de fluorescence.

Nous avons établi différents essais d'interaction entre la CaM1 d'Arabidopsis et la NADK2, une des protéines plastidiales connue d'après la littérature pour être activée par la CaM. Un premier test a consisté à déterminer l'affinité du domaine N-terminal de la NADK2 pour la CaM1 d'Arabidopsis (AtCaM1) marquée avec une sonde Alexa488 ; le second test a consisté à déterminer l'affinité de la CaM1 d'Arabidopsis pour la séquence de 20 acides aminés de la NADK2 censée contenir un site de liaison à la CaM et marquée avec une sonde TamRa. La cohérence de ces essais nous a motivé à les utiliser pour la caractérisation d'autres interactions.

Chapitre 2

En collaboration entre le laboratoire PCV et le laboratoire EDyP du CEA-Grenoble, une analyse à grande échelle des cibles potentielles de la CaM dans le chloroplaste avait été effectuée avant le début de cette thèse. Tout d'abord, des fractions très pures des trois sous-compartiments du chloroplaste (stroma, thylakoides, enveloppe) avaient été obtenues puis soumises à une chromatographie d'affinité pour la CaM ; les protéines qui avaient été retenues sur la matrice CaM en présence de calcium avaient enfin été analysées et identifiées par spectrométrie de masse. Cette approche avait conduit à l'identification de 210 cibles potentielles.

La première partie du travail a consisté en une analyse de cet ensemble de cibles potentielles afin de déterminer leurs caractéristiques. Le groupe apparait très hétérogène en termes du niveau d'abondance de chaque protéine, de leurs fonctions et des processus cellulaires dans lesquels elles sont impliquées. Certaines de ces protéines (24) ont été exclues des analyses suivantes car elles sont très certainement des contaminants d'autres compartiments cellulaires (par exemple, la sous-unité gamma de l'ATP synthase mitochondriale). En parallèle, cette étude a permis d'identifier un groupe de 20 protéines très certainement chloroplastiques mais jamais détectées au cours des analyses protéomiques antérieures car très peu abondantes.

Nous avons ensuite focalisé notre attention sur un sous-ensemble de 20 nouvelles cibles potentielles. La validation a été effectuée par un test de liaison à la CaM *in vitro* appelé « overlay assay » que nous avons optimisé afin de pouvoir comparer en parallèle les signaux obtenus avec différentes protéines. Cette procédure a permis de confirmer toutes les interac-

tions potentielles. Cependant, les protéines ne présentaient pas toutes le même comportement. Elles ont été classées en quatre sous-groupes : protéines à forte intensité de signal calcium-dépendante, protéines à faible intensité de signal calcium-dépendante, protéines à forte intensité de signal calcium-indépendante, et protéines à faible intensité de signal calcium-indépendante. En outre, l'intensité des signaux obtenus était fortement dépendante de la durée de l'incubation en présence de CaM (15 minutes ou trois heures). Ces différences étaient appréciables également pour les contrôles positifs (NADK2 et Tic32).

Nous avons ensuite focalisé notre attention sur un sous-groupe de quatre protéines à fonction enzymatique : Lox2 (lipoxygénase 2), TS2 (thréonine synthase 2), la protéine ceQORH et XK1-like (dont l'activité reste à déterminer). Dans le cas de ceQORH, Lox2 et TS2, l'activité enzymatique en présence et en absence de CaM-calcium a été mesurée sans aucune différence appréciable. L'interaction de ces protéines avec la CaM a été donc validée par le biais d'une chromatographie d'affinité et par un test d'anisotropie de fluorescence avec AtCaM1-Alexa488. La chromatographie d'affinité n'a permis de confirmer les résultats overlay que pour la protéine ceQORH et pour Lox2. Une haute affinité pour la CaM mesurée par anisotropie de fluorescence n'a été observée que pour la ceQORH (Chapitre 3).

Chapitres 3 et 4

Malgré l'absence d'un peptide transit traditionnel à son extrémité N-terminale, les protéines ceQORH (Miras et al, 2002 et 2007) et Tic32 (Chigri et al, 2006) sont adressées au chloroplaste. En outre, d'après la littérature et des résultats préliminaires obtenus au sein du laboratoire PCV, les deux protéines sont capables d'interagir avec la CaM.

Nous avons donc analysé ces interactions plus en détail et quantitativement, afin de mieux comprendre leur éventuel rôle physiologique. Tic32 et ceQORH ont été étudiées en combinaison avec AtCaM avec plusieurs essais d'anisotropie de fluorescence.

Pour la ceQORH, nous avons observé qu'une séquence interne de 20 acides aminés présente une haute affinité pour la CaM, avec un k_D de l'ordre de 10 nM, ce qui correspond aussi à la valeur mesurée pour la protéine entière. Des mutations dans des acides aminés de ce site, estimés importants pour la liaison à la CaM, élèvent effectivement cette valeur de vingt fois (200 nM). Cependant, dans la protéine entière et active, la mutation de ce site n'affecte pas l'interaction avec la CaM.

Cette divergence peut s'expliquer si l'on compare ces résultats avec des expériences de mesure d'activité de la protéine ceQORH. Cette protéine perd son activité quand elle est dénaturée par un excès d'urée, mais se replie en une forme active après dilution de l'urée (renaturation). Cependant, si la rénaturation est effectuée dans un milieu contenant CaM et calcium, l'activité n'est pas récupérée. Ces résultats suggèrent que la CaM empêche le repliement de la protéine dans une conformation active et que la liaison à la ceQORH repliée, bien que possible, n'a plus d'effets sur son activité. Ce mécanisme de contrôle de l'activité pourrait avoir un rôle particulier dans la localisation de la protéine dans le chloroplaste ou dans la membrane plasmique, comme le montre des expériences de localisation *in planta* (D. Salvi et L. Moyet). Les caractéristiques moléculaires de ce système de transport restent à être déterminées.

Nos mesures avec la protéine Tic32 dans sa conformation native a également montré une forte affinité pour la CaM, similaire à celle mesurée avec la protéine ceQORH. En accord avec la littérature, nous avons obeservé que l'interaction avec la CaM avec la protéine Tic32 est déplacée par le NADPH, un des substrats de la protéine. Une concentration assez faible de NADPH (de l'ordre du micromolaire) est toutefois suffisante pour annuler l'interaction avec la CaM, ce qui ouvre la question de la réalité physiologique de cette interaction. Enfin, nous avons aussi testé l'affinité de la région C-ter de la protéine, qui avait été précédemment identifiée comme une région clé pour l'interaction Tic32-CaM. Cette région isolée n'a montré aucune affinité pour la CaM.

Chapitre 5

Le génome d'Arabidopsis contient 7 séquences de protéines CaM et 50 de protéines très similaires appelées CaM-like (CMLs). Dans la séquence de certaines CMLs se trouve non seulement des domaines EF-hand mais aussi des séquences additionnelles aux extrémités N-terminales ou C-terminales qui parfois déterminent la localisation subcellulaire de ces protéines dans la mitochondrie, la vacuole ou d'autres organelles. Malgré la présence de peptides d'adressage au chloroplaste d'un ensemble de CMLs, aucune d'entre elles n'a jamais été observée dans cette organelle. La question de la présence de la CaM ou des CMLs dans le chloroplaste étant de première importance, nous avons essayé d'y répondre par le biais d'une analyse protéomique à grande échelle et d'études préliminaires de localisation subcellulaire dans des protoplastes d'Arabidopsis (pour les CML 35, 36 et 41) en fusionnant ces protéines à

la protéine GFP. À présent, aucune de ces analyses n'a permis d'observer des CaMs ou CMLs dans le chloroplaste.

Chapitre 6

Enfin, nous sommes revenus à l'analyse de la NADK2, notre contrôle positif d'interaction avec la CaM pendant toutes les expériences précédentes. En effet, par une relecture approfondie de la littérature, nous avons constaté que la réalité de cette interaction et son éventuelle fonction physiologique sont encore très contradictoires. Si une activité NADK CaM-dépendante peut être observée dans des extraits cellulaires, la preuve que l'enzyme responsable est la NADK2 n'a toujours pas été donnée, car la NADK2 recombinante n'est pas CaM-sensible. En outre, son affinité pour la CaM mesurée par anisotropie de fluorescence n'atteint pas les valeurs très élevées attendues sur la base du facteur d'activation précédemment mesuré. Nous avons donc commencé à mettre en place une procédure de purification de la forme CaM-dépendante à partir d'extraits végétaux. Des analyses complémentaires seront donc nécessaires avant de pouvoir répondre à cette question biologique du contrôle de la NADK2 par la CaM. En parallèle, nous avons analysé les plantes mutantes *nadk2* et observé un fort impact de l'absence de cette protéine sur la photosynthèse et le développement de la plante.

CONCLUSIONS

De très nombreuses analyses à grande échelle sur les cibles de la CaM ont été conduites sur différents organismes au cours des dix dernières années. Toutefois, comme le montre les divergences que nous avons observées selon les techniques utilisées (overlay, colonne d'affinité, anisotropie de fluorescence) la confirmation des interactions requière des analyses quantitatives qui permettent de supporter et investiguer leur réalité physiologique.

Le présent travail de thèse a permis de mettre en place différents systèmes de mesure des interactions protéine-protéine par anisotropie de fluorescence qui se sont révélé très souples et utiles pour répondre à ces questions. Ils nous ont permis notamment d'aller plus loin dans la caractérisation du rôle de la CaM dans la modulation de la protéine ceQORH et de remettre en question les données de la littérature concernant Tic32 et NADK2.

PUBLICATIONS

Dell'Aglio, E., C. Giustini, D. Salvi, S. Brugière, F. Delpierre, L. Moyet, M. Baudet, D. Seigneurin-Berny, M. Matringe, M. Ferro, N. Rolland, and G. Curien (2013). *Complementary biochemical approaches applied to the identification of plastidial calmodulin-binding proteins.* Molecular Biosystems, **9**(6), 1234-1248.

Publications related to previous works

Volpe, V.*, E. Dell'Aglio*, and P. Bonfante (2013). *The* Lotus japonicus *MAMI gene links root development, arbuscular mycorrhizal symbiosis and phosphate availability*. Plant Sgnaling & Behavior, **8**(3), e23414.

Volpe, V., E. Dell'Aglio, M. Giovannetti, C. Ruberti, A. Costa, A. Genre, M. Guether, and P. Bonfante (2013). *An AM-induced, MYB-family gene of* Lotus japonicus *(LjMAMI) affects root growth in an AM-independent manner*. The Plant Journal, **73**(3), 442-455.

ORAL COMMUNICATION

Groupe Français de Bioénergétique. Carry – Le Rouet, September 2013. *The chloroplast NADP pool in* Arabidopsis thaliana*: synthesis, regulation and physiological consequences on photosynthesis.* Dell'Aglio, E., G. Finazzi, N. Rolland and G. Curien.

Résumé en Français

La calmoduline (CaM) est une protéine modulatrice de la réponse cellulaire chez les eucaryotes composée de quatre domaines de liaison au calcium (Ca^{2+}) et d'une hélice centrale flexible. Elle peut interagir avec d'autres protéines en présence de Ca^{2+}, entraînant l'activation et l'inhibition d'enzymes, l'ouverture de canaux membranaires et modulant le trafic intracellulaire.

L'identification de protéines partenaire de la CaM requière la mise au point de techniques permettant de mesurer les paramètres de la liaison pour un grand nombre de protéines dans des conditions variables mimant l'environnement cellulaire (par exemple en présence de ligands ou d'autres protéines).

Le premier objectif de cette thèse a été de développer une technique de mesure des interactions CaM-partenaire reposant sur des mesures d'anisotropie de fluorescence. Les tests ont été ensuite utilisés pour caractériser de manière quantitative l'interaction préalablement mise en évidence de deux protéines chloroplastiques (NADK2 et Tic32) avec la CaM. Afin d'identifier d'autres cibles chloroplastiques de la CaM nous avons alors effectué une analyse à haut-débit en couplant une purification par affinité à des analyses protéomiques. La validation des interactions a été réalisée grâce à l'utilisation de méthodes biochimiques complémentaires. Nous avons ensuite focalisé notre attention sur la protéine ceQORH dont la très forte affinité pour la CaM a pu être confirmée. Nos résultats fournissent par ailleurs de nouveaux éléments pour la compréhension des effets de ces interactions.

Afin de vérifier la présence de CaM ou de CaM-like dans le chloroplaste nous avons utilisé une approche biochimique et protéomique. Nous avons d'autre part étudié la localisation de CMLs potentiellement chloroplastiques fusionnées à la GFP dans des protoplastes d'*Arabidopsis*. A ce jour ces deux approches ne nous ont pas permis d'identifier ce type de protéines dans les chloroplastes.

Abstract in English

Calmodulin (CaM) is an important modulator of cell responses of eukaryotes. This protein is composed of four calcium (Ca^{2+})-binding sites and a flexible central helix. CaM can interact with other proteins in a Ca^{2+}-dependent way. This leads to a wide variety of effects, such as activation/inhibition of enzymes, opening of membrane channels and regulation of protein trafficking.

The identification of high-affinity CaM targets requires techniques allowing the study of the CaM-binding parameters ofa large number of proteins, and in several conditions mimicking the cell environment (*e.g.* presence of ligands or other proteins).

The first objective of this PhD thesis was to develop flexible and quantitative assays of CaM-partners interactions based on measurements of fluorescence anisotropy. These tests were used to perform a quantitative characterization of the interaction between CaM and two previously identified targets located in Arabidopsis chloroplast (NADK2 and Tic32). We then performed a high-throughput analysis (CaM-affinity chromatography coupled with mass spectrometry) in order to detect new potential plastidial CaM targets. We validated our approach with several biochemical approaches. We finally focused our attention on the ceQORH protein, whose high CaM affinity was confirmed by several approaches. Our results confirm the Ca^{2+} dependent CaM affinity of NADK2, Tic32 and ceQORH and provide new elements for understanding the effects of these interactions.

In addition, in order to verify the presence of CaMs or CaM-like proteins in the chloroplast, we used a biochemical and proteomic approach. We also studied the intracellular localization of some putative plastidial CMLs tagged with GFP in Arabidopsis protoplasts. For the moment, these approaches did not allow identifying such proteins in the chloroplast.